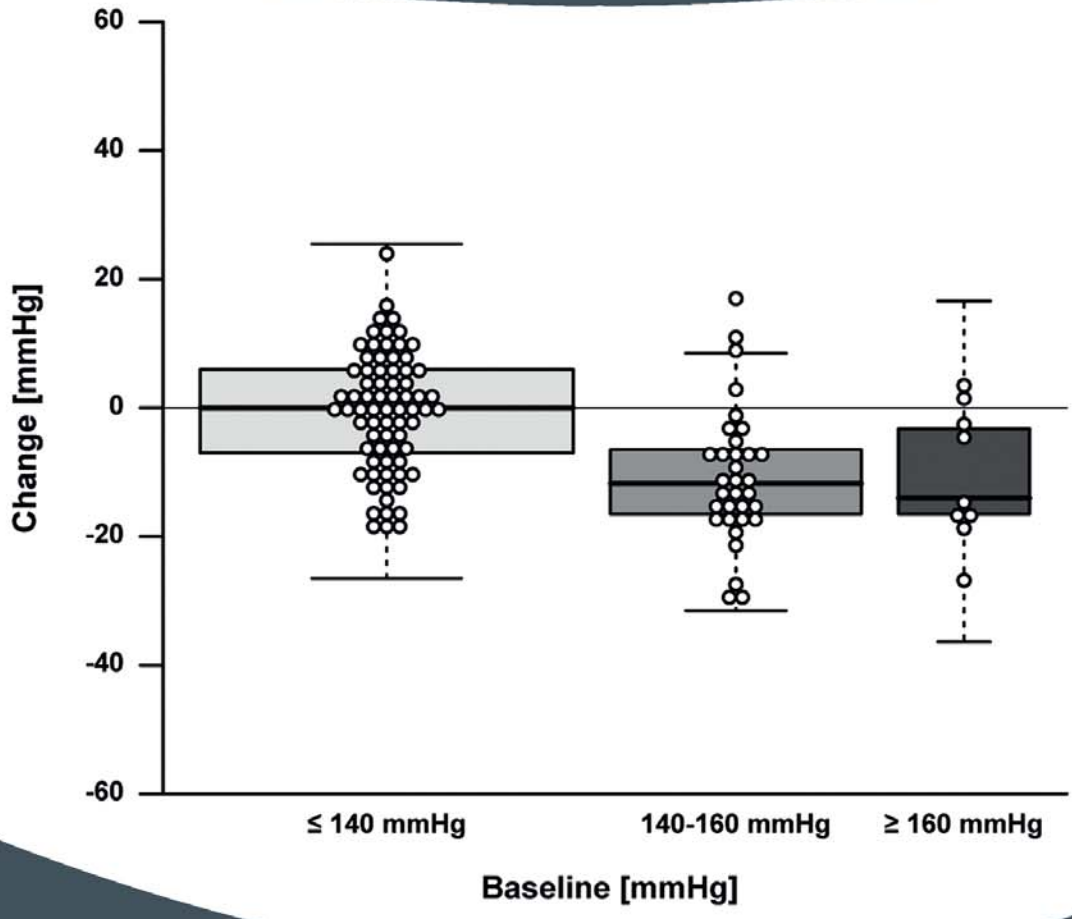

Special Collection on Diet

Effect of the intervention on systolic blood pressure by baseline systolic blood pressure, see van de Rest et al. - "Metabolic effects of a 13-weeks lifestyle intervention in older adults: The Growing Old Together Study."

Diet

AGING

Editorial and Publishing Office Aging
6666 E. Quaker St., Suite 1b
Orchard Park, NY 14127
Phone: 1-800-922-0957
Fax: 1-716-508-8254
e-Fax: 1-716-608-1380

Submission
Please submit your manuscript on-line at http://aging.msubmit.net

Editorial
For editorial inquiries, please call us or email editors@impactaging.com

Production
For questions related to preparation of your article for publication, please call us or email krasnova@impactaging.com

Indexing
If you have questions about the indexing status of your paper, please email kurenova@impactaging.com

Billing/Payments
If you have questions about billing/invoicing or would like to make a payment, please call us or email payment@impactaging.com

External & Legal Affairs
If you have questions about post publication promotion, Altmetric, video interviews or social media, please email RyanJamesJessup@Impactjournals.com

Printing
Each issue or paper can be printed on demand. To make a printing request, please call us or email krasnova@impactaging.com

Publisher's Office
Aging is published by Impact Journals, LLC
To contact the Publisher's Office, please email: publisher@impactjournals.com, visit www.impactjournals.com, or call 1-800-922-0957

Aging (ISSN: 1945 - 4589) is published monthly by Impact Journals LLC
6666 East Quaker St., Suite 1b Orchard Park, NY 14127

Abstracted and/or indexed in: PubMed/Medline (abbreviated as Aging (Albany NY)), PubMed Central , ISI/Web of Science/Thomson Reuters (abbreviated as Aging-US and listed in the cell biology category), and Scopus /Rank Q1 (abbreviated as Aging)

ONLINE ISSN: 1945-4589

AGING

www.aging-us.com

EDITORIAL BOARD

EDITORIAL BOARD

Table of Contents

Effects of dietary restriction on adipose mass and biomarkers of healthy aging in human 1
Originally published in Volume 8, Issue 12 pp 3341—3355

Long-term moderate calorie restriction inhibits inflammation without impairing cell-mediated immunity: a randomized controlled trial in non-obese humans 16
Originally published Volume 8, Issue 7 pp 1416—1431

Measuring aging rates of mice subjected to caloric restriction and genetic disruption of growth hormone signaling 32
Originally published Volume 8, Issue 3 pp 539—546

Metabolic effects of a 13-weeks lifestyle intervention in older adults: The Growing Old Together Study 40
Originally published Volume 8, Issue 1 pp 111—126

Caloric restriction induces heat shock response and inhibits B16F10 cell tumorigenesis both in vitro and in vivo 54
Originally published Volume 7, Issue 4 pp 233—240

Serum from calorie-restricted animals delays senescence and extends the lifespan of normal human fibroblasts in vitro 61
Originally published Volume 7, Issue 3 pp 152—166

Target of rapamycin signalling mediates the lifespan-extending effects of dietary restriction by essential amino acid alteration 76
Originally published Volume 6, Issue 5 pp 390—398

Multiple dietary supplements do not affect metabolic and cardiovascular health 85
Originally published Volume 6, Issue 2 pp 149—157

Using PDE inhibitors to harness the benefits of calorie restriction: lessons from resveratrol 94
Originally published Volume 4, Issue 3 pp 144—145

Long-term calorie restriction, but not endurance exercise, lowers core body temperature in humans 96
Originally published Volume 3, Issue 4 pp 374—379

Adult-onset, short-term dietary restriction reduces cell senescence in mice 102
Originally published Volume 2, Issue 9 pp 555—566

Diet and exercise signals regulate SIRT3 and activate AMPK and PGC-1α in skeletal muscle 114
Originally published Volume 1, Issue 9 pp 771—783

Research Paper

Effects of dietary restriction on adipose mass and biomarkers of healthy aging in human

Daniele Lettieri-Barbato[1], Esmeralda Giovannetti[1], Katia Aquilano[1,2]

[1]Department of Biology, University of Rome Tor Vergata, Rome, Italy
[2]IRCCS San Raffaele La Pisana, Rome, Italy

Correspondence to: Daniele Lettieri-Barbato; **email:** d.lettieribarbato@hotmail.it
Keywords: adipose tissue, aging, calorie restriction, fasting, biomarkers, human, longevity **doi:** 10.18632/aging.101122
Received: October 3, 2016 **Accepted:** November 16, 2016 **Published:** November 29, 2016

ABSTRACT

In developing countries the rise of obesity and obesity-related metabolic disorders, such as cardiovascular diseases and type 2 diabetes, reflects the changes in lifestyle habits and wrong dietary choices. Dietary restriction (DR) regimens have been shown to extend health span and lifespan in many animal models including primates. Identifying biomarkers predictive of clinical benefits of treatment is one of the primary goals of precision medicine. To monitor the clinical outcomes of DR interventions in humans, several biomarkers are commonly adopted. However, a validated link between the behaviors of such biomarkers and DR effects is lacking at present time. Through a systematic analysis of human intervention studies, we evaluated the effect size of DR (i.e. calorie restriction, very low calorie diet, intermittent fasting, alternate day fasting) on health-related biomarkers. We found that DR is effective in reducing total and visceral adipose mass and improving inflammatory cytokines profile and adiponectin/leptin ratio. By analysing the levels of canonical biomarkers of healthy aging, we also validated the changes of insulin, IGF-1 and IGFBP-1,2 to monitor DR effects. Collectively, we developed a useful platform to evaluate the human responses to dietary regimens low in calories.

INTRODUCTION

Aging and wrong lifestyle choices, including inadequate dietary patterns, increase the risk of developing several diseases such as obesity and its-related chronic degenerative diseases. Interestingly, the aging program can be accelerated by obesity [1]. It is thus likely that obesity reduces life- and health span and plays a predominant role in the onset of age-related diseases [2]. In fact, the prevalence of obesity is globally increasing in populations and has become a burden for healthcare systems. Several studies suggest that dietary restriction (DR) regimens (e.g. intermittent fasting, calorie restriction, low calorie diet) reverse obesity and improve health in human by promoting the same molecular and metabolic adaptations that have been shown in animal models of longevity. In particular, DR in humans ameliorates several metabolic and hormonal factors that are implicated in the pathogenesis of an array of age-associated chronic metabolic diseases [3, 4].

At present it is difficult to evaluate the effectiveness of DR on lifespan in humans, so that several works proposed predictive non-invasive biomarkers to evaluate the geroprotective role of DR. However, a miscellaneous of biomarkers is investigated in human intervention studies limiting the statistical robustness of the data. Whether a "biomarker-based" approach could be suitable for evaluating the effectiveness of DR still remains a matter of debate.

Precision medicine is a medical model that proposes the customization of healthcare, with the identification of predictors that can help to find the effectiveness of health-promoting dietary interventions. Biomarkers represent potentially predictive tools for precision medicine but, although affordable 'omics'-based technology has enabled faster identification of putative biomarkers [5], their validation is still hindered by low statistical power as well as limited reproducibility of results.

Herein, through meta-analysis we have evaluated the effect size of DR regimens on adipose mass and well-recognized biomarkers of healthy aging. Overall findings provide the geroprotective footprint of DR in humans and highlight a useful platform to validate or monitor the efficiency of dietary treatments to preserve and improve health span and longevity.

RESULTS

Effects of DR on total and visceral adipose mass

DR regimens are effective in slowing aging, and maintaining healthy status in animals [6, 7]. Adipose mass quickly and dynamically responds to nutrient/

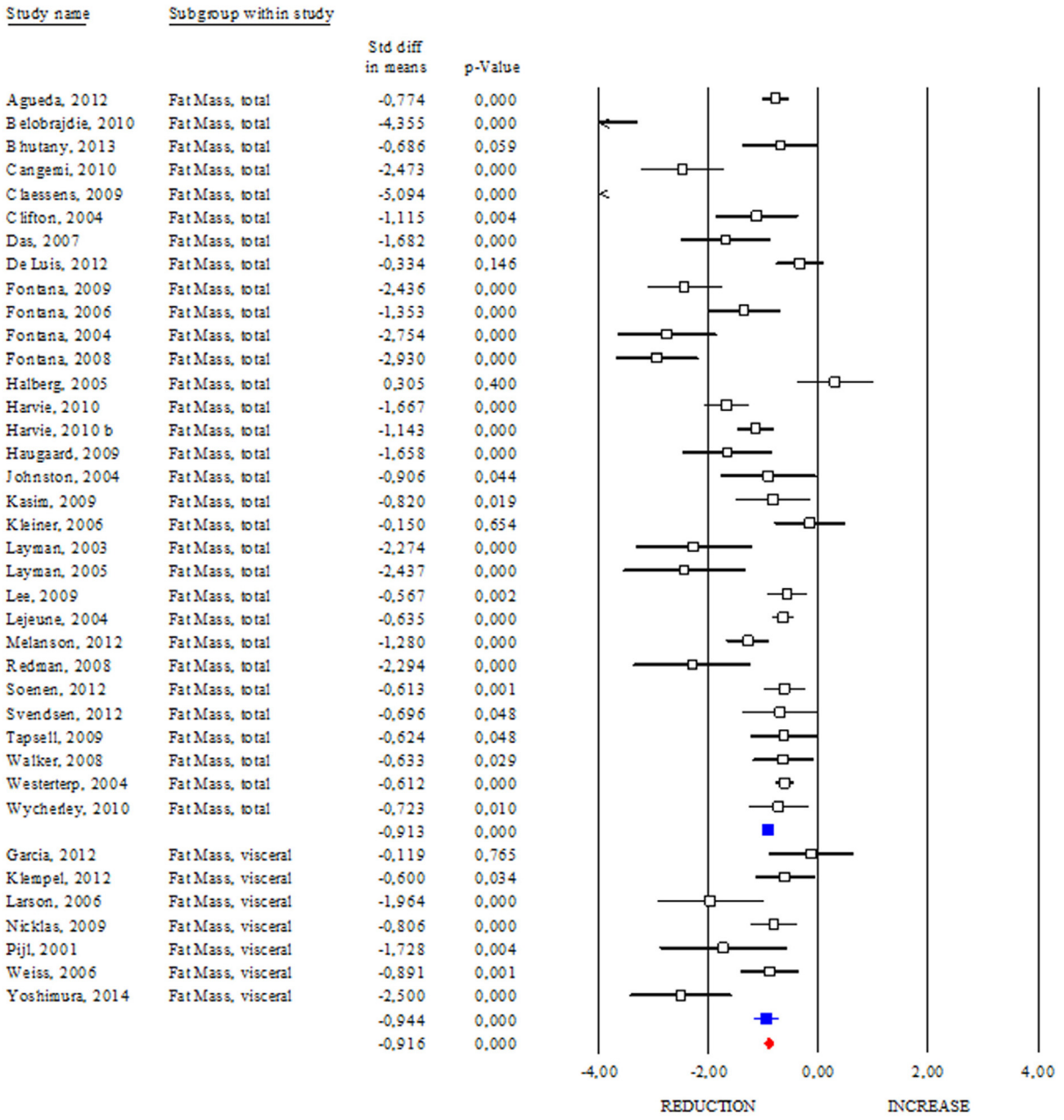

Figure 1. Changes of total and visceral adipose mass after DR. Studies were stratified according to the design of the study. A positive standardized difference in mean (SDM) indicates an increase, whereas a negative SDM indicates the decrease of fat mass (total or visceral). The empty black square indicates the results of each study, whereas empty blu square shows the summary results of each subgroup data. The red diamond resumes overall results of the included studies in the forest plot.

energy fluctuation and its remodelling seems to mediate the beneficial effects of DR [7]. In this section we evaluated the effects of DR on adipose mass (Fig. 1). Interestingly, all studies showed clear evidence on the efficacy of DR in reducing total adipose mass in human (SDM -0.913; 95% CI -0.994, -0.832; p<0.000). Interestingly, we detected higher effectiveness of DR in healthy than unhealthy subjects (SDM -1.843; 95% CI -2.144, -1.542 p<0.000 and SDM -0.813; 95% CI -0.897, -0.728 p<0.000, respectively). Our data reveal that DR was also effective in reducing visceral fat mass (SDM -0.944; 95% CI -1.187, -0.700; p<0.000) (Fig. 1) and identify adipose mass measurement as a feasible approach to evaluate the efficacy of diets low in calories.

Effects of DR on adipokines and DHEA

Among adipokines, adiponectin has an anti-inflammatory function and correlates with healthy metabolic profile. Reduction of adiponectin production is often revealed in obese and diabetic subjects [8]. These evidences highlight adiponectin as a good candidate to monitor healthy status in human. However, conflicting results emerge from circulating adiponectin levels in centenarians [9, 10]. Herein we determined changes of adiponectin levels occurring after DR. As shown in Fig. 2, DR increased adiponectin levels in human (SDM 0.427; 95% CI 0.243, 0.612; p<0.000) independently of healthy status (healthy group: SDM 0.947; 95% CI 0.395, 1.499 p<0.001 and unhealthy group: SDM 0.370; 95% CI 0.155, 0.585 p<0.001). The "satiety hormone" leptin controls dietary behaviour and has been strongly associated with adipose mass. Indeed, reduced leptin levels are associated with diminished visceral adipose mass. However, unclear are evidences about its levels in healthy centenarians [9, 10]. Our data reveal that leptin levels were significantly reduced in DR group (SDM -1.383; 95% CI -1.511, -1.255; P<0.000) (Fig. 3).

The hormonal profile of aging includes a marked decrease in the adrenal hormone dehydroepiandrosterone (DHEA) [11]. DHEA is taken up by adipose tissue and seems to reduce its mass protecting against obesity [12]. Epidemiologic data in the elderly cohort of long-living Okinawans (over 65) show relatively high plasma DHEA levels at older ages than the aged-matched counterpart [13]. However, as disclosed in Suppl. Fig. 1, DHEA levels were unchanged after DR (SDM 0.149; 95% CI -0.342, 0.641 p 0.551). Overall findings suggest a tight relationship between changes in circulating adipokines and reduction of adipose mass occurring after DR. Differently, DHEA modulation seems to be independent of calorie intake.

Effects of DR on insulin, IGF-1, HOMA Index and IGBPs

Insulin and insulin growth factors 1 (IGF-1) signalling is an evolutionary conserved pathway linking nutrient levels to fat mass and lifespan. Generally, reduced level

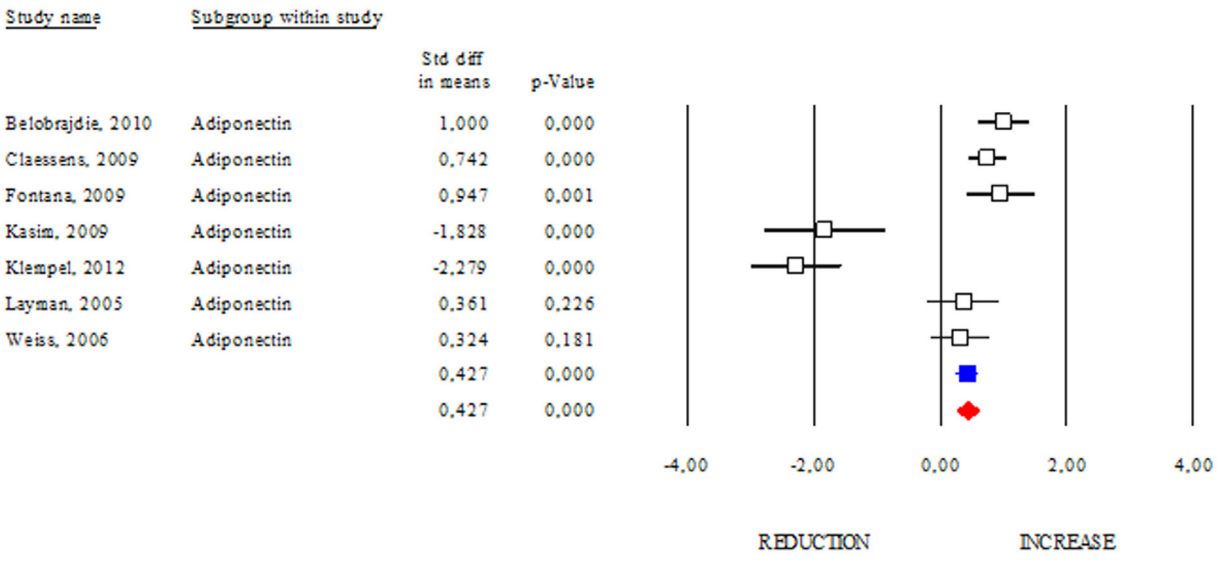

Figure 2. DR effects on circulating adiponectin. Studies were stratified according to the design of the study. A positive standardized difference in mean (SDM) indicates an increase, whereas a negative SDM indicates the decrease of circulating adiponectin. The empty black square indicates the results of each study, whereas empty blu square shows the summary results of each subgroup data. The red diamond resumes overall results of the included studies in the forest plot.

of insulin and IGF-1 is associated with increased longevity from yeasts to mammals [14]. Differently, levels of insulin and IGF-1 are commonly higher in subjects affected by age-related diseases or obesity than lean healthy subjects [15]. In our work, we reported clear evidence about DR effects on insulin and IGF-1 levels in human (Fig. 4). In particular, we observed a significant reduction in insulin both in healthy (SDM -1.019; 95% CI -1.362, -0.675 p<0.000) and unhealthy subjects (SDM -0.811; 95% CI -0.893, -0.730 p<0.000). The same trend was detected by analysing the IGF-1 levels (SDM -0.546; 95% CI -0.750, -0.342 p<0.000). Overall data analyses (SDM -0.779; 95% CI -0.851, -0.706 p<0.000) confirm decreased insulin/IGF-1 levels as downstream effect of DR in human.

The Homeostasis Model Assessment (HOMA) Index is currently a biochemical tool to estimate insulin sensitivity by matching fasting glycaemia and insulinemia [16]. A study carried out on centenarians indicates that they seem to be protected from hyper-insulinaemia, and their insulin resistance is as low, if not lower, than that of healthy younger adults [17]. The correlation between HOMA Index with obesity or aging suggests its prognostic capacity to evaluate the efficacy of health promoting strategies. Accordingly, we reported a significant reduction in the HOMA Index occurring after DR (SDM -0.837; 95% CI -0.990, -0.750 p<0.000) (Fig. 5) and this effect was stronger if dietary treatment was longer than 3 months (data not shown).

The IGF-binding protein 2 (IGFBP2) is known as a carrier protein for IGF-1 limiting its biological action [18]. However, there are several characterized IGFBPs, which seem to improve metabolic status independently of IGFs binding [19]. Interestingly, some papers reported that DR regimens increase circulating levels of IGFBPs [20]. In our work, we analysed the changes in the levels of the best-known IGFBPs after DR. As shown in Fig. 6, DR similarly modulated IGFBP-1 and IGFBP-2 levels (SDM 1.527; 95% CI 1.248, 1.806 p<0.000 and SDM 1.687; 95% CI 1.387, 1.986 p<0.000, respectively). Differently, DR was ineffective in increasing IGFBP-3 levels (SDM -0.045; 95% CI -0.517, 0.427 p=0.853). These results suggest that IGFBP-1 and -2 are more sensitive to DR than IGFBP-3.

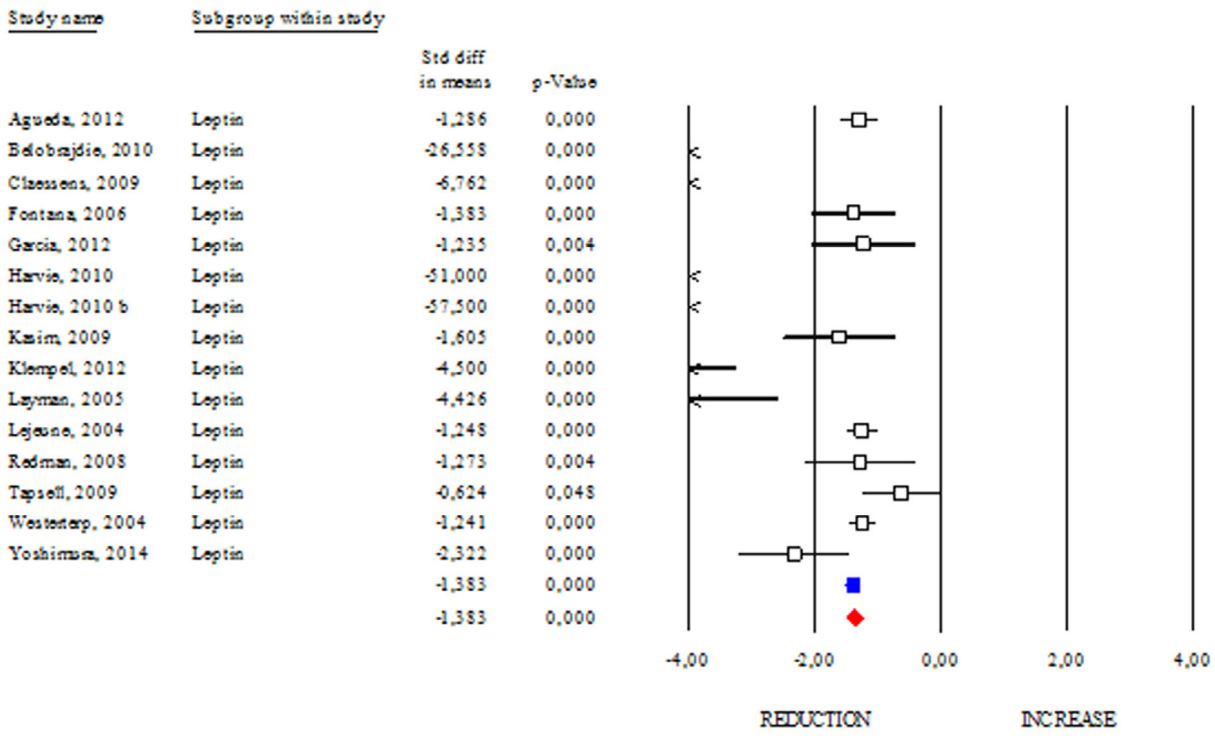

Figure 3. DR effects on circulating leptin. Studies were stratified according to the design of the study. A positive standardized difference in mean (SDM) indicates an increase, whereas a negative SDM indicates the decrease of circulating leptin. The empty black square indicates the results of each study. The red diamond resumes overall results of the included studies in the forest plot.

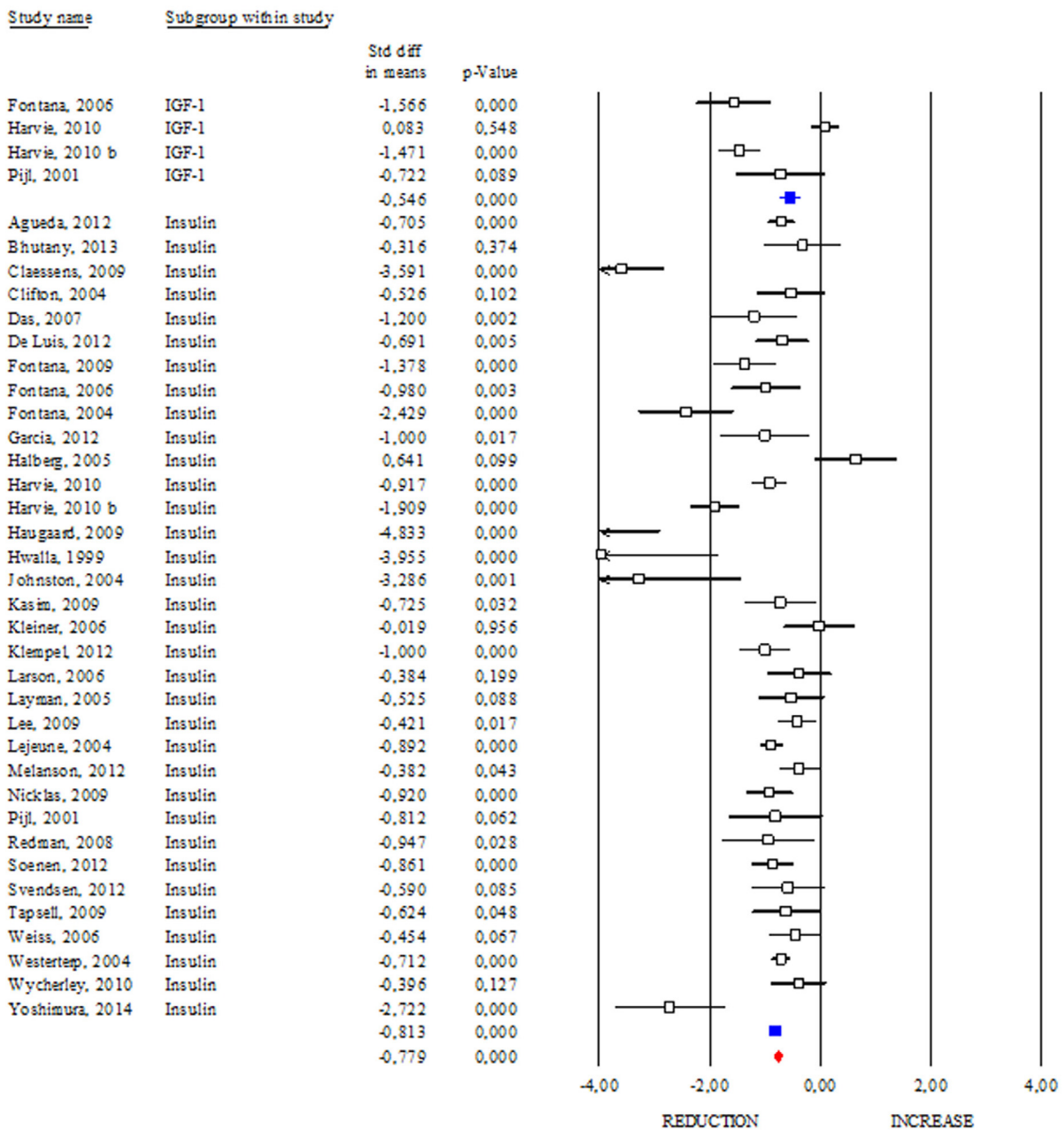

Figure 4. Changes of circulating insulin and insulin growth factor-1 (IGF-1) after DR. Studies were stratified according to the design of the study. A positive standardized difference in mean (SDM) indicates an increase, whereas a negative SDM indicates the decrease of circulating IGF-1 or insulin. The empty black square indicates the results of each study, whereas empty blu square shows the summary results of each subgroup data. The red diamond resumes overall results of the included studies in the forest plot.

Effects of DR on inflammatory markers

One of the common features of aging and obesity is the presence of a chronic sterile low-grade inflammatory status, which contributes to the onset of several metabolic perturbations [21]. In our work we evaluated the changes in circulating inflammatory markers observed after DR (Fig. 7). Interestingly, among the evaluated inflammatory markers, only CRP and IL-6 displayed a significant reduction after DR (SDM -0.715; 95% CI -0.862, -0.568 $p<0.000$ and SDM -0.316; 95% CI -0.515, -0.118 $p<0.002$, respectively). Although IL-1 and TNF-α are cytokines routinely assayed to monitor systemic inflammation, our data revealed that their level

remained unchanged after DR (SDM 0.041; 95% CI -.181, 0.263 p=0.719 and SDM -0.079; 95% CI -0.264, 0.106 p=0.402, respectively). Overall data regarding CRP, IL-6, IL-1 and TNF-α levels revealed anti-inflammatory effect of DR in human (SDM -0.351; 95% CI -0.442, -0.260 p<0.000) (Fig. 7).

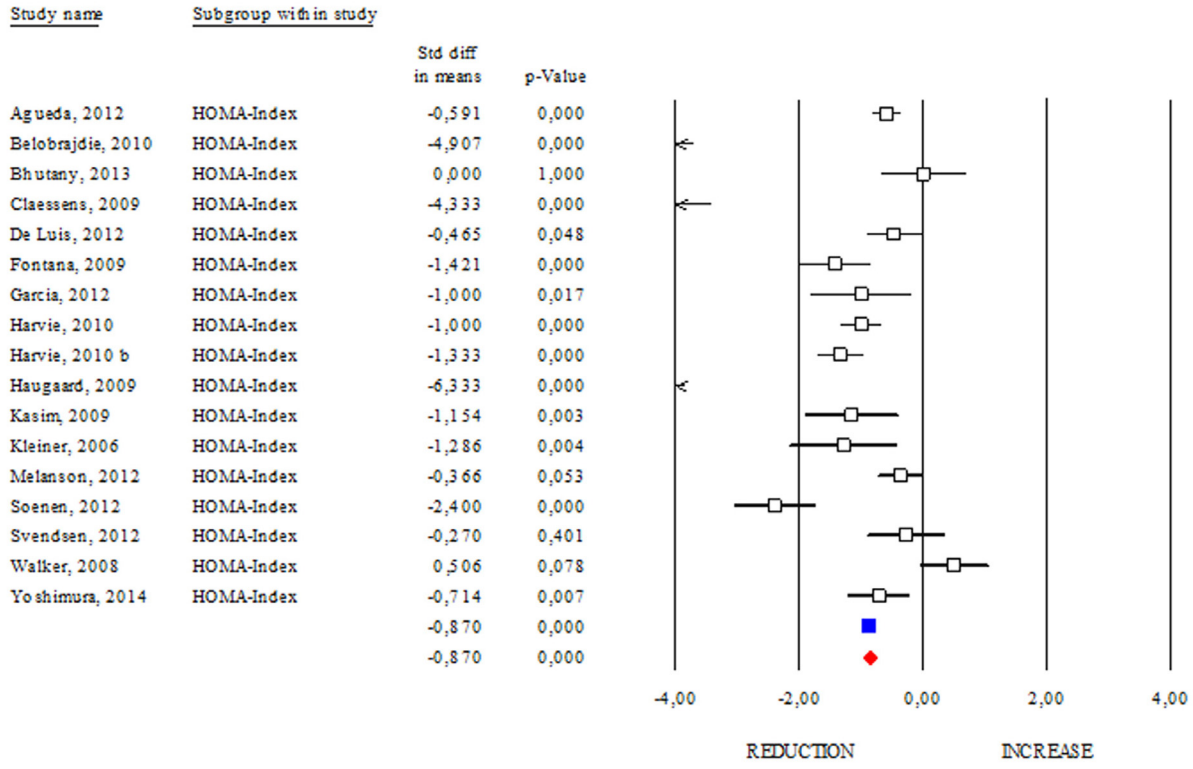

Figure 5. Changes of HOMA Index after DR. Studies were stratified according to the design of the study. A positive standardized difference in mean (SDM) indicates an increase, whereas a negative SDM indicates the decrease of HOMA Index. The empty black square indicates the results of each study. The red diamond resumes overall results of the included studies in the forest plot.

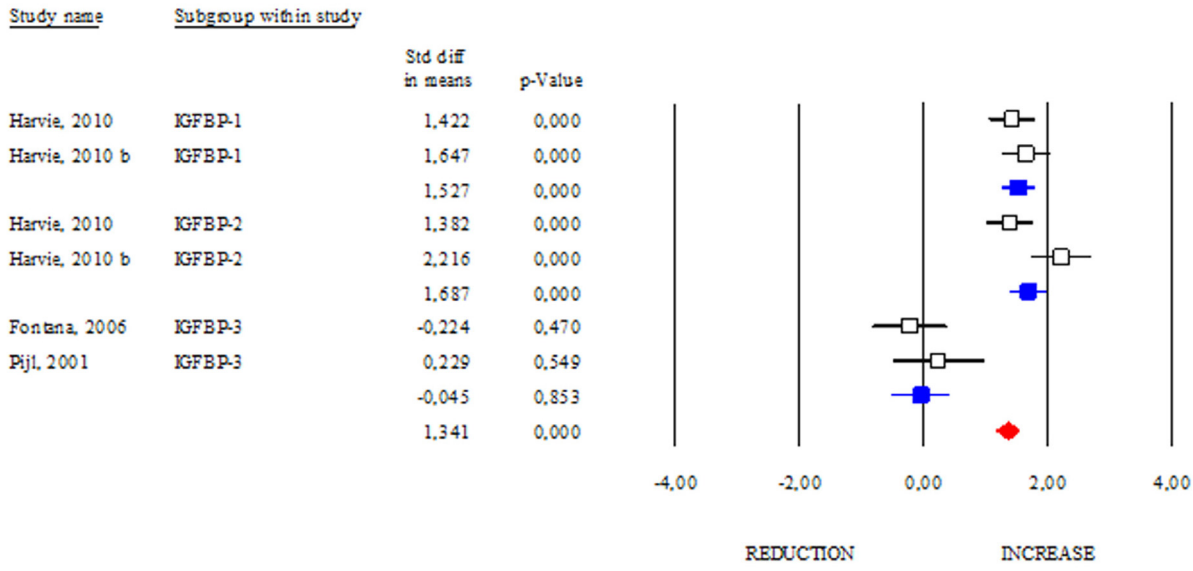

Figure 6. Changes of circulating IGFB-1, IGFBP-2 and IGFBP-3 after DR. Studies were stratified according to the design of the study. A standardized difference in mean (SDM) indicates an increase, whereas a negative SDM indicates the decrease of IGFB-1, IGFBP-2 or IGFBP-3. The empty black square indicates the results of each study, whereas empty blu square shows the summary results of each subgroup data. The red diamond resumes overall results of the included studies in the forest plot.

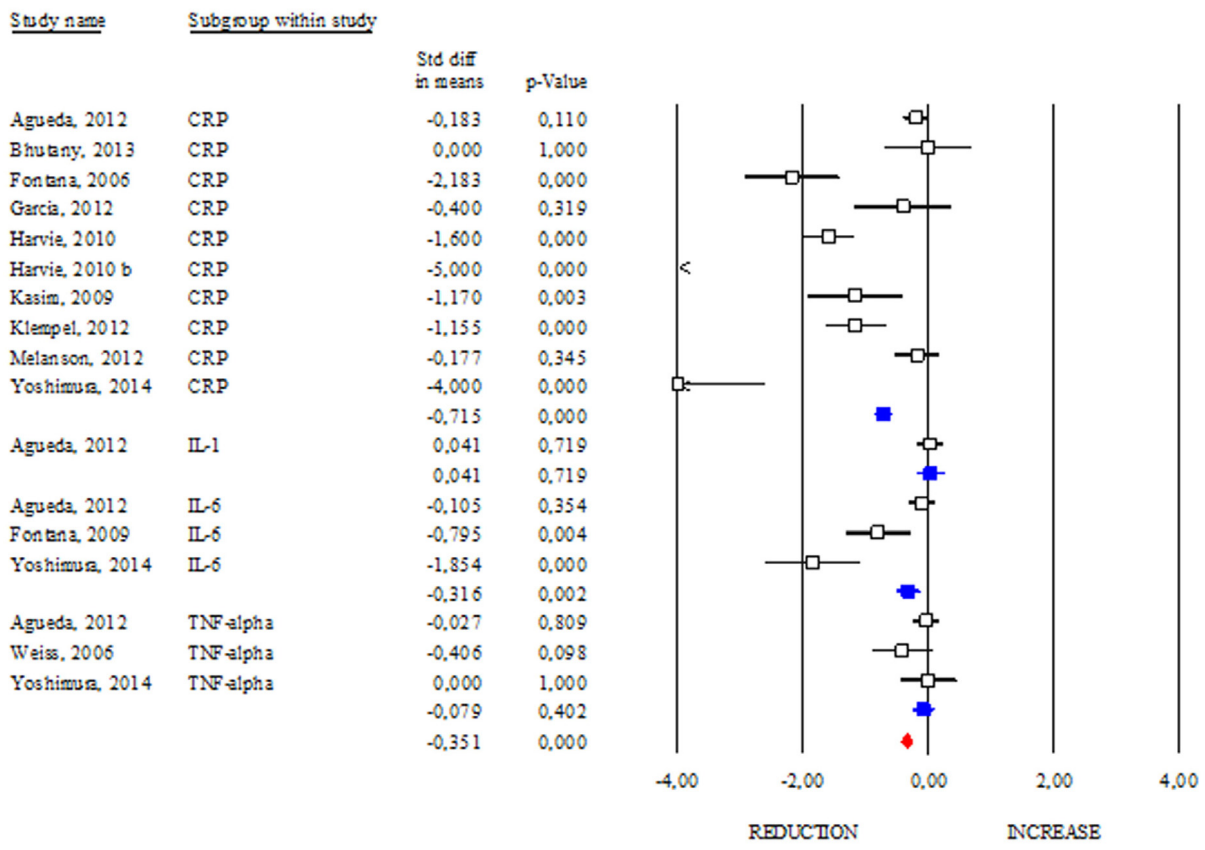

Figure 7. Changes of inflammatory markers after DR. Studies were stratified according to the design of the study. A positive standardized difference in mean (SDM) indicates an increase, whereas a negative SDM indicates the decrease of CRP, IL-1, IL-6 or TNF-alpha. The empty black square indicates the results of each study, whereas empty blu square shows the summary results of each subgroup data. The red diamond resumes overall results of the included studies in the forest plot.

DISCUSSION

Aging is commonly defined as a physiological decline of biological functions in the body. Aging strongly remodels adipose depots by reducing subcutaneous adipose in favour of visceral depots enlargement [22]. Aging and visceral adipose tissue expansion act in synergy in inducing a chronic low grade of inflammatory status, which triggers a systemic metabolic decline in human [21, 23]. DR is a promising and feasible strategy that ameliorates body metabolic and inflammatory profile increasing lifespan through evolutionary-conserved mechanisms [4, 22, 24, 25]. Herein we included all studies evaluating the impact of DR on several healthy-associated markers in human including adipose mass. Increased visceral adiposity leads to chronic inflammation, which is often associated with a number of comorbidities (e.g. hyperinsulinemia, hypertension, insulin resistance, glucose intolerance) and reduced life expectancy [26, 27]. Through this meta-analysis approach, we confirmed the capacity of DR to reduce total and visceral adipose mass and, interestingly, we observed a more effective visceral adipose mass reduction after DR regimens (-20% in DR: SDM -1.081; 95% CI -1.242, -0.921 p<0.000) (-30/40% in DR: SDM -0.893; 95% CI -1.050, -0.737 p<0.000 and >-40% in DR: SDM -0.678; 95% CI -0.800, -0.555 p<0.000). These findings suggest that to obtain a more effective adipose mass loss, 20% in calorie reduction could be an elective strategy. Central or visceral adiposity perturbs systemic inflammation in animal models and human and relatively to this, the healthy effects of DR could be mediated by visceral adiposity reduction. Indeed, DR significantly diminished the markers of inflammation, highlighting the central role of DR-mediated adipose tissue remodelling in improving inflammatory profile in human. Furthermore, DR also increased adiponectin/leptin ratio, which is commonly associated with ameliorated insulin sensitivity in human. In line with this effect, we demonstrated that DR was successful in reducing insulin, IGF-1 and HOMA index.

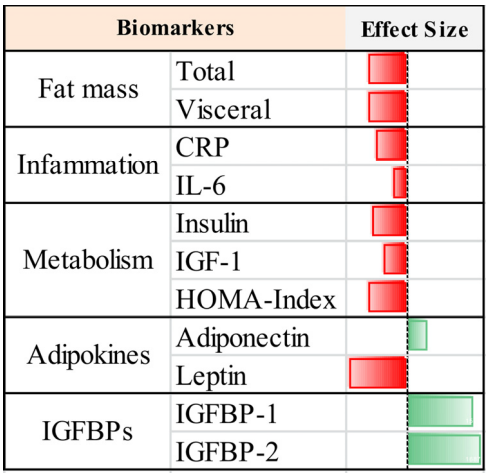

Figure 8. Geroprotective footprint of dietary restriction.

subgroups because it was difficult to collect a good number of subjects.

In conclusion, by a meta-analysis approach we have provided evidences about DR efficiency on key hallmarks of aging (Fig. 8) and built a useful platform to evaluate the responses of human to dietary regimens low in calories (Fig. 9).

MATERIALS AND METHODS

Search strategy and included studies

In our work we analysed human intervention studies and evaluated the impact of DR regimens on adipose mass and some biomarkers of healthy aging (*Geromarkers*). The *Geromarkers* included in our meta-analysis were described in Table 1. Two investigators,

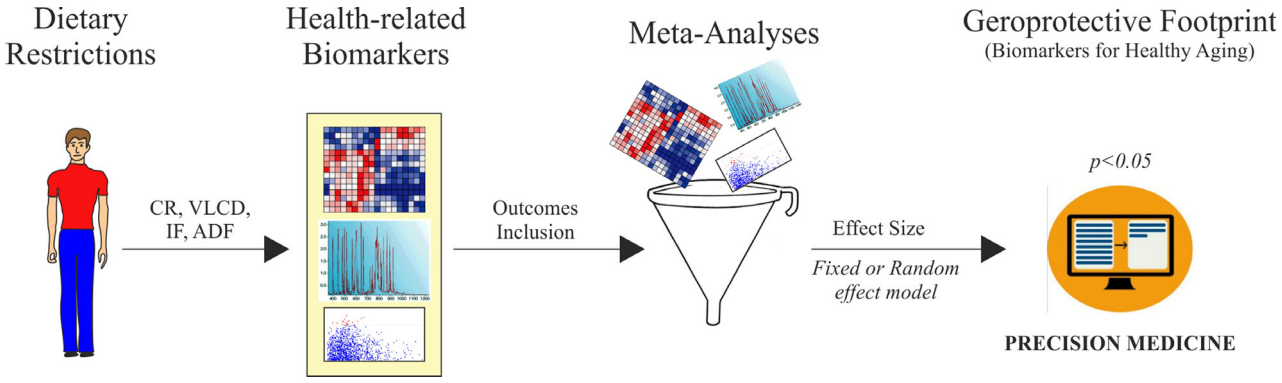

Figure 9. Algorithm development for biomarkers validation of dietary restriction in human. CR: calorie restriction; VLCD: very low calorie diet; IF: intermittent fasting; ADF: alternate-day-fasting.

The insulin growth factor binding proteins (IGFBPs) are a family of proteins that bind to insulin-like growth factors limiting their biological actions [28]. IGFBP-2 is the most abundant among circulating IGFBPs and its anti-diabetic role as well as direct ability to limit adipogenesis has been demonstrated [29, 30]. Actually, high serum levels of IGFBP-2 appear to protect against obesity and type 2 diabetes [30]. IGFBP-1 showed an inverse relation with insulin and BMI in human [31]. Differently, unclear are the evidences about the link between IGFBP-3 and adipose mass. In accordance with the data described above, we observed a strong responsiveness in circulating levels of IGFBP-1 and -2 occurring after DR. However some limitations emerge from this meta-analysis. In particular, statistical analyses on IL-1 and IGFBPs were carried out only evaluating the results obtained from few studies [32-35]. Moreover, it was not possible to evaluate the efficiency of DR in gender or time of treatment

E.G. and D.L.B., independently carried out study selection and included both studies with an experimental design (EXP) and quasi-experimental design (Q-EXP). EXP studies were randomized with a control group and a parallel or crossover design; whereas Q-EXP included observational studies (pre- and post-intervention or pre- and post-data), non-randomized or uncontrolled studies [36]. Q-EXP studies were pooled together with EXP studies only after assessing whether they were in agreement with EXP studies [37]. Candidate studies were searched in PubMed (finalized February 30, 2016) using the terms 'calorie or caloric or dietary restriction', 'fasting or intermittent fasting or alternate day fasting and 'adipose tissue or fat mass or fat tissue''. Inclusion criteria were as follows: human intervention studies with long-term study design (> 3 months); healthy and unhealthy (e.g. dyslipidaemia, obesity, metabolic syndrome) subjects; numerically analysable information about results, study

duration and calories reduced in the study. Studies were excluded when: only abstracts were available; duration time of the study was lesser than 3 months; data presentation was incomplete; information about the DR was incomplete. When necessary, efforts were made to contact investigators for clarification or additional data. This research strategy produced a total of 201 studies. Furthermore, a manual research of references from clinical studies and reviews identified 42 additional studies, for a total of 243 studies to be evaluated, 9 of which are reviews [38-46]. A first screening allowed discarding 147 articles whose titles or abstracts were evidently irrelevant to our aim. Of the remaining 96 studies, 53 were rejected whenever: they presented incomplete data; DR was coupled with physical exercise; there were no reported data on adipose mass; they only presented data on weight and fat mass without other parameters (Fig. 10). Therefore, from 243 initial candidates, the 43 studies available for a formal meta-analysis had the following charac-teristics: they were written in English; they had a period of intervention of at least two weeks; they were carried out exclusively on human subjects. Among the considered studies, 12 were on females [32, 34, 35, 47-55], 4 on males [56-59], and the rest mixed [60-62, 33, 63-85]. Moreover, 30 studies were intervention studies evaluating the efficacy of calorie restriction [33-35, 47-49, 51-53, 56, 58-60, 63-67, 69, 71-73, 75, 76, 79-82, 84, 85]; 4 were intervention studies evaluating the efficacy of intermittent fasting [50, 57, 61, 70]; 9 were intervention studies evaluating the efficacy of low or very low calorie diets [32, 54, 55, 62, 68, 74, 77, 78, 83]. The selected studies included human groups with different BMI. In particular, 10 were studies on obese [34, 35, 48, 50, 53, 54, 58, 61, 64, 68], 16 on overweight [51, 52, 57, 59, 62, 63, 65, 69, 71-73, 77-79, 82, 85], 12 on both obese and overweight [32, 47, 49, 55, 60, 62, 74, 75, 80, 81, 83, 84], 5 on both normal weight and over-

Table 1. Selected biomarkers and number of the studies included in meta-analysis.

Biomarkers	n. of the studies
Fat Mass (total and visceral)	38
Adipokines (adiponectin and leptin)	22
IGFBPs (IGFBP-1, -2, -3)	6
IGF-1	4
HOMA-Index	17
Insulin	34
Inflammation (TNFa, IL-1, IL-6, CRP)	17
DHEA	5

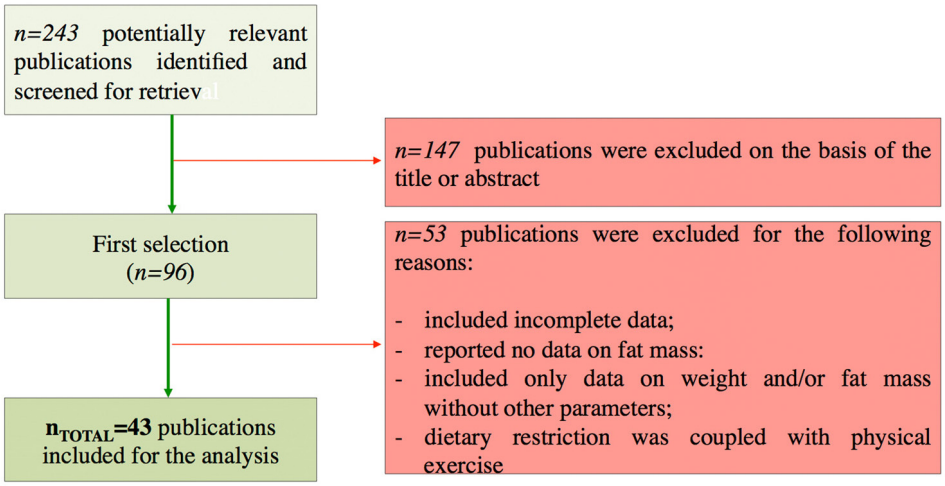

Figure 10. Flow chart of the study identification and selection.

weight [33, 66, 67, 70, 76]. Finally, the studies were on healthy subjects, with the exception of few articles in which subjects were affected by the following pathologies: chronic osteoarthritis [64]; metabolic syndrome [59]; hyperinsulinemia [58, 72], polycystic ovary syndrome [49], type 2 diabetes [84]. Hence, the meta-analysis was based on 43 studies and analysed a total of 2094 subjects. Before analyses, all studies were stratified for gender, healthy status, time of treatment and percentage of calorie reduction and the main characteristics of the included studies were reported in Table 2. Calorie restriction, intermittent or alternate-day-fasting and low calorie diet interventions were overall grouped in dietary restriction (DR) category.

Table 2. Characteristics of the included studies for the meta-analyses.

Study Design				Gender Stratification		Healthy Status Stratification		Time of Treatment	
Unrandomized	Randomized or Controlled	Randomized and Controlled	Cross-Sectional	Yes	No	Yes	No	Brief (<3 months)	Long-Term (>3 months)
4	**14**	**23**	**2**	**16**	**27**	**36**	**2**	**26**	**16**

Data analysis

Relevant data of the 43 studies available were entered for formal meta-analytic evaluation into the Comprehensive Meta-Analysis software (Biostat) [86]. Data analysis was performed as previously described [87]. In particular, for the results showed as post-data only, we selected mean, standard deviation and sample size in each group, or difference in means, sample size and p value between groups. When results were reported as pre- and post-data, we used mean, standard deviation, sample size in each group and correlation between baseline and end-point intervention period, or mean change, standard deviation difference, sample size in each group, correlation between baseline and end-point intervention period. For observational studies considering only one group (pre–post-intervention data), we used mean difference, standard deviation of difference and sample size. In all studies, we assumed the correlation between baseline and end-point study period to be 0.5 to produce the most conservative estimate [37, 88]. To enable a joint comparison, the standardized difference in mean (SDM) was calculated for each outcome. In our analysis, positive SDM indicates increased effect size of DR on outcome considered. The effect sizes of the included studies were pooled both under a 'fixed effects model' or 'random effects model'. Under fixed effects model we assumed that the true effect is the same in all studies. By contrast, under the random effects model we allowed that the true effect may vary from one study to the next [37]. Fixed or random effect model was selected following evaluation of heterogeneity between studies based on the I^2 test for heterogeneity. When I^2 values were low, we selected a fixed effects model, whereas random effects model was selected for I^2 values higher than 75%.

CONFLICTS OF INTEREST

The authors declare no conflict of interests.

FUNDING

This work was supported by "Uncovering Excellence" – University of Rome Tor Vergata and Ministero della Salute (GR-2011-02348047).

REFERENCES

1. Horvath S, Erhart W, Brosch M, Ammerpohl O, von Schönfels W, Ahrens M, Heits N, Bell JT, Tsai PC, Spector TD, Deloukas P, Siebert R, Sipos B, et al. Obesity accelerates epigenetic aging of human liver. Proc Natl Acad Sci USA. 2014; 111:15538–43. doi: 10.1073/pnas.1412759111

2. Tchkonia T, Morbeck DE, Von Zglinicki T, Van Deursen J, Lustgarten J, Scrable H, Khosla S, Jensen MD, Kirkland JL. Fat tissue, aging, and cellular senescence. Aging Cell. 2010; 9:667–84. doi: 10.1111/j.1474-9726.2010.00608.x

3. Al-Regaiey KA. The effects of calorie restriction on aging: a brief review. Eur Rev Med Pharmacol Sci. 2016; 20:2468–73.

4. Most J, Tosti V, Redman LM, Fontana L. Calorie restriction in humans: an update. Ageing Res Rev. 2016S1568-1637(16)30183-0.

5. Pearson ER. Personalized medicine in diabetes: the role of 'omics' and biomarkers. Diabet Med. 2016; 33:712–17. doi: 10.1111/dme.13075

6. Wiesenborn DS, Menon V, Zhi X, Do A, Gesing A, Wang Z, Bartke A, Altomare DA, Masternak MM. The effect of calorie restriction on insulin signaling in skeletal muscle and adipose tissue of Ames dwarf mice. Aging (Albany NY). 2014; 6:900–12.

doi: 10.18632/aging.100700

7. Lettieri Barbato D, Tatulli G, Aquilano K, Ciriolo MR. Erratum: mitochondrial Hormesis links nutrient restriction to improved metabolism in fat cell. Aging (Albany NY). 2016; 8:1571. doi: 10.18632/aging.101003

8. Ghoshal K, Bhattacharyya M. Adiponectin: probe of the molecular paradigm associating diabetes and obesity. World J Diabetes. 2015; 6:151–66. doi: 10.4239/wjd.v6.i1.151

9. Pareja-Galeano H, Santos-Lozano A, Sanchis-Gomar F, Fiuza-Luces C, Garatachea N, Gálvez BG, Lucia A, Emanuele E. Circulating leptin and adiponectin concentrations in healthy exceptional longevity. Mech Ageing Dev. 2016S0047-6374(16)30019-7.

10. Meazza C, Vitale G, Pagani S, Castaldi D, Ogliari G, Mari D, Laarej K, Tinelli C, Bozzola M. Common adipokine features of neonates and centenarians. J Pediatr Endocrinol Metab. 2011; 24:953–57. doi: 10.1515/JPEM.2011.373

11. Samaras N, Samaras D, Frangos E, Forster A, Philippe J. A review of age-related dehydroepiandrosterone decline and its association with well-known geriatric syndromes: is treatment beneficial? Rejuvenation Res. 2013; 16:285–94. doi: 10.1089/rej.2013.1425

12. Karbowska J, Kochan Z. Effects of DHEA on metabolic and endocrine functions of adipose tissue. Horm Mol Biol Clin Investig. 2013; 14:65–74. doi: 10.1515/hmbci-2013-0009

13. Willcox BJ, Willcox DC, Todoriki H, Fujiyoshi A, Yano K, He Q, Curb JD, Suzuki M. Caloric restriction, the traditional Okinawan diet, and healthy aging: the diet of the world's longest-lived people and its potential impact on morbidity and life span. Ann N Y Acad Sci. 2007; 1114:434–55. doi: 10.1196/annals.1396.037

14. Parrella E, Longo VD. Insulin/IGF-I and related signaling pathways regulate aging in nondividing cells: from yeast to the mammalian brain. Sci World J. 2010; 10:161–77. doi: 10.1100/tsw.2010.8

15. Balasubramanian P, Longo VD. Growth factors, aging and age-related diseases. Growth Horm IGF Res. 2016; 28:66–68. doi: 10.1016/j.ghir.2016.01.001

16. Wallace TM, Levy JC, Matthews DR. Use and abuse of HOMA modeling. Diabetes Care. 2004; 27:1487–95. doi: 10.2337/diacare.27.6.1487

17. Curtis R, Geesaman BJ, DiStefano PS. Ageing and metabolism: drug discovery opportunities. Nat Rev Drug Discov. 2005; 4:569–80. doi: 10.1038/nrd1777

18. Kang HS, Kim MY, Kim SJ, Lee JH, Kim YD, Seo YK, Bae JH, Oh GT, Song DK, Ahn YH, Im SS. Regulation of IGFBP-2 expression during fasting. Biochem J. 2015; 467:453–60. doi: 10.1042/BJ20141248

19. Oh Y. IGF-independent regulation of breast cancer growth by IGF binding proteins. Breast Cancer Res Treat. 1998; 47:283–93. doi: 10.1023/A:1005911319432

20. Levine ME, Suarez JA, Brandhorst S, Balasubramanian P, Cheng CW, Madia F, Fontana L, Mirisola MG, Guevara-Aguirre J, Wan J, Passarino G, Kennedy BK, Wei M, et al. Low protein intake is associated with a major reduction in IGF-1, cancer, and overall mortality in the 65 and younger but not older population. Cell Metab. 2014; 19:407–17. doi: 10.1016/j.cmet.2014.02.006

21. Goldberg EL, Dixit VD. Drivers of age-related inflammation and strategies for healthspan extension. Immunol Rev. 2015; 265:63–74. doi: 10.1111/imr.12295

22. Lettieri Barbato D, Aquilano K. Feast and famine: adipose tissue adaptations for healthy aging. Ageing Res Rev. 2016; 28:85–93. doi: 10.1016/j.arr.2016.05.007

23. Minamino T, Orimo M, Shimizu I, Kunieda T, Yokoyama M, Ito T, Nojima A, Nabetani A, Oike Y, Matsubara H, Ishikawa F, Komuro I. A crucial role for adipose tissue p53 in the regulation of insulin resistance. Nat Med. 2009; 15:1082–87. doi: 10.1038/nm.2014

24. Lettieri Barbato D, Aquilano K, Ciriolo MR. FoxO1 at the nexus between fat catabolism and longevity pathways. Biochim Biophys Acta. 2014; 1841:1555–60. doi: 10.1016/j.bbalip.2014.08.004

25. Emran S, Yang M, He X, Zandveld J, Piper MD. Target of rapamycin signalling mediates the lifespan-extending effects of dietary restriction by essential amino acid alteration. Aging (Albany NY). 2014; 6:390–98. doi: 10.18632/aging.100665

26. Fontana L, Hu FB. Optimal body weight for health and longevity: bridging basic, clinical, and population research. Aging Cell. 2014; 13:391–400. doi: 10.1111/acel.12207

27. Guilherme A, Virbasius JV, Puri V, Czech MP. Adipocyte dysfunctions linking obesity to insulin resistance and type 2 diabetes. Nat Rev Mol Cell Biol. 2008; 9:367–77. doi: 10.1038/nrm2391

28. Clemmons DR. Insulin-like growth factor binding proteins and their role in controlling IGF actions. Cytokine Growth Factor Rev. 1997; 8:45–62. doi: 10.1016/S1359-6101(96)00053-6

29. Hedbacker K, Birsoy K, Wysocki RW, Asilmaz E, Ahima RS, Farooqi IS, Friedman JM. Antidiabetic effects of

IGFBP2, a leptin-regulated gene. Cell Metab. 2010; 11:11–22. doi: 10.1016/j.cmet.2009.11.007

30. Wheatcroft SB, Kearney MT, Shah AM, Ezzat VA, Miell JR, Modo M, Williams SC, Cawthorn WP, Medina-Gomez G, Vidal-Puig A, Sethi JK, Crossey PA. IGF-binding protein-2 protects against the development of obesity and insulin resistance. Diabetes. 2007; 56:285–94. doi: 10.2337/db06-0436

31. Janssen JA, Stolk RP, Pols HA, Grobbee DE, Lamberts SW. Serum total IGF-I, free IGF-I, and IGFB-1 levels in an elderly population: relation to cardiovascular risk factors and disease. Arterioscler Thromb Vasc Biol. 1998; 18:277–82. doi: 10.1161/01.ATV.18.2.277

32. Harvie MN, Pegington M, Mattson MP, Frystyk J, Dillon B, Evans G, Cuzick J, Jebb SA, Martin B, Cutler RG, Son TG, Maudsley S, Carlson OD, et al. The effects of intermittent or continuous energy restriction on weight loss and metabolic disease risk markers: a randomized trial in young overweight women. Int J Obes. 2011; 35:714–27. doi: 10.1038/ijo.2010.171

33. Fontana L, Klein S, Holloszy JO. Long-term low-protein, low-calorie diet and endurance exercise modulate metabolic factors associated with cancer risk. Am J Clin Nutr. 2006; 84:1456–62.

34. Pijl H, Langendonk JG, Burggraaf J, Frölich M, Cohen AF, Veldhuis JD, Meinders AE. Altered neuroregulation of GH secretion in viscerally obese premenopausal women. J Clin Endocrinol Metab. 2001; 86:5509–15. doi: 10.1210/jcem.86.11.8061

35. Agueda M, Lasa A, Simon E, Ares R, Larrarte E, Labayen I. Association of circulating visfatin concentrations with insulin resistance and low-grade inflammation after dietary energy restriction in Spanish obese non-diabetic women: role of body composition changes. Nutr Metab Cardiovasc Dis. 2012; 22:208–14. doi: 10.1016/j.numecd.2010.06.010

36. Harris AD, Bradham DD, Baumgarten M, Zuckerman IH, Fink JC, Perencevich EN. The use and interpretation of quasi-experimental studies in infectious diseases. Clin Infect Dis. 2004; 38:1586–91. doi: 10.1086/420936

37. Borenstein M. 2009. Introduction to meta-analysis. Chichester, West Sussex, UK; Hoboken: John Wiley & Sons.

38. Fontana L, Klein S. Aging, adiposity, and calorie restriction. JAMA. 2007; 297:986–94. doi: 10.1001/jama.297.9.986

39. Holloszy JO, Fontana L. Caloric restriction in humans. Exp Gerontol. 2007; 42:709–12. doi: 10.1016/j.exger.2007.03.009

40. Johansson K, Neovius M, Hemmingsson E. Effects of anti-obesity drugs, diet, and exercise on weight-loss maintenance after a very-low-calorie diet or low-calorie diet: a systematic review and meta-analysis of randomized controlled trials. Am J Clin Nutr. 2014; 99:14–23. doi: 10.3945/ajcn.113.070052

41. Longo VD, Fontana L. Calorie restriction and cancer prevention: metabolic and molecular mechanisms. Trends Pharmacol Sci. 2010; 31:89–98. doi: 10.1016/j.tips.2009.11.004

42. Omodei D, Fontana L. Calorie restriction and prevention of age-associated chronic disease. FEBS Lett. 2011; 585:1537–42. doi: 10.1016/j.febslet.2011.03.015

43. Sohal RS, Weindruch R. Oxidative stress, caloric restriction, and aging. Science. 1996; 273:59–63. doi: 10.1126/science.273.5271.59

44. Varady KA, Hellerstein MK. Alternate-day fasting and chronic disease prevention: a review of human and animal trials. Am J Clin Nutr. 2007; 86:7–13.

45. Varady KA. Intermittent versus daily calorie restriction: which diet regimen is more effective for weight loss? Obes Rev. 2011; 12:e593–601. doi: 10.1111/j.1467-789X.2011.00873.x

46. Wycherley TP, Moran LJ, Clifton PM, Noakes M, Brinkworth GD. Effects of energy-restricted high-protein, low-fat compared with standard-protein, low-fat diets: a meta-analysis of randomized controlled trials. Am J Clin Nutr. 2012; 96:1281–98. doi: 10.3945/ajcn.112.044321

47. Clifton PM, Noakes M, Keogh JB. Very low-fat (12%) and high monounsaturated fat (35%) diets do not differentially affect abdominal fat loss in overweight, nondiabetic women. J Nutr. 2004; 134:1741–45.

48. García-Unciti M, Izquierdo M, Idoate F, Gorostiaga E, Grijalba A, Ortega-Delgado F, Martínez-Labari C, Moreno-Navarrete JM, Forga L, Fernández-Real JM, Ibáñez J. Weight-loss diet alone or combined with progressive resistance training induces changes in association between the cardiometabolic risk profile and abdominal fat depots. Ann Nutr Metab. 2012; 61:296–304. doi: 10.1159/000342467

49. Kasim-Karakas SE, Almario RU, Cunningham W. Effects of protein versus simple sugar intake on weight loss in polycystic ovary syndrome (according to the National Institutes of Health criteria). Fertil Steril. 2009; 92:262–70. doi: 10.1016/j.fertnstert.2008.05.065

50. Klempel MC, Kroeger CM, Bhutani S, Trepanowski JF, Varady KA. Intermittent fasting combined with calorie restriction is effective for weight loss and cardio-

protection in obese women. Nutr J. 2012; 11:98. doi: 10.1186/1475-2891-11-98

51. Layman DK, Boileau RA, Erickson DJ, Painter JE, Shiue H, Sather C, Christou DD. A reduced ratio of dietary carbohydrate to protein improves body composition and blood lipid profiles during weight loss in adult women. J Nutr. 2003; 133:411–17.

52. Layman DK, Evans E, Baum JI, Seyler J, Erickson DJ, Boileau RA. Dietary protein and exercise have additive effects on body composition during weight loss in adult women. J Nutr. 2005; 135:1903–10.

53. Nicklas BJ, Wang X, You T, Lyles MF, Demons J, Easter L, Berry MJ, Lenchik L, Carr JJ. Effect of exercise intensity on abdominal fat loss during calorie restriction in overweight and obese postmenopausal women: a randomized, controlled trial. Am J Clin Nutr. 2009; 89:1043–52. doi: 10.3945/ajcn.2008.26938

54. Nørrelund H, Børglum J, Jørgensen JO, Richelsen B, Møller N, Nair KS, Christiansen JS. Effects of growth hormone administration on protein dynamics and substrate metabolism during 4 weeks of dietary restriction in obese women. Clin Endocrinol (Oxf). 2000; 52:305–12. doi: 10.1046/j.1365-2265.2000.00937.x

55. Svendsen PF, Jensen FK, Holst JJ, Haugaard SB, Nilas L, Madsbad S. The effect of a very low calorie diet on insulin sensitivity, beta cell function, insulin clearance, incretin hormone secretion, androgen levels and body composition in obese young women. Scand J Clin Lab Invest. 2012; 72:410–19. doi: 10.3109/00365513.2012.691542

56. Cangemi R, Friedmann AJ, Holloszy JO, Fontana L. Long-term effects of calorie restriction on serum sex-hormone concentrations in men. Aging Cell. 2010; 9:236–42. doi: 10.1111/j.1474-9726.2010.00553.x

57. Halberg N, Henriksen M, Söderhamn N, Stallknecht B, Ploug T, Schjerling P, Dela F. Effect of intermittent fasting and refeeding on insulin action in healthy men. J Appl Physiol (1985). 2005; 99:2128–36. doi: 10.1152/japplphysiol.00683.2005

58. Baba NH, Sawaya S, Torbay N, Habbal Z, Azar S, Hashim SA. High protein vs high carbohydrate hypoenergetic diet for the treatment of obese hyperinsulinemic subjects. Int J Obes Relat Metab Disord. 1999; 23:1202–06. doi: 10.1038/sj.ijo.0801064

59. Lee K, Lee J, Bae WK, Choi JK, Kim HJ, Cho B. Efficacy of low-calorie, partial meal replacement diet plans on weight and abdominal fat in obese subjects with metabolic syndrome: a double-blind, randomised controlled trial of two diet plans - one high in protein and one nutritionally balanced. Int J Clin Pract. 2009; 63:195–201. doi: 10.1111/j.1742-1241.2008.01965.x

60. Belobrajdic DP, Frystyk J, Jeyaratnaganthan N, Espelund U, Flyvbjerg A, Clifton PM, Noakes M. Moderate energy restriction-induced weight loss affects circulating IGF levels independent of dietary composition. Eur J Endocrinol. 2010; 162:1075–82. doi: 10.1530/EJE-10-0062

61. Bhutani S, Klempel MC, Kroeger CM, Trepanowski JF, Varady KA. Alternate day fasting and endurance exercise combine to reduce body weight and favorably alter plasma lipids in obese humans. Obesity (Silver Spring). 2013; 21:1370–79. doi: 10.1002/oby.20353

62. Claessens M, van Baak MA, Monsheimer S, Saris WH. The effect of a low-fat, high-protein or high-carbohydrate ad libitum diet on weight loss maintenance and metabolic risk factors. Int J Obes. 2009; 33:296–304. doi: 10.1038/ijo.2008.278

63. Das SK, Gilhooly CH, Golden JK, Pittas AG, Fuss PJ, Cheatham RA, Tyler S, Tsay M, McCrory MA, Lichtenstein AH, Dallal GE, Dutta C, Bhapkar MV, et al. Long-term effects of 2 energy-restricted diets differing in glycemic load on dietary adherence, body composition, and metabolism in CALERIE: a 1-y randomized controlled trial. Am J Clin Nutr. 2007; 85:1023–30.

64. de Luis DA, Izaola O, García Alonso M, Aller R, Cabezas G, de la Fuente B. Effect of a commercial hypocaloric diet in weight loss and post surgical morbidities in obese patients with chronic arthropathy, a randomized clinical trial. Eur Rev Med Pharmacol Sci. 2012; 16:1814–20.

65. Fontana L, Klein S, Holloszy JO. Effects of long-term calorie restriction and endurance exercise on glucose tolerance, insulin action, and adipokine production. Age (Dordr). 2010; 32:97–108. doi: 10.1007/s11357-009-9118-z

66. Fontana L, Meyer TE, Klein S, Holloszy JO. Long-term calorie restriction is highly effective in reducing the risk for atherosclerosis in humans. Proc Natl Acad Sci USA. 2004; 101:6659–63. doi: 10.1073/pnas.0308291101

67. Fontana L, Weiss EP, Villareal DT, Klein S, Holloszy JO. Long-term effects of calorie or protein restriction on serum IGF-1 and IGFBP-3 concentration in humans. Aging Cell. 2008; 7:681–87. doi: 10.1111/j.1474-9726.2008.00417.x

68. Haugaard SB, Vaag A, Mu H, Madsbad S. Skeletal muscle structural lipids improve during weight-maintenance after a very low calorie dietary intervention. Lipids Health Dis. 2009; 8:34.

doi: 10.1186/1476-511X-8-34

69. Heilbronn LK, de Jonge L, Frisard MI, DeLany JP, Larson-Meyer DE, Rood J, Nguyen T, Martin CK, Volaufova J, Most MM, Greenway FL, Smith SR, Deutsch WA, et al, and Pennington CALERIE Team. Effect of 6-month calorie restriction on biomarkers of longevity, metabolic adaptation, and oxidative stress in overweight individuals: a randomized controlled trial. JAMA. 2006; 295:1539–48. doi: 10.1001/jama.295.13.1539

70. Heilbronn LK, Smith SR, Martin CK, Anton SD, Ravussin E. Alternate-day fasting in nonobese subjects: effects on body weight, body composition, and energy metabolism. Am J Clin Nutr. 2005; 81:69–73.

71. Johnston CS, Tjonn SL, Swan PD. High-protein, low-fat diets are effective for weight loss and favorably alter biomarkers in healthy adults. J Nutr. 2004; 134:586–91.

72. Kleiner RE, Hutchins AM, Johnston CS, Swan PD. Effects of an 8-week high-protein or high-carbohydrate diet in adults with hyperinsulinemia. MedGenMed. 2006; 8:39.

73. Larson-Meyer DE, Heilbronn LK, Redman LM, Newcomer BR, Frisard MI, Anton S, Smith SR, Alfonso A, Ravussin E. Effect of calorie restriction with or without exercise on insulin sensitivity, beta-cell function, fat cell size, and ectopic lipid in overweight subjects. Diabetes Care. 2006; 29:1337–44. doi: 10.2337/dc05-2565

74. Lejeune MP, Kovacs EM, Westerterp-Plantenga MS. Additional protein intake limits weight regain after weight loss in humans. Br J Nutr. 2005; 93:281–89. doi: 10.1079/BJN20041305

75. Melanson KJ, Summers A, Nguyen V, Brosnahan J, Lowndes J, Angelopoulos TJ, Rippe JM. Body composition, dietary composition, and components of metabolic syndrome in overweight and obese adults after a 12-week trial on dietary treatments focused on portion control, energy density, or glycemic index. Nutr J. 2012; 11:57. doi: 10.1186/1475-2891-11-57

76. Meyer TE, Kovács SJ, Ehsani AA, Klein S, Holloszy JO, Fontana L. Long-term caloric restriction ameliorates the decline in diastolic function in humans. J Am Coll Cardiol. 2006; 47:398–402. doi: 10.1016/j.jacc.2005.08.069

77. Redman LM, Rood J, Anton SD, Champagne C, Smith SR, Ravussin E, and Pennington Comprehensive Assessment of Long-Term Effects of Reducing Intake of Energy (CALERIE) Research Team. Calorie restriction and bone health in young, overweight individuals. Arch Intern Med. 2008; 168:1859–66. doi: 10.1001/archinte.168.17.1859

78. Redman LM, Veldhuis JD, Rood J, Smith SR, Williamson D, Ravussin E, Pennington CT, and Pennington CALERIE Team. The effect of caloric restriction interventions on growth hormone secretion in nonobese men and women. Aging Cell. 2010; 9:32–39. doi: 10.1111/j.1474-9726.2009.00530.x

79. Soenen S, Bonomi AG, Lemmens SG, Scholte J, Thijssen MA, van Berkum F, Westerterp-Plantenga MS. Relatively high-protein or 'low-carb' energy-restricted diets for body weight loss and body weight maintenance? Physiol Behav. 2012; 107:374–80. doi: 10.1016/j.physbeh.2012.08.004

80. Tapsell L, Batterham M, Huang XF, Tan SY, Teuss G, Charlton K, Oshea J, Warensjö E. Short term effects of energy restriction and dietary fat sub-type on weight loss and disease risk factors. Nutr Metab Cardiovasc Dis. 2010; 20:317–25. doi: 10.1016/j.numecd.2009.04.007

81. Lasker DA, Evans EM, Layman DK. Moderate carbohydrate, moderate protein weight loss diet reduces cardiovascular disease risk compared to high carbohydrate, low protein diet in obese adults: A randomized clinical trial. Nutr Metab (Lond). 2008; 5:30. doi: 10.1186/1743-7075-5-30

82. Weiss EP, Racette SB, Villareal DT, Fontana L, Steger-May K, Schechtman KB, Klein S, Holloszy JO, and Washington University School of Medicine CALERIE Group. Improvements in glucose tolerance and insulin action induced by increasing energy expenditure or decreasing energy intake: a randomized controlled trial. Am J Clin Nutr. 2006; 84:1033–42.

83. Westerterp-Plantenga MS, Lejeune MP, Nijs I, van Ooijen M, Kovacs EM. High protein intake sustains weight maintenance after body weight loss in humans. Int J Obes Relat Metab Disord. 2004; 28:57–64. doi: 10.1038/sj.ijo.0802461

84. Wycherley TP, Noakes M, Clifton PM, Cleanthous X, Keogh JB, Brinkworth GD. A high-protein diet with resistance exercise training improves weight loss and body composition in overweight and obese patients with type 2 diabetes. Diabetes Care. 2010; 33:969–76. doi: 10.2337/dc09-1974

85. Yoshimura E, Kumahara H, Tobina T, Matsuda T, Ayabe M, Kiyonaga A, Anzai K, Higaki Y, Tanaka H. Lifestyle intervention involving calorie restriction with or without aerobic exercise training improves liver fat in adults with visceral adiposity. J Obes. 2014; 2014:197216. doi: 10.1155/2014/197216

86. Sterne JA, Gavaghan D, Egger M. Publication and related bias in meta-analysis: power of statistical tests and prevalence in the literature. J Clin Epidemiol. 2000; 53:1119–29. doi: 10.1016/S0895-4356(00)00242-0

87. Lettieri-Barbato D, Tomei F, Sancini A, Morabito G, Serafini M. Effect of plant foods and beverages on plasma non-enzymatic antioxidant capacity in human subjects: a meta-analysis. Br J Nutr. 2013; 109:1544–56. doi: 10.1017/S0007114513000263

88. Higgins JP, Green S, and Cochrane Collaboration. 2008. Cochrane handbook for systematic reviews of interventions. Chichester, West Sussex; Hoboken NJ: Wiley-Blackwell.

Research Paper

Long-term moderate calorie restriction inhibits inflammation without impairing cell-mediated immunity: a randomized controlled trial in non-obese humans

Simin N. Meydani[1], Sai K. Das[1], Carl F. Pieper[2], Michael R. Lewis[3], Sam Klein[4], Vishwa D. Dixit[5], Alok K. Gupta[6], Dennis T. Villareal[7], Manjushri Bhapkar[2], Megan Huang[2], Paul J. Fuss[1], Susan B. Roberts[1], John O. Holloszy[4], and Luigi Fontana[4,8,9]

[1]The Jean Mayer USDA Human Nutrition Research Center on Aging at Tufts University, Boston, MA 02111, USA
[2]Duke University Medical Center, Durham, NC 27705, USA
[3]University of Vermont, Burlington, VT 05405, USA
[4]Department of Medicine, Washington University School of Medicine, St Louis, MO 63110, USA
[5]Comparative Medicine and Department of Immunobiology, Yale University School of Medicine, New Haven, CT 06510, USA
[6]Pennington Biomedical Research Center, Baton Rouge, LA 70808, USA
[7]Baylor College of Medicine and Michael E DeBakey VA Medical Center, Houston, TX 77030, USA
[8]Department of Clinical and Experimental Sciences, Brescia University School of Medicine, Brescia, Italy [9]CEINGE Biotecnologie Avanzate, Napoli, Italy

Key words: human, familial longevity, calorie restriction, inflammation, vaccine response, cell-mediated immunity
Received: 05/11/16; Accepted: 06/20/16; Published: 07/13/16 **doi:** 10.18632/aging.100994
Correspondence to: Simin N. Meydani, PhD; **E-mail:** Simin.meydani@tufts.edu

Abstract: **Calorie restriction (CR) inhibits inflammation and slows aging in many animal species, but in rodents housed in pathogen-free facilities, CR impairs immunity against certain pathogens. However, little is known about the effects of long-term moderate CR on immune function in humans. In this multi-center, randomized clinical trial to determine CR's effect on inflammation and cell-mediated immunity, 218 healthy non-obese adults (20-50 y), were assigned 25% CR (n=143) or an ad-libitum (AL) diet (n=75), and outcomes tested at baseline, 12, and 24 months of CR. CR induced a 10.4% weight loss over the 2-y period. Relative to AL group, CR reduced circulating inflammatory markers, including total WBC and lymphocyte counts, ICAM-1 and leptin. Serum CRP and TNF-α concentrations were about 40% and 50% lower in CR group, respectively. CR had no effect on the delayed-type hypersensitivity skin response or antibody response to vaccines, nor did it cause difference in clinically significant infections. In conclusion, long-term moderate CR without malnutrition induces a significant and persistent inhibition of inflammation without impairing key *in vivo* indicators of cell-mediated immunity. Given the established role of these pro-inflammatory molecules in the pathogenesis of multiple chronic diseases, these CR-induced adaptations suggest a shift toward a healthy phenotype.**

INTRODUCTION

Calorie restriction (CR) without malnutrition is the most powerful intervention to increase lifespan in simple model organisms and rodents [1]. CR decreases inflammation, which is believed to protect against age-associated diseases [2, 3]. Low-grade chronic inflammation is deeply implicated in the pathogenesis of multiple age-associated chronic diseases and in the biology of aging itself [4]. Serum concentrations of C-reactive protein (CRP, a highly specific systemic marker of inflammation) and TNF-α (a powerful pro-inflammatory cytokine) are both associated with an increased risk of developing insulin resistance, type 2 diabetes (T2D), cardiovascular disease (CVD) and cancer [5-8]. Excessive adiposity is associated with increased

adipose tissue TNF-α expression [9] and serum TNF-α levels [10], which are reduced by weight loss [9, 11]. However, concerns exist regarding the potential immunosuppressive effects of CR, because some studies have shown a detrimental effect on cell-mediated immune responses in monkeys [12] and increased susceptibility to infection in rodents [13, 14]. On the contrary, other studies in aging mouse and monkeys show that CR can enhance the T cell receptor diversity suggesting improved immune –surveillance [15, 16].

In humans, CR including a restriction of protein and essential nutrients impairs cell-mediated immune responses [17] and increases susceptibility to morbidity and mortality from infectious diseases. However, little is known about the long-term effects of moderate CR with adequate intake of nutrients on inflammatory markers and cell-mediated immune response of healthy adults.

A purpose of this 2-year multicenter randomized controlled trial (RCT) was to evaluate the effects of a 25% CR diet on inflammatory markers [WBC count, high sensitivity CRP (hs-CRP), pro-inflammatory cytokines, adhesion molecules], and *in vivo* measures of cell-mediated immunity [antibody response to 3 vaccines, and delayed-type hypersensitivity skin response (DTH) to three recall antigens] in a large number of healthy, non-obese young and middle-aged individuals. Self-reported infections, allergies and related medications were documented.

RESULTS

Participants and baseline characteristics

As described previously [18], 1,069 interested individuals were invited to an in-person screening evaluation, 238 started baseline testing and 220 were randomized. Two CR participants dropped prior to randomization, resulting in an ITT cohort of 218 (Figure 1 and Table 1). Thirty participants withdrew from the study [4 (5.3%) in the AL and 26 (18.2%) in the CR group (p= 0.01)]. Three CR participants continued the study evaluations beyond withdrawal and were included in analyses. There were no differences at baseline between AL and CR groups in biometric and demographic variables including body weight, body mass index (BMI) and other body composition and demographic variables, blood glucose or lipid profile (Table 1) or for any of the immune and inflammatory outcomes.

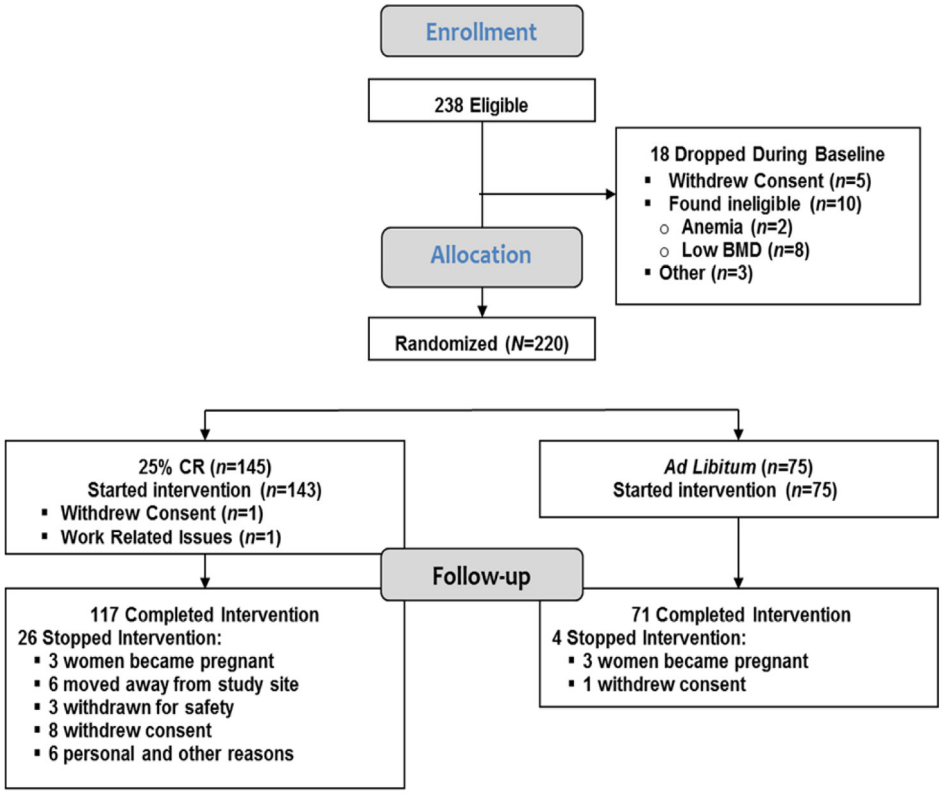

Figure 1. CONSORT diagram. Two hundred and thirty eight individuals were eligible and 220 individuals were randomized. Two individuals, both assigned to the calorie-restricted (CR) group, dropped out prior to starting the intervention, resulting in an intention-to-treat cohort of 218 participants; 75 in the ad libitum (AL) control and 143 in the CR group (Table 1). Thirty participants were withdrawn or dropped from the intervention prior to completion including 4 (5.3%) in the AL control group and 26 (18.2%) in the CR group (p=0.01).

Table 1. Demographic, anthropometric and clinical characteristics at baseline for the 218 participants who started the 2-year intervention *

	Calorie Restriction (n=143)†	Ad Libitum (n=75)†
Race		
White, n (%)	111 (77.6%)	57 (76%)
African American, n (%)	15 (10.5%)	11 (14.7%)
Other, n (%)	17 (11.9%)	7 (9.3%)
Sex (F/M)	99F/44M	53F/22M
Age, y	38.0 (7.2)	37.9 (6.9)
Height, cm	168.9 (8.6)	168.4 (8.3)
Baseline Weight, kg	71.8 (9.2)	71.3 (8.6)
Baseline BMI, kg/m^2	25.1 (1.7)	25.1 (1.6)
Body Fat, %	33.6 (6.6)	32.9 (6.1)
Blood pressure		
SBP, mmHg	112 (9.9)	111 (9.9)
DBP, mmHg	72.1 (7.5)	71.2 (7.1)
Laboratory Values		
Glucose, mg/dL	81.9 (5.6)	83.6 (6.1)
Insulin, µIU/mL	5.4 (0.2)	5.8 (0.3)
HDL-C, mg/dL	49.1 (13.3)	49.2 (11.7)
LDL-C, mg/dL	98.0 (26.5)	105.6 (28.6)
Tg, mg/dL	103.5 (50.5)	106.8 (59.7)

Abbreviations: AL, ad libitum control group; CR, 25% calorie restriction group; SBP, systolic blood pressure; DBP, diastolic blood pressure; HDL-C, high density lipoprotein cholesterol; LDL-C, low density lipoprotein cholesterol; Tg, triglycerides.
* Values represent mean (SD).
† No significant between group differences for all listed variables.

Intervention adherence and body composition

Participant adherence and changes in body composition in response to CR have been published elsewhere [19]. Energy intake was reduced by 19.5 (0.8) % (480 kcal/d) during the first 6-months of CR, and by an average of 9.1 (0.7) % (234 kcal/d) for the remaining 18-mo ($p<0.0001$ vs. AL). CR induced significant reduction in body weight [8.3 (0.3) kg (11.5%) at 1-y and a net change of 7.6 (0.3) kg (10.4%) at 2-y ($p<0.001$)], BMI and % body fat [19]. No significant change was observed in energy intake or body composition in the AL group. Measured by DEXA, CR induced a 6.1% (0.2) kg change in Fat Mass at 1-yr and 5.3 (0.3) kg at 2-yr, but did not change in the AL group.

Moderate CR impacts white blood cell profile

Complete blood count and differentials (CBC-Diff) stayed within normal ranges in both groups. However, compared to AL, CR significantly reduced the number of WBC at month 12 ($p=0.03$), and 24 ($p=0.002$) (Figure 2A). There was a trend for a correlation between changes in BMI from baseline to 24 months and that of WBC number ($r=0.14$, $p=0.07$) when both CR and AL groups were combined.

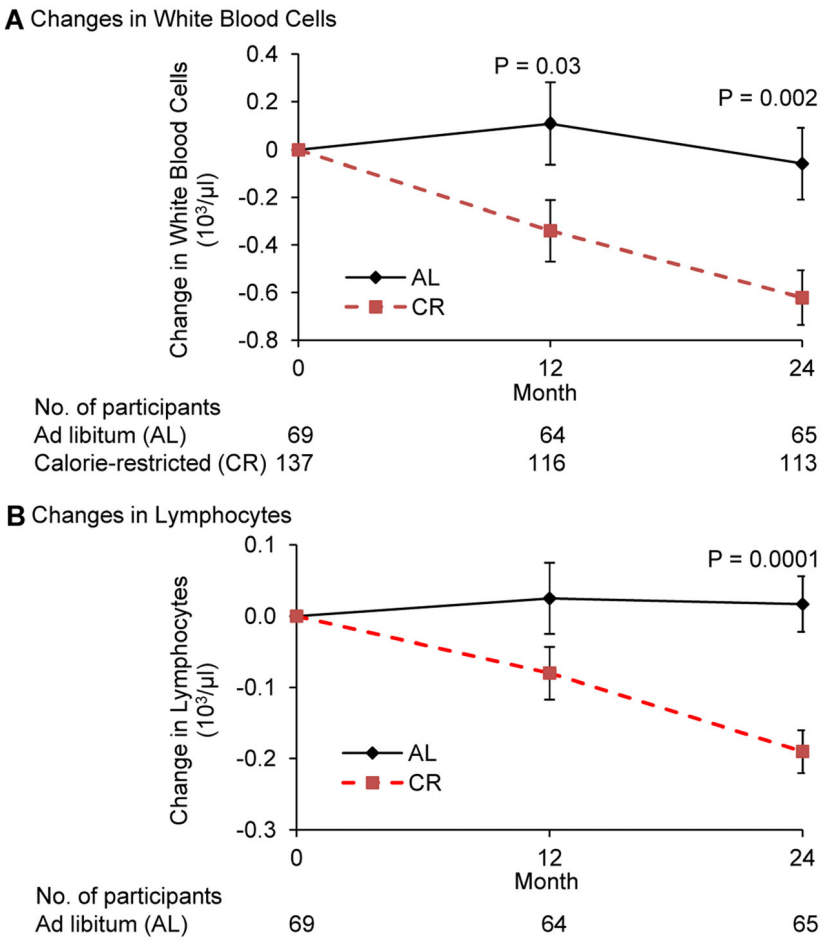

Figure 2. Change in the number of white blood cells and lymphocytes following 2 years of calorie restriction in humans. Panel (**A**) baseline values of white blood cells for ad libitum (AL) and calorie-restricted (CR) groups were 5.9 x 10^3/µl and 6.0 x 10^3/µl, respectively. Panel (**B**) baseline values of lymphocytes for both AL and CR groups were 1.8 x 10^3/µl. Data are mean (SE). The P value comparisons are for AL and CR groups at indicated time points.

Compared to AL, CR significantly reduced the number of lymphocytes at month 24 (p=0.0001) (Figure 2B). The difference in the change in lymphocytes between CR and AL group was -0.106 at 12 months (p=0.09) and -0.207 at month 24. (p<0.0001. A significant correlation between changes in BMI from baseline to month 24 and that of lymphocytes (r=0.20, p=0.006) was observed when both CR and AL groups were combined.

While a significant difference in change in monocytes was observed between the two groups, this was mainly due to an increase in the AL group. The decrease in neutrophils in the CR group at month 24 in comparison to the AL group tended to be significant (p=0.067) (Supplemental Table 1). No significant differences in the eosinophils or basophils were observed (Both groups showed a small but significant increase in basophils; these numbers stayed within normal ranges (Supplemental Table 1).

Moderate CR reduces circulating inflammatory markers

CRP (natLog) decreased significantly in the CR compared to AL group at both months 12 and 24 (p=0.001) (Figure 3A). The correlation between change in BMI and change in the natural logarithm of CRP trended toward significance (r=0.15, p=0.05).

Plasma TNF-α decreased significantly in both AL and CR groups at month 12 (-0.34 vs. -0.30 pg/mL;

p=0.012, p=0.0024 for AL and CR, respectively); further declines in the CR group between month 12 and 24 (p=0.018) resulted in a significantly higher decrease in TNF-α in CR compared to AL group at month 24 (p=0.025) (Figure 3B). A significant correlation between changes in BMI from baseline to 24 months and that of TNFα (r=0.15, p=0.04) was observed when both CR and AL groups were combined.

Compared to AL group, there was a significant decline in serum ICAM-1 levels in the CR group from baseline to month 12 (P<0.0001), however, ICAM levels in the AL group decreased significantly between month 12 and 24 (P<0.0001) resulting in a non-significant difference between the AL and CR groups at month 24 (P=0.14) (Figure 3C**).** A significant correlation between change in BMI from baseline to 24 months and that of ICAM-1 (r=0.17, p=0.02) was observed when both CR and AL groups were combined.

The change in leptin level was significantly greater in CR compared to AL group at both month 12 and 24 (p<0.0001) (Figure 3D**).** In addition, a significant correlation was observed between changes in BMI from baseline to month 24 months and changes in leptin when both CR and AL groups were combined (r=0.60, p=0.001).

No significant changes were observed for IL-6, IL-8, and MCP-1 (data not shown).

Response to vaccine

Antibody responses to vaccines were measured at the end of the intervention. Three vaccines, Hepatitis A (HEP-A) (primary T cell-dependent), tetanus/diphtheria (TD) (secondary T cell-dependent) and pneumococcal (B cell dependent) (PN) were administered at month 17. A booster shot for HEP-A was administered at month

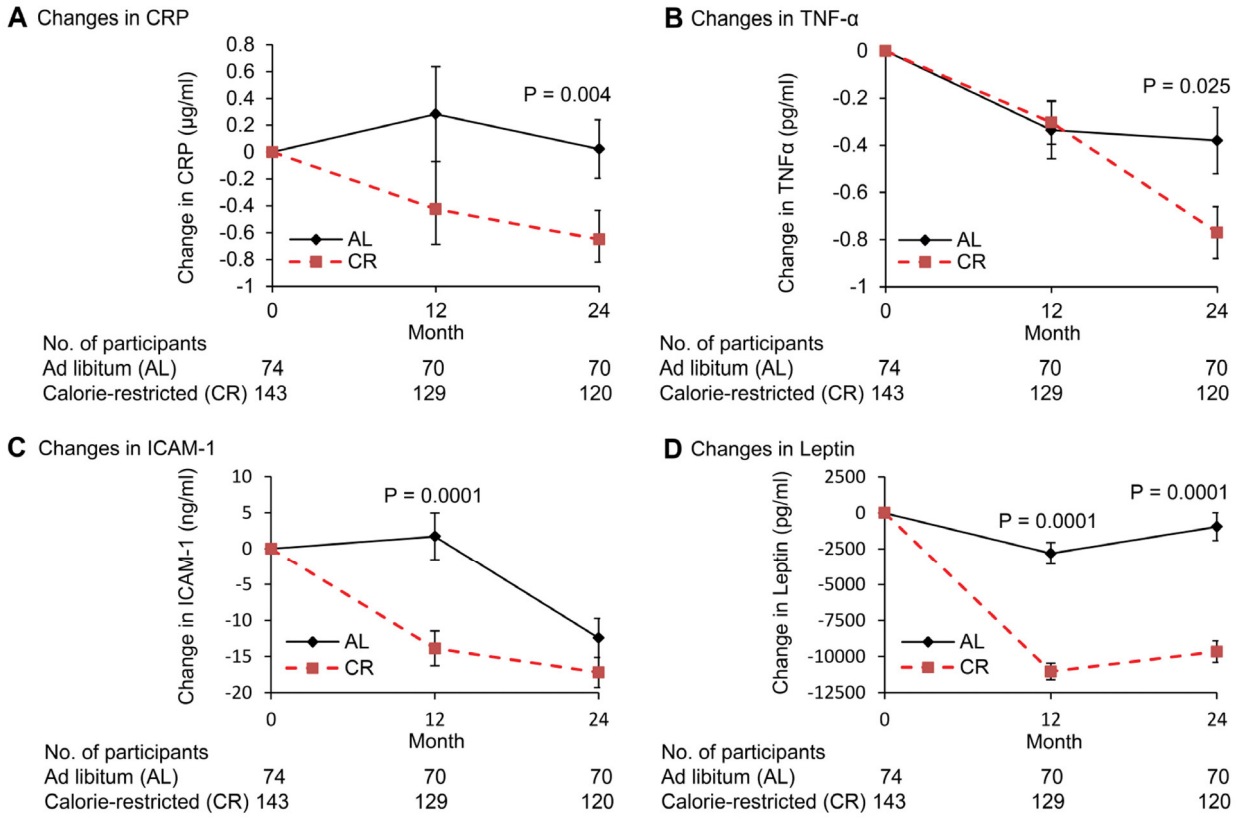

Figure 3. Change in plasma concentrations of inflammation markers following 2 years of calorie restriction in humans. Panel (**A**) baseline values of C-reactive protein (hs-CRP) for ad libitum (AL) and calorie-restricted (CR) groups were 1.1 and 1.5 µg/mL, respectively. Panel (**B**) baseline values of tumor necrosis factor-alpha (TNF-α) for AL and CR groups were 3.1 and 3.5 pg/ml, respectively. Panel (**C**) baseline values of intercellular adhesion molecule-1 (ICAM-1) for AL and CR groups were 165.4 and 165.0 ng/ml, respectively. Panel (**D**) baseline values of leptin for AL and CR groups were 17.7 and 16.9 ng/ml, respectively. Data are mean (SE). The P value comparisons are for AL and CR groups at indicated time points.

23. Blood for antibody response was collected at month 17 (before vaccination), 18, and 24 (after vaccination) for all vaccines, and 23 for before HEP-A booster. There was no significant difference between AL and CR groups in pre-vaccination (month 17 and 23) or post-vaccination (month 18 and 24) levels of antibodies to Hepatits A HEP-A, TD), or any of the PN IgG serotypes (1, 2, 3, 4, 5, 6, 7F, 8, 9N, 9V, 10A, 11A, 12F, 14, 15B, 17F, 18C, 19A, 19F, 20, 22F, 23F, 33F) (Supplemental Table 3).

For HEP-A antibody level, the majority of subjects within both AL and CR groups had levels above the detection limit and thus quantitative values could not be obtained. However, there were no differences between AL and CR groups in % participants who had values above the detection limit at any time point for HEP-A or other vaccines.

DTH

There was no significant difference at baseline between AL and CR groups in the diameter of induration at 24 or 48 h for individual antigens or for total diameter of induration (Table 2**)**, nor in number of positive antigens.

Table 2. Effect of calorie restriction on delayed-type hypersensitivity skin response at 48 hours*

	Time point		
Variable	Baseline	Month 12	Month 24
Trichophyton (diameter of induration, mm)			
AL	0.9 (0.3)	2.2 (0.6)	3.1 (0.8)
CR	1.5 (0.4)	1.1 (0.5)	1.8 (0.7)
p-value	0.79	0.294	0.381
Tetanus (diameter of induration, mm)			
AL	12.1 (1.1)	10.5 (1.3)	9.7 (1.1)†, ‡
CR	13.5 (1.0)	10.5 (1.0)†	8.0 (0.9)†
p-value	0.812	1	0.407
Candida (diameter of induration, mm)			
AL	7.5 (0.9)	9.2 (1.3)	9.4 (1.2)
CR	9.5 (0.8)	10.0 (1.0)	8.7 (0.9)
p-value	0.167	1	1
Total Diameter of Induration (mm) for all observed values			
AL	20.5 (1.7)	20.6 (2.2)	21.5 (1.9)
CR	24.4 (1.4)	21.2 (1.6)	18.2 (1.6)†, §
p-value	0.127	1	0.353
Number of Positive Responses (> 5mm)			
AL	1.48 (0.09)	1.64 (0.11)	1.72 (0.13)
CR	1.59 (0.07)	1.69 (0.08)	1.59 (0.07)
p-value	0.392	0.737	0.361

Abbreviations: AL, ad libitum control group; CR, 25% calorie restriction group.
* Results are mean (SE). Predicted values based on statistical analysis.
† Significantly different from baseline within each treatment group at $p<0.05$.
‡ $p<0.016$ for response to *Tetanus toxoid*.
§ $p<0.001$ for total diameter of induration.

There were no significant main effects of treatment or time and their interaction or in the change during 2-years in the total number of positive antigens or total diameter of induration for positive responses (≥5mm) or all observed responses at 24 or 48 hours between CR and AL groups. A significant within CR group change from baseline to month 24 (p=0.001) in total diameter of induration (Table 2**)** was observed and both groups showed a significant decline in the diameter of induration for positive responses (values ≥5mm) to *Tetanus toxoid* (p=0.016). The reason for this decline is not clear and cannot be explained by any methodological inconsistency, changes in participants' health status, timing of administration of DTH, or timing of tetanus vaccination.

Infection

Incidence of total infections or organ-specific infections, allergies and associated medications as well as severity of infections and allergies over the 24-month follow-up did not significantly differ between AL and CR groups (Supplemental Tables 3A and B). This was true for the annualized rate of infection and allergies with the exception of lower respiratory (CR group tended to have a lower rate 0.046 vs 0.015; p=0.058) and eye infections (CR group had a higher rate 0.00 vs 0.019; p=0.036) (Supplemental Table 3A).

DISCUSSION

This is the first RCT to test the long-term effects of moderate CR without malnutrition in a large sample of young and middle-aged non-obese individuals using a variety of inflammatory and immune outcomes. We show that 25% CR for 24 mo persistently reduced circulating inflammatory markers including WBC count. Serum concentrations of CRP and TNF-α were about 40% and 50% lower in the CR group, respectively. Furthermore, despite a major reduction in body fat and circulating leptin levels, a significant impairment in key in vivo measures of adaptive immune function with CR was not observed in our study and this finding is supported by the lack of clinically significant differences in self-reported infection rate between CR and AL groups.

Low-grade chronic inflammation is implicated in the pathogenesis of multiple age-associated chronic diseases and in the biology of aging itself [4]. On the other hand, research on rodents housed in pathogen-free facilities and data from undernourished children and adults living in third world countries suggest that a chronic reduction in energy intake may impair adaptive immunity against pathogens by lowering leptin and other nutrient-sensing pathways [17, 20] While data from animal and observational human studies show that CR without malnutrition inhibits inflammation [3, 20-22], this RCT is the first to show a causal relationship in humans. The WBC count has been broadly used as a non-specific marker of systemic inflammation [23], with higher levels, even when within the clinical reference range, associated with an increased risk of developing insulin resistance, T2D [24], hypertension [25], CVD [26], and cancer [27]. Moreover, the relative risk of CVD and cancer mortality increases in a dose-dependent manner with increasing WBC count, independent of other risk factors [28]. Data from previous weight loss studies in obese individuals have shown that CR reduces total WBC count, IL-1β, IL-6, and TNF-α [29]. We found that CR induced a significant reduction in total WBC, lymphocyte and monocyte count, as well as a strong trend (p=0.067) for a decrease in neutrophils, suggesting that CR has metabolic benefits even in non-obese individuals. The anti-inflammatory effect of CR is further supported by the CR-induced decrease in serum levels of CRP, TNF-α, ICAM-1, and leptin [30]. However, in our study the serum concentrations of other pro-inflammatory cytokines and chemokines (IL-6, IL-8, MCP-1) were not significantly altered by CR, probably because our volunteers were healthy, young to middle-aged and non-obese, with relatively low levels of visceral adiposity [31]. Since obesity-associated increase in circulating IL-6 is mainly contributed by increased output from the visceral adipose tissue [31], it is possible that a reduction in visceral fat mass would lead to more pronounced IL-6-lowering effect in an obese individual relative to their non-obese counterpart with an already low IL-6 level.

The mechanisms underlying the anti-inflammatory effect of CR are not entirely clear. It is hypothesized that the reductions in fat mass and leptin largely explain the beneficial effect of CR on inflammation. However, our findings suggest that other metabolic and molecular factors may play a role, because peak reduction in circulating leptin levels at month 12 were not accompanied by a significant reduction in serum TNF-α levels. Thus, the significant reduction in CRP and TNF-α concentrations observed at 24 months may be due to CR-induced alterations of the neuroendocrine system through the down-regulation of nutrient-sensing pathways that impact mitochondrial function, redox status and inflammatory gene activation [32-35].

A major finding of this study is the lack of significant negative effects of CR on key *in vivo* indicators of cell-mediated immunity. There is controversy in the literature regarding the impact of CR on cell-mediated

immunity. Although some animal studies indicate that age-associated impairment of immune function may be improved by CR, and short-term CR in a small number of subjects improved T cell-mediated function [36], others have raised concern regarding the potential adverse impact of CR on cell-mediated immunity and resistance to pathogens. For example, CR mice were shown to have lower natural killer cell activity, decreased survival, and delayed viral clearance compared to ad-libitum fed mice [13, 14], which can be reversed by re-feeding [37]. CR also caused higher mortality from polymicrobial sepsis [38] and West Nile Virus [39], and more susceptibility to the intestinal parasite (Heligmosomoides bakeri) infection [40] in mice. In this study, despite a ~57% decrease in leptin, CR did not exert any detrimental effect on the two best available *in vivo* indicators of acquired (specific) immunity, i.e., antibody production to vaccines and DTH to recall antigens. This difference might be due to moderate level of CR (25%) administered in the current study compared to that used in several animal studies which can be as high as 40%. Taken together, these results suggest that moderate CR without malnutrition is safe and does not adversely affect immune response to pathogens, which is also supported by the lack of clinically significant differences in self-reported infection rate between CR and AL groups. It will be interesting to determine if lower than 25% CR would be effective in reducing inflammation.

In conclusion, data from this unique RCT showed that moderate long-term CR without malnutrition decreases inflammation in non-obese, healthy adults, as demonstrated by reduced number of WBC, lymphocytes, and neutrophils in blood, as well as reduced circulating levels of CRP, leptin, TNF-α, and ICAM-1, with no significant adverse effect on key *in vivo* indicators of cell-mediated immunity. These CR-induced changes suggest a shift toward a healthy phenotype, given the established role of these pro-inflammatory molecules as risk markers in the development of metabolic syndrome and age-related chronic diseases, in particular CVD, T2D and cancer.

METHODS

Overview. The Comprehensive Assessment of Long-term Effects of Reducing Intake of Energy (CALERIE) Phase 2 Study was a two-year, multi-center, parallel-group, single-blind RCT of healthy individuals receiving an intervention to reduce energy intake by 25% (CR) or maintain habitual ad libitum intake (AL-control) group. Clinical outcomes were assessed every 6-mo as detailed elsewhere [19, 41]. The study protocol (ClinicalTrials.gov ID:NCT00427193), was approved by the institutional review boards at all research sites, and participants provided written informed consent. Exclusion criteria for administration of vaccine and/or DTH included history of allergic reactions, infection or exposure to antibiotics in the previous two-weeks, non-steroidal anti-inflammatory drugs within 72 h, vaccination within last 6-wk, steroids >10 mg/d, or any immunosuppressive medication. For Hepatitis A only participants were screened out of the vaccination testing if they had previously received a vaccination.

Baseline testing was conducted over six weeks and included evaluations of health status and doubly labeled water (DLW) measurements of energy expenditure to individualize the 25% CR prescription. Fasting blood samples were collected for immune parameters. DTH and vaccines were administered as indicated below.

Following baseline testing, participants were randomized to either AL or CR in a 2:1 allocation in favor of CR. Randomization was stratified by site (3 sites), sex, and BMI (normal weight, overweight).

The intervention targeted an immediate and sustained 25% CR [42, 43]. Control participants were advised to continue their current diets. No specific level of physical activity was recommended. Percent CR was calculated and adherence evaluated from DLW measurements at months 12 and 24 [43]. Participants (both CR and AL) received a multivitamin and mineral supplement (Nature Made Multi Complete, Pharmavite, Mission Hills, CA) plus a calcium supplement (1000 mg/d, Douglas Laboratories, Pittsburgh, PA) to ensure current recommendations for micronutrients were met regardless of the intervention allocation.

Outcome assessments. Participants were weighed in a pre-weighed hospital gown after an overnight fast (Scale Tronix 5200, White Plains, NY). Height was measured twice using a wall-mounted stadiometer. Percent body fat, lean mass, and bone were measured by dual X-ray absorptiometry (DXA; Hologic Inc., Bedford, MA) and analyzed using Hologic software version Apex 3.3.

As part of safety testing, participants record signs, symptoms, adverse events, and medication use in a diary and hematology, serum chemistry and urinalysis were monitored every 3-mo [41]. Self-reported infection, allergy, and antibiotic use and duration were recorded throughout the study and coded for severity (mild, moderate, and severe) by the Coordinating Center in accordance with MedRA version 14.1 and WHO Drug Dictionary Enhanced-March 2012 guidelines.

Immune and inflammatory markers. Inflammatory markers were measured in fasting blood at baseline, month 12 and 24, and analyzed at the University of Vermont. Hs-CRP was measured using particle-enhanced immunonephelometric assay (BN II, Siemens, Deerfield, IL; CV=3.2 ± 2.5%); TNF-α, monocyte chemoattractant protein-1 (MCP-1), leptin, IL-1β, and IL-8 using the multiplex immunoassay (Human Adipokine Panel B, Millipore, Billerica, MA; Bio-Plex 200, Bio-Rad Laboratories, Hercules, CA; CV=6.1±1.7%, 6.4±2.1%, 4.3±1.5%, 8.0±4.4% and 8.7±3.9%, respectively); and IL-6 and intracellular adhesion molecule-1 (ICAM-1) using ELISA (R&D Systems, Minneapolis, MN; CV=7.9±3.1% and 8.2±1.2%, respectively). Complete blood count and WBC differential (CBC-Diff) were assayed using automated methods (Esoterix Inc., a LabCorp Company, Cranford, NJ).

In vivo cell-mediated immunity was assessed using delayed type hypersensitivity skin response (DTH) and antibody response to 3 vaccines. DTH, which determines ability of immune response to antigens to which it has been previously exposed, was assessed using Mantoux test. Three recall antigens [*Tetanus toxoid* (Aventis Pasteur), *Candida albicans* (Candin; Allermed Laboratories, San Diego, CA), and *Trichophyton* species (*Trichophyton mentagrophytes* in conjunction with *Trichophyton rubrum*; Hollister-Stier Labs, Spokane, WA)] and a negative control (0.9% normal saline) were used. Antigens were employed in a standard volume of 0.1 mL except *Tetanus toxoid* [0.025 mL (0.2 limit of flocculation units per dose)] and were injected intradermally on the volar surface of the forearm by trained research staff. Vertical and horizontal diameters of induration after 24 and 48 h were measured, and mean values ≥5 mm were considered positive. Total diameter of induration was calculated from sum of the means of the 3 antigens.

Antibody responses to vaccines were measured at the end of the intervention. Three vaccines, Hepatitis A (HEP-A) (primary T cell-dependent), tetanus/diphtheria (TD) (secondary T cell-dependent) and pneumococcal (B cell dependent) (PN) were administered at month 17. A booster shot for HEP-A was administered at month 23. Blood for antibody response was collected at month 17 (before vaccination), 18, and 24 (after vaccination) for all vaccines, and 23 for before HEP-A booster. Anti-HEP-A virus (anti-HAV) antibodies (total immuno-globulin, IgM and IgG) were measured by chemi-luminescent immunoassay (Elecsys, Roche Diagnostics, Indianapolis, IN; CV=1.9 ± 1.4%), anti-diphtheria, and anti-tetanus toxoid IgG antibodies by EIA, and anti-*Streptococcus pneumonia* IgG antibodies (23 serotypes) by microsphere photometry at Mayo Medical Laboratories, Rochester, MN.

Complete blood count with differentials(CBC). CBC and white cell differential were assayed using automated methods employed by Esoterix Inc. (A LabCorp Company, Cranford, NJ)

Infection, asthma, allergies and antibiotic use. Self-reported infection, and asthma, allergy and antibiotic use, and their start and end date were recorded throughout the intervention period and coded based on severity (mild, moderate and severe) by the Coordinating Center in accordance with MedRA version 14.1 and WHO Drug Dictionary Enhanced-March 2012 guidelines.

Statistical methods. Methods for the overall CALERIE study have been described elsewhere [19]. Briefly, intention-to-treat analysis was performed by including all available observations. For continuous outcomes (CBC-Diff and inflammatory markers) repeated Mixed models analysis [44-46] were used to examine change from baseline, controlling for site, sex, BMI stratum, and the baseline value for the outcome of interest. Significant between-group differences at each time point were tested at α=0.05. Bonferroni correction was applied where appropriate [47] for between group p values while within group changes p-values were always protected by a Bonferroni correction.

For values beyond the limits of detection of the assay for antibody response, a parametric regression model used in survival analysis [48] was applied. Values above or below detection limits were considered censored at those points. Between-group tests were performed using the lognormal distribution for the outcome adjusting for site, sex, and BMI stratum.

For the three DTH antigens, individual positive values were analyzed using the generalized estimating equation model [49] with the logit link and the Bernoulli variance. The number of positive antigens (0, 1, 2 or 3) was treated as a binomial outcome and analyzed in a similar manner. The induration diameters were treated as continuous and were analyzed using the repeated measures model described above.

The annualized infection, allergy, and associated medication rates were derived as the total number of episodes (or drugs) divided by the amount of follow-up time. For any outcome, a between-group comparison was performed using a generalized linear model [50] with the *ln* link and the Poisson variance, adjusting for site, sex and BMI stratum; the natural logarithm of the

amount of follow-up time contributed by each participant was included as an offset. The incidence of any infection was treated as a binary outcome, and analyzed using the same *ln*-Poisson model with the modification suggested by Zou [51].

All analyses were performed by the statistical unit at Duke University Clinical Research Institute (DCRI, Durham, NC) using SAS software version 9.2 (SAS Institute Inc., Cary, NC).

Funding

The National Institute on Aging, National Institutes of Health Cooperative Agreements (U01AG022132, U01AG020478, U01AG020487, and U01AG020480); USDA Specific Cooperative Agreement #58-1950-0-014.

Clinical Trial Registry Number and Website

CALERIE, ID:NCT00427193, ClinicalTrials.gov.

Conflict of Interests Statement

None of the authors have conflict of interest.

REFERENCES

1. Fontana L, Partridge L and Longo VD. Extending healthy life span--from yeast to humans. Science. 2010;328:321-26.

2. Franceschi C and Campisi J. Chronic inflammation (inflammaging) and its potential contribution to age-associated diseases. J Gerontol A Biol Sci Med Sci. 2014; 69 Suppl 1:4-9.

3. Meyer TE, Kovacs SJ, Ehsani AA, Klein S, Holloszy JO and Fontana L. Long-term caloric restriction ameliorates the decline in diastolic function in humans. J Am Coll Cardiol. 2006; 47:398-402.

4. Howcroft TK, Campisi J, Louis GB, Smith MT, Wise B, Wyss-Coray T, Augustine AD, McElhaney JE, Kohanski R and Sierra F. The role of inflammation in age-related disease. Aging (Albany NY). 2013; 5:84-93. doi: 10.18632/aging.100531.

5. Koenig W. High-sensitivity C-reactive protein and atherosclerotic disease: from improved risk prediction to risk-guided therapy. Int J Cardiol. 2013; 168:5126-34.

6. Hotamisligil GS, Shargill NS and Spiegelman BM. Adipose expression of tumor necrosis factor-alpha: direct role in obesity-linked insulin resistance. Science. 1993; 259:87-91.

7. Lavie CJ, Milani RV, Verma A and O'Keefe JH. C-reactive protein and cardiovascular diseases--is it ready for primetime? Am J Med Sci. 2009; 338:486-92.

8. Taube A, Schlich R, Sell H, Eckardt K and Eckel J. Inflammation and metabolic dysfunction: links to cardiovascular diseases. Am J Physiol Heart Circ Physiol. 2012; 302:2148-65.

9. Kern PA, Saghizadeh M, Ong JM, Bosch RJ, Deem R and Simsolo RB. The expression of tumor necrosis factor in human adipose tissue. Regulation by obesity, weight loss, and relationship to lipoprotein lipase. J Clin Invest. 1995; 95:2111-19.

10. Zahorska-Markiewicz B, Janowska J, Olszanecka-Glinianowicz M and Zurakowski A. Serum concentrations of TNF-alpha and soluble TNF-alpha receptors in obesity. Int J Obes Relat Metab Disord. 2000; 24:1392-95.

11. Formoso G, Taraborrelli M, Guagnano MT, D'Adamo M, Di Pietro N, Tartaro A and Consoli A. Magnetic resonance imaging determined visceral fat reduction associates with enhanced IL-10 plasma levels in calorie restricted obese subjects. PLoS One. 2012; 7:52774.

12. Roecker EB, Kemnitz JW, Ershler WB and Weindruch R. Reduced immune responses in rhesus monkeys subjected to dietary restriction. J Gerontol A Biol Sci Med Sci. 1996; 51:276-79.

13. Gardner EM. Caloric restriction decreases survival of aged mice in response to primary influenza infection. J Gerontol A Biol Sci Med Sci. 2005; 60:688-94.

14. Ritz BW, Aktan I, Nogusa S and Gardner EM. Energy restriction impairs natural killer cell function and increases the severity of influenza infection in young adult male C57BL/6 mice. J Nutr. 2008; 138:2269-75.

15. Messaoudi I, Warner J, Fischer M, Park B, Hill B, Mattison J, Lane MA, Roth GS, Ingram DK, Picker LJ, Douek DC, Mori M and Nikolich-Zugich J. Delay of T cell senescence by caloric restriction in aged long-lived nonhuman primates. Proc Natl Acad Sci U S A. 2006; 103:19448-53.

16. Yang H, Youm YH and Dixit VD. Inhibition of thymic adipogenesis by caloric restriction is coupled with reduction in age-related thymic involution. J Immunol. 2009; 183:3040-52.

17. Schaible UE and Kaufmann SH. Malnutrition and infection: complex mechanisms and global impacts. PLoS Med. 2007; 4:115.

18. Stewart TM, Bhapkar M, Das S, Galan K, Martin CK, McAdams L, Pieper C, Redman L, Roberts S, Stein RI, Rochon J and Williamson DA. Comprehensive Assessment of Long-term Effects of Reducing Intake of Energy Phase 2 (CALERIE Phase 2) screening and recruitment: methods and results. Contemp Clin Trials. 2013; 34:10-20.

19. Ravussin E, Redman LM, Rochon J, Das SK, Fontana L, Kraus WE, Romashkan S, Williamson DA, Meydani SN, Villareal DT, Smith SR, Stein RI, Scott TM, et al. A 2-Year Randomized Controlled Trial of Human Caloric Restriction: Feasibility and Effects on Predictors of Health Span and Longevity. J Gerontol A Biol Sci Med Sci. 2015; 70:1097-1104.

20. Lam QL and Lu L. Role of leptin in immunity. Cell Mol Immunol. 2007; 4:1-13.

21. Ershler WB, Sun WH, Binkley N, Gravenstein S, Volk MJ, Kamoske G, Klopp RG, Roecker EB, Daynes RA and Weindruch R. Interleukin-6 and aging: blood levels and mononuclear cell production increase with advancing age and in vitro production is modifiable by dietary restriction. Lymphokine Cytokine Res. 1993; 12:225-30.

22. Fontana L. Neuroendocrine factors in the regulation of inflammation: excessive adiposity and calorie restriction. Exp Gerontol. 2009; 44:41-45.

23. Rienstra M, Sun JX, Magnani JW, Sinner MF, Lubitz SA, Sullivan LM, Ellinor PT and Benjamin EJ. White blood cell count and risk of incident atrial fibrillation (from the Framingham Heart Study). Am J Cardiol. 2012; 109:533-37.

24. Lorenzo C, Hanley AJ and Haffner SM. Differential white cell count and incident type 2 diabetes: the Insulin Resistance Atherosclerosis Study. Diabetologia. 2014; 57:83-92.

25. Shankar A, Klein BE and Klein R. Relationship between white blood cell count and incident hypertension. Am J Hypertens. 2004; 17:233-39.

26. Margolis KL, Manson JE, Greenland P, Rodabough RJ, Bray PF, Safford M, Grimm RH, Jr., Howard BV, Assaf AR and Prentice R. Leukocyte count as a predictor of cardiovascular events and mortality in postmenopausal women: the Women's Health Initiative Observational Study. Arch Intern Med. 2005; 165:500-508.

27. Toriola AT, Cheng TY, Neuhouser ML, Wener MH, Zheng Y, Brown E, Miller JW, Song X, Beresford SA, Gunter MJ, Caudill MA and Ulrich CM. Biomarkers of inflammation are associated with colorectal cancer risk in women but are not suitable as early detection markers. Int J Cancer. 2013; 132:2648-58.

28. Shankar A, Wang JJ, Rochtchina E, Yu MC, Kefford R and Mitchell P. Association between circulating white blood cell count and cancer mortality: a population-based cohort study. Arch Intern Med. 2006; 166:188-94.

29. Chae JS, Paik JK, Kang R, Kim M, Choi Y, Lee SH and Lee JH. Mild weight loss reduces inflammatory cytokines, leukocyte count, and oxidative stress in overweight and moderately obese participants treated for 3 years with dietary modification. Nutr Res. 2013; 33:195-203.

30. Loffreda S, Yang SQ, Lin HZ, Karp CL, Brengman ML, Wang DJ, Klein AS, Bulkley GB, Bao C, Noble PW, Lane MD and Diehl AM. Leptin regulates proinflammatory immune responses. FASEB J. 1998; 12:57-65.

31. Fontana L, Eagon JC, Trujillo ME, Scherer PE and Klein S. Visceral fat adipokine secretion is associated with systemic inflammation in obese humans. Diabetes. 2007; 56:1010-13.

32. Bordone L and Guarente L. Calorie restriction, SIRT1 and metabolism: understanding longevity. Nat Rev Mol Cell Biol. 2005; 6:298-305.

33. Guarente L. Mitochondria--a nexus for aging, calorie restriction, and sirtuins? Cell. 2008; 132:171-76.

34. Barzilai N, Huffman DM, Muzumdar RH and Bartke A. The critical role of metabolic pathways in aging. Diabetes. 2012; 61:1315-22.

35. Hotamisligil GS and Erbay E. Nutrient sensing and inflammation in metabolic diseases. Nat Rev Immunol. 2008; 8:923-34.

36. Ahmed T, Das SK, Golden JK, Saltzman E, Roberts SB and Meydani SN. Calorie restriction enhances T-cell-mediated immune response in adult overweight men and women. J Gerontol A Biol Sci Med Sci. 2009; 64:1107-13.

37. Clinthorne JF, Adams DJ, Fenton JI, Ritz BW and Gardner EM. Short-term re-feeding of previously energy-restricted C57BL/6 male mice restores body weight and body fat and attenuates the decline in natural killer cell function after primary influenza infection. J Nutr. 2010; 140:1495-1501.

38. Sun D, Muthukumar AR, Lawrence RA and Fernandes G. Effects of calorie restriction on polymicrobial peritonitis induced by cecum ligation and puncture in young C57BL/6 mice. Clin Diagn Lab Immunol. 2001; 8:1003-11.

39. Goldberg EL, Romero-Aleshire MJ, Renkema KR, Ventevogel MS, Chew WM, Uhrlaub JL, Smithey MJ, Limesand KH, Sempowski GD, Brooks HL and Nikolich-Zugich J. Lifespan-extending caloric restriction or mTOR inhibition impair adaptive immunity of old mice by distinct mechanisms. Aging Cell. 2015; 14:130-38.

40. Kristan DM. Chronic calorie restriction increases susceptibility of laboratory mice (Mus musculus) to a primary intestinal parasite infection. Aging Cell. 2007; 6:817-25.

41. Rochon J, Bales CW, Ravussin E, Redman LM, Holloszy JO, Racette SB, Roberts SB, Das SK, Romashkan S, Galan KM, Hadley EC and Kraus WE. Design and conduct of the CALERIE study: comprehensive assessment of the long-term effects of reducing intake of energy. J Gerontol A Biol Sci Med Sci. 2011; 66:97-108.

42. Pieper C, Redman L, Racette S, Roberts S, Bhapkar M, Rochon J, Martin C, Kraus W, Das S, Williamson D and Ravussin E. Development of adherence metrics for caloric restriction interventions. Clin Trials. 2011; 8:155-64.

43. Rickman AD, Williamson DA, Martin CK, Gilhooly CH, Stein RI, Bales CW, Roberts S and Das SK. The CALERIE Study: design and methods of an innovative 25% caloric restriction intervention. Contemp Clin Trials. 2011; 32:874-81.

44. Diggle PJ, Heagerty P, Liang K-Y and Zeger SL. Analysis of Longitudinal Data. 2002. New York: Oxford University Press.

45. Fitzmaurice G, Laird NM and Ware JH. Applied Longitudinal Analysis. 2002. New York City: Wiley.

46. Jennrich RI and Schluchter MD. Unbalanced repeated-measures models with structured covariance matrices. Biometrics. 1986; 42:805-20.

47. Wright S. Adjusted P-values for simultaneous inference. Biometrics. 1992; 48:1005-13.

48. Lawless J. Statistical Models and Methods for Lifetime Data. 2003.New York: John Wiley & Sons.

49. Liang KY. Longitudinal data analysis using generalized linear models. Biometrika 1986; 78:13-22.

50. McCullagh P and Nelder JA. Generalized Linear Models. 1989. London New York: Chapman and Hall.

51. Zou G. A modified poisson regression approach to prospective studies with binary data. Am J Epidemiol. 2004; 159:702-06.

SUPPLEMENTAL DATA

Appendix Table 1. Effect of calorie restriction on white blood cells*

Variable (time)	Treatment Group		p-value ‡
	CR	AL	
Total monocytes (10^3/μL)			
Baseline	0.33 (0.01)	0.32 (0.01)	
Mo. 12	0.32 (0.01)	0.37 (0.01) †	0.004
Mo. 24	0.32 (0.01)	0.35 (0.01) †	0.034
Total Neutrophils (10^3/μL)			
Baseline	3.68 (0.11)	3.60 (0.13)	
Mo. 12	3.41 (0.12) †	3.71 (0.16)	0.106
Mo. 24	3.24 (0.10) †	3.54 (0.14)	0.067
Total Eosinophils (10^3/μL)			
Baseline	0.14 (0.01)	0.11 (0.01)	
Mo. 12	0.14 (0.01)	0.12 (0.01)	0.095
Mo. 24	0.13 (0.01)	0.15 (0.01)	0.102
Total Basophils (10^3/μL)			
Baseline	0.01 (0.001)	0.02 (0.002)	
Mo. 12	0.021 (0.002) †	0.025 (0.002) †	0.378
Mo. 24	0.020 (0.002) †	0.024 (0.002) †	0.443

* Results are mean (SE) and reflect predicted values at months 12 and 24 based on intention-to-treat (ITT) statistical analysis, p-values reflect the ITT analyses for changes from baseline at each time point.

† Significantly different from baseline within the same treatment group.

‡ Values reflect difference in change from baseline between treatment groups at each time point.

Appendix Table 2. Effect of calorie restriction on antibody response to Hepatitis A, Tetanus/Diphtheria and Pneumococcal vaccines						
	Median (IQR)*			% with detectable values		
Time (Mos.)	17	18	24	17	18	24
Hepatitis A (IU/L)						
AL	9.7 (7.8, 11.7)	41.7 (29.5, 53.7)	NA	42.9%	27.5%	0%†
CR	8.6 (7.5, 10.3)	37.3 (26.0, 53.0)	28.5 (16.4, 40.7)	28.0%	23.2%	5.1%†
p-value	0.601‡	0.983‡	NA	0.670	0.832	0.332
Tetanus (IU/mL)						
AL	2.43 (1.8, 3.5)	4.95 (3.8, 5.9)	3.31 (2.6, 4.1)	90.2%	51.7%	79.3%
CR	2.56 (1.7, 3.9)	4.37 (3.3, 5.7)	3.70 (2.6, 5.0)	93.1%	52.9%	79.4%
p-value	0.675	0.775	0.940	0.499‡	0.876‡	0.992‡
Diphtheria (IU/mL)						
AL	0.36 (0.2, 0.7)	1.1 (0.7, 1.9)	0.77 (0.4, 1.1)	100%	93.3%	98.3%
CR	0.35 (0.2, 0.7)	1.1 (0.7, 1.5)	0.75 (0.4, 1.3)	98%	87.3%	100%
p-value	0.350	0.644	0.901	0.273	0.416	0.196
Pneumonia IgG Serotype 1 (µg/mL)						
AL	1.5 (0.8, 4.5)	10.0 (3.7, 35.4)	8.1 (3.1, 30.5)	85.7%	95.1%	100%
CR	1.7 (0.8, 3.9)	7.0 (2.5, 23.7)	6.3 (2.9, 21.3)	77.9%	96.1%	94.6%
p-value	0.604	0.474	0.233	0.356	0.624	0.314
Pneumonia IgG Serotype 2 (µg/mL)						
AL	0.65 (0.4, 1.3)	5.5 (2.2, 9.3)	4.3 (2.1, 12.5)	88.9%	94.3%	100%
CR	0.70 (0.4, 1.5)	3.7 (1.7, 10.7)	3.5 (1.4, 9.9)	80.4%	100%	98.8%
p-value	0.437	0.553	0.296	0.185	0.448	0.456
Pneumonia IgG Serotype 3 (µg/mL)						
AL	1.0 (0.5, 2.8)	3.8 (1.6, 8.0)	2.9 (1.1, 7.7)	90.5%	98.4%	98.1%
CR	1.2 (0.5, 2.8)	3.2 (1.8, 7.1)	2.5 (1.2, 6.6)	88.3%	99.0%	98.9%
p-value	0.853	0.973	0.599	0.971	0.702	0.676
Pneumonia IgG Serotype 4 (µg/mL)						
AL	0.5 (0.2, 1.6)	1.3 (0.5, 3.6)	1.1 (0.4, 3.9)	76.2%	100%	100%
CR	0.4 (0.2, 1.0)	1.7 (0.9, 4.2)	1.2 (0.7, 3.2)	78.8%	98.1%	97.8%
p-value	0.856	0.158	0.598	0.498	1.00	1.00
Pneumonia IgG Serotype 5 (µg/mL)						
AL	2.8 (1.0, 5.2)	4.7 (2.6, 13.4)	4.1 (2.3, 11.3)	96.8%	100%	100%
CR	3.0 (1.2, 5.1)	4.5 (2.0, 12.8)	4.9 (2.1, 11.5)	95.2%	100%	100%
p-value	0.788	0.792	0.944	0.611	0.611	0.611
Pneumonia IgG Serotype 8 (µg/mL)						
AL	1.1 (0.6, 2.6)	3.5 (1.8, 7.5)	3.0 (1.5, 6.9)	100%	100%	100%
CR	1.1 (0.5, 2.6)	2.6 (1.2, 6.4)	2.6 (1.3, 5.3)	99.0%	99.0%	98.9%
p-value	0.511	0.433	0.357	0.436	0.444	0.455
Pneumonia IgG Serotype 14 (µg/mL)						
AL	3.2 (1.3, 5.2)	11.7 (4.3, 30.6)	13.6 (4.2, 29.4)	74.6%	93.4%	86.5%
CR	2.2 (1.2, 4.8)	9.7 (2.8, 31.7)	9.5 (3.0, 27.8)	72.1%	90.4%	90.3%
p-value	0.423	0.357	0.908	0.726	0.498	0.487
Pneumonia IgG Serotype 20 (µg/mL)						
AL	0.8 (0.4, 1.8)	3.0 (1.0, 11.9)	2.5 (0.9, 5.3)	79.4%	98.4%	96.2%
CR	0.8 (0.5, 1.8)	2.2 (0.9, 7.6)	2.1 (0.7, 5.9)	75.0%	94.2%	93.5%
p-value	0.777	0.215	0.514	0.723	0.503	0.910
Pneumonia IgG Serotype 6B (µg/mL)						
AL	2.5 (1.2, 5.2)	5.1 (2.8, 11.9)	4.3 (2.3, 10.2)	85.7%	93.4%	92.3%
CR	2.7 (1.4, 4.8)	5.2 (3.0, 12.7)	5.3 (2.8, 11.9)	82.7%	96.2%	92.4%
p-value	0.876	0.401	0.564	0.854	0.187	0.630

Pneumonia IgG Serotype 7F (µg/mL)						
AL	3.0 (1.7, 6.8)	5.2 (2.6, 11.4)	4.8 (2.5, 9.6)	98.4%	96.7%	98.1%
CR	2.8 (1.5, 5.3)	4.8 (2.3, 10.1)	4.8 (2.7, 9.3)	95.2%	95.2%	97.8%
p-value	0.395	0.639	0.910	0.280	0.385	0.927
Continued to next page						
	Median (IQR)*			% with detectable values		
Time (Mos.)	17	18	24	17	18	24
Pneumonia IgG Serotype 9N (µg/mL)						
AL	1.3 (0.7, 3.2)	2.4 (1.2, 8.0)	2.5 (1.2, 6.5)	90.5%	100%	100%
CR	1.4 (0.6, 3.5)	2.8 (1.2, 6.0)	2.7 (1.2, 6.3)	77.9%	95.1%	95.7%
p-value	0.140	0.633	0.674	0.083	0.734	0.457
Pneumonia IgG Serotype 9V (µg/mL)						
AL	2.1 (1.0, 4.0)	3.9 (1.3, 11.2)	4.3 (1.7, 9.1)	95.2%	96.7%	96.2%
CR	1.9 (1.0, 4.7)	3.4 (1.6, 8.2)	3.5 (1.6, 8.4)	92.3%	96.2%	96.8%
p-value	0.636	0.162	0.215	0.461	0.851	0.845
Pneumonia IgG Serotype 10A (µg/mL)						
AL	1.9 (0.9, 5.0)	3.4 (1.6, 13.9)	2.8 (1.3, 8.0)	85.7%	88.5%	92.3%
CR	2.7 (0.9, 5.0)	3.8 (1.3, 9.5)	3.0 (1.1, 8.0)	76.9%	89.4%	89.2%
p-value	0.393	0.681	0.325	0.168	0.859	0.551
Pneumonia IgG Serotype 11A (µg/mL)						
AL	1.1 (0.5, 2.2)	3.4 (1.9, 8.8)	2.9 (1.5, 6.8)	87.3%	98.4%	100%
CR	1.2 (0.5, 4.2)	4.1 (2.0, 8.6)	3.6 (1.6, 8.1)	94.2%	100%	98.9%
p-value	0.093	0.799	0.905	0.118	0.194	0.455
Pneumonia IgG Serotype 12F (µg/mL)						
AL	0.4 (0.2, 1.0)	0.6 (0.3, 2.0)	0.7 (0.3, 2.5)	81.0%	91.8%	90.4%
CR	0.6 (0.3, 2.1)	1.2 (0.4, 3.9)	1.0 (0.4, 4.1)	74.0%	92.3%	89.2%
p-value	0.626	0.211	0.395	0.308	0.908	0.830
Pneumonia IgG Serotype 15B (µg/mL)						
AL	0.8 (0.4, 1.6)	3.7 (1.7, 13.7)	3.0 (1.5, 11.9)	84.1%	98.4%	100%
CR	0.8 (0.4, 2.0)	4.1 (1.6, 13.0)	4.0 (1.6, 10.4)	84.6%	98.1%	96.8%
p-value	0.577	0.650	0.672	0.933	0.452	0.192
Pneumonia IgG Serotype 17F (µg/mL)						
AL	3.2 (1.5, 6.4)	12.1 (4.7, 21.9)	10.3 (4.0, 19.8)	85.7%	98.4%	100%
CR	3.0 (1.6, 6.0)	11.1 (5.0, 24.8)	10.8 (5.7, 19.4)	89.4%	98.1%	97.8%
p-value	0.739	0.785	0.897	0.476	0.896	0.289
Pneumonia IgG Serotype 18C (µg/mL)						
AL	0.6 (0.3, 1.4)	3.5 (1.0, 10.2)	3.4 (1.1, 9.4)	68.3%	98.4%	92.3%
CR	0.8 (0.5, 2.0)	4.4 (1.5, 10.8)	4.3 (1.3, 8.6)	71.2%	98.1%	97.8%
p-value	0.239	0.303	0.344	0.693	0.896	0.109
Pneumonia IgG Serotype 19A (µg/mL)						
AL	4.7 (2.6, 12.5)	8.5 (3.6, 24.8)	11.3 (4.8, 23.7)	76.2%	88.3%	86.3%
CR	4.3 (2.3, 9.4)	13.0 (5.7, 38.0)	12.9 (4.8, 39.2)	79.4%	89.0%	89.9%
p-value	0.798	0.451	0.581	0.628	0.611	0.957
Pneumonia IgG Serotype 19F (µg/mL)						
AL	2.7 (1.3, 5.1)	5.2 (2.6, 16.6)	3.9 (2.0, 13.8)	74.6%	86.9%	90.4%
CR	2.9 (1.5, 5.6)	8.4 (2.9, 18.0)	5.9 (2.5, 12.0)	84.6%	91.3%	93.5%
p-value	0.063	0.228	0.256	0.062	0.200	0.254
Pneumonia IgG Serotype 22F (µg/mL)						
AL	4.2 (2.1, 8.0)	5.2 (2.7, 10.2)	4.9 (2.5, 10.6)	96.8%	95.1%	98.1%
CR	3.3 (1.6, 8.8)	3.6 (2.0, 10.1)	4.5 (2.0, 9.0)	91.3%	96.2%	95.7%
p-value	0.165	0.413	0.379	0.031	0.503	0.453

Pneumonia IgG Serotype 23F (µg/mL)						
AL	7.8 (3.2, 16.4)	8.8 (3.3, 20.0)	8.1 (3.4, 21.0)	95.2%	93.4%	96.2%
CR	7.5 (2.8, 16.2)	9.3 (3.7, 21.0)	9.6 (3.5, 18.8)	92.3%	94.2%	93.5%
p-value	0.532	0.726	0.505	0.461	0.524	0.511
Pneumonia IgG Serotype 33F (µg/mL)						
AL	1.2 (0.6, 2.9)	4.3 (1.3, 13.0)	4.4 (1.5, 11.2)	85.7%	100%	98.1%
CR	0.9 (0.5, 2.4)	5.0 (1.8, 9.6)	4.2 (1.8, 12.5)	89.4%	96.2%	97.8%
p-value	0.363	0.636	0.980	0.285	0.444	0.441

* Based on observations within detectable range. IQR, Inter-Quartile Range
† For Hepatitis A values reflect those above the detectable range.
‡ p-values are from statistical analysis accounting for censoring.
NA: Since majority of values were beyond the detectable range quantitative analysis could not be performed.

Appendix Table 3A. Annualized Rate of Infections, Allergies and Associated Medications Over the 24-Month Follow-up

	AL (N=75)			CR (N=143)			
Event	**Total No. Episodes***	**Average No. Days†**	**Annualized Rate‡**	**Total No. Episodes***	**Average No. Days†**	**Annualized Rate‡**	**p-value§**
All Infections	156	14.5	1.032	239	9.8	0.897	0.2838
Total respiratory infections	115	11.9	0.761	169	7.2	0.635	0.2099
Upper respiratory infections	108	10.9	0.715	165	6.9	0.620	0.3684
Lower respiratory infections	7	1.0	0.046	4	0.2	0.015	0.0583
GI infections	7	0.2	0.046	18	0.4	0.068	0.3602
Skin infections	9	0.7	0.060	7	0.2	0.026	0.1161
Urinary track infections	6	0.5	0.040	11	0.4	0.041	0.9154
Ear infections	4	0.3	0.026	2	0.1	0.008	0.1420
Eye infections	0	0.0	0.000	5	0.1	0.019	0.0357
Oral dental infections	6	0.3	0.040	19	0.9	0.071	0.1445
Allergies	36	1.3	0.238	47	1.2	0.176	0.1912
OTC Medication Use	190	145.0	1.257	346	229.9	1.299	0.7120
Allergy Medication Use	82	55.5	0.543	138	50.8	0.518	0.7871
Antibiotics Medication Use	71	35.6	0.470	139	33.9	0.522	0.4516

* Total number of distinct episodes summed across participants in that treatment arm.
† The total number of days during which the event was prevalent across participants in that treatment arm, divided by the number of participants in that treatment group
‡ Total number of distinct events divided by the total amount of follow-up time in that treatment arm, standardized to 365 days in a calendar year.
§ The p-value is derived from the Poisson regression model comparing the number of distinct episodes between the two groups.

Appendix Table 3B. Distribution of the Severity of the Events, Pooled Across all Events Among Participants Who Experienced the Event at Least Once

	AL (N=75)				CR (N=143)			
Event	**No. Pts >=1 event***	**Mild†**	**Moderate**	**Severe**	**No. Pts >=1 event***	**Mild†**	**Moderate**	**Severe**
All Infections	53	70 (44.9%)	64 (41.0%)	22 (14.1%)	89	99 (41.4%)	111 (46.4%)	29 (12.1%)
Total respiratory infections	48	51 (44.3%)	51 (44.3%)	13 (11.3%)	79	71 (42.0%)	77 (45.6%)	21 (12.4%)
Upper respiratory infections	46	49 (45.4%)	47 (43.5%)	12 (11.1%)	79	70 (42.4%)	74 (44.8%)	21 (12.7%)
Lower respiratory infections	5	2 (28.6%)	4 (57.1%)	1 (14.3%)	4	1 (25.0%)	3 (75.0%)	0
GI infections	7	2 (28.6%)	1 (14.3%)	4 (57.1%)	14	6 (33.3%)	8 (44.4%)	4 (22.2%)
Skin infections	7	6 (66.7%)	3 (33.3%)	0	7	3 (42.9%)	3 (42.9%)	1 (14.3%)
Urinary track infections	4	2 (33.3%)	3 (50.0%)	1 (16.7%)	8	1 (9.1%)	10 (90.9%)	0
Ear infections	3	0	1 (25.0%)	3 (75.0%)	2	0	0	2 (100.0%)
Eye infections	0	0	0	0	4	3 (60.0%)	2 (40.0%)	0
Oral dental infections	4	3 (50.0%)	3 (50.0%)	0	7	10 (52.6%)	8 (42.1%)	1 (5.3%)
Allergies	16	27 (75.0%)	6 (16.7%)	3 (8.3%)	23	28 (59.6%)	13 (27.7%)	6 (12.8%)

* Number of participants who experienced the event at least once in that treatment arm.
† The frequency and percent of all such events pooled across all events across all participants who experienced that event at least once.

Research Paper

Measuring aging rates of mice subjected to caloric restriction and genetic disruption of growth hormone signaling

Jacob J.E. Koopman[1,2], Diana van Heemst[1,2], David van Bodegom[1,2], Michael S. Bonkowski[3,4], Liou Y. Sun[3,5], and Andrzej Bartke[3]

[1]Section of Gerontology and Geriatrics, Department of Internal Medicine, Leiden University Medical Center, Leiden, the Netherlands
[2]Leyden Academy on Vitality and Ageing, Leiden, the Netherlands
[3]Division of Geriatric Research, Department of Internal Medicine, Southern Illinois University School of Medicine, Springfield, IL 62794-9628, USA
[4]Paul F. Glenn Laboratory, Department of Biology, Massachusetts Institute of Technology, Cambridge, MA 02139, USA
[5]Department of Biology, University of Alabama at Birmingham, Birmingham, AL 35294, USA

Key words: aging, aging rate, mice, caloric restriction, growth hormone, Gompertz model
Received: 01/12/16; Accepted: 02/03/16; Published: 03/07/16 **doi:** 10.18632/aging.100919
Correspondence to: Jacob J.E. Koopman, MD/PhD; **E-mail:** j.j.e.koopman@lumc.nl

Abstract: Caloric restriction and genetic disruption of growth hormone signaling have been shown to counteract aging in mice. The effects of these interventions on aging are examined through age-dependent survival or through the increase in age-dependent mortality rates on a logarithmic scale fitted to the Gompertz model. However, these methods have limitations that impede a fully comprehensive disclosure of these effects. Here we examine the effects of these interventions on murine aging through the increase in age-dependent mortality rates on a linear scale without fitting them to a model like the Gompertz model. Whereas these interventions negligibly and non-consistently affected the aging rates when examined through the age-dependent mortality rates on a logarithmic scale, they caused the aging rates to increase at higher ages and to higher levels when examined through the age-dependent mortality rates on a linear scale. These results add to the debate whether these interventions postpone or slow aging and to the understanding of the mechanisms by which they affect aging. Since different methods yield different results, it is worthwhile to compare their results in future research to obtain further insights into the effects of dietary, genetic, and other interventions on the aging of mice and other species.

INTRODUCTION

Extensive experiments have demonstrated that caloric restriction and genetic disruption of growth hormone signaling can profoundly counteract aging in mice [1]. Caloric restriction — or dietary restriction — is an environmental intervention, whereby the usual *ad libitum* dietary intake is limited to an intake of 30-40% less. Mice subjected to caloric restriction can live up to 60% longer, suffer less often and at higher ages from age-associated disorders, and exhibit less molecular stress and damage [2, 3]. Disruption of growth hormone signaling is a genetic intervention, whereby the production of growth hormone-releasing hormone, growth hormone, or the receptor of growth hormone is impaired, so that the effects of growth hormone are annulled. Mice with disrupted growth hormone signaling can live up to 70% longer, suffer less often and at higher ages from age-associated disorders, have youthful metabolic characteristics such as a higher insulin sensitivity, and have an enhanced resistance against molecular-genetic stress and damage [4-7].

A population's aging is defined as an increase in the risk of death with increasing age [8, 9]. Following this definition, the effects of caloric restriction and genetic disruption of growth hormone signaling on aging are generally examined through age-dependent survival or age-dependent mortality. Age-dependent survival can easily be determined and depicted for relatively small populations and reveals the effects on life expectancy. However, since age-dependent survival and life expectancy do not reveal at which ages and to what extent the risk of death increases, they conceal the effects on aging [10-12]. Age-dependent mortality reveals the effects on aging when it is expressed as an age-dependent mortality rate, which describes the age-dependent risk of death. Age-dependent mortality rates are generally fitted to the Gompertz model, after which they increase linearly with age on a logarithmic scale. The linear increase of such a modeled mortality rate is classically interpreted as an aging rate [8, 10]. However, the use of the Gompertz model constrains mortality rates to increase linearly on a logarithmic scale, which may not correspond with the increases in the crude age-dependent mortality rates, especially in relatively small populations [13, 14]. Moreover, it has been demonstrated theoretically and empirically that the linear increase in a mortality rate on a logarithmic scale, as modeled by the Gompertz model, is an inaccurate measure of the aging rate [15-18]. Therefore, alternative methods are needed to accurately examine the effects of interventions such as caloric restriction and genetic disruption of growth hormone signaling on age-dependent mortality rates.

We have validated a method to derive aging rates from the increase in a mortality rate with age on a linear scale instead of a logarithmic scale [16, 17]. We have substantiated elsewhere that aging is measured more accurately on a linear than a logarithmic scale [18]. This method can be applied without the need to fit the mortality rates to the Gompertz model or any similar model [14]. In this manner, the method does not assume mortality rates to conform to any specific age pattern, but is sensitive to changes in the crude mortality rates at all ages and is solely based on and closely aligns with the definition of aging as an increase in the risk of death with age. As an advantageous consequence, the method is applicable to populations of any species and of relatively small sizes. Here we compare this method with the classically used method in order to examine the effects of caloric restriction and genetic disruption of growth hormone signaling on murine aging.

RESULTS

We derived aging rates from age-dependent mortality rates in two study populations of mice, referred to as Population A and Population B. Both populations included four groups of mice subjected to caloric restriction, disruption of growth hormone signaling, both, or none of these interventions. In Population A, caloric restriction entailed an intake of 30% less than the *ad libitum* dietary intake and growth hormone signaling was disrupted by knockout of the growth hormone receptor gene *Ghr/Ghrbp* [19]. In Population B, caloric restriction entailed an intake of 40% less than the *ad libitum* dietary intake and growth hormone signaling was disrupted by knockout of the growth hormone-releasing hormone gene *Ghrh* [20]. The sizes and life expectancies of the four groups of mice in each population are given in Table 1.

Figures 1A and 1B show the age-dependent survival of the groups of mice in both study populations. These two figures have been published previously [19, 20] and are given here as references. In Population A, the mice subjected to caloric restriction, disruption of growth hormone signaling, or both survived longer than the mice not subjected to these interventions. In Population B, the mice subjected to both caloric restriction and disruption of growth hormone signaling survived longest, the mice subjected to either of these interventions had intermediate survival, and the mice not subjected to these interventions survived shortest. Aging rates cannot be discerned from these figures.

Figures 1C and 1D show the age-dependent mortality rates of the groups of mice in both study populations on a logarithmic scale. In Population A, the mice subjected to caloric restriction, disruption of growth hormone signaling, or both had similar mortality rates that were lower at all ages than that of the mice not subjected to these interventions. In Population B, the mice subjected to both caloric restriction and disruption of growth hormone signaling had the lowest mortality rate, the mice subjected to either of these interventions had intermediate mortality rates, and the mice not subjected to these interventions had the highest mortality rate. The mortality rates of all groups of mice in both populations increased in a linear manner.

The linear increase in mortality rate with age on a logarithmic scale is classically interpreted as an aging rate. This linear increase is most accurately — and therefore most often — measured using the Gompertz model or a similar model [21]. We measured the linear increase in the mortality rate of each group of mice in both populations by fitting each age-dependent mortality rate to the Gompertz model. The aging rates estimated by this classical method did not differ consistently between the groups of mice in both study populations, as reported in Table 2.

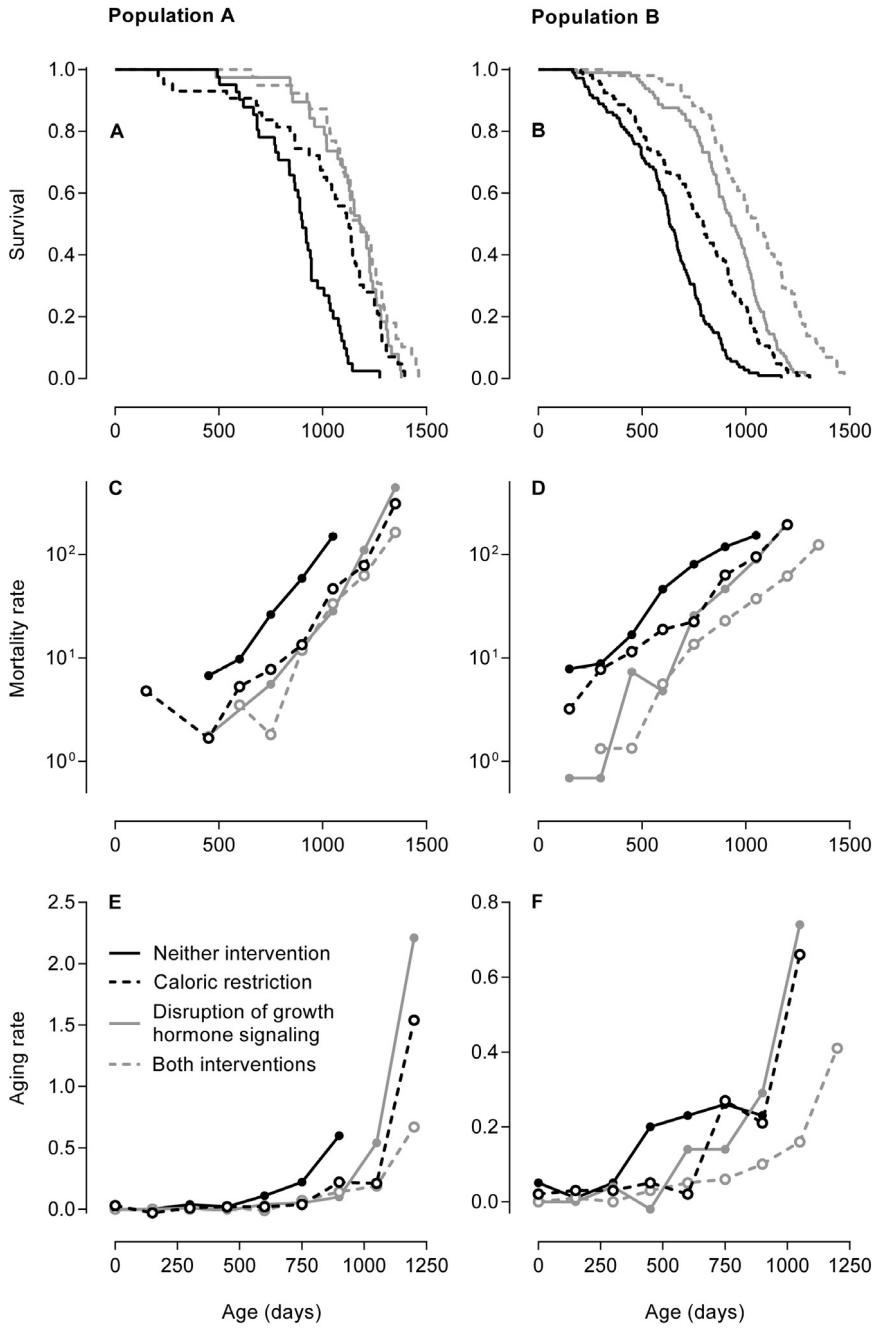

Figure 1. Three methods to examine the effects of caloric restriction and/or genetic disruption of growth hormone signaling on aging in mice. In Population A, caloric restriction entailed an intake of 30% less than the *ad libitum* dietary intake and growth hormone signaling was disrupted by knockout of the growth hormone receptor gene *Ghr/Ghrbp* [19]. In Population B, caloric restriction entailed an intake of 40% less than the *ad libitum* dietary intake and growth hormone signaling was disrupted by knockout of growth hormone-releasing hormone gene *Ghrh* [20]. **(A, B)** Age-dependent survival of the groups of mice in Population A (**A**) and Population B (**B**) depicted as Kaplan-Meier curves. These two figures have been published previously [19, 20] and are given here as references. The copyright of Figure 1A is with the National Academy of Sciences of the USA; the copyright of Figure 1B is with the authors of the original publication [20]. **(C, D)** Age-dependent mortality rates of the groups of mice in Population A (**C**) and Population B (**D**) given on a logarithmic scale. The mortality rates are expressed in deaths per 10,000 mice per day. The linear increase in mortality rate on a logarithmic scale is classically interpreted as an aging rate. **(E, F)** Age-dependent aging rates of the groups of mice in Population A (**E**) and Population B (**F**). Contrary to the aging rates estimated by the classical method in Table 2, these aging rates were calculated without modeling the age-dependent mortality rates, describe the increases in the mortality rates on a linear scale, and are dependent on age themselves. The aging rates are expressed in deaths per 10,000 mice per day per day, which equals the change in mortality rate per day.

Alternatively to the aging rates estimated by the classical method, we calculated aging rates as the increases in the mortality rates with age on a linear scale without fitting the mortality rates to the Gompertz model or any similar model. Figures 1E and 1F show these aging rates for the different groups of mice in both study populations. The aging rates of all groups of mice in both populations increased with age in an exponential manner. In Population A, the aging rates of the mice subjected to caloric restriction, disruption of growth hormone signaling, or both increased at higher ages and to higher levels than that of the mice not subjected to these interventions. In Population B, the aging rate of the mice subjected to both caloric restriction and disruption of growth hormone signaling increased at the highest ages to an intermediate level, the aging rates of mice subjected to either of these intervention were similar and increased at intermediate ages to the highest levels, and the aging rate of mice not subjected to these interventions increased at the lowest ages to the lowest level.

We repeated our analyses after stratifying male and female mice, which yielded similar results (data not shown).

Table 1. Life expectancies of mice subjected to caloric restriction and/or genetic disruption of growth hormone signaling.

Caloric restriction	–	+	–	+
Disruption of growth hormone signaling	–	–	+	+
Population A				
Number of mice	41	43	38	39
Median life expectancy	903	1127	1181	1188
Increase in median life expectancy	Ref.	25%	31%	32%
Maximal life expectancy	1275	1395	1379	1462
Increase in maximal life expectancy	Ref.	9%	8%	15%
Population B				
Number of mice	108	105	97	102
Median life expectancy	634	794	931	1056
Increase in median life expectancy	Ref.	25%	47%	67%
Maximal life expectancy	1171	1307	1308	1537
Increase in maximal life expectancy	Ref.	12%	12%	31%

Median and maximal life expectancies are given in days. Increases in median and maximal life expectancies are given relative to the mice not subjected to caloric restriction or disruption of growth hormone signaling (Ref.).

Table 2. Aging rates of mice subjected to caloric restriction and/or genetic disruption of growth hormone signaling according to the classical method.

Caloric restriction	–	+	–	+
Disruption of growth hormone signaling	–	–	+	+
Population A	6.1 (4.6 to 7.5)	4.9 (3.6 to 6.2)	7.6 (5.6 to 9.6)	6.4 (4.9 to 8.0)
Population B	4.5 (3.8 to 5.3)	3.9 (3.2 to 4.6)	5.7 (4.8 to 6.6)	4.5 (3.8 to 5.2)

Aging rates estimated by the classical method are given with 95% confidence intervals and are shown × 1000 for legibility. These aging rates are expressed in units per day. These aging rates were estimated using the Gompertz model, equal the Gompertz model's parameter γ, and describe the linear increases in the mortality rates on a logarithmic scale.

DISCUSSION

This study aims to examine the effects of caloric restriction and genetic disruption of growth hormone signaling on murine aging by comparing a method that calculates an aging rate as the increase in a mortality rate with age on a linear scale without the need to fit the mortality rate to the Gompertz model or any similar model with the classically used model that estimates an aging rate as the increase in a mortality rate with age on a logarithmic scale modeled with the Gompertz model. It shows that the methods yield different results. According to the classical method, these interventions negligibly and non-consistently affected the aging rates (Table 2). By contrast, according to the alternative method studied here, the aging rates of mice subjected to caloric restriction or disruption of growth hormone signaling increased at higher ages and to higher levels as compared with mice not subjected to these interventions (Figures 1E and 1F).

A key question in research on aging is whether increases in life expectancy reflect a postponement or a slowing of aging. The answer to this question is pivotal to gain insight in the mechanisms of aging, to identify interventions that modulate these mechanisms, and to predict the effects of such interventions on aging [22]. However, with respect to caloric restriction and disruption of growth hormone signaling, a clear answer to this question is lacking. While caloric restriction has long been assumed to slow aging, it is debated whether it postpones aging instead [3, 9, 23, 24]. Likewise, some presume that genetic disruption of growth hormone signaling slows aging [4], whereas others pose that it rather postpones aging [10].

Research on the effects of caloric restriction and disruption of growth hormone signaling — and other interventions — on aging is hampered by the variety of methods that measure aging through the increase in the risk of death with age [8, 9, 15, 16, 18]. The examination of age-dependent survival is unsuitable to reveal the effects of the interventions on aging and to distinguish between postponed and slowed aging [9-11, 23]. The classically used method, which fits age-dependent mortality rates to the Gompertz model and interprets their linear increases on a logarithmic scale as aging rates, suits this purpose. It identifies a slowing of aging as a flattening of a mortality rate's linear increase and identifies a postponement of aging as a lowering of a mortality rate while its linear increase remains unaltered [8, 10, 24]. However, the validity of the classical method has been disputed [15-17].

According to the classical method, caloric restriction and disruption of growth hormone signaling did not affect the aging rates, but would be interpreted to postpone aging. The alternative method studied here, by contrast, yields age-dependent aging rates that allow for a more variegated assessment beyond the question of a mere postponement or slowing of aging. This method interprets these interventions to affect the aging rates in an age-dependent manner: aging was slowed at lower ages, postponed until higher ages, but quickened at higher ages. Such a pattern resembles a compression of aging, whereby aging is postponed as well as intensified, reflected by a risk of death that increases sharply at a high age [25]. A compression of aging also becomes apparent from the life expectancies of the mice (Table 1): these interventions bring about an increase in median life expectancy that is two to four times larger

than the increase in maximal life expectancy, indicating a sharper increase in the risk of death at a higher age. This effect was shared by caloric restriction and genetic disruption of growth hormone signaling. When both interventions were applied jointly, their effects were mutually reinforced only in Population B — subjected to a caloric restriction of 40% of the *ad libitum* dietary intake and knockout of the growth hormone-releasing hormone gene — but not in Population A — subjected to a caloric restriction of 30% of the *ad libitum* dietary intake and knockout of the growth hormone receptor gene. These results are in line with previous observations in these populations of mice (Figures 1A and 1B) [19, 20].

The classical method has been employed intensively to study the effects of caloric restriction on murine aging. It has yielded inconsistent results in individual studies [3, 9, 23, 26]. When these individual studies are compiled, it has yielded the conclusions that caloric restriction both postpones and slows [27] or only slows aging in mice [21], while disagreement exists over the correct application of the classical method [21]. Since the alternative method studied here yields different conclusions about the effects of these interventions on murine aging, it calls for a reevaluation of the previous studies with the use of this method.

The effects of caloric restriction and genetic disruption of growth hormone signaling on murine aging are not universally equal. They differ, for example, between sexes and genetic backgrounds of mice [5, 6, 26, 28, 29]. We found similar effects in male and female mice in two genetically distinct populations. More research is warranted to establish whether the alternative method studied here finds similar effects in other study populations of mice or, if different effects are found, which of the populations' characteristics explain the differences in the results. Moreover, the method explored here can be used to examine the effects on aging of other interventions and in other species.

This study explores the different methods to examine the effects of caloric restriction and genetic disruption of growth hormone signaling on murine aging. It is beyond the aim of this study to discuss the mechanisms through which these interventions influence aging; these mechanisms are elaborately discussed in other publications, such as those referenced here. Still, the alternative method studied here may provide insight into these mechanisms. The question whether caloric restriction and disruption of growth hormone signaling postpone or slow aging is often related to the accumulation of physical damage that is thought to underlie aging, for example due to oxidative stress. While a postponement of aging is regarded to reflect an improvement of health at all ages, only a slowing of aging is regarded to reflect a decreased pace at which damage accumulates or an increased ability with which the damage can be repaired [3, 9, 23, 24]. In addition, the age at which mortality rates start to increase is related to the pace at which damage accumulates [30]. As the alternative method points to a compression of aging, it suggests that the accumulation of damage is modulated differently at different ages and suggests that aging is modulated through more complex mechanisms than a simple increase or decrease of the pace at which damage accumulates.

In conclusion, this study shows that, depending on the method that is used, different effects are found of caloric restriction and genetic disruption of growth hormone signaling on murine aging. Whereas these interventions negligibly and non-consistently affect aging rates according to the classical method to calculate aging rates, they slow aging at lower ages and quicken aging at higher ages according to the alternative method that has been validated previously. This conclusion warrants a reevaluation of previous studies on the effects of these interventions on murine aging with the use of the alternative method. Moreover, the alternative method can be applied in future research to obtain further insights into the effects of dietary, genetic, and other interventions on aging of mice and other species.

METHODS

Mice. Data on the mortality of mice subjected to caloric restriction and with genetic disruption of growth hormone signaling were derived from two previous studies. Mice without a receptor of growth hormone and growth-hormone binding protein were developed by targeted disruption of the *Ghr/Ghrbp* gene in 129/Ola mice and provided by Dr. Kopchick at Ohio University [31]. These mutant mice do not express the receptor of growth hormone and are consequently resistant to growth hormone. Their phenotypically normal siblings served as controls. Both the mutant and wild-type mice were divided in two groups, of which one was fed *ad libitum* and the other was subjected to caloric restriction from 56 days of age onward. Caloric restriction was gradually introduced with an intake of 10% less than the *ad libitum* dietary intake in the initial week, 20% less in the second week, and 30% less throughout the subsequent weeks [19]. We refer to this population of mice as Population A.

Mice without production of growth hormone-releasing hormone were developed by targeted disruption of the

Ghrh gene in mice with a mixed C57BL/6 and 129/Sv background and provided by Dr. Salvatori at Johns Hopkins University School of Medicine [32]. These mutant mice do not secrete growth hormone-releasing hormone and consequently do not secrete growth hormone. Their phenotypically normal siblings served as controls. Both the mutant and wild-type mice were divided in two groups, of which one was fed *ad libitum* and the other was subjected to caloric restriction from 84 days of age onward with an intake of 40% less than the *ad libitum* dietary intake [20]. We refer to this population of mice as Population B.

All mice were bred and housed at Southern Illinois University School of Medicine under controlled temperature (20-23 °C) and light conditions (12-hours light/12-hours dark cycles) and were fed Lab Diet Formula 5001 (Nestlé Purina, St. Louis, MO). Regular testing for bacterial and viral infections was negative. Few mice appearing near death, having a tumor that bled, or having a tumor that approached 10% of the body weight were euthanized. All animal protocols were in strict accordance with the recommendations in the Guide for the Care and Use of Laboratory Animals of the National Institutes of Health and were approved by the Animal Care and Use Committee of Southern Illinois University School of Medicine.

Mortality rates. Mortality rates were calculated per group of mice per interval of 150 days of age. Mortality rates were calculated by dividing the number of mice that died by the number of days lived by all mice in the age interval of interest. If only one mouse died in the last age interval, the corresponding mortality rate was excluded.

The age-dependent mortality rate of each group of mice was fitted to the Gompertz model using Stata/SE 12.1 (StataCorp, College Station, TX) in order to obtain estimates of the Gompertz model's parameters. The Gompertz model describes mortality rate m at age t by $m(t) = \alpha\, e^{\gamma t}$, where α and γ are the model's parameters. The linear increase in a mortality rate with age on a logarithmic scale is described by γ and classically interpreted as an aging rate.

Aging rates. Alternatively to the classically estimated aging rates, aging rates were derived from age-dependent mortality rates per group of mice per interval of 150 days of age without fitting the mortality rates to the Gompertz model or any similar model. The aging rate in each age interval was calculated as the absolute difference in mortality rate between the age interval of interest and the subsequent age interval divided by the difference in age between both age intervals, as described previously in more detail [14].

ACKNOWLEDGEMENTS

The authors are grateful for the assistance of Adam Spong in conducting the study of the mice in Population B.

Funding

This research was supported by the European Commission Project Switchbox (FP7, Health-F2-2010-259772). The funder had no role in the design, conduct, interpretation, documentation, and publication of the study.

Author Contributions

Conception and design of the study: JJEK, DvH, DvB. Provision of the data: MSB, LYS, AB. Analyses: JJEK. Interpretation of the results: JJEK, DvH, AB. Intellectual contributions to the manuscript: all authors. All authors read and approved the manuscript.

Conflict of interest statement

The authors have no conflict of interests to declare.

REFERENCES

1. Vanhooren V and Libert C. The mouse as a model organism in aging research: usefulness, pitfalls and possibilities. Ageing Res Rev. 2013; 12:8-21.

2. Weindruch R and Sohal RS. Caloric intake and aging. N Engl J Med. 1997; 337:986-994.

3. Masoro EJ. Overview of caloric restriction and ageing. Mech Ageing Dev. 2005; 126:913-922.

4. Flurkey K, Papaconstantinou J, Miller RA, and Harrison DE. Lifespan extension and delayed immune and collagen aging in mutant mice with defects in growth hormone production. Proc Natl Acad Sci USA. 2001; 98:6736-6741.

5. Bartke A. Impact of reduced insulin-like growth factor-1/insulin signaling on aging in mammals: novel findings. Aging Cell. 2008; 7:285-290.

6. Junnila RK, List EO, Berryman DE, Murrey JW, and Kopchick JJ. The GH/IGF-1 axis in ageing and longevity. Nat Rev Endocrinol. 2013; 9:366-376.

7. Brown-Borg HM. The somatotropic axis and longevity in mice. Am J Physiol Endocrinol Metab. 2015; 309:E503-E510.

8. Finch CE. Longevity, Senescence, and the Genome. Chicago: University of Chicago Press, 1990; 12-32.

9. Masoro EJ. Caloric restriction and aging: controversial issues. J Gerontol A Biol Sci Med Sci. 2006; 61:14-19.

10. de Magalhães JP, Cabral JAS, and Magalhães D. The influence of genes on the aging process of mice: a statistical assessment of the genetics of aging. Genetics. 2005; 169:265-274.

11. Curtsinger JW, Gavrilova NS, and Gavrilov LA. Biodemography of aging and age-specific mortality in Drosophila melanogaster. In: Masoro EJ and Austad SN (eds). Handbook of the Biology of Aging. San Diego: Elsevier, 2006; 261-288.

12. Baudisch A. The pace and shape of ageing. Methods Ecol Evol. 2011; 2:375-382.
13. Horiuchi S and Wilmoth JR. Deceleration in the age pattern of mortality at older ages. Demography. 1998; 35:391-412.
14. Koopman JJE, Rozing MP, Kramer A, Abad JM, Finne P, Heaf JG, Hoitsma AJ, De Meester JMJ, Palsson R, Postorino M, Ravani P, Wanner C, Jager KJ, et al. Calculating the rate of senescence from mortality data: an analysis of data from the ERA-EDTA Registry. J Gerontol A Biol Sci Med Sci. 2015, in press.
15. Driver C. The Gompertz function does not measure ageing. Biogerontology. 2001; 2:61-65.
16. Rozing MP and Westendorp RGJ. Parallel lines: nothing has changed? Aging Cell. 2008; 7:924-927.
17. Koopman JJE, Rozing MP, Kramer A, de Jager DJ, Ansell D, De Meester JMJ, Prütz KG, Finne P, Heaf JG, Palsson R, Kramar R, Jager KJ, Dekker FW, and Westendorp RGJ. Senescence rates in patients with end-stage renal disease: a critical appraisal of the Gompertz model. Aging Cell. 2011; 10:233-238.
18. Koopman JJE, Wensink MJ, Rozing MP, van Bodegom D, and Westendorp RGJ. Intrinsic and extrinsic mortality reunited. Exp Gerontol. 2015; 67:48-53.
19. Bonkowski MS, Rocha JS, Masternak MM, Al Regaiey KA, and Bartke A. Targeted disruption of growth hormone receptor interferes with the beneficial actions of calorie restriction. Proc Natl Acad Sci USA. 2006; 103:7901-7905.
20. Sun LY, Spong A, Swindell WR, Fang Y, Hill C, Huber JA, Boehm JD, Westbrook R, Salvatori R, and Bartke A. Growth hormone-releasing hormone disruption extends lifespan and regulates response to caloric restriction in mice. eLife. 2013; 2:e01098.
21. Simons MJP, Koch W, and Verhulst S. Dietary restriction of rodents decreases aging rate without affecting initial mortality rate: a meta-analysis. Aging Cell. 2013; 12:410-414.
22. Vaupel JW. Biodemography of human ageing. Nature. 2010; 464:536-542.
23. Merry BJ. Dietary restriction in rodents: delayed or retarded ageing? Mech Ageing Dev. 2005; 126:951-959.
24. Partridge L. The new biology of ageing. Phil Trans R Soc Lond B Biol Sci. 2010; 365:147-154.
25. Fries JF. Aging, natural death, and the compression of morbidity. N Engl J Med. 1980; 303:130-135.
26. Liao CY, Rikke BA, Johnson TE, Diaz V, and Nelson JF. Genetic variation in the murine lifespan response to dietary restriction: from life extension to life shortening. Aging Cell. 2010; 9:92-95.
27. Nakagawa S, Lagisz M, Hector KL, and Spencer HG. Comparative and meta-analytic insights into life extension via dietary restriction. Aging Cell. 2012; 11:401-409.
28. Swindell WR. Dietary restriction in rats and mice: a meta-analysis and review of the evidence for genotype-dependent effects on lifespan. Ageing Res Rev. 2012; 11:254-270.
29. Mulvey L, Sinclair A, and Selman C. Lifespan modulation in mice and the confounding effects of genetic background. J Genet Genomics. 2014; 41:497-503.
30. Salinari G and De Santis G. On the beginning of mortality acceleration. Demography. 2015; 52:39-60.
31. Zhou Y, Xu BC, Maheshwari HG, He L, Reed M, Lozykowski M, Okada S, Cataldo L, Coschigamo K, Wagner TE, Baumann G, and Kopchick JJ. A mammalian model for Laron syndrome produced by targeted disruption of the mouse growth hormone receptor/binding protein gene (the Laron mouse). Proc Natl Acad Sci USA 1997; 94:13215-13220.
32. Alba M and Salvatori R. A mouse with targeted ablation of the growth hormone-releasing hormone gene: a new model of isolated growth hormone deficiency. Endocrinology. 2004; 145:4134-4143.

Research Paper

Metabolic effects of a 13-weeks lifestyle intervention in older adults: The Growing Old Together Study

Ondine van de Rest[1,#], Bianca A.M. Schutte[2,#], Joris Deelen[2,#], Stephanie A.M. Stassen[3], Erik B. van den Akker[2,4], Diana van Heemst[3], Petra Dibbets-Schneider[5], Regina. A. van Dipten-van der Veen[1], Milou Kelderman[1], Thomas Hankemeier[6], Simon P. Mooijaart[3], Jeroen van der Grond [5], Jeanine J. Houwing-Duistermaat [7], Marian Beekman [2], Edith J.M. Feskens [1], P. Eline Slagboom[2]

[1]Division of Human Nutrition, Wageningen University, 6700 EV Wageningen, The Netherlands
[2]Department of Molecular Epidemiology, Leiden University Medical Center, 2300 RC Leiden, The Netherlands
[3]Department of Gerontology and Geriatrics, Leiden University Medical Center, 2300 RC Leiden, The Netherlands [4]The Delft Bioinformatics Lab, Delft University of Technology, 2628 CD Delft, The Netherlands
[5]Department of Radiology, Leiden University Medical Center, 2300 RC Leiden, The Netherlands
[6]Division of Analytical Biosciences, Leiden Academic Centre for Drug Research, Leiden University, Leiden 2300 RA, The Netherlands
[7]Department of Medical Statistics, Leiden University Medical Center, 2300 RC Leiden, The Netherlands
[#] Equally contributed to this work

Key words: lifestyle intervention, older adults, caloric restriction, physical activity, metabolic health, healthy ageing
Received: 11/12/15; Accepted: 01/19/16; Published: 01/25/16 **doi:** 10.18632/aging.100877
Correspondence to: P. Eline Slagboom, PhD; **E-mail:** P.Slagboom@lumc.nl

Abstract: For people in their 40s and 50s, lifestyle programs have been shown to improve metabolic health. For older adults, however, it is not clear whether these programs are equally healthy. In the Growing Old Together study, we applied a 13-weeks lifestyle program, with a target of 12.5% caloric restriction and 12.5% increase in energy expenditure through an increase in physical activity, in 164 older adults (mean age=63.2 years; BMI=23-35 kg/m^2). Mean weight loss was 4.2% (SE=2.8%) of baseline weight, which is comparable to a previous study in younger adults. Fasting insulin levels, however, showed a much smaller decrease (0.30 mU/L (SE=3.21)) and a more heterogeneous response (range=2.0-29.6 mU/L). Many other parameters of metabolic health, such as blood pressure, and thyroid, glucose and lipid metabolism improved significantly. Many ^{1}H-NMR metabolites changed in a direction previously associated with a low risk of type 2 diabetes and cardiovascular disease and partially independently of weight loss. In conclusion, 25% reduction in energy balance for 13 weeks induced a metabolic health benefit in older adults, monitored by traditional and novel metabolic markers.

INTRODUCTION

Worldwide, the proportion of older and highly aged people in the population is rising fast [1]. Metabolic and physical health generally decline among older adults, be it in a highly heterogeneous fashion [2]. Hence, there is an urge to stimulate healthy ageing among the increasing group of older adults. Metabolic health can successfully be improved by lifestyle changes, such as dietary restriction and/or increased physical activity [3-

9], thereby reducing the risk for cardiovascular disease (CVD). An example of a lifestyle intervention showing this metabolic improvement in young adults (28-45 years of age) is the CALERIE study, a 6-month lifestyle intervention reducing energy balance by 25% in 12 overweight individuals (body mass index (BMI) 25-30 kg/m^2) [6]. As yet, it is unclear whether a 25% reduction in energy balance likewise improves metabolic health in older adults and is feasible in this age group.

Poor metabolic health is generally marked by high levels of total cholesterol, glucose, insulin, triglycerides, and blood pressure and low levels of HDL cholesterol, free triiodothyronine (fT3), and adiponectin [10-13], except in highly aged individuals (above 75 years) [14,15]. Remarkably, the majority of parameters of poor metabolic health inversely associate with familial longevity, as shown by comparison of middle-aged offspring of long-lived subjects and their spouses [16-19]. Besides clinical markers, metabolic health can also be monitored by novel technologies, such as Nuclear Magnetic Resonance (NMR), which are able to measure large numbers of metabolites in an affordable and standardized way. Distinct profiles of metabolites have been demonstrated to associate with intake of specific food components [20,21], (future) type 2 diabetes (T2D) [22-24] and CVD [18,25,26], showing the potential of metabolomics to monitor metabolic health. However, it has not yet been established which optimal set of markers monitors the metabolic effects of a lifestyle change in older adults.

In the Growing Old TOgether (GOTO) study we investigated the effect of a lifestyle intervention in older adults by both clinical and metabolomic profiles. Participants reduced energy balance by 25% for 13 weeks, targeted by 12.5% reduction in caloric intake and 12.5% increase in physical activity, corresponding to one of the three intervention conditions previously applied in the CALERIE study [6]. In CALERIE, 12 participants received this intervention. The GOTO study consisted of 164 individuals (mean age 63.2 years) with a BMI of 23-35 kg/m^2, which are mostly couples of whom one was member of a longevity family and the other their spouse. Since fasting insulin was one of the markers that showed a reduction within three months in the CALERIE study [6], this parameter was used as our primary outcome. In addition, we measured the response to the intervention by other established markers of metabolic health, state-of-the-art metabolic profiles measured with Hydrogen-1 NMR (^{1}H-NMR), and quality of life (QoL).

RESULTS

Longevity family members and controls are largely similar on baseline

Of the 164 individuals who started the intervention study, one dropped out prior to completion of the study (Fig. 1). A selection of the clinical baseline characteristics of the participants according to familial background, i.e. longevity family member or control, is depicted in Table 1 (complete clinical baseline characteristics are provided in Supplementary Table 1A). Baseline characteristics of ^{1}H-NMR metabolites are shown in Supplementary Table 1B. Gender differences were observed for many parameters. In contrast to the Leiden Longevity Study as a whole, in which many metabolic parameters differ significantly between longevity family members and controls [16,18,19], we observed only few significant differences in the parameters at baseline between the small groups included in the GOTO study. Therefore, we studied the effects of the intervention in both groups combined.

Intervention improves body composition and metabolic health

The effect of the 13-weeks lifestyle change on clinical parameters is depicted in Table 2 and Supplementary Table 2A. For the primary outcome, i.e. fasting insulin, a minor mean (SE) decrease of 0.30 mU/L (3.21 mU/L) and a considerable heterogeneity (range -11.5-10.5 mU/L) was observed (Supplementary Fig. 1). Measures of body composition generally improved, as shown by a mean weight loss of 3.3 kg (0.18 kg), i.e. 4.2% (2.8%) of baseline weight (Fig. 2), a body fat mass decrease of 11.7% (8.9%), and a fat free mass decrease of 0.7 kg (0.1 kg). Measures of health and functioning showed a significant decrease of 4.3 mmHg (1.0 mmHg) in systolic and 1.7 mmHg (0.6 mmHg) in diastolic blood pressure. We noted that the changes in weight and systolic blood pressure (Fig. 3), but not in insulin levels, were dependent on baseline levels.

Resting energy expenditure (REE) significantly decreased with 49.2 kcal/day (8.0 kcal/day). Hand grip strength was not changed by the lifestyle change, but physical functioning, mental QoL in women, and the Framingham Risk Score improved. The diagnostic measures showed a significant decrease in total and LDL cholesterol, HDL cholesterol in women, fT3, and leptin levels and an increase in adiponectin levels in men.

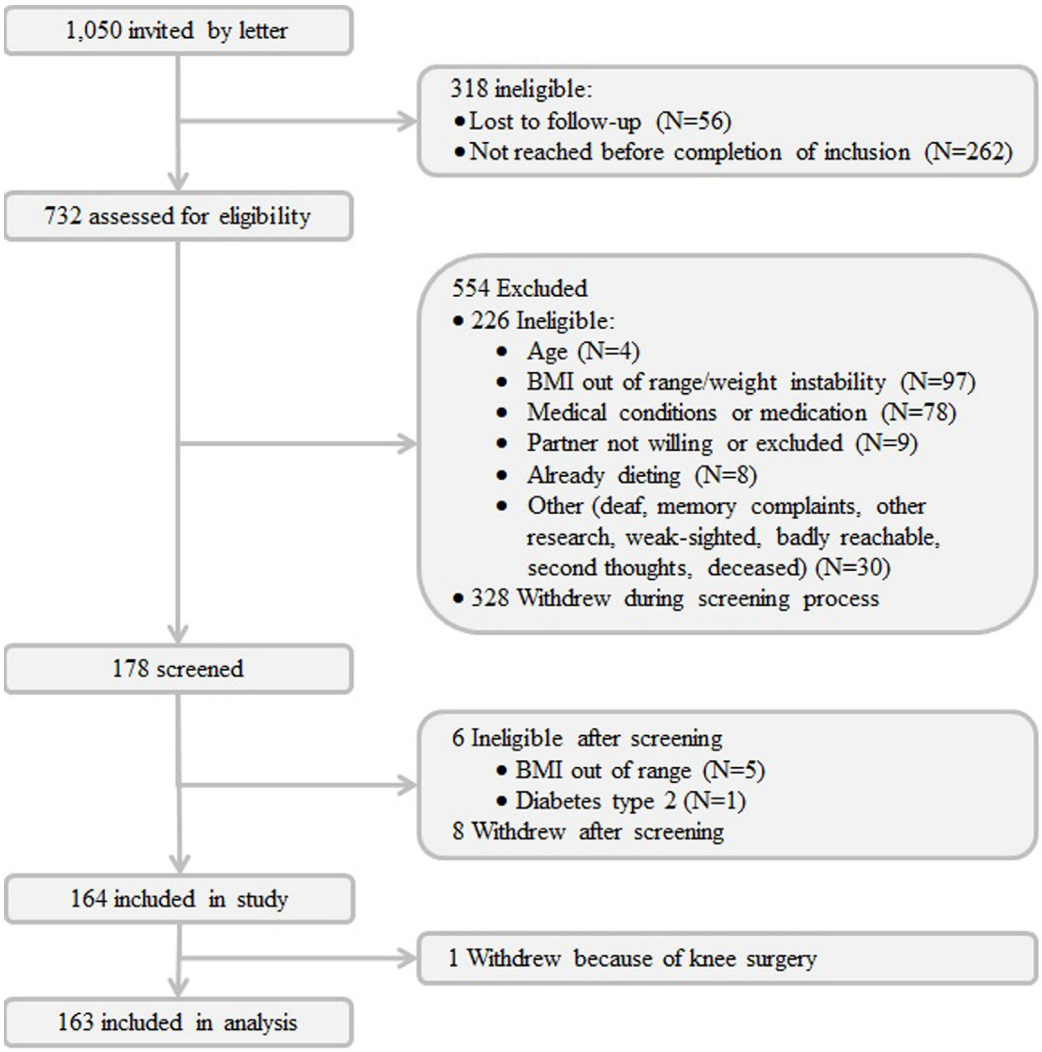

Figure 1. Flow chart of participants in the trial.

Plasma metabolite profile changes due to 3 months lifestyle intervention

To determine the overall effect of the intervention on the ^{1}H-NMR metabolites, we performed Principle Component Analysis. This analysis indicated that a major part of the variation in the metabolites (PC1, explaining 32.4% of the total variance) could be attributed to the effects of the lifestyle intervention (Fig. 4). As shown in Supplementary Fig. 2, the intervention effect, as represented by PC1, coincides with many of the measured ^{1}H-NMR metabolites. The effects of the intervention on the single ^{1}H-NMR metabolites in fasting blood are depicted in Fig. 5 and Supplementary Table 2B. Multiple amino acids levels changed significantly and include a decrease of the branched-chain amino acid leucine and the aromatic amino acid tyrosine. In addition, the levels of multiple glycolysis-related metabolites, ketone bodies, fatty acids, metabolites involved in fluid balance and inflammation, apolipoproteins, lipid concentrations, and lipoprotein particle sizes showed a significant decrease. Citrate levels, large HDL cholesterol concentrations, and HDL particle size, on the other hand, increased after the lifestyle change. For several HDL-related metabolites we observed an opposite effect of the intervention in men and women.

Table 1. Baseline characteristics of parameters of body composition, health and functioning, and diagnostic measurements.

Characteristic		n	Longevity family members	n	Controls
Women, n (%)			39 (43.3)		42 (56.8)
Age, mean (SD) [range], years		90	63.4 (5.4) [49.1-75.1]	74	62.4 (6.1) [46.7-73.5]
Body composition, mean (SD) [range]					
Weight, kg		89	79.8 (9.6) [62.5-105.7]	73	79.0 (10.2) [60.5-102.4]
	Men	50	84.3 (8.0) [67.2-105.7]	31	85.4 (8.1) [70.1-102.4]
	Women	39	74.1 (8.4) [62.5-95.4]	42	74.1 (8.9) [60.5-100.4]
BMI, kg/m^2		89	27.0 (2.6) [22.9-34.2]	73	26.9 (2.4) [22.9-33.5]
Waist circumference, cm		90	96.2 (7.9) [74-122]	74	96.1 (8.2) [77-112]
	Men	51	98.1 (7.4) [80-122]	32	100.1 (6.4) [89-112]
	Women	39	93.6 (7.9) [74-112]	42	93.0 (8.1) [77-111]
Health and functioning, mean (SD) [range]					
Systolic blood pressure, mm Hg[a]		65	135.4 (15.9) [111-196]	48	137.8 (17.1) [101-173]
Diastolic blood pressure, mm Hg[a]		65	83.5 (7.4) [64-101]	48	84.7 (9.2) [65-108]
Medication use, *n* (%)					
Lipid-lowering agent		90	11 (12.2)	74	18 (24.3)
Antihypertensive agent		90	23 (25.6)	74	26 (35.1)
Diagnostic measurements, mean (SD) [range]					
Fasting glucose, mmol/L		90	5.0 (0.5) [3.6-6.5]	74	5.0 (0.6) [4.0-7.6]
Fasting insulin, mU/L[b]		90	9.4 (5.1) [2.0-29.6]	74	9.0 (3.9) [2.0-22.6]
HOMA-IR		88	1.2 (0.6) [0.4-3.8]	72	1.2 (0.5) [0.4-2.7]
Total cholesterol, mmol/L[c]		79	5.5 (1.0) [3.3-8.6]	56	5.5 (1.0) [3.2-8.0]
HDL cholesterol, mmol/L[c]		79	1.6 (0.4) [0.6-3.1]	56	1.4 (0.4) [0.6-2.3]
	Men	43	1.4 (0.3) [1.0-2.0]	23	1.1 (0.2) [0.6-1.6]
	Women	36	1.7 (0.5) [0.6-3.1]	33	1.6 (0.3) [1.2-2.3]
LDL cholesterol, mmol/L[c]		79	3.5 (0.8) [1.8-6.4]	56	3.4 (0.9) [1.6-6.0]

[a] Individuals using antihypertensive agents were removed before analysis.
[b] Natural log transformed parameter was used for analysis.
[c] Individuals using lipid-lowering agents were removed before analysis.
Parameters were analysed separately in men and women if there was a significant gender-difference at baseline. BMI, body mass index; HOMA-IR, homeostatic model assessment - insulin resistance; HDL, high density lipoprotein; LDL, low density lipoprotein.

Effects of lifestyle intervention at old age (partly) independent of weight loss

To investigate whether the observed response mainly coincides with the change in weight, we adjusted for weight loss. For most of the parameters of health and functioning, diagnostic measurements, and ^{1}H-NMR metabolites, adjustment for weight loss reduced the effects of the intervention. However, the changes in fT3, total, VLDL, LDL, and IDL cholesterol, as well as those in phosphoglycerides, cholines, sphingomyelines, and some glycolysis intermediates, remained largely unchanged after this adjustment (Table 2, Supplementary Table 2A and Supplementary Table 2B).

Finally, the beneficial effects on physical functioning and mental QoL in women were also largely independent of weight loss (Table 2 and Supplementary Table 2A).

Hence, the effect of the lifestyle change on many of the metabolic parameters and well-being in this study occurs partly or fully independent of the observed loss in weight.

Table 2. Effects of the intervention on parameters of body composition, health and functioning, and diagnostic measurements.

Characteristic, mean (SE)		n	Difference	P-value[a]
Body composition				
Weight, kg		161	-3.34 (0.18)	<0.001
	Men	80	-3.42 (0.27)	<0.001
	Women	81	-3.25 (0.23)	<0.001
BMI, kg/m^2		161	-1.13 (0.06)	<0.001
Waist circumference, cm		163	-4.3 (0.4)	<0.001
	Men	82	-4.4 (0.6)	<0.001
	Women	81	-4.2 (0.6)	<0.001
Body fat, %		161	-2.26 (0.16)	<0.001
	Men	80	-2.22 (0.23)	<0.001
	Women	81	-2.29 (0.21)	<0.001
Fat free mass, kg^2		161	-0.67 (0.10)	<0.001
	Men	80	-0.83 (0.16)	<0.001
	Women	81	-0.51 (0.13)	<0.001
Health and functioning				
Systolic blood pressure, mm Hg[b]		113	-4.33 (0.98)	<0.001*
Diastolic blood pressure, mm Hg[b]		113	-1.66 (0.61)	0.007
REE, kcal/day		126	-49.2 (8.0)	<0.001*
	Men	65	-46.59 (11.76)	<0.001
	Women	61	-51.94 (10.79)	<0.001*
Handgrip strength, kg		153	0.38 (0.32)	0.25
	Men	76	0.24 (0.53)	0.65
	Women	77	0.51 (0.38)	0.18
Physical functioning		159	0.14 (0.05)	0.008*
Physical quality of life		157	-0.18 (0.61)	0.77
	Men	82	-0.72 (0.83)	0.39
	Women	75	0.42 (0.92)	0.65
Mental quality of life		157	0.9 (0.70)	0.19
	Men	82	-1.13 (0.84)	0.18
	Women	75	3.13 (1.12)	0.005*
FRS, %		163	-0.51 (0.23)	0.03
	Men	82	-0.65 (0.43)	0.13
	Women	81	-0.37 (0.15)	0.01

Table 2. Effects of the intervention on parameters of body composition, health and functioning, and diagnostic measurements. (continued).

Characteristic, mean (SE)		n	Difference	P-value[a]
Diagnostic measurements				
Fasting glucose, mmol/L		163	-0.06 (0.04)	0.16
Fasting insulin, mU/L[c]		163	-0.05 (0.03)	0.04
HOMA-IR		153	-0.03 (0.03)	0.33
Total cholesterol, mmol/L[d]		135	-0.29 (0.06)	<0.001[#]
HDL cholesterol, mmol/L[d]		135	-0.01 (0.02)	0.49
	Men	66	0.04 (0.02)	0.11
	Women	69	-0.06 (0.03)	0.02*
LDL cholesterol, mmol/L[d]		135	-0.26 (0.05)	<0.001[#]
Triglycerides, mmol/L[c,d]		135	-0.04 (0.03)	0.11
fT3, pmol/L		163	-0.14 (0.03)	<0.001[#]
fT4, pmol/L		163	-0.07 (0.09)	0.44
TSH, mU/L[d]		163	-0.04 (0.03)	0.17
DHEAS, nmol/L[c]		163	-0.02 (0.01)	0.20
	Men	82	-0.01 (0.02)	0.47
	Women	81	-0.02 (0.02)	0.28
Leptin, µg/L[c]		163	-0.26 (0.03)	<0.001*
	Men	82	-0.29 (0.04)	<0.001*
	Women	81	-0.23 (0.03)	<0.001*
Adiponectin, mg/L[b]		163	0.04 (0.01)	0.005
	Men	82	0.09 (0.02)	<0.001
	Women	81	-0.01 (0.02)	0.76
IGF-1, nmol/L		163	0.10 (0.24)	0.67
	Men	82	0.36 (0.31)	0.24
	Women	81	-0.17 (0.35)	0.64
IGFBP-3, mg/L		163	-0.05 (0.05)	0.37
IGF-1:IGFBP-3		163	0.004 (0.003)	0.21
	Men	82	0.009 (0.006)	0.14
	Women	81	-0.001 (0.003)	0.82
CRP (high-sensitivity), mg/L[c]		163	-0.11 (0.07)	0.09

* P-value < 0.05 after adjustment for weight loss. [#] P-value < 0.001 after adjustment for weight loss.

[a] P-value refers to difference between baseline and end.

[b] Individuals using antihypertensive agents were removed before analysis.

[c] Natural log transformed parameter was used for analysis.

[d] Individuals using lipid-lowering agents were removed before analysis.

Parameters were analysed separately in men and women if there was a significant gender-difference at baseline. BMI, body mass index; REE, resting energy expenditure; FRS, Framingham risk score; HOMA-IR, homeostatic model assessment - insulin resistance; HDL, high density lipoprotein; LDL, low density lipoprotein; fT3, free triiodothyronine; fT4, free thyroxine; TSH, thyroid stimulating hormone; DHEAS, dehydroepiandrosterone-sulfate; IGF-1, insulin-like growth factor 1; IGFBP-3, insulin-like growth factor binding protein 3; CRP, C-reactive protein.

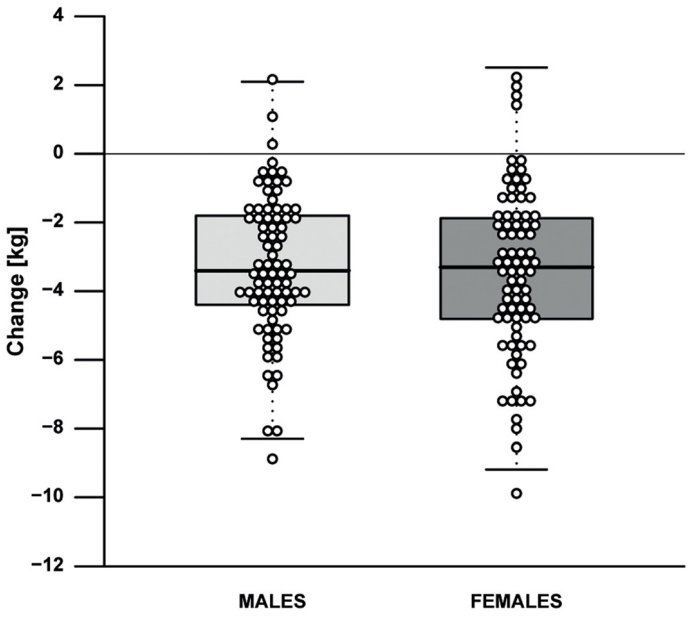

Figure 2. Effect of the intervention on weight by gender.

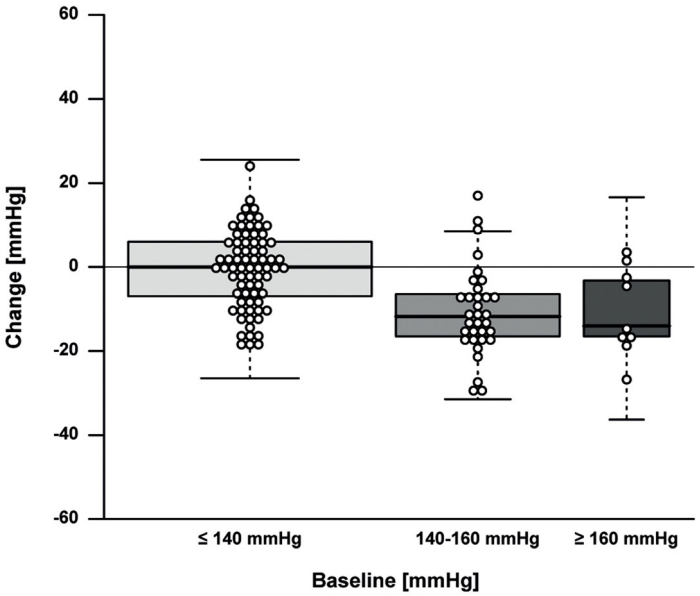

Figure 3. Effect of the intervention on systolic blood pressure by baseline systolic blood pressure.

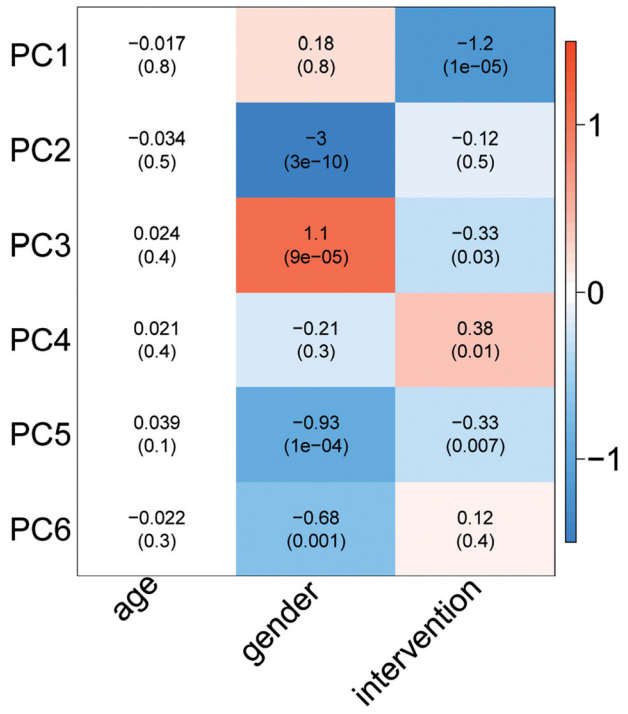

Figure 4. Effect of age, gender, and intervention on ^{1}H-NMR metabolite-based PC's. The colour of the blocks represents the magnitude of the effect, while the P-value is mentioned between brackets.

DISCUSSION

A 13-weeks lifestyle change among older adults aimed at combining 12.5 % decreased energy intake and 12.5% increased physical activity improved parameters of body composition, relevant clinical markers, such as fasting insulin, our primary endpoint, blood pressure, glucose, lipid and thyroid metabolism, and ^{1}H-NMR metabolites. In addition, physical functioning and mental QoL in women improved. For most of the parameters, the improvements were, at least partly, independent of weight loss, indicating that we monitored aspects of metabolic health additional to weight loss.

The GOTO study shows that one of the intervention conditions previously pioneered by the CALERIE study in younger and more overweight subjects [6] seems generally feasible, since only one drop-out was observed and metabolic health was generally improved. The older adults in GOTO generally lost weight during the intervention and the mean change in weight was comparable to CALERIE. The mean change in fasting insulin, however, was much smaller in GOTO (0.30 mU/L) than in CALERIE (2.06 mU/L) and the heterogeneity in response was much larger (range -11.5 – 10.5 mU/L and -8 – 2 mU/L, respectively). There could be several explanations for this difference. First, the sample size of the GOTO study is almost 14 times as large as the 'calorie restriction with exercise' study group in CALERIE and may have estimated the effect of the intervention more accurately. Second, the baseline and response variation in insulin and other metabolic variables was larger in GOTO than in CALERIE, which might be caused by the higher mean age of our population (mean age 63 years (GOTO) versus 39 years (CALERIE)) and broader range in baseline BMI. Third, because the intervention in GOTO was less controlled, the outcome was likely more heterogeneous. Heterogeneous responses to lifestyle interventions should be further explored and carefully monitored in even larger studies of older adults.

The potential improvement of metabolic health is reflected in the change of clinical parameters as well as metabolites. The observed decrease in leucine, tyrosine, glucose, pyruvate, glycerol, total fatty acids, monounsaturated fatty acids, α-acid glycoprotein, lipid concentrations, and VLDL particle size and increase in fatty acid chain length and citrate imply a decreased future CVD risk based on a previous prospective study, including older adults, using the same ^{1}H-NMR assay [26]. This would correspond with reduced FRS in women after the lifestyle change. In addition, the observed decrease in leucine, tyrosine, glucose, 3-hydroxybutyrate, and creatinine and increase in glycine is considered beneficial with respect to (risk of) T2D [22-24]. The observed gender difference in HDL metabolites in response to the intervention may be due to the fact that women already displayed more beneficial levels at baseline as compared to men, while the observed decrease in HDL metabolites in men may be caused by a decrease in alcohol intake [27].

Unlike insulin, blood pressure levels, and the Framingham Risk Score, parameters indicative of lipid and thyroid metabolism, as well as several ^{1}H-NMR metabolites, changed largely independent of the reduction in body weight. Such changes may point at the occurrence of metabolic shifts in response to dietary changes and increase in physical activity, exemplified by decreased fT3 levels, which were also observed in the CALERIE study after 3 months [6]. Basically, our data suggest that the effects of the intervention on metabolic health can be monitored by a combination of weight, fT3 levels, and a single ^{1}H-NMR metabolite assay.

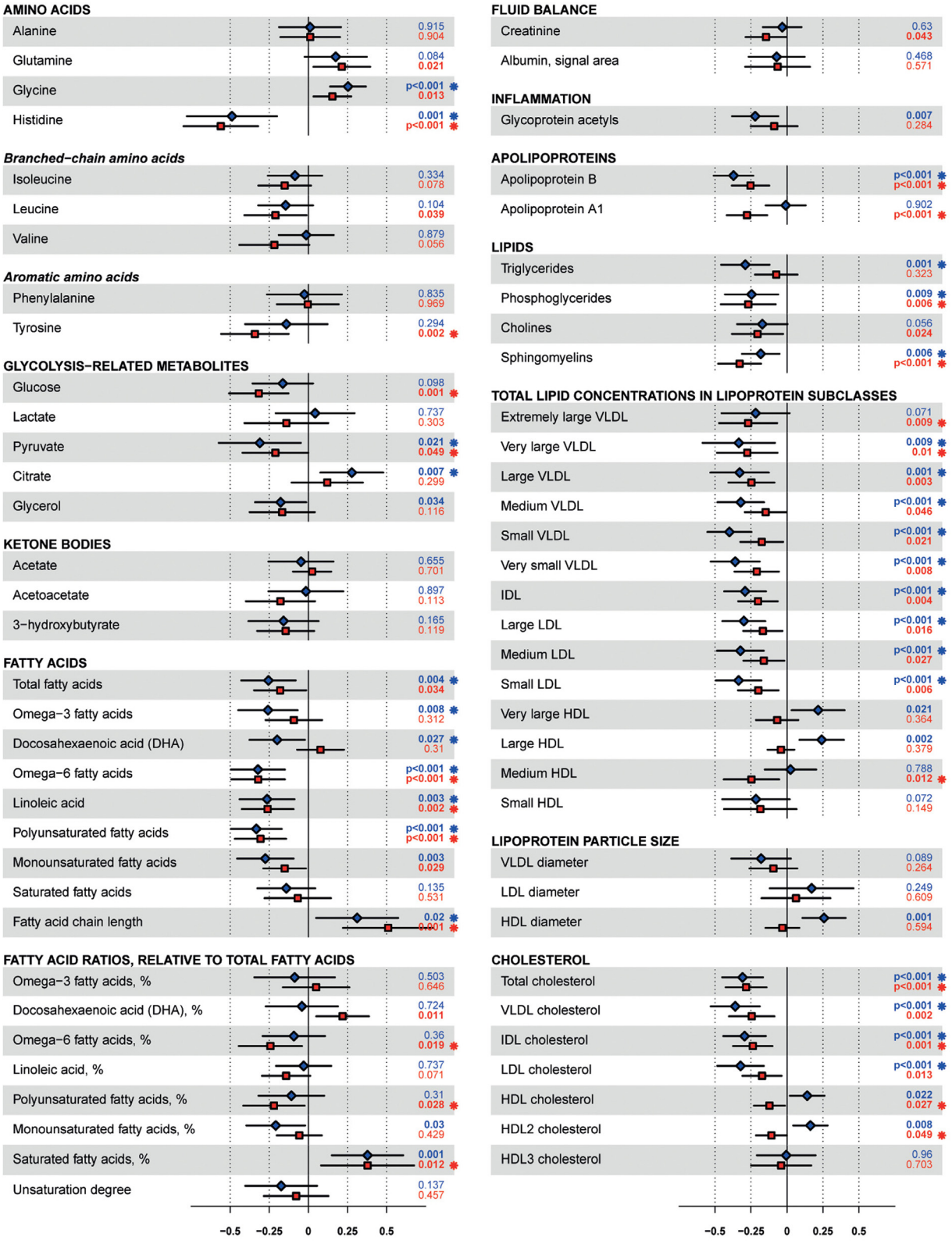

Figure 5. Effects of the intervention on ^{1}H-NMR metabolites. Effect sizes are per 1-SD log-transformed metabolite concentration and adjusted for age and gender. Squares indicate mean and error bars denote 95% confidence intervals. Blue squares indicate males, red squares indicate females. Individuals using lipid-lowering agents were removed before analysing fatty acids, fatty acids ratios, apolipoproteins, lipids, total lipid concentrations in lipoprotein subclasses, lipoprotein particle size and cholesterol. VLDL, very low density lipoprotein; IDL, intermediate density lipoprotein; LDL, low density lipoprotein; HDL, high density lipoprotein.

Next to metabolic health, we observed an improvement of mental health status in women, which was independent of weight loss. The positive effect of social interaction by participating in a trial may underlay this improvement. However, physical activity has also been described to improve mental health [28,29]. This effect was not observed in men, which may be explained by their better mental health at baseline. Mental health improvements may stimulate compliance to a lifestyle change over time. In our study, an additional questionnaire showed that 66% of the participants indicated that they maintained their new lifestyle one year after the intervention, possibly contributed by a 'buddy' effect for these older adult couples.

In conclusion, reducing energy balance by 25% for 13 weeks by a modest change in dietary habits and physical exercise seemed generally feasible in older adults (mean age 63 years) and resulted in a weight change comparable to younger adults. Despite a considerable heterogeneity in response, metabolic health was generally beneficially influenced, as reflected by most markers of body composition, blood pressure, physical functioning, glucose, lipid, and thyroid metabolism, and a range of metabolites that could be measured with a well-standardized ^{1}H-NMR assay. We conclude that monitoring of the response to an intervention among elderly is optimized by applying metabolomics assays in addition to clinical markers of metabolic health. The response to the lifestyle intervention applied in GOTO, as measured by metabolomics profiles and parameters of wellbeing, can be used as reference for more specific dietary interventions that the ageing field is planning [30].

METHODS

Study population. Participants for the GOTO study were recruited from the Leiden Longevity Study (LLS), a longitudinal cohort consisting of 421 families of long-lived Caucasian siblings, together with their offspring and the partners thereof [31]. For the current intervention couples consisting of offspring from the long-lived siblings and their current partners were included. In case one of the two was not eligible to participate, single offspring or controls were included to obtain the required sample size. Individuals of ages between 46 and 75 years and having a BMI ≥23 ≤35 kg/m^2 were recruited between February and October 2012. Potential participants underwent a telephonic screening and a screenings home visit. Exclusion criteria were: type I or type II diabetes (on diabetic medication); fasting blood glucose level ≥7.0 mmol/L; weight change ≥3 kg over the past 6 months; engagement in heavy/intensive physical activity (top sport or physically heavy work); any disease or condition that seriously affects body weight and/or body composition including active types of cancer; heart failure (NYHA III/VI), COPD (GOLD III/VI); recent (<3 months prior to intervention) immobilisation for >1 week; psychiatric or behavioural problems; use of thyroid medication, immunosuppressive drugs (e.g. prednisone, methotrexate, biologicals (TNF-alpha antagonists); concurrent participation in any other intervention study or weight management program, or not having a general practitioner. The Medical Ethical Committee of the Leiden University Medical Center approved the study and all participants signed written informed consent. All experiments were performed in accordance with relevant and approved guidelines and regulations. This trial was registered at the Dutch Trial Register (http://www.trialregister.nl) as NTR3499.

Intervention. The intervention comprised 13 weeks of 25% lowered energy balance by 12.5% reduction in energy intake and 12.5% increase in physical activity. Baseline energy intake and expenditure were assessed by an online version of a 150-item food frequency questionnaire (FFQ) [32] and by the International Physical Activity Questionnaire- Short Form (IPAQ-SF) [33]. The IPAQ-SF collects information on time spent walking, in moderate and vigorous physical activity, and sitting over the last seven days to estimate the total metabolic equivalent (MET) in minutes per week.

Individual guidelines were prescribed by respectively a dietician and physiotherapist in consultation with the participant to match the subjects' preferences and physical capabilities. The dietary guidelines were as much as possible according to the 'Dutch Guidelines for a healthy diet' [34]. Participants were advised to increase the amount of physical activity in such a way it fitted in their daily life pattern, as couple or alone, by walking, cycling, adjusted activities in and around the house and participation in local sport activities and facilities.

During the intervention participants had weekly contact with the dietician and physiotherapist by phone, email or at the participants home (alternating schedule) to check and stimulate adherence to the intervention and to discuss practical problems and solutions. To optimally guide the participants, both dietician and physio-therapist combined elements from the Attitude, Social influence and self-Efficacy model (ASE) [35], the Stages of Change Model [36] and Motivational Interviewing [37].

Participants daily recorded their eating behaviour and physical activity in a diary. To quantitatively assess

dietary intake two telephonic 24-h recalls were performed during the first month and two during the last month of the intervention. Days of the recall were unannounced to the participant and randomized to obtain a good distribution of the different days of the week, including weekend days. During the monthly home visits body weight and body composition were measured. To quantitatively determine physical activity prior to the intervention and at the end of the intervention accelerometers worn at home during seven days on wrist and ankle (GENEActiv, Activinsights, Kimbolton, UK) were used.

Anthropometrics. Height and weight were measured to the nearest 0.1 cm and 0.1 kg, respectively (Seca Clara 803, Seca Deutschland, Hamburg, Germany), with the person dressed in light clothing and without shoes. Waist circumference was measured to the nearest cm at the midpoint between the lowest rib and the top of the iliac crest with a non-elastic tape in standing position without shoes. Fat free mass and fat mass were measured using the In-Body 720 body composition analyser (Biospace, Cerritos, CA, USA).

Blood pressure. Trained staff members measured blood pressure in sitting position after a 10-minute rest on the dominant arm using a validated blood pressure device (Maxi-Stabil 3, Welch Allyn, Leiden, the Netherlands). Blood pressure was measured 4 times, twice in the first part of the afternoon and twice at the end of the afternoon. Systolic and diastolic blood pressures were calculated as the average of the four measurements.

Energy metabolism. Resting metabolic rate was measured 65 minutes after a standardized meal by indirect calorimetry, using a ventilated hood system (Care Fusion Canopy Jaeger Oxycon Pro, CareFusion Germany, Hoechberg, Germany). The standardized meal was 500 kcal and consisted of one raisin bun, one whole-wheat bun with margarine and 20 grams of Gouda cheese and a cup of tea without milk or sugar. Participants were lying on a bed under the ventilated hood in a quiet, temperature controlled room for 30 minutes. The initial 5 minutes of the measurement were not used for the analysis. VO2 and VCO2 were measured every minute. Resting energy expenditure (REE) and respiratory quotient (RQ) were calculated using the formulas:

$$REE = 3.91\ VO2 + 1.10\ VCO2 - 1.93N.$$
$$RQ = VCO2 / VO2$$

To exclude outliers in energy expenditure, the degree of variation based on the coefficient of variation (CV) was examined based on the mean and the SD of five data points that were used. Data per 5 consecutive minutes was included if the RQ data over these 5 minutes had a CV <5%.

Physical performance. Physical performance was assessed by the short physical performance battery (SPPB), which consisted of three components: balance, gait speed, and chair rise ability [38]. Handgrip strength was determined by three consecutive measures using a hand dynamometer (Jamar, Lafayette Instrument, Lafayette, IN, USA) at both hands.

Quality of life. Quality of life was assessed using the Short Form Health Survey-12 (SF-12). This questionnaire [39] distinguishes physical and mental health, each assessed by six items.

Framingham risk score. The Framingham risk score (FRS), which estimates the 10-year risk for developing coronary heart disease, was calculated using the criteria proposed by the Expert Panel on Detection, Evaluation, and Treatment of High Blood Cholesterol in Adults [40]. The score is based on the age, gender, total and HDL cholesterol serum level, smoking status, and systolic blood pressure of an individual.

Diagnostic measurements. All measurements were performed in fasted serum collected by venipuncture. Cholesterol, free thyroxine (fT4), glucose, high-density lipoprotein (HDL) cholesterol, triglycerides, high-sensitivity C-reactive protein (hsCRP), and thyroid stimulating hormone (TSH) were measured on the Roche/Hitachi Modular P800 analyzer (Roche Diagnostics, Almere, The Netherlands). Dehydro-epiandrosterone sulfate (DHEAS), insulin, insulin-like growth factor 1 (IGF-1), and insulin-like growth factor 1 binding protein 3 (IGF-BP3) were assessed on the Immulite 2000 XPi (Siemens, Eschborn, Germany). Adiponectin and leptin were determined using Human Adiponectin and Leptin RIA kits (EMD Millipore Corporation, Billerica, MA, USA). Free triiodothyronine (fT3) was determined using the ARCHITECT Free T3 assays (Abbott Laboratories, Abbott Park, IL, USA) on the Hitachi Modular E170 analyzer (Roche Diagnostics). Coefficients of variation for all laboratory analyses were <8%. Low-density lipoprotein (LDL) cholesterol was calculated using the Friedewald formula [41], while the homeostasis model assessment-estimated insulin resistance (HOMA-IR) was calculated using the publically available HOMA calculator (https://www.dtu.ox.ac.uk/homacalculator) [42].

Hydrogen-1 Nuclear Magnetic Resonance metabolites. ^{1}H-NMR metabolites were measured using a previously described platform [43]. For our analysis we used the

total lipid concentrations, fatty acid composition, and low-molecular-weight metabolites, including amino acids, glycolysis-related metabolites, ketone bodies and metabolites involved in fluid balance and immunity. All metabolite concentrations were natural log-transformed and scaled to standard deviation units before analysis.

Statistical analysis. Baseline differences between longevity family members and controls were calculated using a linear mixed model adjusted for age, gender (fixed effects), and household (random effects). The effects of the intervention were determined using a linear mixed model adjusted for age, gender, status (longevity family member or control) (fixed effects), household, and individual (random effects). Parameters were analyzed separately in men and women if there was a significant gender-difference at baseline. For additional analyses, weight was added to the model to determine weight loss-independent effects.

Principle Component Analyses and the following association analyses with age, gender and intervention were performed in R [44]. Principle Components (PCs) were computed using the function *prcomp* of the *stats* package [44]. Association analyses with the obtained PCs were performed using mixed linear models, function *lmer*, of package *lmerTest* [45]. Heatmaps were drawn to visualize the magnitude of the statistics from the association analyses using *labeledHeatmap* of the *WGCNA* package [46].

Sample size calculation was based on fasting insulin as primary end point, whereby we assumed a decrease of 21% (9.75 to 7.69 μIU/mL), since this was observed after 3 months in the calorie restriction with exercise group of the CALERIE study [6], which is comparable to our study. As the mean fasting insulin levels (μIU/mL) in longevity family members and controls in the complete LLS cohort were 6.93 (SD=4.3) and 8.70 (SD=6.6), respectively, and a correlation of 0.6 between repeated insulin measurements was assumed [47], we based our power calculation on an expected mean decrease of 1.65 μIU/mL, SD 4.9. With a power of 80% and an α of 5% this translates in a required sample size of 72 individuals. In a recent large meta-analysis, genetic background did not influence the association of healthy diet with fasting glucose or insulin [48]. Nevertheless, we doubled the sample size of our study to account for potential differences between longevity family members and controls in response to the intervention. Taking into account a dropout rate of 10%, we aimed to include 80 couples in the intervention.

All statistical analyses were performed with STATA/SE 11.2 (StataCorp LP, College Station, TX, USA) and SPSS Statistics v20 (IBM Corp, Armonk, NY, USA) and a $P \leq 0.05$ was considered significant.

ACKNOWLEDGEMENTS

We thank all staff members and Bachelor's and Master's students who contributed to the preparation, design, and performance of this intervention trial and/or assisted on the project. Last but not least, our gratitude goes to all participants who did their very best to adhere to the intervention guidelines and underwent all measurements at baseline and end.

Funding

The research leading to these results has received funding from the European Union's Seventh Framework Programme (FP7/2007-2011) under grant agreement number 259679. This study was financially supported by the Netherlands Consortium for Healthy Ageing (grant 050-060-810), in the framework of the Netherlands Genomics Initiative, Netherlands Organization for Scientific Research (NWO); by BBMRI-NL, a Research Infrastructure financed by the Dutch government (NWO 184.021.007) and by the Netherlands CardioVascular Research Initiative (CVON201-03). The funding agencies had no role in the design and conduct of the study; collection, management, analysis, and interpretation of the data; and preparation, review, or approval of the manuscript.

Author contributions

O.v.d.R, D.v.H, M.B., E.J.M.F, P.E.S designed the study. B.A.M.S, J.D., S.A.M.S., P.D.S., R.A.v.D.v.d.V., M.K. acquired the data. O.v.d.R, B.A.M.S, J.D., E.B.v.d.A, E.J.M.F., P.E.S. analysed the data. O.v.d.R, B.A.M.S, J.D., J.J.H.D. did statistical analysis. O.v.d.R, B.A.M.S, J.D., M.B., E.J.M.F., P.E.S drafted the manuscript. O.v.d.R, B.A.M.S, J.D., D.v.H, E.B.v.d.A, T.H., S.P.M., J.v.d.G., M.B., E.J.M.F., P.E.S critically revised the manuscript for important intellectual content. M.B., E.J.M.F., P.E.S. obtained funding.

Conflict of interest statement

The authors declare no competing financial interests.

REFERENCES

1. National Institute on Ageing, National Institutes of Health, U.S.Department of Health and Human Services, WHO. Global health and ageing. 2011.

2. Rejeski WJ, Mihalko SL. Physical activity and quality of life in older adults. J Gerontol A Biol Sci Med Sci 2001; 56 Spec No 2: 23-35.

3. Pittas AG, Roberts SB, Das SK et al. The effects of the dietary glycemic load on type 2 diabetes risk factors during weight loss. Obesity (Silver Spring) 2006; 14:2200-2209.
4. Layman DK, Evans E, Baum JI, Seyler J, Erickson DJ, Boileau RA. Dietary protein and exercise have additive effects on body composition during weight loss in adult women. J Nutr 2005; 135: 1903-1910.
5. Vroege DP, Wijsman CA, Broekhuizen K et al. Dose-response effects of a Web-based physical activity program on body composition and metabolic health in inactive older adults: additional analyses of a randomized controlled trial. J Med Internet Res 2014; 16: e265.
6. Heilbronn LK, de JL, Frisard MI et al. Effect of 6-month calorie restriction on biomarkers of longevity, metabolic adaptation, and oxidative stress in overweight individuals: a randomized controlled trial. JAMA 2006; 295:1539-1548.
7. Josse AR, Atkinson SA, Tarnopolsky MA, Phillips SM. Increased consumption of dairy foods and protein during diet- and exercise-induced weight loss promotes fat mass loss and lean mass gain in overweight and obese premenopausal women. J Nutr 2011; 141:1626-1634.
8. Roumen C, Corpeleijn E, Feskens EJ, Mensink M, Saris WH, Blaak EE. Impact of 3-year lifestyle intervention on postprandial glucose metabolism: the SLIM study. Diabet Med 2008; 25: 597-605.
9. Wijsman CA, Westendorp RG, Verhagen EA et al. Effects of a web-based intervention on physical activity and metabolism in older adults: randomized controlled trial. J Med Internet Res 2013; 15: e233.
10. Roef GL, Rietzschel ER, Van Daele CM et al. Triiodothyronine and free thyroxine levels are differentially associated with metabolic profile and adiposity-related cardiovascular risk markers in euthyroid middle-aged subjects. Thyroid 2014; 24: 223-231.
11. Barazzoni R, Silva V, Singer P. Clinical biomarkers in metabolic syndrome. Nutr Clin Pract 2014; 29:215-221.
12. Alberti KG, Eckel RH, Grundy SM et al. Harmonizing the metabolic syndrome: a joint interim statement of the International Diabetes Federation Task Force on Epidemiology and Prevention; National Heart, Lung, and Blood Institute; American Heart Association; World Heart Federation; International Atherosclerosis Society; and International Association for the Study of Obesity. Circulation 2009; 120: 1640-1645.
13. Okamoto Y, Kihara S, Funahashi T, Matsuzawa Y, Libby P. Adiponectin: a key adipocytokine in metabolic syndrome. Clin Sci (Lond) 2006; 110: 267-278.
14. Molander L, Lovheim H, Norman T, Nordstrom P, Gustafson Y. Lower systolic blood pressure is associated with greater mortality in people aged 85 and older. J Am Geriatr Soc 2008; 56: 1853-1859.
15. Weverling-Rijnsburger AW, Blauw GJ, Lagaay AM, Knook DL, Meinders AE, Westendorp RG. Total cholesterol and risk of mortality in the oldest old. Lancet 1997; 350: 1119-1123.
16. Rozing MP, Westendorp RG, de Craen AJ et al. Low serum free triiodothyronine levels mark familial longevity: the Leiden Longevity Study. J Gerontol A Biol Sci Med Sci 2010; 65: 365-368.
17. Atzmon G, Pollin TI, Crandall J et al. Adiponectin levels and genotype: a potential regulator of life span in humans. J Gerontol A Biol Sci Med Sci 2008; 63: 447-453.
18. Vaarhorst AA, Beekman M, Suchiman EH et al. Lipid metabolism in long-lived families: the Leiden Longevity Study. Age (Dordr) 2011; 33: 219-227.
19. Wijsman CA, Rozing MP, Streefland TC et al. Familial longevity is marked by enhanced insulin sensitivity. Aging Cell 2011; 10: 114-121.
20. Lankinen M, Kolehmainen M, Jaaskelainen T et al. Effects of whole grain, fish and bilberries on serum metabolic profile and lipid transfer protein activities: a randomized trial (Sysdimet). PLoS One 2014; 9: e90352.
21. Erkkila AT, Schwab US, Lehto S et al. Effect of fatty and lean fish intake on lipoprotein subclasses in subjects with coronary heart disease: a controlled trial. J Clin Lipidol 2014; 8: 126-133.
22. Stancakova A, Civelek M, Saleem NK et al. Hyperglycemia and a common variant of GCKR are associated with the levels of eight amino acids in 9,369 Finnish men. Diabetes 2012; 61: 1895-1902.
23. Suhre K, Meisinger C, Doring A et al. Metabolic footprint of diabetes: a multiplatform metabolomics study in an epidemiological setting. PLoS One 2010; 5: e13953.
24. Fiehn O, Garvey WT, Newman JW, Lok KH, Hoppel CL, Adams SH. Plasma metabolomic profiles reflective of glucose homeostasis in non-diabetic and type 2 diabetic obese African-American women. PLoS One 2010; 5: e15234.
25. Soininen P, Kangas AJ, Wurtz P, Suna T, Ala-Korpela M. Quantitative serum nuclear magnetic resonance metabolomics in cardiovascular epidemiology and genetics. Circ Cardiovasc Genet 2015; 8: 192-206.
26. Wurtz P, Havulinna AS, Soininen P et al. Metabolite profiling and cardiovascular event risk: a prospective study of 3 population-based cohorts. Circulation 2015; 131: 774-785.
27. Brien SE, Ronksley PE, Turner BJ, Mukamal KJ, Ghali WA. Effect of alcohol consumption on biological markers associated with risk of coronary heart disease: systematic review and meta-analysis of interventional studies. BMJ 2011; 342: d636.
28. Dishman RK, Berthoud HR, Booth FW et al. Neurobiology of exercise. Obesity (Silver Spring) 2006; 14: 345-356.
29. Dunn AL, Jewell JS. The Effect of Exercise on Mental Health. 2010; 9: 202-207.
30. Longo VD, Antebi A, Bartke A et al. Interventions to Slow Aging in Humans: Are We Ready? Aging Cell. 2015; 14:497-510.
31. Schoenmaker M, de Craen AJ, de Meijer PH et al. Evidence of genetic enrichment for exceptional survival using a family approach: the Leiden Longevity Study. Eur J Hum Genet 2006; 14: 79-84.
32. Feunekes GI, Van Staveren WA, De Vries JH, Burema J, Hautvast JG. Relative and biomarker-based validity of a food-frequency questionnaire estimating intake of fats and cholesterol. Am J Clin Nutr 1993; 58:489-496.
33. Craig CL, Marshall AL, Sjostrom M et al. International physical activity questionnaire: 12-country reliability and validity. Med Sci Sports Exerc 2003; 35: 1381-1395.
34. Health Council of the Netherlands. Guidelines for a healthy diet 2006. The Hague: Health Council of the Netherlands, 2006
35. de Vries H, Dijkstra M, Kuhlman P. Self-efficacy: the third factor besides attitude and subjective norm as a predictor of behavioural intentions. 1988; 3: 273.
36. Prochaska JO, DiClemente CC, Norcross JC. In search of how people change. Applications to addictive behaviors. Am Psychol 1992; 47: 1102-1114.

37. Miller WR. Motivational Interviewing: Preparing people for change. New York, NY, US: Guilford Press; 2002.
38. Guralnik JM, Simonsick EM, Ferrucci L et al. A short physical performance battery assessing lower extremity function: association with self-reported disability and prediction of mortality and nursing home admission. J Gerontol 1994; 49: M85-M94.
39. Ware J, Jr., Kosinski M, Keller SD. A 12-Item Short-Form Health Survey: construction of scales and preliminary tests of reliability and validity. Med Care 1996; 34: 220-233.
40. Expert Panel on Detection EaToHBCiA. Executive Summary of The Third Report of The National Cholesterol Education Program (NCEP) Expert Panel on Detection, Evaluation, And Treatment of High Blood Cholesterol In Adults (Adult Treatment Panel III). JAMA 2001; 285: 2486-2497.
41. Friedewald WT, Levy RI, Fredrickson DS. Estimation of the concentration of low-density lipoprotein cholesterol in plasma, without use of the preparative ultracentrifuge. Clin Chem 1972; 18: 499-502.
42. Wallace TM, Levy JC, Matthews DR. Use and abuse of HOMA modeling. Diabetes Care 2004; 27: 1487-1495.
43. Soininen P, Kangas AJ, Wurtz P et al. High-throughput serum NMR metabonomics for cost-effective holistic studies on systemic metabolism. Analyst 2009; 134: 1781-1785.
44. A Language and Environment for Statistical Computing. 2015.
45. Kuznetsova A, Brockhoff PB, Christensen, RHB. lmerTest: Tests in Linear Mixed Effects Models. R package version 2.0-29. 2015.
46. Langfelder P, Horvath S. WGCNA: an R package for weighted correlation network analysis. BMC Bioinformatics 2008; 9: 559.
47. Mensink M, Feskens EJ, Saris WH, De Bruin TW, Blaak EE. Study on Lifestyle Intervention and Impaired Glucose Tolerance Maastricht (SLIM): preliminary results after one year. Int J Obes Relat Metab Disord 2003; 27: 377-384.
48. Nettleton JA, Hivert MF, Lemaitre RN et al. Meta-analysis investigating associations between healthy diet and fasting glucose and insulin levels and modification by loci associated with glucose homeostasis in data from 15 cohorts. Am J Epidemiol 2013; 177: 103-115.

Research Paper

Caloric restriction induces heat shock response and inhibits B16F10 cell tumorigenesis both *in vitro* and *in vivo*

Marta G. Novelle[1,3], Ashley Davis[1], Nathan L. Price[1], Ahmed Ali[1], Stefanie Fürer-Galvan[1], Yongqing Zhang[2], Kevin Becker[2], Michel Bernier[1], and Rafael de Cabo[1]

[1]Translational Gerontology Branch, National Institute on Aging, National Institutes of Health, Baltimore, MD 21224, USA
[2]Gene Expression and Genomics Unit, National Institute on Aging, National Institutes of Health, Baltimore, MD 21224, USA
[3]Department of Physiology, CIMUS, University of Santiago de Compostela-Instituto de Investigación Sanitaria, 15782 Santiago de Compostela, Spain; CIBER Fisiopatología de la Obesidad y Nutrición (CIBERobn), 15706 Santiago de Compostela, Spain

Key words: caloric restriction, heat shock, stress response, tumorigenesis, aging
Received: 12/01/14; Accepted: 03/24/15; Published: 04/05/15 **doi:** 10.18632/aging.100732
Correspondence to: Rafael de Cabo, PhD; **E-mail:** decabora@grc.nia.nih.gov

Abstract: Caloric restriction (CR) without malnutrition is one of the most consistent strategies for increasing mean and maximal lifespan and delaying the onset of age-associated diseases. Stress resistance is a common trait of many long-lived mutants and life-extending interventions, including CR. Indeed, better protection against heat shock and other genotoxic insults have helped explain the pro-survival properties of CR. In this study, both *in vitro* and *in vivo* responses to heat shock were investigated using two different models of CR. Murine B16F10 melanoma cells treated with serum from CR-fed rats showed lower proliferation, increased tolerance to heat shock and enhanced HSP-70 expression, compared to serum from *ad libitum*-fed animals. Similar effects were observed in B16F10 cells implanted subcutaneously in male C57BL/6 mice subjected to CR. Microarray analysis identified a number of genes and pathways whose expression profile were similar in both models. These results suggest that the use of an *in vitro* model could be a good alternative to study the mechanisms by which CR exerts its anti-tumorigenic effects.

INTRODUCTION

Aging is a complex multifactorial process, whereby organisms undergo major cell degeneration and loss of function. During aging, irreversible and deleterious processes are triggered by accumulation of damaged cellular macromolecules [1, 2]. Several theories have been proposed to explain these processes [3, 4], but the exact molecular mechanisms behind aging remains unknown. Cellular damage may result from oxidative stress, toxic metabolic byproducts, endoplasmic reticulum stress and mitochondrial unfolded protein responses, or exposure to heat stress, among others. Several heat shock proteins (HSP) function as molecular chaperones by preventing misfolding and aggregation of other proteins. This induction of cytoprotective responses promotes longevity [5, 6]; conversely, aging is associated with down-regulation in HSP expression in neuronal tissue, skeletal and cardiac muscle, and the liver [7, 8]. Stimulation of HSP synthesis has been suggested as a viable strategy to counteract the negative effects of aging and eliciting a 'low-grade' stress response may help organisms live longer and improve their survival [9].

More than 8 decades ago, McCay and colleagues observed that severe reduction in calorie intake while maintaining sufficient micronutrient levels for optimum health resulted in lifespan extension [10]. Since then,

numerous studies have reported that lifelong caloric restriction (CR) extends mean and maximum lifespan and delays age-associated diseases in a wide variety of species [11, 12]. Many of the beneficial effects of CR are mediated by altering the expression of several HSPs, notably Hsp70, and the activation of heat shock transcription factor 1 [13-15]. In this context, our group has demonstrated that exposure of HepG2 cells to human serum from CR participants conferred significant cytoprotection against heat stress [7]. Moreover, cells treated with human serum from CR volunteers trigger a transcriptional up-regulation of numerous genes and pathways implicated in stress resistance through activation of the transcription factor NF-E2-related factor (NRF2) [16]. NFR2 plays a key role in maintaining homeostasis during oxidative stress and exposure to carcinogens by coordinately regulating the expression of antioxidants and detoxification enzymes [17] that boost protection against cancer [18].

The anti-tumorigenic properties of CR on spontaneously arising tumors and in experimental cancer models are well-documented [19]. For example, 15 days of 40% CR significantly reduces the growth of brain tumors in mice by reducing angiogenesis and increasing tumor cell apoptosis [20]. The combination of fasting and chemotherapy retards the growth of human breast cancer tumors in mice [21] and delays the progression of pancreatic cancer lesions in a mouse model [22]. The use of the mouse as an experimental tool in cancer research is cumbersome, time-consuming and expensive, and, therefore, has compelled us to explore an alternative approach to study anti-cancer therapies.

In this manuscript we present a new approach to investigate a central mechanism by which CR activates a stress response pathway to combat tumorigenesis. The stress response of murine B16F10 melanoma cells maintained in culture medium supplemented with serum from rats fed CR and *ad libitum* (AL) diet was evaluated and compared to that of mice injected with B16F10 melanoma cells and maintained on either CR or AL. In the latter experimental model, mice were subjected to heat stress followed by the monitoring of a melanoma-specific Hsp70 reporter expression. These results combined with microarray analysis illustrated alteration of a common set of cancer-related genes using in *vitro* and *in vivo* testing.

RESULTS

Growth rate and heat shock response of B16F10 melanoma cells maintained in serum from CR-fed animals

Proliferation of B16F10 melanoma cells was carried out in the presence of serum from rats fed either AL or CR diet. A significant reduction in cell growth was observed following incubation with CR serum as compared to AL serum controls (Fig. 1a). Exposure of B16F10 cells to heat stress (45°C) for 1 h caused a significant difference in survival depending on whether these cells were maintained in CR or AL serum (Fig. 1b). Our observations that CR serum decreased heat-dependent cellular cytotoxicity support previously published results from this laboratory [23].

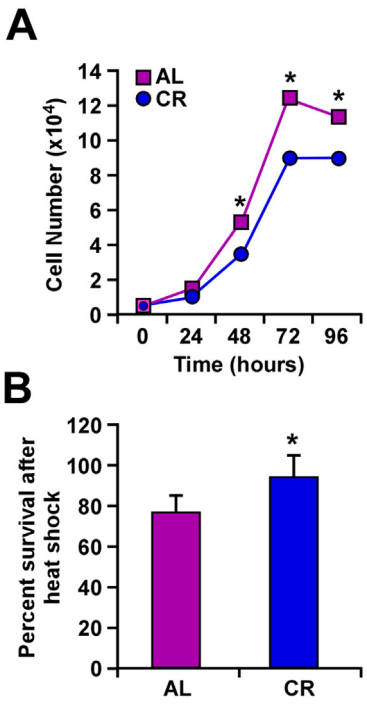

Figure 1. Caloric restriction slows cellular growth and improves response to heat shock. (**A**) B16F10 melanoma cells were maintained in culture with serum from AL- and CR-fed rats over a period of 96 h. The number of cells was counted at 24-h intervals. (**B**) Percent of cells surviving a 1-h treatment at 45°C when maintained in culture with serum from either AL- or CR-fed rats. Data are represented as the mean ± SEM. *, $p < 0.05$.

Reduction in the number and size of tumors in mice on caloric restriction

To evaluate the effect of CR on tumor growth *in vivo*, mouse B16F10 melanoma cells that were stably transfected with Hsp70-GFP plasmid, were implanted subcutaneously in male C57BL/6 mice fed either a CR or AL diet. A significant decrease in the size and weight of tumors was observed in CR-fed mice along with delayed tumor growth both in the periscapular region and lower back area (Fig. 2).

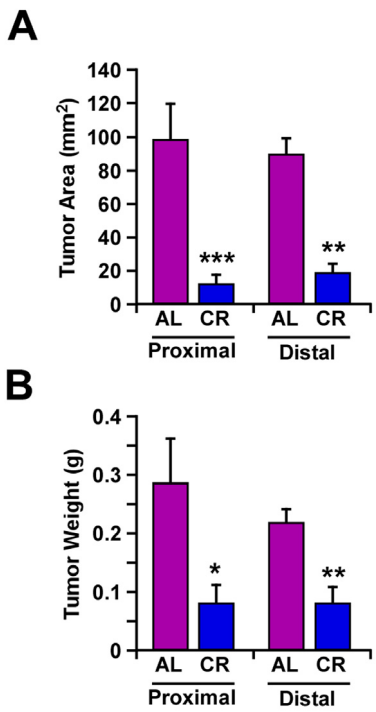

Figure 2. Caloric restriction decreased melanoma tumor growth *in vivo*. In AL- and CR-fed mice, mouse tumor xenografts were formed by implanting B16F10 melanoma cells, at the periscapular region (proximal area) and in the lower back over the hip (distal area). Tumor area (mm^2) (**A**) and individual tumor weight (g) (**B**) were determined after 14 days. Data are represented as the mean ± SEM. n=10/per group. *, p< 0.05, **, p<0.01, *** p<0.001.

Heat stress-mediated induction of Hsp70 expression both in *in vitro* and *in vivo* models

Changes in HSP expression play an important role in the ability of cells to respond to environmental stressors. Earlier work has shown an elevation in Hsp70 expression in B16F10 melanoma cells cultured with serum from CR-fed animals [23]. Here, we compared the effects of CR alone, heat shock alone or the combination 'CR + heat shock' using B16F10 melanoma cells stably expressing GFP-tagged Hsp70 construct under the control of rat *hsp70.1* promoter [24]. The results indicate that the heat-mediated induction of Hsp70 expression was significantly higher when B16F10 cells and tumor-bearing animals were subjected to CR (Fig. 3).

Microarray analysis of B16F10 melanoma cells used in *in vitro* and *in vivo* settings

DNA microarray analysis was performed to compare the global transcriptional effect of CR in B16F10 melanoma cells either grown in culture or implanted in mice. Principal Component Analysis (PCA) revealed inherent *in vivo* and *in vitro* differences that must be taken into account when comparing the impact of CR in gene expression profile. Nevertheless, Venn diagram indicated that both models shared 55 up-regulated and 17 down-regulated transcripts, which were significantly enriched in the CR versus AL pairwise comparisons (Fig. 4a, Supplemental Table 1). Among these shared transcripts, MAP Kinase Interacting Serine/Threonine

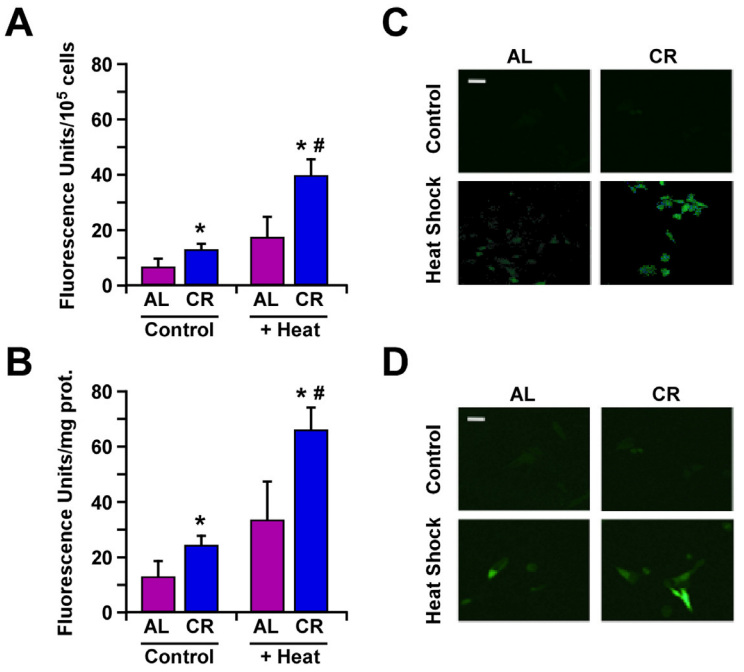

Figure 3. Caloric restriction improves protection against heat shock through increased expression of Hsp70. (**A**) B16F10 melanoma cells stably transfected with a plasmid encoding GFP-tagged Hsp70 construct were maintained in medium supplemented with 10% serum from AL- or CR-fed rats and then subjected or not to heat shock stress for 45 min. Bars represent fluorescence intensity per 10^5 cells. Cell culture experiments were performed as three or more replicates. (**B**) B16F10 tumor xenografts from mice fed either AL or CR diet were subjected to heat shock stress for 45 min and sacrificed after 4h. Bars represent fluorescence intensity per mg of tumor proteins; n=10 per group. Data, obtained by fluorimetery, are represented as the means ± SEM. *, p <0.05 *vs.* AL group; #, p<0.05 *vs.* CR group. (**C**) Images of B16F10 cells and (**D**) tumor cells depicting GFP fluorescence were detected by confocal microscopy. White bar, 20 µm.

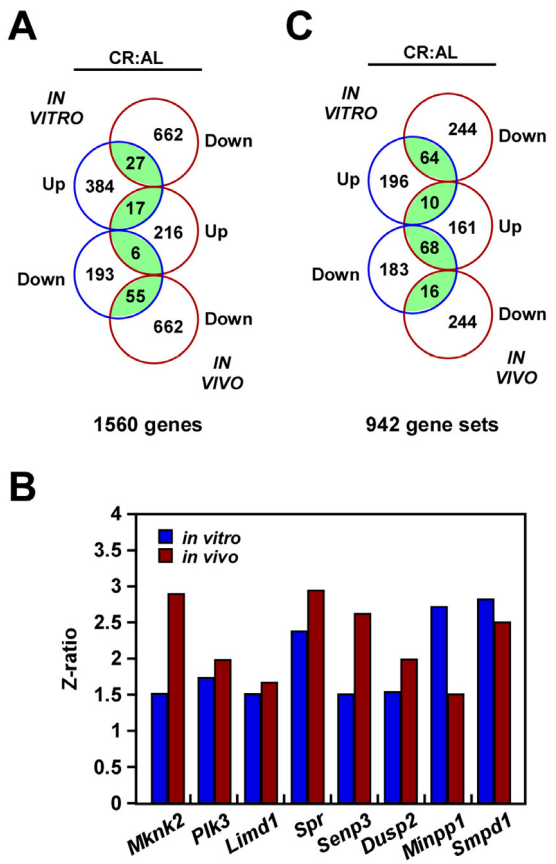

Figure 4. Gene expression profiling in response to caloric restriction. (**A**) Venn diagram showing the overlap of gene **transcripts** with significant change in expression in the CR *versus* AL pairwise comparisons by both B16F10 melanoma cells growing in culture (*in vitro*) and as tumor xenografts (*in vivo*). (**B**) Effect of CR on the expression of a select group of transcripts. (**C**) Venn diagram showing the overlap of gene sets with significant change in expression in the CR *versus* AL pairwise comparisons.

Kinase 2 (*Mknk2*) [25], polo-like kinase 3 (*Plk3*) [26] and LIM Domains Containing 1 (*Limd1*) [27] are implicated in tumorigenesis, whereas *Spr* and *Semp3*, which encode for Sepiapterin Reductase and SUMO1/Sentrin/SMT3 Specific Peptidase 3, are involved in stress response [28, 29]. DUSP2 is an important member of the dual-specificity protein phosphatase subfamily, which is implicated in inflammatory response and reported to be upregulated both with CR and heat shock [30]. Moreover, there is an increased expression of *Minpp1*, which encodes for Multiple Inositol Polyphosphate Phosphatase 1. This phosphatase is induced in response to heat shock, osmotic and oxidative stress conditions, thereby contributing to the regulation of ER stress and apoptosis [31]. Finally, upregulation of *Smpd1* (Sphingomyelin phosphodiesterase 1, also known as ASM) was also observed in both experimental models with CR (Fig. 4b). Its activity is expressed at high levels in cancer cells under the control of an inducible expression of hsp70.1 protein [32]. Using parametric analysis of gene set enrichment, 26 gene sets were identified whose expression levels were significantly altered in the same direction by CR in both experimental models (Fig. 4c, Supplemental Table S2).

DISCUSSION

The aging process involves multiple physiological mechanisms and represents one of the main risk factors for several human pathologies, such as cancer, diabetes, and cardiovascular disease. Dietary CR retards the aging process and age-related disease pathogenesis [33, 34], and many studies have tried to elucidate the exact mechanism(s) by which CR acts (reviewed in [35]). Our work demonstrates that CR significantly decreases tumor cell proliferation, in agreement with previous studies [36, 37], and this phenomenon takes place whether B16F10 melanoma cells were cultured with serum from CR-fed animals or these tumor cells were implanted in CR-fed mice. Moreover, the process of tumorigenesis was significantly decreased in CR-fed animals after heat stress. Hsp70 is one of several heat-shock proteins implicated in the regulation of cancer cell growth. HSPs sustain tumor survival and drive tumor growth [38]; however, induction of Hsp70 family members results in cellular protection against un-favorable environmental conditions, including elevated temperatures, oxidative stress, exposure to heavy metals, proteasome inhibitors, and infection [39]. CR has been previously shown to restore the ability of cells to mount a heat shock response through increase in Hsp70-mediated thermotolerance [40], an observation that was confirmed in the present study. Moreover, B16F10 melanoma cells subjected to heat shock stress showed greater survival when maintained in CR serum as compared to serum from AL-fed animals. It would appear that heat stress and CR acted cooperatively to enhance cell survival, possibly via activation of the deacetylase SIRT1 [40, 41]. It is interesting to note that the combination of heat stress with CR caused a synergistic increase in Hsp70-GFP expression when compared to either condition alone both *in vitro* and *in vivo*.

Microarray results reinforce the idea that despite significant genome-wide gene expression variation between the two experimental models, the expression profile of several transcripts implicated in tumorigenesis and stress response exhibited a comparable pattern,

whether B16F10 melanoma cells were cultured in CR serum or implanted in mice fed a CR diet. Although this *in vitro* model is quite distant from a physiological setting, it displayed a number of molecular pathways similar to the ones observed *in vivo*.

In conclusion, our findings indicate that the impact of CR on the regulation of several pathways implicated in tumorigenesis on an *in vivo* model of heat stress response can be replicated *in vitro* using tumor cells incubated with serum from CR-fed animals. The idea that hormones and nutrients present in serum, whose levels are altered during CR, are involved in homeostasis control mechanisms, including the aging process, has been suggested [7, 16, 23]. These results support the notion that *in vitro* testing may be well suited for the study of molecular aspects of CR that have not been elucidated yet.

MATERIALS AND METHODS

Animals and dietary manipulation. The mice were single-housed in duplex caging in a room maintained at a constant temperature (20-22 °C) and humidity (30-70%) in a light:dark 12:12-h schedule, according to established animal protocols and NIH guidelines. Male C57BL/6 mice (3 month old) were fed on a standard purified mouse diet (NIH-31) *ad libitum* (AL; n=10) or maintained on a 40% calorie restriction regimen (CR; n=10) during six weeks. Body weight and food intake was recorded weekly (supplemental figure 1 a, b).

Cell culture. B16F10 melanoma cells (ATCC® CRL-6475™) were purchased from American Type Culture Collection (Manassas, VA); they were cultured in Dulbecco's Modified Essential Medium (DMEM) supplemented with 10% fetal bovine serum and penicillin/streptomycin (Gibco, Gaithersburg, MD) under standard cell culture conditions. Cells were incubated in media with 10% serum from AL- or CR-fed rats (as described previously [23]). Briefly, serum was obtained from overnight fasted, anesthetized 6-month-old male Fisher 344 rats from three different cohorts. The blood collection took place between 7-11:00 a.m. After a 1-h incubation in a water bath at 45°C, cells were trypsinized, washed twice with phosphate-buffered saline (Invitrogen, Grand Island, NY), and then seeded at $1.5x10^5$ cells/well in 96-well plates. Cell proliferation assays were carried out during 96 h by the addition of a tetrazolium salt solution, WST-8, to each well according to the manufacturer's protocol (Dojindo, Indianapolis, IN). The absorbance of the formazan dye formed was measured at 450nm using the Perkin Elmer HTS 7000 Plus BioAssay reader.

Heat shock treatment of B16F10 melanoma xenografts in vivo. One month into the study, mice were injected with $1x10^6$ B16F10 melanoma cells stably transfected with a plasmid containing *GFP* gene linked to rat stress-inducible *hsp70.1* gene promoter [24] in the periscapular region (proximal) and in the lower back over the hip (distal area). After a two-week period, five mice were randomly chosen from each group and placed in a tumor hyperthermia induction chamber (THIC) constructed in our facility. Mice were anesthetized with isoflurane droplets in a closed chamber prior to being placed in the THIC and maintained under anesthesia for the reminder of the experiment. Two membranous tubes filled with pre-warmed water were placed over the proximal (45°C) and distal (27°C) tumors of the anesthetized mice *(supplemental figure 1 c, d)*. The water temperature was maintained throughout the duration of the experiment. After a 45-min heat treatment, the mice recovered for 4 h and then euthanized by cervical dislocation, according to the AAALAC guidelines.

Melanoma tumor growth *in vivo*. Tumor xenografts were formed by implanting murine B16F10 melanoma cells at the periscapular region and in the lower back of AL- and CR-fed mice. Fourteen days later, animals were euthanized and tumors were excised for the determination of the tumor area using a caliper. Tumor weight was also recorded.

GFP fluorescence detection. Experiments were carried out as indicated, using B16F10 melanoma cells stably expressing a plasmid encoding GFP-tagged Hsp70 that were either maintained in culture or used as tumor xenografts in mice. GFP fluorescence was monitored using both a confocal microscope (Axiovert-200, Zeiss LSM 510) to obtain images and a fluorimeter (Perkin-Elmer LS-55 and HTS 7000 Plus BioAssay reader) to accurately quantify GFP expression levels, which were normalized per 10^5 cells (in culture) or mg of tumor proteins.

Microarray analysis. RNA was isolated from B16F10 melanoma cells maintained in culture and as tumor xenografts. For microarray analysis, RNA was processed, reverse transcribed, labeled and hybridized to Mouse 15K cDNA arrays and read on an Illumina BeadArray 500GX reader. Raw data were subjected to Z normalization to ensure compatibility using the formula: z(raw data)=[ln (raw data) – avg(ln(raw data))]/[std dev(ln (raw data))], where ln is natural logarithm, avg is the average over all genes of an array, and std dev is the standard deviation over all genes of an array (Cheadle et al., 2003). The Z ratio (between treatment A and B) is given by z(A)-z(B)/std dev.

Individual genes with Z ratio > 1.5 in both directions, *P* value < 0.05, and false discovery rate > 0.3 were considered significantly changed. All raw data were deposited in the NCBI Gene Expression Omnibus under accession number GSE67430.

Statistical analysis. Statistical analyses were performed using Microsoft Excel software (Microsoft Corp., Redmond, WA). Unpaired t-tests were used for all analyses. Statistical significance was established at $p<0.05$. Data are expressed as means ± standard error of the mean (SEM).

ACKNOWLEDGEMENTS

We would like to thank Dr. Zdzislaw Krawczyk for giving us the plasmid encoding GFP-tagged Hsp70. This work has been supported by the Intramural Research Program of the National Institute on Aging, National Institutes of Health. MGN was supported by CIBER de Fisiopatología de la Obesidad y Nutrición (CIBERobn), an initiative of ISCIII, Spain.

Conflict of interest statement

The authors have no conflict of interests to declare.

REFERENCES

1. Chondrogianni N, Sakellari M, Lefaki M, Papaevgeniou N and Gonos ES. Proteasome Activation Delays Aging in Vitro and in Vivo. Free Radic Biol Med. 2014;71:303-320.

2. López -Otin C, Blasco MA, Partridge L, Serrano M and Kroemer G. The hallmarks of aging. Cell. 2013; 153:1194-1217.

3. Jin K. Modern Biological Theories of Aging. Aging Dis. 2010; 1:72-74.

4. Wiggins J and Bitzer M. Slowing the aging process. Clin Geriatr Med. 2013; 29:721-730.

5. Shore DE, Carr CE and Ruvkun G. Induction of cytoprotective pathways is central to the extension of lifespan conferred by multiple longevity pathways. PLoS Genet. 2012;8:e1002792.

6. Shore DE and Ruvkun G. A cytoprotective perspective on longevity regulation. Trends Cell Biol. 2013; 23:409-420.

7. Allard JS, Heilbronn LK, Smith C, Hunt ND, Ingram DK, Ravussin E and de CR. In vitro cellular adaptations of indicators of longevity in response to treatment with serum collected from humans on calorie restricted diets. PLoS One. 2008;3:e3211.

8. Hall DM, Xu L, Drake VJ, Oberley LW, Oberley TD, Moseley PL and Kregel KC. Aging reduces adaptive capacity and stress protein expression in the liver after heat stress. J Appl Physiol (1985). 2000; 89:749-759.

9. Rattan SI, Fernandes RA, Demirovic D, Dymek B and Lima CF. Heat stress and hormetin-induced hormesis in human cells: effects on aging, wound healing, angiogenesis, and differentiation. Dose Response. 2009; 7:90-103.

10. McCay CM, Crowell MF and Maynard LA. The effect of retarded growth upon the length of life span and upon the ultimate body size. 1935. Nutrition. 1989;5:155-171.

11. McDonald RB and Ramsey JJ. Honoring Clive McCay and 75 years of calorie restriction research. J Nutr. 2010; 140:1205-1210.

12. Mercken EM, Carboneau BA, Krzysik-Walker SM and de Cabo R. Of mice and men: the benefits of caloric restriction, exercise, and mimetics. Ageing Res Rev. 2012; 11:390-398.

13. Brown MK and Naidoo N. The endoplasmic reticulum stress response in aging and age-related diseases. FPHYS. 2012; 3:263.

14. Morimoto RI and Cuervo AM. Proteostasis and the aging proteome in health and disease. J Gerontol A Biol Sci Med Sci. 2014; 69 Suppl 1:S33-38.

15. Sinclair DA. Toward a unified theory of caloric restriction and longevity regulation. Mech Ageing Dev. 2005; 126:987-1002.

16. Omodei D, Licastro D, Salvatore F, Crosby SD and Fontana L. Serum from humans on long-term calorie restriction enhances stress resistance in cell culture. Aging (Albany NY). 2013; 5:599-606.

17. Martin-Montalvo A, Villalba JM, Navas P and de Cabo R. NRF2, cancer and calorie restriction. Oncogene. 2011; 30:505-520.

18. Jaramillo MC and Zhang DD. The emerging role of the Nrf2-Keap1 signaling pathway in cancer. Genes Dev. 2013; 27:2179-2191.

19. Hursting SD, Smith SM, Lashinger LM, Harvey AE and Perkins SN. Calories and carcinogenesis: lessons learned from 30 years of calorie restriction research. Carcinogenesis. 2010; 31:83-89.

20. Mukherjee P, Abate LE and Seyfried TN. Antiangiogenic and proapoptotic effects of dietary restriction on experimental mouse and human brain tumors. Clin Cancer Res. 2004; 10:5622-5629.

21. Lee C, Safdie FM, Raffaghello L, Wei M, Madia F, Parrella E, Hwang D, Cohen P, Bianchi G and Longo VD. Reduced levels of IGF-I mediate differential protection of normal and cancer cells in response to fasting and improve chemotherapeutic index. Cancer Res. 2010; 70:1564-1572.

22. Lanza-Jacoby S, Yan G, Radice G, LePhong C, Baliff J and Hess R. Calorie restriction delays the progression of lesions to pancreatic cancer in the LSL-KrasG12D; Pdx-1/Cre mouse model of pancreatic cancer. Exp Biol Med (Maywood). 2013; 238:787-797.

23. De Cabo R, Fürer-Galban S, Anson RM, Gilman C, Gorospe M and Lane MA. An in vitro model of caloric restriction. Exp Gerontol. 2003; 38:631-639.

24. Wysocka A and Krawczyk Z. Green fluorescent protein as a marker for monitoring activity of stress-inducible hsp70 rat gene promoter. Mol Cell Biochem. 2000; 215:153-156.

25. Ueda T, Sasaki M, Elia AJ, Chio II, Hamada K, Fukunaga R and Mak TW. Combined deficiency for MAP kinase-interacting kinase 1 and 2 (Mnk1 and Mnk2) delays tumor development. PNAS. 2010; 107(32):13984-13990.

26. Strebhardt K. Multifaceted polo-like kinases: drug targets and antitargets for cancer therapy. Nat Rev Drug Discov. 2010; 9:643-660.

27. Sharp TV, Munoz F, Bourboulia D, Presneau N, Darai E, Wang HW, Cannon M, Butcher DN, Nicholson AG, Klein G, Imreh S and Boshoff C. LIM domains-containing protein 1 (LIMD1), a tumor suppressor encoded at chromosome 3p21.3, binds pRB and represses E2F-driven transcription. PNAS. 2004; 101:16531-16536.

28. Rochette L, Lorin J, Zeller M, Guilland JC, Lorgis L, Cottin Y and Vergely C. Nitric oxide synthase inhibition and oxidative

stress in cardiovascular diseases: possible therapeutic targets? Pharmacol Ther. 2013; 140:239-257.
29. Wang Y, Yang J and Yi J. Redox sensing by proteins: oxidative modifications on cysteines and the consequent events. Antioxid Redox Signal. 2012;16:649-657.
30. Lang R, Hammer M and Mages J. DUSP meet immunology: dual specificity MAPK phosphatases in control of the inflammatory response. J Immunol. 2006; 177:7497-7504.
31. Kilaparty SP and Ali N. Changes in expression of Multiple Inositol Polyphosphate Phosphatase1 (Minpp1) under Apoptotic and Cellular Stress Conditions. FASEB J. 2013;27:834.14
32. Zhu H, Yoshimoto T and Yamashima T. Heat shock protein 70.1 (Hsp70.1) affects neuronal cell fate by regulating lysosomal acid sphingomyelinase. J Biol Chem. 2014; 289:27432-27443.
33. Mercken EM, Crosby SD, Lamming DW, JeBailey L, Krzysik-Walker S, Villareal DT, Capri M, Franceschi C, Zhang Y, Becker K, Sabatini DM, de Cabo R and Fontana L. Calorie restriction in humans inhibits the PI3K/AKT pathway and induces a younger transcription profile. Aging Cell. 2013; 12:645-651.
34. Omodei D and Fontana L. Calorie restriction and prevention of age-associated chronic disease. FEBS Lett. 2011; 585:1537-1542.
35. De Cabo R, Carmona-Gutierrez D, Bernier M, Hall MN and Madeo F. The search for antiaging interventions: from elixirs to fasting regimens. Cell. 2014;157:1515-1526.
36. De Lorenzo MS, Baljinnyam E, Vatner DE, Abarzua P, Vatner SF and Rabson AB. Caloric restriction reduces growth of mammary tumors and metastases. Carcinogenesis. 2011; 32:1381-1387.
37. Minor RK, López M, Younts CM, Jones B, Pearson KJ, Anson RM, Dieguez C and de Cabo R. The arcuate nucleus and neuropeptide Y contribute to the antitumorigenic effect of calorie restriction. Aging Cell. 2011; 10:483-492.
38. Daugaard M, Jaattela M and Rohde M. Hsp70-2 is required for tumor cell growth and survival. Cell Cycle. 2005; 4:877-880.
39. Westerheide SD and Morimoto RI. Heat shock response modulators as therapeutic tools for diseases of protein conformation. J Biol Chem. 2005; 280:33097-33100.
40. Raynes R, Leckey BD, Jr., Nguyen K and Westerheide SD. Heat shock and caloric restriction have a synergistic effect on the heat shock response in a sir2.1-dependent manner in Caenorhabditis elegans. J Biol Chem. 2012; 287:29045-29053.
41. Westerheide SD, Anckar J, Stevens SM, Jr., Sistonen L and Morimoto RI. Stress-inducible regulation of heat shock factor 1 by the deacetylase SIRT1. Science. 2009; 323:1063-1066.

Research Paper

Serum from calorie-restricted animals delays senescence and extends the lifespan of normal human fibroblasts *in vitro*

Rafael de Cabo[1*], Lijuan Liu[1*], Ahmed Ali[1], Nathan Price[1], Jing Zhang[1], Mingyi Wang[1], Edward Lakatta[2], and Pablo M. Irusta[1, 3]

[1] Experimental Gerontology Section, Translational Gerontology Branch, NIA/NIH, Baltimore, MD 21224, USA
[2] Laboratory of Cardiovascular Science and Cardiovascular Function Section, NIA/NIH, Baltimore, MD 21224, USA
[3] Department of Human Science, Georgetown University Medical Center, Washington, DC 20057 USA
[*] These authors contributed equally to this work

Key words: human diploid fibroblasts, senescence, caloric restriction, lifespan extension, SIRT1, aging
Received: 08/12/14; Accepted: 01/11/15; Published: 01/13/15 **doi:** 10.18632/aging.100719
Correspondence to: Rafael de Cabo, PhD; Pablo M. Irusta, PhD; **E-mail:** decabora@grc.nia.nih.gov; pmi2@georgetown.edu

Abstract: The cumulative effects of cellular senescence and cell loss over time in various tissues and organs are considered major contributing factors to the ageing process. In various organisms, caloric restriction (CR) slows ageing and increases lifespan, at least in part, by activating nicotinamide adenine dinucleotide (NAD^+)-dependent protein deacetylases of the sirtuin family. Here, we use an *in vitro* model of CR to study the effects of this dietary regime on replicative senescence, cellular lifespan and modulation of the SIRT1 signaling pathway in normal human diploid fibroblasts. We found that serum from calorie-restricted animals was able to delay senescence and significantly increase replicative lifespan in these cells, when compared to serum from *ad libitum* fed animals. These effects correlated with CR-mediated increases in SIRT1 and decreases in p53 expression levels. In addition, we show that manipulation of SIRT1 levels by either over-expression or siRNA-mediated knockdown resulted in delayed and accelerated cellular senescence, respectively. Our results demonstrate that CR can delay senescence and increase replicative lifespan of normal human diploid fibroblasts *in vitro* and suggest that SIRT1 plays an important role in these processes. (185 words).

INTRODUCTION

The multifactorial process of ageing is thought to involve the cumulative effects of cell loss in various tissues and organs throughout life due in part to cellular senescence [1-9]. Age-associated cell loss and the consequent generation of hostile microenvironments are believed to render the elderly susceptible to various stresses, e.g. overloading cholesterol and oxidative stress [10-15]. These age-associated metabolic dysfunctions further contribute to fragility of otherwise healthy older cells and organs, exacerbating the ageing process. Normal human diploid somatic cells cultured in the laboratory, recapitulate the senescence process observed in ageing cells by displaying a finite replicative lifespan [3,6,16]. After a limited number of cellular divisions, these cells enter a state of replicative senescence, which is characterized by irreversible growth arrest and secretion of senescence-associated bioactive factors like matrix metalloproteinases (MMPs) [17,18].

In a wide range of organisms ranging from yeast to mammals, calorie restriction (CR) has proven to be a highly reproducible intervention for extending lifespan as well as effectively retarding the onset and reducing the incidence of age-related diseases [19-25]. Several beneficial CR-associated effects are due to decreased levels of oxidative stress and maintained metabolic homeostasis [26-28]. Nicotinamide adenine dinucleotide (NAD^+)-dependent protein deacetylases of the sirtuin family are induced by CR in all experimental systems studied and have been postulated to be at the core of most of these effects [29-32]. In *Saccharomyces*

cerevisiae, *Caenorhabditis elegans* and *Drosophila melanogaster* increased Sir2 levels have been directly associated with lifespan extension [33-37] and the mammalian SIRT1 protein is regarded as one of the candidate mediators of the longevity effect of CR in rodents [38-40]. Supporting this notion, it has been shown that over-expression of SIRT1 in transgenic mice results in physiologic responses that resemble CR treatments [41], and pharmacological interventions with molecules that activate SIRT1 (e.g. resveratrol) extend the lifespan of mice fed a high fat diet [42,43].

We have previously described an *in vitro* model of CR using cell cultures grown in medium supplemented with serum from animals on CR diets [44]. Many of the features of CR, including reduced cellular proliferation, enhanced stress responsiveness and changes in gene expression could effectively be reproduced in this system. In particular, CR serum leads to increased SIRT1 protein levels in cultured cells [38]. Thus, several effects of CR appear to be mediated by circulating factors in the sera of the animals subjected to the dietary regimen and can be recapitulated *in vitro*. In this study we investigated the effects of CR on replicative senescence. To this end, we cultured normal human diploid fibroblasts *in vitro* in the presence of serum from rats fed on CR (40%) versus *ad libitum* (AL) diets, and assessed the consequences on replicative capacity, cellular lifespan and modulation of the SIRT1 signaling pathway.

RESULTS

CR serum delays the onset of senescent phenotypic changes and extends the replicative lifespan of normal human diploid fibroblasts *in vitro*

Normal human diploid cells grown *in vitro* exhibit a restricted population doubling potential and eventually enter an irreversible growth-arrested state known as replicative senescence, which has been proposed to reflect cellular ageing [45,46]. To determine whether CR can affect senescence entry and lifespan of normal human diploid fibroblasts *in vitro*, three independent normal human fibroblast cell lines were subpassaged in media supplemented with either 10 % CR rat serum or 10% AL rat serum, and analyzed until they reached senescence. Figure 1A shows the growth curves under these conditions for the three cell lines tested, namely IMR-90 (I90-79) (left panel), IMR (I90-26) (middle panel), and WI-38 (AG06814N) (right panel). Exposure of cultured IMR-90 (I90-79) and WI-38 cells to CR serum induced a significant increase in population doubling levels (PDL) and all three cell lines showed a profound delayed in the onset of senescent growth arrest. The average lifespan (cumulative PDL time) of these cells in the presence of CR serum was markedly increased when compared to that of cells grown in medium containing AL serum.

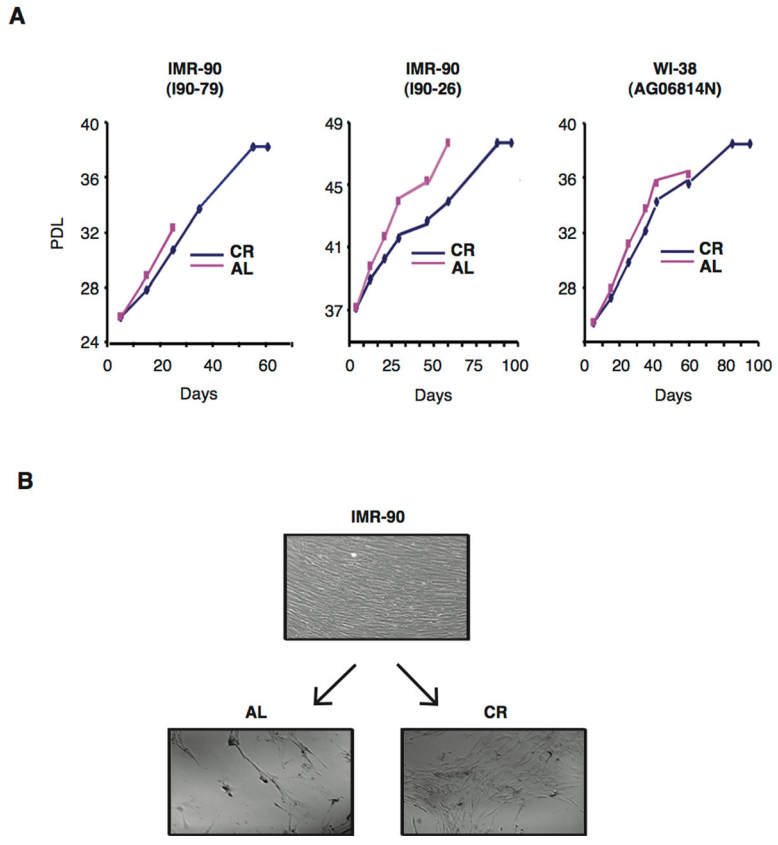

Figure 1. CR serum delays senescence and extends the lifespan of normal human diploid fibroblasts. (**A**) Cumulative growth curves of various normal human fibroblast lines cultured in medium containing 10% of either AL (red lines) or CR (blue lines) rat serum. Data obtained with IMR-90 (I90-79) (left panel), IMR-90 (I90-26) (middle panel) and WI-38 (right panel) are shown. PDL, population doublings (**B**) Representative photomicrographs of early passage IMR-90 cells (PDL 25) grown in medium with 10% FBS (upper panel) and after undergoing serial subpassages in the present of AL (left panels) or CR (right panels) rat serums are shown. Original magnification: X100.

To examine phenotypic changes during serial cultivation, fibroblast morphology was assessed throughout the study. Early passage IMR-90 fibroblasts (PDL 25) grown in 10% FBS displayed a typical spindle-shaped fibroblastic phenotype, grew to confluency, and were contact-inhibited (Fig. 1B, upper panel). Subsequent subpassage of these cells for 60 days in medium supplemented with 10% AL rat serum resulted in dramatic morphological changes, such as enlarged and flattened cell shapes as well as low saturation densities, both typical manifestations of senescence (Fig. 1B, lower left panel). In contrast, CR rat serum-treated cells during the same time period retained fibroblastic morphology and attained higher saturation densities, indicating that CR serum was able to delay the passage-induced senescent phenotype (Fig. 1B, lower right panel).

CR serum treatment reduces SA-β-gal activity in normal human diploid fibroblasts

Senescent cells contain elevated levels of senescence-associated β-galactosidase (SA β-gal), an endogenous β-galactosidase that is active at pH 6.0 [47]. To determine whether CR serum affected the level of SA β-gal activity in normal human diploid fibroblasts, IMR-90 and WI-38 cells were grown in the presence of various sera, fixed at different passage numbers and stained with a β-gal substrate for microscopic analysis. As shown in Figure 2A**,** IMR-90 fibroblasts cultured in normal DMEM medium supplemented with 10 % FBS displayed a 15.8 fold increase in the percentage of SA β-gal-positive cells from PDL 21 to PDL 55. Similarly, the percentage of SA β-gal-positive WI-38 fibroblasts cultured in DMEM supplemented with 10% FBS showed an 8.3 fold increase from PDL 24 to PDL 40 (Fig. 2B). When IMR-90 cells grown in the presence of rat sera were analyzed, we found that at PDL 37, the percentage of SA β-gal-positive fibroblasts cultured in DMEM containing 10 % CR serum was reduced more than 8 folds compared to that of cells of the same passage number grown in 10% AL serum (Fig. 2C). A similar but more modest effect was also observed in WI-38 cells at PDL 36 (Fig. 2D). Thus, CR serum was able to significantly reduce the amount of passage-induced SA-β-Gal activity in two independent lines of normal human diploid fibroblasts.

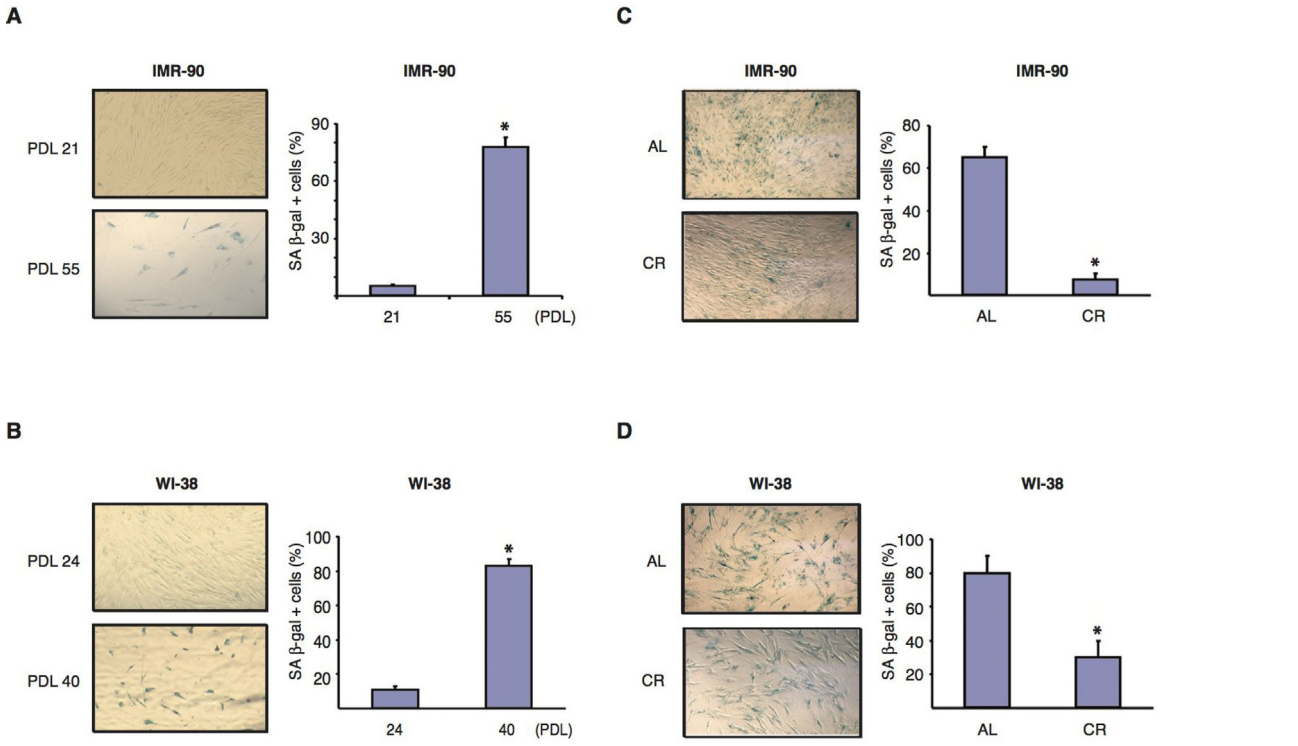

Figure 2. CR serum reduces SA-β-gal activity in normal human diploid fibroblasts. (**A** and **B**) Representative photomicrographs of SA-β-gal staining (left panels) of IMR-90 fibroblasts at PDL 21 and 55 (**A**) and of WI-38, fibroblasts at PDL 24 and 40 (**B**). Data were obtained from cells cultured in medium supplemented with 10% FBS. Original magnification: X100. Graphs on the right show the average percentage of β-gal positive cells shown in left panels, and represent the average -/+ SEM from three independent experiments. * = statistically significant ($p<0.05$) for early vs. late passage. (**C** and **D**) Representative photomicrographs of SA-β-gal staining (left panels) of IMR-90 (PDL37) fibroblasts (**C**) and WI-38 (PDL36) cells (**D**) cultured for one week in the presence of AL (upper panels) or CR serum (lower panels). Original magnification: X100. Graphs on the right show the average percentage of β-gal positive cells shown in left panels. Data represent the average -/+ SEM from three independent experiments. * = statistically significant ($p<0.05$) CR vs. AL.

CR serum treatment significantly decreases the senescence-associated activation of MMP-2 in normal human diploid fibroblasts

Cells undergoing replicative senescence contain elevated levels of secreted matrix metalloproteinase type-2 (MMP-2) activity. Full enzymatic activity of MMP-2 requires that the enzyme be cleaved by membrane-tethered MT-MMPs, in particular membrane type-1 matrix metalloproteinase (MT1-MMP)[48-51]. To assess the effects of CR serum on the activation of MMP-2, we performed gelatin zymography studies. As shown in Figure 3A, increasing passage numbers of normal human fibroblasts in DMEM 10 % FBS led to a significant increase in MMP-2 processing and activity in both IMR-90 cells (passaged from PDL 30 to PDL 36; left panel) and WI-38 cells (passaged from PDL 33 to PDL 39; right panel). When the levels of MMP-2 activity in IMR-90 (PDL 35) fibroblasts grown in medium containing either rat AL or CR serum were analyzed, we found that CR treatment significantly reduced MMP-2 activation Fig. 3B). Similar results were observed when WI-38 (PDL 36) cells exposed to AL or CR serum were examined Fig. 3B).

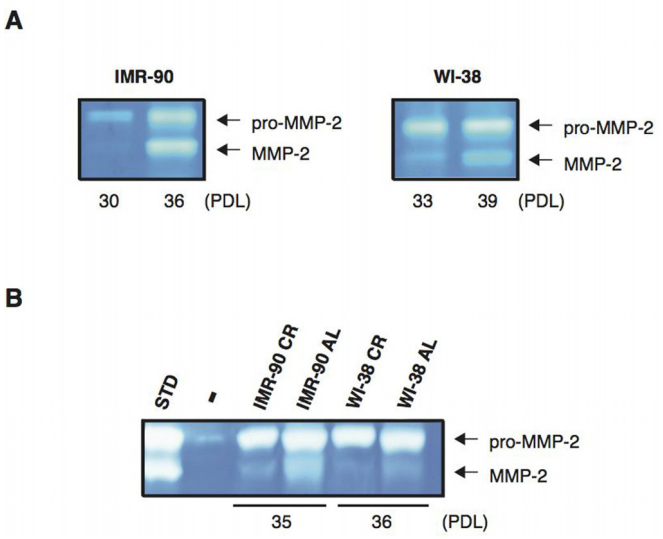

Figure 3. CR treatment reduces MMP-2 activity in normal human diploid fibroblasts. (**A**) Gelatin zymograms of protein extracts from IMR-90 cells at PDL 30 and 36 (left panel), and from WI-38 cells at PDL 33 and 39 (right panel) are shown. These cells were cultured in DMEM with 10% FBS prior to processing. (**B**) Gelatin zymograms of protein extracts from IMR-90 at PDL 35 and WI-38 at PDL 36 that were cultured in the presence of sera from AL or CR rats, as indicated, are shown. The unprocessed pro-form of MMP-2 (pro-MMP-2) and the mature, cleaved form of MMP-2 (MMP-2) are indicated. MMP-2 standard control (STD) and negative control sample (-) are shown.

SIRT1 protein expression is downregulated in normal human fibroblasts during senescence and CR serum-treatment delays this effect

At the cellular level, CR treatment is believed to enhance resistance to various forms of stress at least in part via the upregulation of sirtuins [38,52-54]. Since CR serum had such a profound effect on the development of a senescent phenotype in human fibroblasts (Figs. 1 and 2), we first analyzed the levels of SIRT1 protein in IMR-90 and WI-38 cells at different passage numbers to determine whether its expression was modulated during the senescence process. As shown in Figures 4A and B, the amount of SIRT1 protein in IMR-90 fibroblasts grown in the presence of 10% FBS progressively declined with increasing cumulative PDL (left panels). Specifically, between PDL 20 and PDL50 cells underwent a dramatic 50% reduction in SIRT1 protein levels. Similarly, the amount of SIRT1 in WI-38 fibroblasts was significantly decreased from PDL 24 to PDL 40 (Fig.4A and B, right panels). These results indicate that as human fibroblasts are passaged *in vitro* and progress toward replicative senescence, SIRT1 protein expression is significantly downregulated.

IMR-90 fibroblasts grown in the presence of 10% rat AL serum also showed a marked decline in SIRT1 levels from early (PDL 32) to late (PDL 45) passages Fig. 4C and D, left panels). Interestingly, despite the fact that IMR-90 fibroblasts grown in the presence of 10% rat CR serum also experienced a reduction in SIRT1 levels from PDL32 to PDL45, the overall SIRT1 protein levels in these cells were much higher than those observed in AL serum-treated controls. Specifically, the amount of SIRT1 protein found in IMR-90 fibroblasts grown in the presence of CR serum at PDL45 was 15-20% higher than that present in IMR-90 fibroblasts grown with AL-serum at PDL32 Fig. 4C and D, left panels). CR rat serum also preserved SIRT1 protein levels in WI-38 fibroblasts when compared to AL rat serum treatment at an intermediate (PDL 37) passage number Fig. 4C and D, right panels). These results indicate that CR serum treatment significantly prevents the senescence-associated SIRT1 downregulation displayed by normal human fibroblasts *in vitro*.

Senescence in normal human fibroblasts is delayed by SIRT1 overexpression

The correlation between increased SIRT1 levels and senescence retardation displayed by normal human diploid fibroblasts treated with CR-serum suggested that SIRT1 may play an important role in this process. To investigate the effects of SIRT1 modulation on

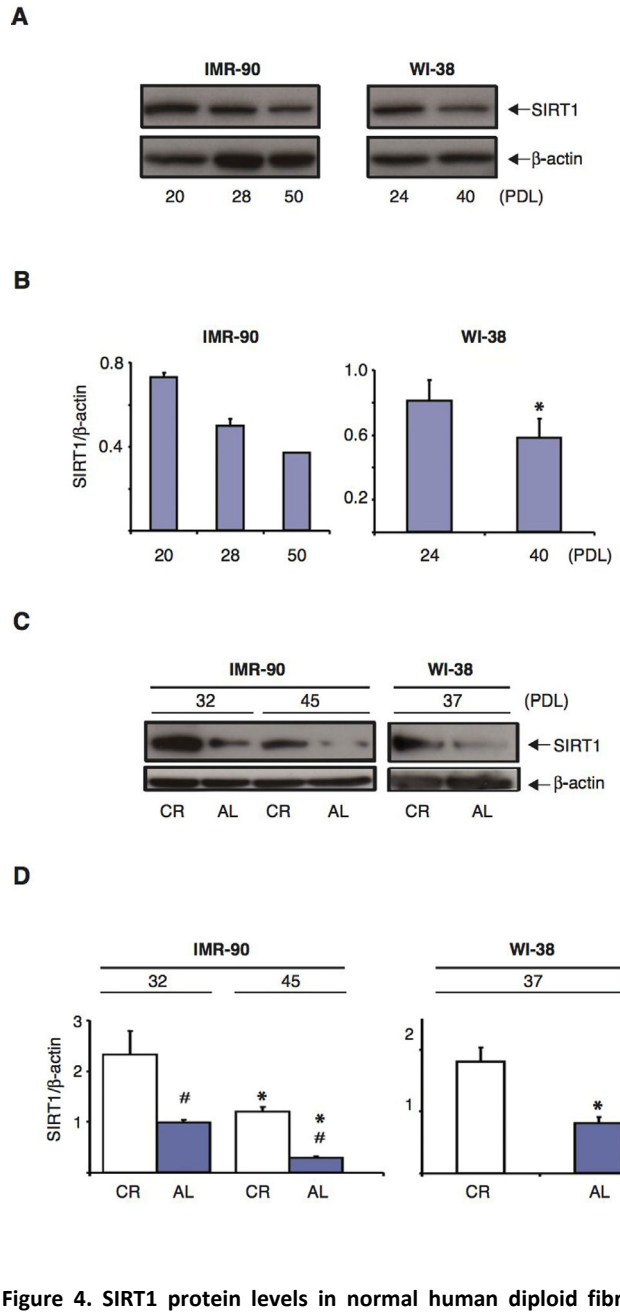

Figure 4. SIRT1 protein levels in normal human diploid fibroblasts decrease with increasing passage number and CR treatment retards this effect. (**A**) Representative immunoblots for SIRT1 (upper panels) and β-actin (lower panels) proteins from IMR-90 cells (left panel) and WI-38 cells (right panel) at different passage number. (**B**) Quantification of SIRT1 protein levels shown in (**A**), after correction for β-actin loading controls. Data represent the average -/+ SEM from three independent experiments; *= statistically significant ($p<0.05$). (C) Representative immunoblots of SIRT1 (upper panels) and β-actin (lower panels) proteins from IMR-90 cells at PDL 32 and PDL 45 (left panels) and WI-38 cells at PDL 37 (right panels) cultured for one week in media containing 10% CR or AL serum. (**D**) Quantification of SIRT1 protein levels shown in (C), after correction for β-actin loading control. Data represent the average -/+ SEM from three independent experiments (*and #= statistically significant ($p<0.05$) for PDL effect and CR vs. AL effect, respectively).

senescence in these cells, we first induced SIRT1 overexpression in IMR-90 and WI-38 fibroblasts at a late passage number, and analyzed cells for the development of a senescent phenotype. To this end, IMR-90 (PDL 48) and WI-38 (PDL 41) cells grown in DMEM supplemented with 10% FBS were transfected with either a plasmid coding for SIRT1 (pSIRT1) or a control empty plasmid (Vector). As shown in Figure 5A, twenty-four hours after transfection, SIRT1 levels were significantly increased in pSIRT1-transfected cells compared to vector-transfected controls. Remarkably, after two weeks in culture, IMR-90 and WI-38 fibroblasts overexpressing SIRT1 displayed a significantly higher cellular density than control cells Fig. 5B). Thus, overexpression of SIRT1 in late passage human fibroblasts grown in medium containing FBS resulted in delayed senescent growth arrest.

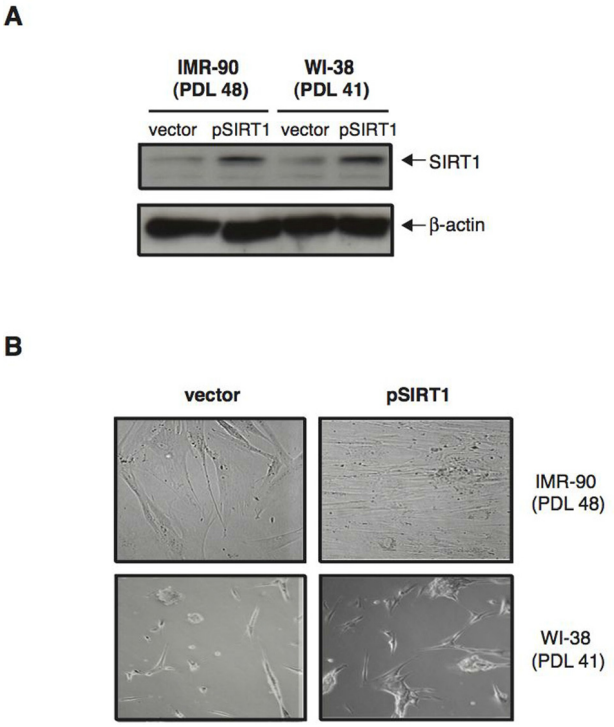

Figure 5. Over-expression of SIRT1 in normal human diploid fibroblasts delays senescence. (**A**) Representative immunoblots for SIRT1 (upper panel) and β-actin (lower panel) proteins from IMR-90 (PDL 48) and WI-38 (PDL 41) cells 24 hours after transfection with either pSIRT1 (second and fourth lane) or a control plasmid (vector; first and third lanes) and cultured in medium supplemented with 10 % FBS. (**B**) Representative phase-contrast photomicrographs of IMR-90 cells (PDL 48) and WI-38 cells (PDL 41) two weeks after transfection with either pSIRT1 or vector control. Original magnification: X200.

Senescence in normal human fibroblasts is accelerated by siRNA-induced downregulation of SIRT1 and CR serum partially rescues this effect

We then tested whether downregulation of SIRT1 levels in normal human fibroblasts could accelerate cellular senescence. To this end, IMR-90 cells were infected with Ad-SIRT1-siRNA, an adenoviral vector that has been shown to efficiently knockdown SIRT1 gene expression [38]. Immunoblot analysis showed that forty-eight hours after Ad-SIRT1-siRNA infection of IMR-90 (PDL 37), approximately 80% of the SIRT1 protein was downregulated when compared to SIRT1 levels in cells infected with an empty adenoviral control Fig. 6A). Similar results were observed with later passage IMR-90 (PDL 50) fibroblasts (data not shown). Interestingly, after 72 hours in culture in DMEM 10% FBS, the percentage of senescent IMR-90 (PDL 50) cells infected with Ad-SIRT1-siRNA was approximately 4-fold higher than that of cells infected with the control adenoviral vector, as measured by SA-β-GAL expression Fig. 6B and C). Interestingly, the knockdown of SIRT1 in early passage IMR-90 cells (PDL 29) led to a significant increase in MMP-2 activation Fig. 6D). These results indicate that reduction of SIRT1 protein levels alone can have a significant impact on the development of senescence manifestations in normal human fibroblasts.

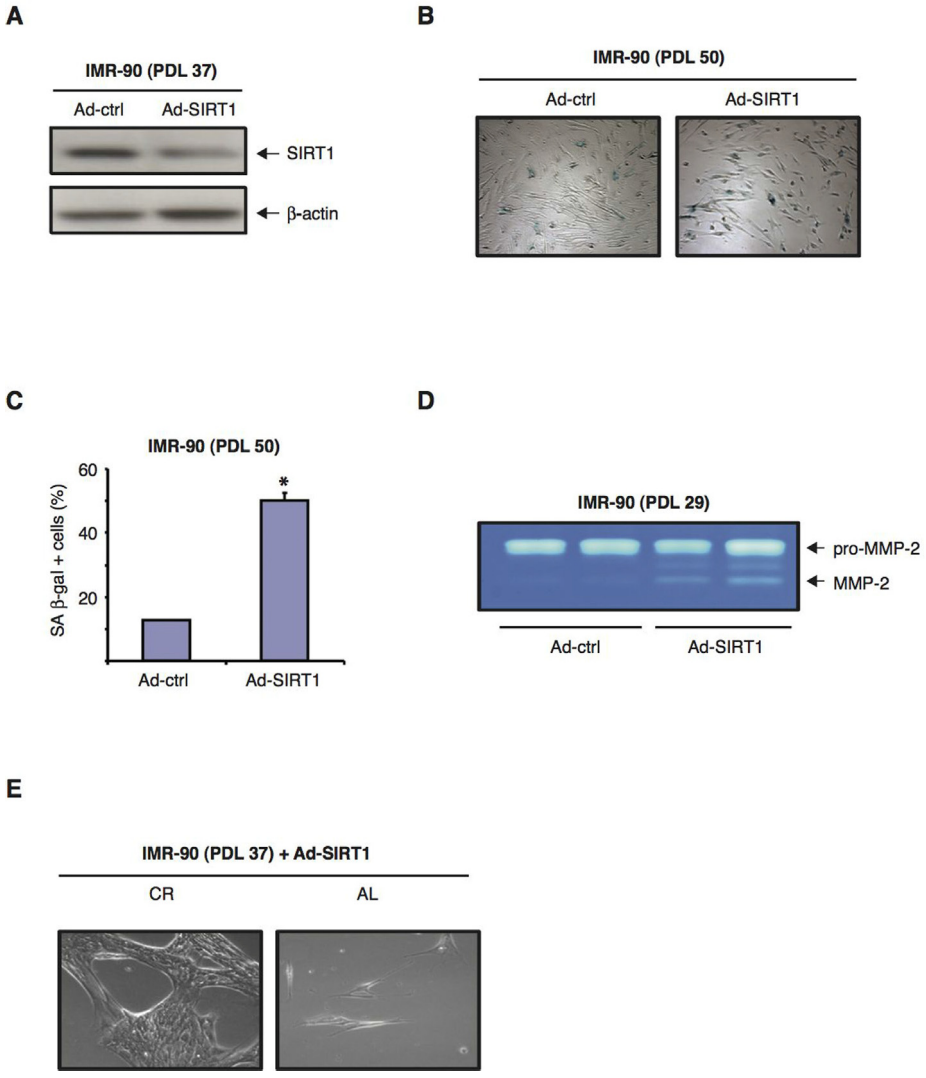

Figure 6. SIRT1 siRNA-mediated downregulation exacerbates the development of senescence in normal human diploid fibroblasts. (**A**) Representative immunoblots for SIRT1 (upper panel) and β-actin (lower panel) proteins from IMR-90 cells (PDL 37) forty-eight hours after infection with either Ad-SIRT1 or an empty adenoviral vector as negative control (Ad-ctrl). (B) Representative phase-contrast photomicrographs showing SA β-gal staining of IMR-90 cells at PDL 50 forty-eight hours post-infection with either Ad-SIRT1 or Ad-ctrl (negative control). Original magnification: X100. (**C**) Quantification of the percentage of SA β-gal positive cells shown in (**B**).(**D**) Representative zymograms from early passage IMR-90 (PDL 29) cells seventy-two hours after transfection with Ad-SIRT1 siRNA or Ad-ctrl vector. Representative data from three independent experiments are shown. (**E**) Phase-contrast (photomicrographs of IMR-90 at PDL 37 infected with Ad-SIRT1, and subsequently incubated for 72 hours in media containing 10% of either CR (left panel) or AL (right panel) rat serum**.** Original magnification: X200.

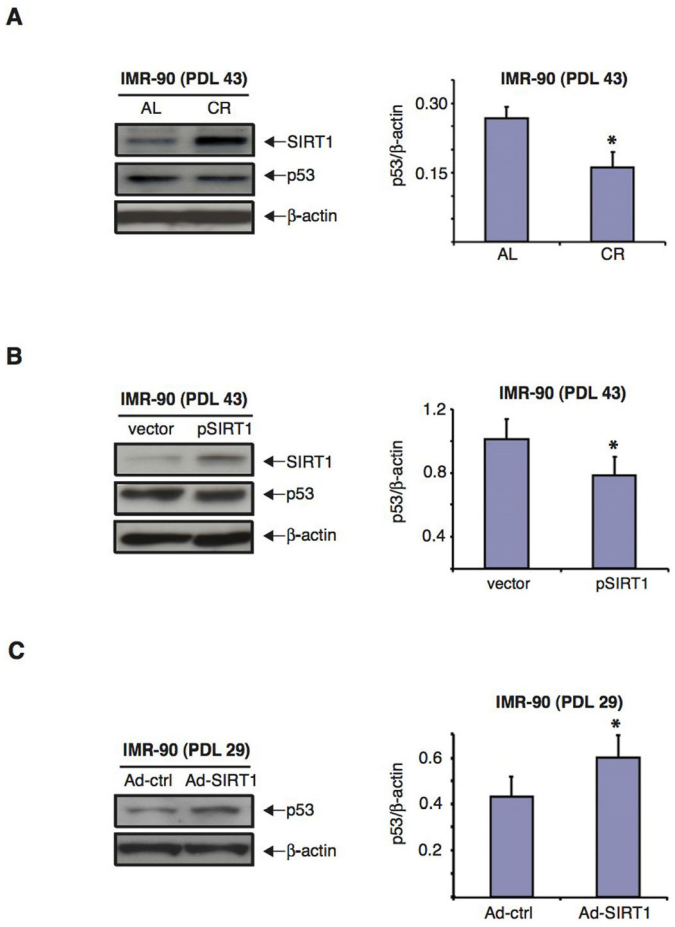

Figure 7. CR serum and over-expression of SIRT1 decrease p53 levels whereas SIRT1 knockdown increases them in IMR-90 cells. (**A**) Representative immunoblots for SIRT1 (upper panel), p53 (middle panel) and β-actin (lower panel) proteins of cell extracts from IMR-90 cells (PDL 43) cultured for 72 hours in media with CR (second lane) or AL (first lane) rat serum. Right panel shows the quantification of p53 levels for immunoblots shown on the left after correction for actin controls (* = p< 0.05 CR vs. AL). (**B**) Representative immunoblots for SIRT1 (upper panel), p53 (middle panel) and β-actin (lower panel) proteins of extracts from IMR-90 cells (PDL 43) transfected twenty four hours prior to lysis with either pSIRT1 or empty vector. Right panel shows the quantification of p53 levels for the immunoblots shown on the left after correction for actin controls (* = p<0.05, pSIRT1 vs. vector). (**C**) Representative immunoblots for p53 (upper panel) and β-actin (lower panel) of proteins extracts from IMR-90 cells (PDL 29) forty-eight hours after infection with either Ad-SIRT1 or Ad-ctrl (negative control). Data shown in **A**, **B** and **C** are representative of three independent experiments per group.

When low passage IMR-90 cells (PDL 37) infected with Ad-SIRT1-siRNA were subsequently exposed to medium containing 10% CR rat serum for 72 hours, their growth rate was improved (i.e. they attained higher cellular density) compared to that displayed by the same cells treated with medium containing 10 % AL serum Fig. 6E). Therefore, even in the context of siRNA-induced SIRT1 downregulation, CR serum treatment still to some extent retarded the development of a senescent phenotype in normal human fibroblasts.

Modulation of SIRT1 levels by either over-expression, knockdown or CR-treatment is associated with altered p53 levels

The tumor suppressor p53 signaling pathway plays a major role in the development of senescence [3,8,55,56], and it has been reported that SIRT1 can modulate cellular stress responses and survival through regulation of p53 [38,57-60]. Since CR treatment delayed senescence and efficiently preserved SIRT1 expression in IMR-90 human diploid fibroblasts with increasing cumulative PDLs, we tested whether p53 levels were also modulated by CR treatment in these cells. As shown in Figure 7A, we found that CR serum treatment of IMR-90 fibroblasts at PDL43 was accompanied by a decrease in p53 protein levels when compared to AL serum treatment**.** Specifically, the amount of p53 present in cells cultured in medium with CR serum was 1.6-fold lower than that of the same cells cultured in medium with AL serum (Fig.7A, right panel)**.** Overexpression of SIRT1 in pSIRT1-transfected IMR-90 (PDL 43) fibroblasts grown in normal medium caused a significant decrease in p53 expression levels (Fig.7B**).** Conversely, the knockdown of SIRT1 in early passage IMR-90 (PDL 29) fibroblasts enhanced p53 expression (Fig. 7C).

DISCUSSION

Several physiological consequences of CR regimes, including reduced cellular proliferation and increased stress resistance in certain cell types, can be reproduced *in vitro* by culturing cells with serum obtained from

animals that were fed CR diets. For instance, FaO cells (a transformed rat hepatoma cell line) and rat primary hepatocytes exposed to CR sera from either rats or Rhesus monkeys have been shown to display enhanced responsiveness to stresses such as heat shock-induced toxicity and oxidative stress by hydrogen peroxide (H2O2) [44]. A similar observation was recently made with sera collected from human participants of the FEAST study, which induced a form of CR by alternate-day fasting or ADF (i.e. short, regular intervals of complete caloric deprivation). The study compared the effects on human hepatoma HepG2 cells of sera collected from individuals at baseline (before dieting) versus sera collected from the same individuals at the end of the dieting period [53]. Interestingly, cells cultured in sera from participants following the ADF regime showed decreased proliferation and increased resistance to heat shock stress.

Other consequences of CR regimes, like their beneficial effects on the cardiovascular system, appear to be accompanied by cellular proliferation. Csiszar et al. reported that human endothelial cells cultured with sera derived from *Macaca mulatta* on long-term CR displayed increased migration, proliferation and formation of capillary-like structures when compared to cells treated with sera derived from ad-libitum-fed control monkeys [61]. These effects were correlated with upregulated vascular endothelial growth factor (VEGF) signaling, and suggest that increased angiogenesis caused by circulating serum factors could be a potential mechanism by which CR improves cardiac function and prevents vascular cognitive impairment *in vivo*.

While all of the reported CR-mediated effects *in vitro* have been observed after incubation of cells for short periods with CR sera from various species, little is known about the long-term effects of CR serum treatment in cultured cells. An important cellular consequence of the process of ageing is replicative senescence, whereby cells lose their replicative capacity and irreversibly exit the cell cycle. Decreased senescence *in vivo* is believed to contribute to delayed ageing and the increased tolerance to stress observed in organisms subjected to CR regimens [3,8]; however, the study of this cellular process *in vivo* (either in animals or humans) is experimentally challenging. Therefore, we decided to test the effects of CR serum on cellular senescence *in vitro* using normal human diploid fibroblasts, which undergo replicative senescence after several passages in culture. Our results clearly show that CR serum can significantly delay senescence progression of these cells, resulting in increased replicative lifespan. This was exemplified by delayed appearance of senescent morphological changes, decreased levels of p53 and reduced activity of senescence markers such as SA β-galactosidase and MMP-2, with the consequent increased in cumulative PDL (Figs. 1, 2, 3 and 7).

The molecular mechanisms mediating the health benefits associated with CR are not fully understood, and while some may be shared among different target organs and cell types, others are likely to be cell-type specific. For instance, it was recently reported that CR conferred persisting anti-oxidative, pro-angiogenic, and anti-inflammatory cellular effects in rat cerebro-microvascular endothelial cells, in part by modulating the levels and activities of Nrf2, NFkB, and miR-144 [62]. Among the most ubiquitous molecular targets of CR are the sirtuin proteins, whose levels are increased in all animal models of CR, suggesting these enzymes play a major role in CR-induced physiologic activities. Studies performed in yeast, flies, worms and mice have shown that increased sirutin activity due to either protein over-expression or treatment with sirtuin-activating compounds such as resveratrol, can *per se* recapitulate several of the effects mediated by CR [33-37,41-43]. Importantly, the CR-associated SIRT1 increases observed in animals can be recapitulated in *in vitro* models of CR. CR-sera from rats and monkeys as well as from human participants in the FEAST study have all consistently induced increased levels of SIRT1 in various cell types exposed to these sera for short time periods [38,53]. In human cells, CR serum-mediated induction of SIRT1 leads to the sequestration of proapoptotic factors and consequent promotion of cell survival [38]. Here, we show that SIRT1 levels decline with passage number *in vitro* as IMR-90 and WI-38 normal human fibroblasts progress toward replicative senescence (Fig. 4A and B). This is in accordance with previous reports showing reduced SIRT1 levels in senescent human and mouse fibroblasts, human smooth muscle cells (SMC) as well as human endothelial cells [63-66]. Interestingly, when IMR-90 and WI-38 cells were repeatedly passaged in the presence of CR rat serum they displayed much higher levels of SIRT1 than control cells passaged in AL serum (Fig. 4C and D). Therefore, CR serum protects cells from SIRT1 decreases associated with the senescence process throughout long time periods. Furthermore, experiments where SIRT1 levels were experimentally manipulated at different passage numbers suggested that this protein is important for the proper execution of the senescence program (i.e. triggering it when eliminated by siRNA-knockdown and delaying it when over-expressed) (Figs. 5 and 6). Previous studies testing the ability of SIRT1 to delay senescence and increase replicative lifespan have produced conflicting results. Over-expression of SIRT1

in mouse embryo fibroblasts and articular chondrocytes has been reported to inhibit senescence [67,68], whereas reduced SIRT1 activity has been shown to induce senescence in human breast cancer MCF-7 cells, endothelial cells and articular chondrocytes [64,65,68]. However, others have found that SIRT1 over-expression does not affect the replicative lifespan of human fibroblasts [69]. Importantly, mouse embryonic fibroblasts from SIRT1-deficient animals displayed increased rather than decreased replicative lifespan [70]. Ho *et al.* have suggested that some of these differences may be explained by different levels of activity of the NAD+ salvage pathway under various experimental paradigms [63]. These authors observed that in SMCs, SIRT1 over-expression conferred significant extension of replicative lifespan only when the activity of the nicotinamide phosphorybosiltransferase (Nampt), a rate-limiting enzyme for NAD+ salvage, was also increased [63]. Nampt activity has been shown to decline as cells progress toward senescence [71-75]. Therefore, it is possible that in IMR-90 and WI-38 cells the basal activity of Nampt (and/or other NAD+- generating enzymes) is sufficiently high to allow SIRT1-mediated senescence modulation and/or that the sera tested in our study contain factors that can enhance their function. Future experiments should test these possibilities. We observed that CR serum-treatment of early passage IMR-90 cells undergoing siRNA-induced SIRT1 downregulation (and therefore accelerated senescence) still had some retarding effect regarding the appearance of a senescent phenotype Fig. 6E). This result suggests that in addition to elevating SIRT1 levels, CR treatment exerts a wider effect on senescence progression in these cells. Whether results obtained with this *in vitro* system are a reflection of the modulation of senescence in organisms undertaking CR diets remains to be determined.

Additional effects of CR on the senescence program likely include the nutrient sensor mammalian target of rapamycin (mTOR), which is implicated in stimulating cell growth and an array of cellular functions [76, 77]. Nutrients as well as insulin and other growth factors activate mTOR, which can lead to accelerated cellular senescence [78, 79, 80]. Conversely, Rapamycin has been shown to delay cellular senescence through the inhibition of mTOR [81, 82]. Interestingly, Resveratrol can suppress cellular senescence at least in part by antagonizing the mTOR pathway through the activation of Sirt1 [83, 84]. CR serum has less nutrient availability and leads to elevated levels of Sirt1, a combination that would be expected to inhibit mTOR signaling [85].

Responses to CR treatment are expected to vary vastly between normal and cancerous cells. For instance, cancer cells typically show sustained aerobic glycolysis, a phenomenon known as the Warburg effect, and therefore are likely to be much more sensitive to nutrient deprivation during CR than normal cells [86]. Under certain experimental paradigms, cancerous cells also appear to display higher sensitivity than normal cells to CR-mediated reductions in the levels of circulating factors like Insulin-like growth factor 1 (IGF-1) [87, 88]. This increased sensitivity, at least in tumors of epithelial origin, appears to be dependent on the activity of the phosphoinositide 3-kinase (PI3K)/AKT signaling pathway [89, 90]. Differences in the activities of several other signaling molecules, including mTOR and Sirtuins, have also been implicated in the differential effects of CR on normal versus tumor cells [91].

Abrogation of programmed senescence appears to be a fundamental prerequisite for tumor formation [3,7,9,19]. In that regard, the senescence-suppressing effects of CR would be predicted to have tumorigenic activity; however, long term CR in various animal models has been consistently associated with lower cancer risk [92-97]. Clearly, other beneficial effects of CR must operate to prevent cancerous changes in long-lived cells. On the other hand, and despite the predicted anti-tumor activity of replicative senescence, this process might also contribute to tumor formation and spread under certain circumstances (e.g. through the microenvironmental disruption that results from the secretion of extracellular matrix-degrading proteases by senescent cells). The expression of MT1-MMP and the activation of MMP-2, for instance, strongly correlate with tumor growth, neovascularization, and metastasis [98-108]. In addition, MMP-2 protein levels have been shown to increase in all tumor-derived fibroblast lines [17,109]. Our data show that whereas normal senescent human diploid fibroblasts produced high levels of MMP-2, CR serum treatment led to a significant reduction in MMP-2 activity associated with passage number Fig. 3). Whether this effect is representative of *in vivo* consequences of CR and could contribute to its anti-tumor activity remains an interesting possibility. The reduction in MMP-2 displayed by CR-treated human diploid fibroblasts in this study correlated with increased SIRT1 levels, and knockdown of SIRT1 in early passage cells enhanced MMP-2 activation to levels comparable to those associated with cells at a much later passage number (i.e. senescent) (Fig. 6D). These data highlight the potential beneficial effect of interventions based on CR or SIRT1-agonists like resveratrol against tumor-promoting MMP-2 activity.

SIRT1 has been shown to regulate cellular responses to diverse stresses in part through deacetylation of the

tumor-suppressor p53 and the consequent down-regulation of its transcriptional activity in various cell types, including neurons, cardiac myocytes, and smooth muscle cells [110-118]. Several lines of evidence show that p53 also plays a central role in the progression of cellular replicative senescence. Elimination of p53 activity from pre-senescent cells through sequestration by viral oncoproteins extends the lifespan of human cells by as much as 200 population doublings [119,120]. Similarly, introduction of dominant negative versions of mutant p53 also increases cellular lifespan [91] and micro-injection of anti-p53 antibodies into senescent human fibroblast reinitiates DNA synthesis and allows further population doublings [121]. Our data indicate that CR-mediated modulation of SIRT1 signaling in human diploid fibroblasts directly correlated with decreased expression levels of p53 (Fig. **7**). Once again, how a treatment like CR can lead to both lower p53 levels and reduced cancer risk remains to be elucidated. Manipulation of SIRT1 levels by silencing or overexpressing SIRT1 also resulted in increased and decreased p53 levels, respectively (Fig. **7**). A recent report showed that normal human fibroblasts *in vitro* and colon adenomas *in vivo* displayed a particular senescence-associated signature of p53 isoform expression, with elevated levels of p53β and reduced ⊗133p53 [56]. Whether CR treatment results in altered expression of any of these isoforms should be investigated.

In summary, this study demonstrates that delayed senescence onset, one of the anti-ageing effects believed to be exerted by CR, can be induced *in vitro* in cells incubated in media supplemented by serum collected from animals fed a CR diet. Specifically, exposure of normal human diploid fibroblasts to CR rat serum compared to AL rat serum resulted in i) sustained increases in SIRT1 levels, ii) decreased p53 levels, iii) delayed morphologic senescent changes, iv) reduced activities of SA β-gal and MMP-2, and v) increased replicative lifespan. The modulation of cellular senescence by CR serum described here further validates the use of this *in vitro* model to investigate the mechanisms behind the beneficial effects of CR. We now have an experimental system to identify CR serum components or CR-mimetic compounds that regulate senescence and to study the molecular consequences of their effects. We also show that manipulation of SIRT1 levels by either over-expression (mimicking the effects of CR serum) or knockdown of this protein (mimicking the effects of AL serum) resulted in delayed and accelerated cellular senescence, respectively. Taken together, these findings indicate that the modulation of the SIRT1 signaling pathway *per se* can have a significant impact on the progression of the senescence program in normal human fibroblasts, and suggest that SIRT1 plays an important role in CR-mediated senescence retardation and replicative lifespan extension in these cells.

MATERIALS AND METHODS

Animals, dietary manipulations and sera. Male Fisher-344 rats fed either an AL or CR diet were used in these experiments. AL animals were fed a NIH-31 standard diet while CR animals were given a vitamin- and mineral-fortified version of the same diet. CR animals were in a 60% calorie restriction since weaning (i.e. 40% less food (by weight) than the average AL consumption). Water was available ad libitum for both groups. Animals were maintained under controlled conditions including 12 on/12 off light cycle, with appropriate temperature and humidity. The animal protocol used was approved by the Institutional Animal Care and Use Committee of the Gerontology Research Center and complied with the guide for the care and use of laboratory animals (NIH publication No. 3040-2, revised 1999).

Sera from these animals were collected every other week during a 6-month period. All sera were obtained from fasted, anesthetized animals. Rats were anesthetized and a 21-gauge catheter was inserted into the tail vein. 1.5 ml of whole blood was then collected and allowed to clot for 20-30 minutes, followed by centrifugation for 20 min at 2500 rpm. Sera were removed from the centrifuged samples and stored frozen until used. All sera utilized were thawed and heat inactivated at 56 ^{o}C prior to use in cell culture experiments.

Cell culture. IMR-90 (I90-79), IMR-90 (I90-26) and WI-38 (AG06814-N) with PDL at freeze of 17, 30 and 15, respectively, were purchased from Coriell Institute for Medical Research (Camden, NJ). These cells were grown in Minimum Essential Medium (MEM) (1X), with 2mM L-glutamine, 100 µg/ml penicillin, and 100 µg/ml streptomycin and supplemented with either 10% fetal bovine serum (FBS) or 10% serum from AL- or CR-fed rats. Cells were maintained at 37°C under a humidified 5% CO_2 and 95% O_2 air atmosphere. Except for experiments describing Figure 1, IMR-90 (I90-79) cells were utilized for all other experiments.

Transfections and infections. The pSIRT1 expression vector, adenovirus SIRT1 siRNA (Ad-SIRT1), and their respective negative controls were kindly provided by Dr. D. Sinclair (Harvard University) and have been previously described [38]. Cells were transfected with pSIRT1 or control plasmid (empty vector) using

Lipofectamine 2000 (Invitrogen, Carlsbad, CA) following manufacturer's instructions. Adenoviral infections with either Ad-SIRT1 or Ad-control were carried out at a multiplicity of infection (MOI) of 100, as previously described [38].

SA-β-galactosidase assay. The percentage of SA-β-gal-expressing cells was determined as previously described [47]. Briefly, cells in 6-well plates were washed twice in PBS, fixed for 5 min in 4% paraformaldehyde in PBS and washed three times in PBS. The cells were then incubated overnight at 37 °C with fresh SA-β-gal staining solution (1 mg of [5-bromo-4-chloro-3-indolyl β-D-galactopyranoside]/ml of 5 mM potassium ferrocyanide, 5 mM potassium ferricyanide, 150 mM NaCl, 2 mM $MgCl_2$ in 40 mM citric acid/sodium phosphate, pH 6.0) and examined under the microscope.

Western blotting. Whole-cell lysates were prepared by scraping cells in Laemmli buffer (0.12 M Tris, pH 6.8, 4% (w/v) SDS, 20% (v/v) glycerol) containing a protease inhibitor cocktail (Sigma, St. Louis, MO). Proteins were then separated by SDS/PAGE under reducing conditions on a 12% gel and transferred to PVDF membranes. Unspecific binding was blocked by incubation in 5% milk blocking buffer (PBS, 5% nonfat milk and 0.1% Tween 20). Membrane bound proteins were then immunoblotted with antibodies to p53 (ab7757-100, abcam), actin (Santa Cruz Biotech, Santa Cruz, CA), or Sirt1 (Millipore, Billerica, MA). Signals were developed using ECL reagent (Amersham Pharmacia Biotech, Buckinghamshire, England) and densities of the bands were evaluated using a Syngene Gene Genius Bio-Imaging System (Imgen, Alexandria, VA). Protein loading was evaluated either using b-actin antibody (Santa Cruz) or Ponseau S staining (Sigma-Aldrich).

Gelatin zymography. Gelatin zymography was performed as previously described with some modifications [48]. Briefly, cells were lysed in SDS-sample buffer and aliquots (equivalent to 10^5 cells per lane) were loaded without reduction onto 10% Novex gelatin zymogram gels (Invitrogen), run at 125 V for 90 minutes, and incubated in Novex Zymogram renature buffer for 30 minutes (to remove SDS and renature the MMP-2 species). Then the gels were incubated in developing buffer at 37° C for 4 hours to induce gelatin lysis by renatured MMP-2.

Statistical analysis. All results are expressed as the mean ± SEM. Statistical comparisons for multiple group differences were made via a one-way or two-way ANOVA, followed by Bonferoni post hoc tests; and for two group comparisons were determined via Student's t-tests. A p value of < 0.05 was considered statistically significant.

ACKNOWLEDGEMENTS

We thank Dr. Robin Minor (NIA, NIH) for carefully reading this manuscript and providing helpful comments.

Conflict of interest statement

The authors have no conflict of interests to declare.

REFERENCES

1. Lakatta EG, Levy D. Arterial and cardiac aging: major shareholders in cardiovascular disease enterprises: Part I: aging arteries: a "set up" for vascular disease. Circulation. 2003; 107:139–146.

2. Dickstein DL, Kabaso D, Rocher AB, Luebke JI, Wearne SL, Hof PR. Changes in the structural complexity of the aged brain. Aging Cell. 2007; 6:275–284.

3. Collado M, Blasco MA, Serrano M. Cellular senescence in cancer and aging. Cell. 2007;130:223–233.

4. Minamino T, Komuro I. Vascular aging: insights from studies on cellular senescence, stem cell aging, and progeroid syndromes. Nat Clin Pract Cardiovasc Med. 2008; 5:637–648.

5. Campisi J. Cellular senescence as a tumor-suppressor mechanism. Trends in cell biology. 2001; 11:S27–S31.

6. Jeyapalan JC, Sedivy JM. Cellular senescence and organismal aging. Mechanisms of ageing and development. 2008; 129:467–474.

7. Campisi J. Senescent Cells, Tumor Suppression, and Organismal Aging: Good Citizens, Bad Neighbors. Cell. 2005; 120:513–522.

8. Campisi J, d' Adda di Fagagna F. Cellular senescence: when bad things happen to good cells. Nat Rev Mol Cell Biol. 2007; 8:729–740.

9. López-Otín C, Blasco MA, Partridge L, Serrano M, Kroemer G. The Hallmarks of Aging. Cell. 2013; 153:1194–1217.

10. Ashford JW, Atwood CS, Blass JP, Bowen RL, Finch CE, Iqbal K, Joseph JA, Perry G. What is aging? What is its role in Alzheimer's disease? What can we do about it? J Alzheimers Dis. 2005; 7:247–253.

11. Atwood CS, Barzilai N, Bowen RL, Brown-Borg HM, Jarrard DF, Fu VX, Heilbronn LK, Ingram DK, Ravussin E, Schwartz RS, Weindruch R. Pennington scientific symposium on mechanisms and retardation of aging. Exp Gerontol. 2003; 38:1217–1226.

12. Butler RN, Warner HR, Williams TF, Austad SN, Brody JA, Campisi J, Cerami A, Cohen G, Cristofalo VJ, Drachman DA, Finch CE, Fridovich I, Harley CB, et al. The aging factor in health and disease: the promise of basic research on aging. Aging Clin Exp Res. 2004; 16:104–111.

13. Gambino V, De Michele G, Venezia O, Migliaccio P, Dall'Olio V, Bernard L, Minardi SP, Della Fazia MA, Bartoli D, Servillo G, Alcalay M, Giorgio M, Scrable H, et al. Oxidative stress activates a specific p53 transcriptional response that regulates cellular senescence and aging. Aging Cell. 2013; 12:435–445.

14. Baraibar MA, Friguet B. Oxidative proteome modifications target specific cellular pathways during oxidative stress, cellular senescence and aging. Exp Gerontol. 2013; 48:620–625.

15. Cui H, Kong Y, Zhang H. Oxidative Stress, Mitochondrial Dysfunction, and Aging. Journal of Signal Transduction. 2011; 2012:646354.

16. Harley CB, Vaziri H, Counter CM, Allsopp RC. The telomere hypothesis of cellular aging. Exp Gerontol. 1992; 27:375–382.

17. Kang MK, Kameta A, Shin K-H, Baluda MA, Kim H-R, Park N-H. Senescence-associated genes in normal human oral keratinocytes. Exp Cell Res. 2003; 287:272–281.

18. Rodier F, Campisi J. Four faces of cellular senescence. *J* Cell Biol. 2011;192:547–556.

19. Ingram DK, Zhu M, Mamczarz J, Zou S, Lane MA, Roth GS, de Cabo R. Calorie restriction mimetics: an emerging research field. Aging Cell. 2006; 5:97–108.

20. Guarente L, Picard F. Calorie restriction--the SIR2 connection. Cell. 2005; 120:473–482.

21. Weindruch R, Sohal RS. Seminars in medicine of the Beth Israel Deaconess Medical Center. Caloric intake and aging. N Engl J Med. 1997; 337:986–994.

22. Weindruch R, Walford RL, Fligiel S, Guthrie D. The retardation of aging in mice by dietary restriction: longevity, cancer, immunity and lifetime energy intake. J Nutr. 1986; 116:641–654.

23. Fontana L, Klein S. Aging, adiposity, and calorie restriction. JAMA: the journal of the American Medical Association. 2007; 297:986–994.

24. Spindler SR. Caloric restriction: from soup to nuts. Ageing research reviews. 2010; 9:324–353.

25. Baur JA, Ungvari Z, Minor RK, Le Couteur DG, de Cabo R. Are sirtuins viable targets for improving healthspan and lifespan? Nat Rev Drug Discov. 2012; 11:443–461.

26. Kim JD, McCarter RJ, Yu BP. Influence of age, exercise, and dietary restriction on oxidative stress in rats. Aging (Milano). 1996; 8:123–129.

27. López-Lluch G, Hunt N, Jones B, Zhu M, Jamieson H, Hilmer S, Cascajo MV, Allard J, Ingram DK, Navas P, de Cabo R. Calorie restriction induces mitochondrial biogenesis and bioenergetic efficiency. Proc Natl Acad Sci USA. 2006; 103:1768–1773.

28. Civitarese AE, Carling S, Heilbronn LK, Hulver MH, Ukropcova B, Deutsch WA, Smith SR, Ravussin E, CALERIE Pennington Team. Calorie restriction increases muscle mitochondrial biogenesis in healthy humans. PLoS medicine. 2007; 4:e76.

29. Nemoto S, Fergusson MM, Finkel T. Nutrient availability regulates SIRT1 through a forkhead-dependent pathway. Science. 2004; 306:2105–2108.

30. Blander G, Guarente L. The Sir2 family of protein deacetylases. Annu Rev Biochem. 2004; 73:417–435.

31. Bordone L, Guarente L. Calorie restriction, SIRT1 and metabolism: understanding longevity. Nat Rev Mol Cell Biol. 2005; 6:298–305.

32. Longo VD, Kennedy BK. Sirtuins in Aging and Age-Related Disease. Cell. 2006; 126:257–268.

33. Lin SJ, Defossez PA, Guarente L. Requirement of NAD and SIR2 for life-span extension by calorie restriction in Saccharomyces cerevisiae. Science. 2000; 289:2126–2128.

34. Rogina B, Helfand SL. Sir2 mediates longevity in the fly through a pathway related to calorie restriction. Proc Natl Acad Sci USA. 2004; 101:15998–16003.

35. Tissenbaum HA, Guarente L. Increased dosage of a sir-2 gene extends lifespan in Caenorhabditis elegans. Nature. 2001; 410:227–230.

36. Fontana L, Partridge L, Longo VD. Extending Healthy Life Span—From Yeast to Humans. Science. 2010; 328:321–326.

37. Schmeisser K, Mansfeld J, Kuhlow D, Weimer S, Priebe S, Heiland I, Birringer M, Groth M, Segref A, Kanfi Y, Price NL, Schmeisser S, Schuster S, et al. Role of sirtuins in lifespan regulation is linked to methylation of nicotinamide. Nat Chem Biol. 2013; 9:693–700.

38. Cohen HY, Miller C, Bitterman KJ, Wall NR, Hekking B, Kessler B, Howitz KT, Gorospe M, de Cabo R, Sinclair DA. Calorie restriction promotes mammalian cell survival by inducing the SIRT1 deacetylase. Science. 2004; 305:390–392.

39. Leibiger IB, Berggren P-O. Sirt1: a metabolic master switch that modulates lifespan. Nat Med. 2006; 12:34–36.

40. Haigis MC, Sinclair DA. Mammalian Sirtuins: Biological Insights and Disease Relevance. Annu Rev Pathol. 2010; 5:253–295.

41. Bordone L, Cohen D, Robinson A, Motta MC, van Veen E, Czopik A, Steele AD, Crowe H, Marmor S, Luo J, Gu W, Guarente L. SIRT1 transgenic mice show phenotypes resembling calorie restriction. Aging Cell. 2007; 6:759–767.

42. Baur JA, Pearson KJ, Price NL, Jamieson HA, Lerin C, Kalra A, Prabhu VV, Allard JS, Lopez-Lluch G, Lewis K, Pistell PJ, Poosala S, Becker KG et al. Resveratrol improves health and survival of mice on a high-calorie diet. Nature. 2006; 444:337–342.

43. Price NL, Gomes AP, Ling AJ, Duarte FV, Martin-Montalvo A, North BJ, Agarwal B, Ye L, Ramadori G, Teodoro JS, Hubbard BP, Varela AT, Davis JG et al. SIRT1 is required for AMPK activation and the beneficial effects of resveratrol on mitochondrial function. Cell metabolism. 2012; 15:675–690.

44. De Cabo R, Fürer-Galbán S, Anson RM, Gilman C, Gorospe M, Lane MA. An in vitro model of caloric restriction. Exp Gerontol. 2003; 38:631–639.

45. Smith JR, Hayflick L. Variation in the life-span of clones derived from human diploid cell strains. J Cell Biol. 1974; 62:48–53.

46. Muller M. Cellular Senescence: Molecular Mechanisms, *In Vivo* Significance, and Redox Considerations. Antioxidants & Redox Signaling. 2009; 11:59–98.

47. Dimri GP, Lee X, Basile G, Acosta M, Scott G, Roskelley C, Medrano EE, Linskens M, Rubelj I, Pereira-Smith O. A biomarker that identifies senescent human cells in culture and in aging skin in vivo. Proc Natl Acad Sci USA. 1995; 92:9363–9367.

48. Deryugina EI, Ratnikov B, Monosov E, Postnova TI, DiScipio R, Smith JW, Strongin AY. MT1-MMP initiates activation of pro-MMP-2 and integrin alphavbeta3 promotes maturation of MMP-2 in breast carcinoma cells. Exp Cell Res. 2001; 263:209–223.

49. Sato H, Takino T, Okada Y, Cao J, Shinagawa A, Yamamoto E, Seiki M. A matrix metalloproteinase expressed on the surface of invasive tumour cells. Nature. 1994; 370:61–65.

50. Seiki M. Membrane-type matrix metalloproteinases. APMIS. 1999; 107:137–143.

51. Sato H, Takino T, Miyamori H. Roles of membrane-type matrix metalloproteinase-1 in tumor invasion and metastasis. Cancer Science. 2005; 96:212–217.

52. Anderson RM, Latorre-Esteves M, Neves AR, Lavu S, Medvedik O, Taylor C, Howitz KT, Santos H, Sinclair DA. Yeast life-span extension by calorie restriction is independent of NAD fluctuation. Science. 2003; 302:2124–2126.

53. Allard JS, Heilbronn LK, Smith C, Hunt ND, Ingram DK, Ravussin E; Pennington CALERIE Team, de Cabo R. In vitro cellular adaptations of indicators of longevity in response to treatment with serum collected from humans on calorie restricted diets. PLoS ONE. 2008; 3:e3211.

54. Ungvari Z, Kaley G, Cabo R de, Sonntag WE, Csiszar A. Mechanisms of Vascular Aging: New Perspectives. J Gerontol A Biol Sci Med Sci. 2010; 65A:1028–1041.

55. Halazonetis TD, Gorgoulis VG, Bartek J. An oncogene-induced DNA damage model for cancer development. Science. 2008; 319:1352–1355.

56. Fujita K, Mondal AM, Horikawa I, Nguyen GH, Kumamoto K, Sohn JJ, Bowman ED, Mathe EA, Schetter AJ, Pine SR, Ji H, Vojtesek B, Bourdon JC, et al. p53 isoforms Δ133p53 and p53β are endogenous regulators of replicative cellular senescence. Nature cell biology. 2009; 11:1135–1142.

57. Smith J. Human Sir2 and the "silencing" of p53 activity. Trends Cell Biol. 2002; 12:404–406.

58. Lee JT, Gu W. SIRT1: Regulator of p53 Deacetylation. Genes Cancer. 2013; 4:112–117.

59. Hori YS, Kuno A, Hosoda R, Horio Y. Regulation of FOXOs and p53 by SIRT1 Modulators under Oxidative Stress. PLoS ONE. 2013; 8:e73875.

60. Rufini A, Tucci P, Celardo I, Melino G. Senescence and aging: the critical roles of p53. Oncogene. 2013; 32:5129-5143.

61. Csiszar A, Sosnowska D, Tucsek Z, Gautam T, Toth P, Losonczy G, Colman RJ, Weindruch R, Anderson RM, Sonntag WE, Ungvari Z. Circulating factors induced by caloric restriction in the nonhuman primate Macaca mulatta activate angiogenic processes in endothelial cells. J Gerontol A Biol Sci Med Sci. 2012; 68235-249.

62. Csiszar A, Gautam T, Sosnowska D, Tarantini S, Banki E, Tucsek Z, Toth P, Losonczy G, Koller A, Reglodi D, Giles CB, Wren JD, Sonntag WE, Ungvari Z. Caloric restriction confers persistent anti-oxidative, pro-angiogenic, and anti-inflammatory effects and promotes anti-aging mi-RNA expression profile in cerebromicrovascular endothelial cells of aged rats. Am J Physiol Heart Circ Physiol. 2014; 307:H292-306.

63. Ho C, van der Veer E, Akawi O, Pickering JG. SIRT1 markedly extends replicative lifespan if the NAD+ salvage pathway is enhanced. FEBS Lett. 2009; 583:3081–3085.

64. Ota H, Tokunaga E, Chang K, Hikasa M, Iijima K, Eto M, Kozaki K, Akishita M, Ouchi Y, Kaneki M. Sirt1 inhibitor, Sirtinol, induces senescence-like growth arrest with attenuated Ras-MAPK signaling in human cancer cells. Oncogene. 2006; 25:176–185.

65. Ota H, Akishita M, Eto M, Iijima K, Kaneki M, Ouchi Y. Sirt1 modulates premature senescence-like phenotype in human endothelial cells. J Mol Cell Cardiol. 2007; 43:571–579.

66. Gorenne I, Kumar S, Gray K, Figg N, Yu H, Mercer J, Bennett M. Vascular Smooth Muscle Cell Sirtuin 1 Protects Against DNA Damage and Inhibits Atherosclerosis. Circulation. 2013; 127:386–396.

67. Langley E, Pearson M, Faretta M, Bauer UM, Frye RA, Minucci S, Pelicci PG, Kouzarides T. Human SIR2 deacetylates p53 and antagonizes PML/p53-induced cellular senescence. EMBO J. 2002; 21:2383–2396.

68. Hong E-H, Lee S-J, Kim J-S, Lee KH, Um HD, Kim JH, Kim SJ, Kim JI, Hwang SG. Ionizing radiation induces cellular senescence of articular chondrocytes via negative regulation of SIRT1 by p38 kinase. J Biol Chem. 2010; 285:1283–1295.

69. Michishita E, Park JY, Burneskis JM, Barrett JC, Horikawa I. Evolutionarily conserved and nonconserved cellular localizations and functions of human SIRT proteins. Mol Biol Cell. 2005; 16:4623–4635.

70. WW, Saito S, Franco S, Kaushal D, Cheng HL, Fischer MR, Stokes N, Murphy MM, Appella E, Alt FW. Mammalian SIRT1 limits replicative life span in response to chronic genotoxic stress. Cell Metab. 2005; 2:67–76.

71. Van der Veer E, Nong Z, O'Neil C, Urquhart B, Freeman D, Pickering JG. Pre-B-cell colony-enhancing factor regulates NAD+-dependent protein deacetylase activity and promotes vascular smooth muscle cell maturation. Circ Res. 2005; 97:25–34.

72. Kendal CE, Bryant-Greenwood GD. Pre-B-cell colony-enhancing factor (PBEF/Visfatin) gene expression is modulated by NF-kappaB and AP-1 in human amniotic epithelial cells. Placenta. 2007; 28:305–314.

73. Nakahata Y, Sahar S, Astarita G, Kaluzova M, Sassone-Corsi P. Circadian control of the NAD+ salvage pathway by CLOCK-SIRT1. Science. 2009; 324:654–657.

74. Borradaile NM, Pickering JG. Nicotinamide phosphoribosyltransferase imparts human endothelial cells with extended replicative lifespan and enhanced angiogenic capacity in a high glucose environment. Aging Cell. 2009; 8:100–112.

75. Zhang LQ, Heruth DP, Ye SQ. Nicotinamide Phosphoribosyl-transferase in Human Diseases. J Bioanal Biomed. 2011; 3:013–025.

76. Wullschleger S, Loewith R, Hall HN. TOR Signaling in Growth and Metabolism. Cell. 2006; 124:471-484.

77. Yan L, Mieulet V, Lamb RF. Nutrient regulation of mTOR1 and cell growth. Cell Cycle. 2010; 9:13, 2473-2474.

78. Blagosklonny MV. Cell cycle arrest is not yet senescence, which is not just cell cycle arrest: terminology for TOR-driven aging. Aging (Albany NY). 2012; Vol 4 No. 3.

79. Leontieva OV, Blagosklonny MV. DNA damaging agents and p53 do not cause senescence in quiescent cells, while consecutive re-activation of mTOR is associated with conversion to senescence. Aging (Albany NY). 2010; 2:924-935.

80. Zoncu R, Sabatini DM, Efeyan A. mTOR: from growth signal integreation to cancer, diabetes and ageing. Nat Rev Cell Biol. 2011; 12:21-25.

81. Leontieva OV, Demidenko ZN, Gudkov AV, Blagosklonny MV. Elimination of Proliferating Cells Unmasks the Shift from Senescence to Quiescence Cause by Rapamycin. PLOS One. 2011; 6:e26126.

82. Kolesnichenko M, Hong L, Liao R, Vogt PK, Sun P. Attentuation of TORC1 signaling delays replicative and oncogenic RAS-induced senescence. Cell Cycle. 2012; 11:2391-401.

83. Demidenko ZN, Blagosklonny MV. At concentrations that inhibit mTOR, resveratrol suppresses cellular senescence. Cell Cycle. 2009; 8:1901-1904.

84. Ghosh HS, McBurney M, Robbins PD. SIRT1 Negatively Regulates the Mammalian Target of Rapamycin. PLOS One. 2010; 5:e9199.

85. Tucci P. Caloric restriction: is mammalian life extension liked to p53. Aging (Albany NY). 2012; 4:525-534.

86. Kim JW, Dang CV. Cancer's molecular sweet tooth and the Warburg effect. Cancer Res. 2006; 66:8927-30.

87. Dunn SE, Kari FW, French J, Leininger JK, Travlos G, Wilson R, Barrett JC. Dietary restriction reduces insulin-like growth factor I levels, which modulates apoptosis, cell proliferation, and tumor

progression in p53-deficient mice. Cancer Res. 1997; 57:4667-4672.

88. Majeed N, Blouin MJ, Kaplan-Lefko PJ, Barry-Shaw J, Greenberg NM, Gaudreau P, Bismar TA, Pollak M. A germ line mutation that delays prostate cancer progression and prolongs survival in a murine prostate cancer model. Oncogene. 2005; 24:4736-4740.

89. Kalaany NY and Sabatini DM. Tumours with PI3K activation are resistant to dietary restriction. Nature. 2009; 458: 725-731.

90. Curry NL, Mino-Kenudson M, Oliver TG, Yilmaz OH, Yilmaz VO, Moon JY, Jacks T, Sabatini DM, Kalaany NY. Pten-null tumors cohabiting the same lung display differential AKT activation and sensitivity to dietary restriction. Cancer Discov. 2013; 3:908-921.

91. Ophelie Meynet and Jean-Ehrland Ricci. Caloric restriction and cancer: molecular mechanisms and clinical implications. Trends in Molecular Medicine. 2014;20:419-27

92. Albanes D, Winick M. Are cell number and cell proliferation risk factors for cancer? J Natl Cancer Inst. 1988; 80:772–774.

93. James SJ, Muskhelishvili L. Rates of apoptosis and proliferation vary with caloric intake and may influence incidence of spontaneous hepatoma in C57BL/6 x C3H F1 mice. Cancer Res. 1994; 54:5508–5510.

94. Pearson KJ, Lewis KN, Price NL, Chang JW, Perez E, Cascajo MV, Tamashiro KL, Poosala S, Csiszar A, Ungvari Z, Kensler TW, Yamamoto M, Egan JM, et al. Nrf2 mediates cancer protection but not prolongevity induced by caloric restriction. Proc Natl Acad Sci USA. 2008; 105:2325–2330.

95. Lanza-Jacoby S, Yan G, Radice G, LePhong C, Baliff J, Hess R. Calorie restriction delays the progression of lesions to pancreatic cancer in the LSL-KrasG12D; Pdx-1/Cre mouse model of pancreatic cancer. Exp Biol Med (Maywood). 2013; 238:787–797.

96. Colman RJ, Anderson RM, Johnson SC, Kastman EK, Kosmatka KJ, Beasley TM, Allison DB, Cruzen C, Simmons HA, Kemnitz JW, Weindrunch R. Caloric restriction delays disease onset and mortality in rhesus monkeys. Science. 2009; 325:210-214.

97. Mattison JA, Roth GS, Beasley TM, Tilmont EM, Handy AM, Herbert RL, Longo DL, Allison DB, Young JE, Bryant M, Bernard D, Ward WF, Qi W, Ingram DK, de Cabo R. Nature. 2012; 489: 318-321.

98. Brooks PC, Silletti S, von Schalscha TL, Friedlander M, Cheresh DA. Disruption of angiogenesis by PEX, a noncatalytic metalloproteinase fragment with integrin binding activity. Cell. 1998; 92:391–400.

99. Deryugina EI, Bourdon MA, Reisfeld RA, Strongin A. Remodeling of collagen matrix by human tumor cells requires activation and cell surface association of matrix metalloproteinase-2. Cancer Res. 1998; 58:3743–3750.

100. Hotary K, Allen E, Punturieri A, Yana I, Weiss SJ. Regulation of cell invasion and morphogenesis in a three-dimensional type I collagen matrix by membrane-type matrix metalloproteinases 1, 2, and 3. J Cell Biol. 2000; 149:1309–1323.

101. Itoh T, Tanioka M, Yoshida H, Yoshioka T, Nishimoto H, Itohara S. Reduced angiogenesis and tumor progression in gelatinase A-deficient mice. Cancer Res. 1998; 58:1048–1051.

102. McQuibban GA, Gong JH, Tam EM, McCulloch CA, Clark-Lewis I, Overall CM. Inflammation dampened by gelatinase A cleavage of monocyte chemoattractant protein-3. Science. 2000; 289:1202–1206.

103. Shankavaram UT, Lai WC, Netzel-Arnett S, Mangan PR, Ardans JA, Caterina N, Stetler-Stevenson WG, Birkedal-Hansen H, Wahl LM. Monocyte membrane type 1-matrix metallo-proteinase. Prostaglandin-dependent regulation and role in metalloproteinase-2 activation. J Biol Chem. 2001; 276:19027–19032.

104. Deryugina EI, Quigley JP. Pleiotropic roles of matrix metalloproteinases in tumor angiogenesis: Contrasting, overlapping and compensatory functions. Biochimica et Biophysica Acta (BBA) - Molecular Cell Research. 2010; 1803:103–120.

105. Ota I, Li X-Y, Hu Y, Weiss SJ. Induction of a MT1-MMP and MT2-MMP-dependent basement membrane transmigration program in cancer cells by Snail1. PNAS. 2009; 106:20318–20323.

106. Thiolloy S, Edwards JR, Fingleton B, Rifkin DB, Matrisian LM, Lynch CC. An Osteoblast-Derived Proteinase Controls Tumor Cell Survival via TGF-beta Activation in the Bone Microenvironment. PLoS ONE. 2012; 7:e29862.

107. Bauvois B. New facets of matrix metalloproteinases MMP-2 and MMP-9 as cell surface transducers: Outside-in signaling and relationship to tumor progression. Biochimica et Biophysica Acta (BBA) - Reviews on Cancer. 2012; 1825:29–36.

108. Genís L, Gálvez BG, Gonzalo P, Arroyo AG. MT1-MMP: Universal or particular player in angiogenesis? Cancer Metastasis Rev. 2006; 25:77–86.

109. Hornebeck W. Down-regulation of tissue inhibitor of matrix metalloprotease-1 (TIMP-1) in aged human skin contributes to matrix degradation and impaired cell growth and survival. Pathol Biol. 2003; 51:569–573.

110. Araki T, Sasaki Y, Milbrandt J. Increased nuclear NAD biosynthesis and SIRT1 activation prevent axonal degeneration. Science. 2004; 305:1010–1013.

111. Kaula SC, Reddelb RR, Sugiharac T, Mitsuia Y, Wadhwac R. Inactivation of p53 and life span extension of human diploid fibroblasts by mot-2. FEBS Lett. 2000; 474:159–164.

112. Alcendor RR, Gao S, Zhai P, Zablocki D, Holle E, Yu X, Tian B, Wagner T, Vatner SF, Sadoshima J. Sirt1 regulates aging and resistance to oxidative stress in the heart. Circ Res. 2007; 100:1512–1521.

113. Van der Veer E, Ho C, O'Neil C, Barbosa N, Scott R, Cregan SP, Pickering JG. Extension of human cell lifespan by nicotinamide phosphoribosyltransferase. J Biol Chem. 2007; 282:10841–10845.

114. Cheng H-L, Mostoslavsky R, Saito S, Manis JP, Gu Y, Patel P, Bronson R, Appella E, Alt FW, Chua KF. Developmental defects and p53 hyperacetylation in Sir2 homolog (SIRT1)-deficient mice. Proc Natl Acad Sci USA. 2003; 100:10794–10799.

115. Finkel T, Deng C-X, Mostoslavsky R. Recent progress in the biology and physiology of sirtuins. Nature. 2009; 460:587–591.

116. Donmez G, Guarente L. Aging and disease: connections to sirtuins. Aging Cell. 2010; 9:285–290.

117. Salminen A, Kaarniranta K. SIRT1: Regulation of longevity via autophagy. Cellular Signalling. 2009; 21:1356–1360.

118. Kim DH, Jung YJ, Lee JE, Lee AS, Kang KP, Lee S, Park SK, Han MK, Lee SY, Ramkumar KM, Sung MJ, Kim W. SIRT1 activation by resveratrol ameliorates cisplatin-induced renal injury through deacetylation of p53. American Journal of Physiology - Renal Physiology. 2011; 301:F427–F435.

119. Kyo S, Nakamura M, Kiyono T, Maida Y, Kanaya T, Tanaka M, Yatabe N, Inoue M. Successful immortalization of

endometrial glandular cells with normal structural and functional characteristics. Am J Pathol. 2003; 163:2259–2269.

120. Tsuruga Y, Kiyono T, Matsushita M, Takahashi T, Kasai H, Matsumoto S, Todo S. Establishment of immortalized human hepatocytes by introduction of HPV16 E6/E7 and hTERT as cell sources for liver cell-based therapy. Cell Transplant. 2008; 17:1083–1094.

121. Davis T, Singhrao SK, Wyllie FS, Haughton MF, Smith PJ, Wiltshire M, Wynford-Thomas D, Jones CJ, Faragher RG, Kipling D. Telomere-based proliferative lifespan barriers in Werner-syndrome fibroblasts involve both p53-dependent and p53-independent mechanisms. J Cell Sci. 2003; 116:1349–1357.

Research Paper

Target of rapamycin signalling mediates the lifespan-extending effects of dietary restriction by essential amino acid alteration

Sahar Emran[1], Mingyao Yang[1,2], Xiaoli He[1], Jelle Zandveld[3], and Matthew D. W. Piper[1]

[1] Institute of Healthy Ageing, Department of Genetics, Evolution and Environment, University College London, London WC1E 6BT, United Kingdom
[2] Institute of Animal Genetics and Breeding, Sichuan Agricultural University, Chengdu, Sichuan, 611130, China
[3] Laboratory of Genetics, Wageningen University and Research Centre, 6708 PB, Wageningen, The Netherlands

Key words: Drosophila melanogaster, rapamycin, target of rapamycin signalling, phenotyping, lifespan, stress response, essential amino acids
Received: 3/13/14; Accepted: 5/14/14; Published: 5/19/14 **doi:** 10.18632/aging.100665
Correspondence to: Matthew Piper, PhD; **E-mail:** m.piper@ucl.ac.uk

Abstract: Dietary restriction (DR), defined as a moderate reduction in food intake short of malnutrition, has been shown to extend healthy lifespan in a diverse range of organisms, from yeast to primates. Reduced signalling through the insulin/IGF-like (IIS) and Target of Rapamycin (TOR) signalling pathways also extend lifespan. In *Drosophila melanogaster* the lifespan benefits of DR can be reproduced by modulating only the essential amino acids in yeast based food. Here, we show that pharmacological downregulation of TOR signalling, but not reduced IIS, modulates the lifespan response to DR by amino acid alteration. Of the physiological responses flies exhibit upon DR, only increased body fat and decreased heat stress resistance phenotypes correlated with longevity via reduced TOR signalling. These data indicate that lowered dietary amino acids promote longevity via TOR, not by enhanced resistance to molecular damage, but through modified physiological conditions that favour fat accumulation.

INTRODUCTION

Dietary restriction (DR) is an intervention whereby a considerable reduction of food intake, just short of malnutrition, extends lifespan. This has been demonstrated to be effective in a wide range of evolutionarily diverse organisms, from yeast [1] to invertebrates [2] and mammals [3], and is considered one of the most robust environmental interventions to extend lifespan in laboratory organisms. Moreover, the longevity promoting effects of DR are accompanied by a range of health benefits. DR rodents had a delayed onset or a lesser severity of age-related diseases such as cancer, autoimmune diseases and motor dysfunction [4–6] and improved memory [7]. In *C. elegans*, DR was shown to reduce proteotoxicity [8]. DR rhesus monkeys were found to have improved triglyceride, cholesterol and fasting glucose profiles, and a reduced incidence of diabetes, cancer, cardiovascular disease and brain atrophy [9].

The molecular mechanisms underlying the physiological changes elicited by DR have yet to be elucidated, however, experimental data point towards nutrient signalling pathways as playing an important role. The evolutionarily conserved Target of Rapamycin Complex 1 (TORC1) pathway senses amino acid availability and signals to enhance translation via activation of S6 kinase-1 (S6K1) and inhibition of eIF4E binding protein-1(4E-BP1). TORC1 also regulates transcription and autophagy in response to a range of signals, including nutrient availability, cellular energy levels, and growth factors, in such a way that growth rates match resources [10]. Experimental validation of a role for TORC1 in determining lifespan has come from a range of laboratory organisms. Lifespan extension by inhibition of TORC1 pathway genes has been demonstrated in *S.cerevisiae* [11], *C.elegans* [12], *D. Melanogaster* [13] and in mice [14–19]. How TORC1 inhibition promotes longevity is unknown.

Another nutrient sensing pathway that is commonly associated with modified ageing is the insulin/insulin-like growth factor signalling (IIS) network. Mutations in components of the IIS pathway have extended lifespan in a host of model organisms [20]. Because the IIS pathway senses nutrients, considerable effort has been made to assess the role for IIS in modulating the longevity responses to DR. While IIS does not seem to be solely accountable for DR, some experimental data suggest overlapping mechanisms for IIS- and DR-mediated lifespan extension [21].

Recent work has shown that adjustments to the dietary amino acid balance can mimic the benefits to lifespan by DR in *D. melanogaster* [22]. Supplementing a DR diet with the ten essential amino acids (EAA) phenocopy the effects of full feeding (FF) on lifespan and fecundity, indicating that the beneficial effects of DR are a consequence of improved amino acid balance. Experimentally, the addition of EAAs to DR (DR+EAA) offers a sharper instrument with which to dissect the potential causes of lifespan change in response to nutritional balance than the FF condition, which is achieved by increasing the concentration of dietary yeast. Here we characterize physiological and metabolic parameters that define DR and fully fed flies with the aim of identifying candidate factors for causation of the lifespan response to DR.

RESULTS

TORC1 signalling but not IIS signalling is required for the effect of EAA on lifespan and fecundity

Dietary restricted (DR) flies are longer-lived than fully fed flies, but produce fewer eggs. The effect of full feeding to shorten lifespan and increase egg laying can be mimicked by the addition of the 10 essential amino acids (EAA) to DR food (Figures 1a-1c).

To assess the role of the longevity-associated nutrient signalling pathways as potential mediators of the effect of EAA on lifespan, we tested the response to DR of flies that are long lived due to deletion for genes encoding three of the *Drosophila* insulin-like peptides, (DILPs) *ilp*2, *ilp*3 and *ilp*5. We found no difference between the responses of wild type and DILP mutant flies to the addition of EAA to DR food, indicating that IIS is not required for the lifespan extension by DR (data not shown). In contrast, addition of the TORC1 inhibitor rapamycin extended the lifespan of flies on DR+EAA such that their lifespan was not shorter than those subjected to DR (Figure 2a). Rapamycin treatment also prevented the increase in egg laying seen for EAA addition to DR food, in fact egg laying was effectively blocked by rapamycin treatment. We also found that

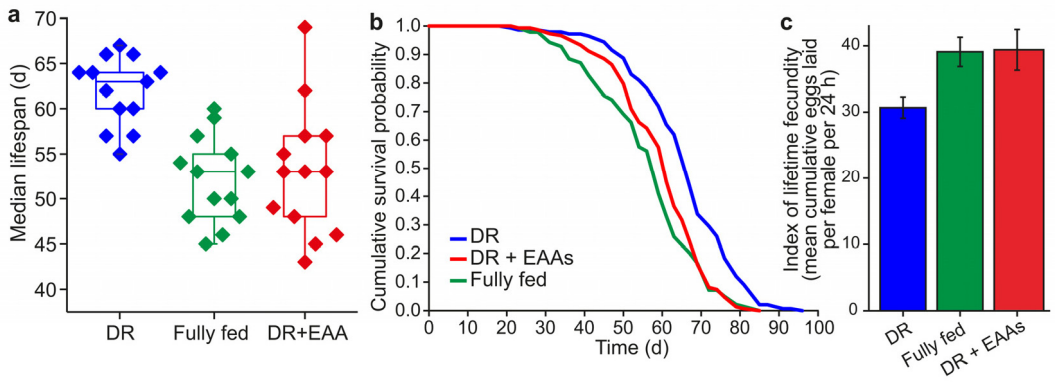

Figure 1. Amino acids mediate lifespan and fecundity changes under DR. (a) Summary of *Drosophila* median lifespans under dietary restriction (DR), full feeding (FF) and essential amino acid supplementation of DR (DR+EAA) (n=13 biological replicates; DR vs FF, P<0.001; FF vs DR+EAA, P=0.9383; DR vs DR+EAA, P=0.002; Wilcoxon rank-sum test) **(b)** A representative lifespan experiment: adding EAAs to DR food shortened lifespan (P< 0.001) to that of FF flies (P=0.194); n=150 per treatment; compared using the log-rank test. **(c)** Adding EAAs to DR food increased egg-laying (P<0.001) to that of FF flies (P<0.936). Fecundity: mean±s.e.m.; n=15; compared using the Wilcoxon rank-sum test.

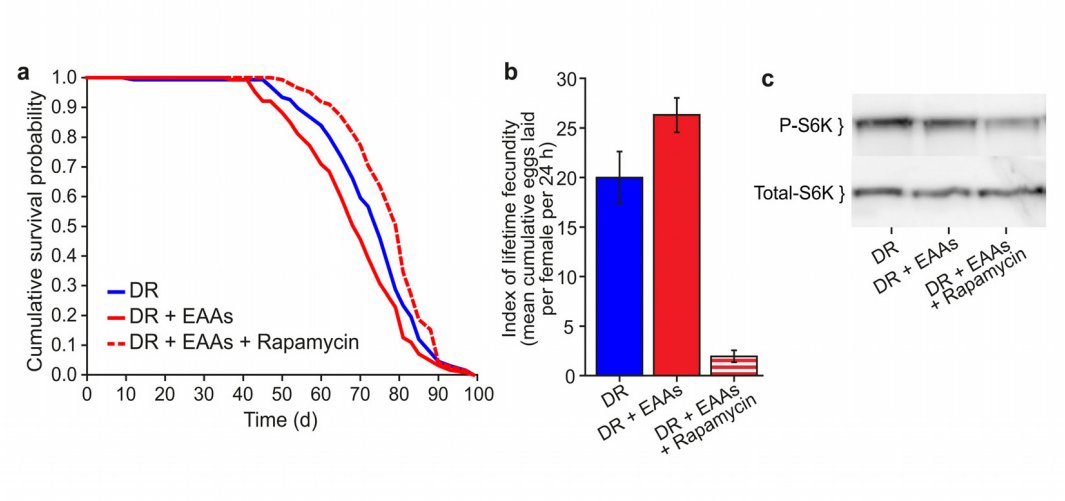

Figure 2. Effect of Rapamycin treatment on EAA-supplemented flies. (a) Rapamycin treatment extended the lifespan of DR+EAA flies beyond that of DR (DR+EAA vs DR+EAA+Rapamycin, $P<0.001$; DR vs DR+EAA, $P<0.012$). $n=150$ per treatment; log-rank test. **(b)** Rapamycin treatment decreased the lifetime fecundity of DR+EAA flies ($P<0.001$). Fecundity: mean±s.e.m.; $n=10$; Wilcoxon rank-sum test. **(c)** Levels of phospho-T398-S6K were measured from whole-fly protein extracts. Treatment with rapamycin for 7 days decreased phospho-T398-S6K levels in DR+EAA+Rapamycin flies relative to DR+EAA flies.

phosphorylation of the TORC1 target S6K was reduced by the addition of rapamycin (Figures 2b, 2c). Together, these data are consistent with TORC1 signalling playing a role in mediating the change in lifespan upon DR.

EAA supplementation alters responses of DR flies to H_2O_2 stress, heat stress, starvation stress, and TAG levels

We set out to identify phenotypic correlates of lifespan change under our dietary conditions in order to understand the causal mechanisms of increased lifespan under DR. Long-lived animal models often have an associated increase in the ability to resist environmental stresses and this is assumed to reflect a general increase in their health. Long-lived insulin/IGF-like signalling (IIS) mutant flies have been shown to be resistant to acute toxic doses of DDT, paraquat and hydrogen peroxide (H_2O_2) [23–25]. We tested whether long-lived DR flies are protected from the harmful effects of these compounds. We found that DR flies were significantly more resistant than DR+EAA flies to a toxic dose of H_2O_2, whereas no difference was apparent for paraquat (Figures 3a, 3b). Surprisingly, DR flies were more sensitive to a toxic dose of DDT than DR+EAA flies (Figure 3c), indicating that, at least for DDT resistance, DR does not protect against this toxin in the same way that lowered insulin signalling does.

Long-lived DR *C. elegans* have increased resistance to heat stress [26,27]. Upon testing the response of flies to heat shock stress, we found that DR flies were significantly less resistant than DR+EAA flies (Figure 3d), indicating that longevity associated with amino acid reduction comes at a cost to heat stress resistance.

Finally, we found that DR flies showed greater resistance to starvation than DR+EAA flies (Figure 3e), suggesting a possible mechanistic relationship between longevity and starvation resistance. Resistance to starvation stress could depend on the availability of enhanced energy stores within the fly. While we found no difference between groups in the levels of the storage carbohydrates glycogen or trehalose (Figure 3f, 3g) we did find that DR flies had significantly higher levels of triacylglycerides (TAG) than DR+EAA flies (Figure 3h). It is possible that this difference in TAG levels is causative of the longevity differences between DR and DR+EAA flies such that increased TAG confers some benefit to survival.

Increased TAG and decreased heat-stress resistance correlate with increased lifespan with DR

If the above phenotypes induced by DR are causally linked to longevity through reduced TORC1 signalling, it should be possible to reproduce the same

physiological outcomes by treating flies with rapamycin. We therefore tested the effect of rapamycin on DR+EAA flies for H_2O_2 stress resistance, starvation sensitivity, heat shock stress resistance and TAG levels (Figures 4a-d). Of these, heat stress resistance and TAG levels changed upon rapamycin treatment of DR+EAA flies, such that the responses became more similar to DR flies; Like DR, rapamycin treatment increased the sensitivity of EAA-treated DR flies to a 39ºC heat stress, and increased their TAG content. There was no effect of rapamycin on the response of EAA-treated flies to H_2O_2 stress or to starvation stress.

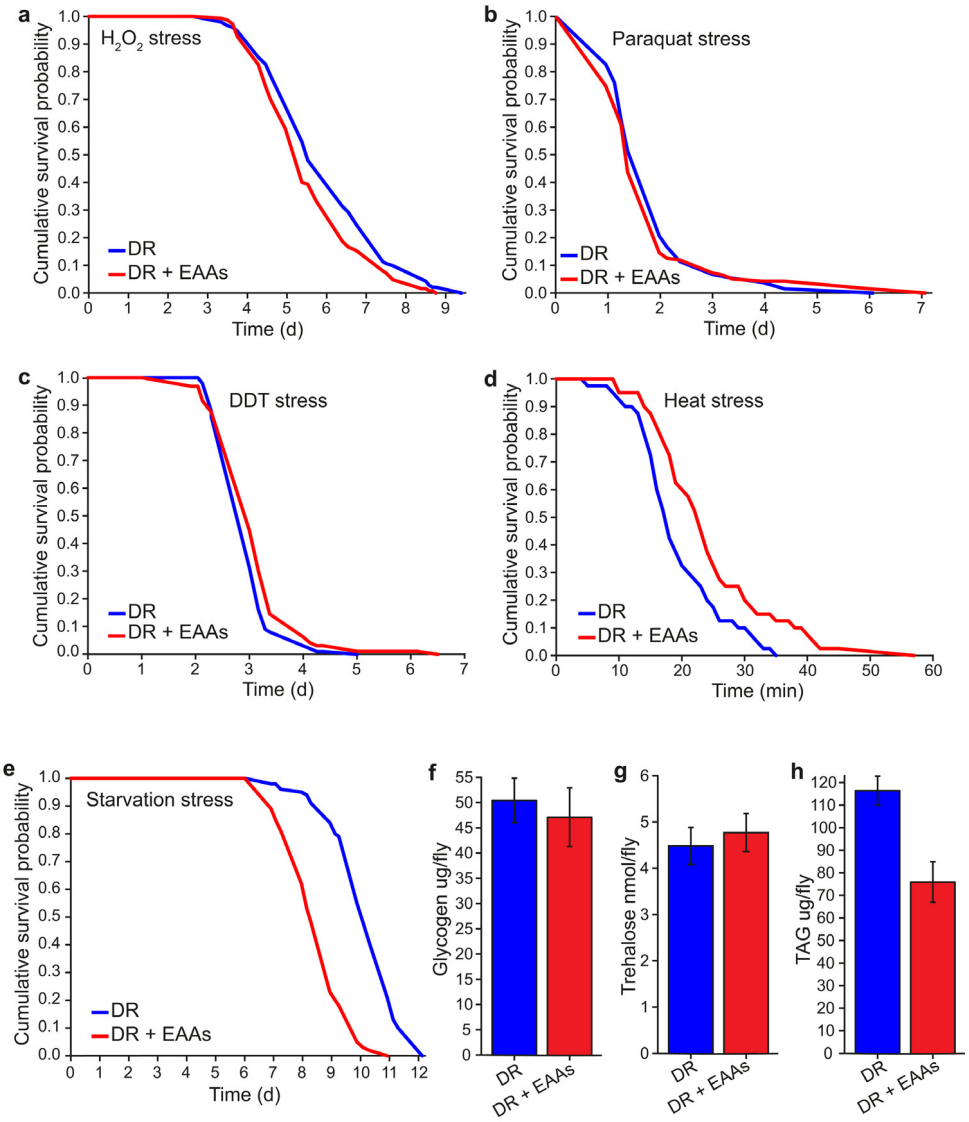

Figure 3. Phenotype comparisons between dietary restricted flies and those supplemented with EAAs. (a) DR+EAA flies showed a decreased resistance to hydrogen peroxide toxicity compared to DR flies (P=0.013; n=150 flies per condition). **(b)** There was no difference between DR and DR+EAA flies in their sensitivity to paraquat stress (P=0.517; n=150 flies per condition). **(c)** DR+EAA flies showed only a marginal, but significantly improved tolerance to DDT compared to that of DR flies (P=0.042, n=100 flies per condition). **(d)** DR+EAA flies were significantly more resistant to a 39ºC heat stress compared to DR flies (P<0.001; n=40 flies per condition). **(e)** DR+EAA flies were significantly more sensitive to starvation than DR flies (P<0.001; n=100 flies per condition). **(f)** After 7 days of treatment there was no difference in the amounts of glycogen measured for DR+EAA flies compared to DR flies (P=0.656; n= 6). **(g)** There was no difference in the levels of trehalose measured for DR+EAA flies compared to DR flies (P=0.630; n=6 flies per condition). **(h)** DR+EAA flies had significantly reduced levels of TAG compared to DR flies (P<0.001; n=6 flies per condition). For figures a-e, P values were calculated using the log-rank test. For figures f-h, P values were calculated by T-test, and error bars represent the s.e.m.

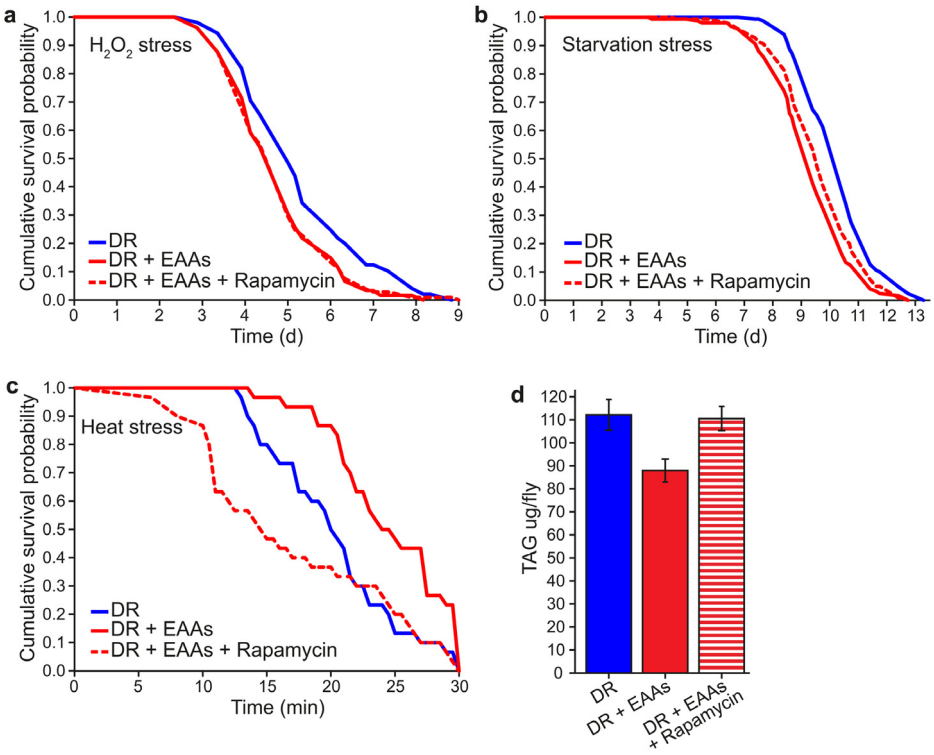

Figure 4. The effect of rapamycin to alter phenotypic differences between DR and DR+EAA flies. **(a)** Rapamycin had no effect on the sensitivity of DR+EAA flies to H_2O_2 stress (*P*=0.963; *n*=105 flies per condition). **(b)** Rapamycin had no effect on the sensitivity of DR+EAA flies to starvation stress (*P*=0.071; *n*=150 flies per condition). **(c)** Rapamycin, like DR, increased the sensitivity of DR+EAA flies to a 39ºC heat stress (*P*<0.001; *n*=30 flies per condition). For figures a-c, *P* values were calculated using the log-rank test. **(d)** Rapamycin treatment increased the triacyglyceride (TAG) levels of DR+EAA flies to the level of DR (*P*=0.011; *n*=6; T-test; error bars represent the s.e.m).

DISCUSSION

We have described the physiological and metabolic features that define long-lived DR flies in order to understand the mechanisms by which longevity is achieved. Our data indicate that dietary amino acids modify TORC1 signalling, which in turn alters lifespan outcomes. We also found that both dietary amino acid manipulation and TORC1 modification in flies alter TAG levels, such that higher body fat may play a causal role in enhancing fly lifespan in response to dietary restriction.

We found that the lifespan of insulin-mutant flies responded in a similar way to DR as wild-types, indicating that reduced IIS is not required for the lifespan-extending effects of DR. This appears to contrast previous studies that have reported interacting effects of IIS on DR, such that lifespan modification in response to yeast dilution is abolished in some IIS mutants [22,23,28]. These differences could be due to the fact that in the current study we modulated lifespan by adjusting EAA alone, rather than yeast. In doing so, we report a markedly different sampling of nutritional space than for yeast dilution, since we change the ratio of EAAs to all other dietary components, such as lipids, carbohydrates, non-essential amino acids, vitamins and trace elements. This may also explain why the phenotypes of our long-lived flies are somewhat different from those of other organisms subjected to DR. Interestingly, our experiments also showed that long-lived DR flies had decreased resistance to DDT, which is the opposite phenotype seen for IIS mutant flies, in which longevity is accompanied by dFOXO-

dependent DDT resistance [23,29]. Together, these data suggest that the beneficial effects on lifespan of DR can be achieved independently of IIS, similar to that reported by Tatar [21]. Moreover, it has been suggested that the effects of IIS on longevity are dependent on the status of TOR activity [30].

One of the strategies taken to understand the mechanisms by which dietary or genetic treatments enhance longevity is to seek out correlated physiological changes that may provide insights into the treatment's mode of action. A common mechanistic explanation for longevity requires enhancing systems to protect against the damaging side-effects of aerobic metabolism, such as that caused by oxidative stress or endogenous lipophilic toxins [31,32]. In our analyses, we found no evidence for broad-spectrum enhanced protection against stressors under DR. Thus, the mechanism for increased longevity under DR may not involve enhanced resistance to stress. Similar observations in studies on worms [33,34] has led to an alternative hypothesis that "hypertrophy" caused by inappropriate continuation of early-life growth programmes into later life is detrimental to an organism and causes ageing [35–38]. This explanation also implicates high levels of TOR signalling as its mechanism.

We found increased TAG levels correlated with longer life in our flies subjected to DR or rapamycin treatment. DR by yeast restriction in *Drosophila* has also been shown to increase lipid content [39–41], and several rodent studies show that higher fat levels correlate with increased lifespan [42–44]. In a recent study, Kapahi and colleagues showed that DR flies have increased TAG, and demonstrated an increased requirement for muscle-specific fatty-acid synthesis and breakdown in extending lifespan under DR [45]. Moreover, some long-lived TOR and IIS pathway mutants have increased fat levels [46–49]. Given that not all fat mutants are long-lived [50], it is likely that if fat levels are causally involved in extending life, the quality of fat accumulated is important. It would be interesting in future work to determine how lipid profiles change under different dietary conditions, to identify the specific types of lipids that are altered, and whether experimental manipulation can enhance lifespan.

EXPERIMENTAL PROCEDURES

General Methods

Standard laboratory food . Dietary restriction medium (1xSYA) contained100 g/l yeast (1x; MP Biomedicals, OH, USA), 50 g/l sucrose (Tate & Lyle, London, UK), 15 g/l agar (Sigma-Aldrich, Dorset, UK), and 30ml/l nipagin (Chemlink Specialities, Manchester, UK) and 3ml/l propionic acid (Sigma-Aldrich, Dorset, UK).This diet and its method of preparation is described in Bass et al., 2007 [51]. The fully fed medium (2xSYA) was prepared in the same way, except that it contained 200g/l yeast.

Experimental food. Rapamycin (LC Laboratories, MA, USA) was dissolved in ethanol and added to 1xSYA food at a final concentration of 200μM. Essential amino acids (Sigma-Aldrich, Dorset, UK) were dissolved in MiliQ water, and added to 1xSYA food at concentrations shown in Table 1. As control measures, ethanol alone was added to the food conditions that did not contain rapamycin, and water was added to food conditions that did not contain essential amino acids.

Table 1. Quantities of each of the essential amino acids added to 1l of 1xSYA food medium.

Essential amino acid (Sigma-Aldrich)	Concentration in 1xSYA medium (g/l)
L-arginine	0.43
L-histidine	0.21
L-isoleucine	0.34
L-leucine	0.48
L-lysine	0.52
L-methionine	0.10
L-phenylalanine	0.26
L-threonine	0.37
L-tryptophan	0.09
L-valine	0.40

Fly stocks and husbandry. The wild-type Dahomey strain was originally collected in 1970 from Dahomey (now known as the Republic of Benin) and since maintained as a large outbred stock with overlapping generations at 25°C on a 12h light:12h dark cycle. These conditions allow for inter-generational breeding and the life expectancy of flies remain similar to that of newly caught wild flies [52]. Flies used for experimentation came from parental flies of the same age at egg laying, thereby controlling for the effects of parental age on lifespan [53].

Insulin-signalling mutant flies lacking the *Drosophila* insulin-like peptides (DILPs) *ilp*2, *ilp*3 and *ilp*5 were generated as described in Gronke et al., 2010 [23]. These flies were backcrossed into a control $white^{Dahomey}$ background stock, which was derived by backcrossing w^{1118} into the outbred wild-type Dahomey background [24]. All mutations were back-crossed into their control backgrounds for a minimum of 6 generations.

Lifespan. All experiments were conducted at 25°C on a 12h light:12h dark cycle, at a constant humidity of 65%. Flies were reared at a standard larval density of ~300 flies per bottle, and all experimental adults were collected within a 12 hour period after eclosion. Flies were allowed to mate for 48 hours after eclosion before the experimental females were separated out under CO_2 anaesthesia. Females were then randomly allocated to the experimental food treatments and housed in plastic vials containing food at a density of 10 flies per vial, with 15 vials per condition (n=150). Flies were transferred to a fresh food source 3 times per week, during which any deaths and censors were recorded.

Fecundity. Lifetime fecundity was measured as the cumulative total for days 7, 14, 21 and 28 of the mean number of eggs laid per female fly over each 24-hour period. Eggs in each vial were counted by eye using a light microscope after 18-24 hours exposure to flies.

Western blots. Protein extracts for western blot analysis were made from whole flies, sampled after 7 days of food treatment, using a TCA-based extraction protocol. 10µl of each sample was loaded into a 12% SDS-PAGE gel and blots were probed with anti-phospho-Thr398- S6K antibody (#9209, Cell Signaling Technologies, MA, USA), and total-S6K (re-made using a peptide sequence previously used to generate the total S6K antibody in Stewart et al., 1996 [54]). Both antibodies were used at a dilution of 1:12000 and normalised by probing with an anti-actin antibody at a dilution of 1:5000. Secondary antibodies conjugated to HRP (AbCam, Cambridge, UK) were used at a dilution of 1:5000, and the signals were detected by chemiluminescence.

Stress Experiments

Experimental flies were reared and housed as described for the lifespan experiment. Mated female flies were kept on the experimental food types for 7 days before being transferred to the stress conditions.

Paraquat, DDT and H_2O_2 stress. The orally administered stressors were as made up follows: 1xSYA containing 20mM paraquat (Sigma-Aldrich, Dorset, UK), 1xSYA containing 0.03% w/v DDT (Supelco Sigma-Aldrich, Dorset, UK), 1.5% agar medium containing 5% H_2O_2 (Sigma-Aldrich, Dorset, UK) and 50g/l sucrose, or plain 1.5% agar medium for the starvation experiment.

Heat shock. Experimental flies were transferred singly into dry empty 2ml glass vials, plugged with cotton wool and placed into a water bath set at 39°C. The time taken for each fly to fall onto its back and stop twitching (knockout) was recorded.

Metabolic measurements

Experimental flies were reared and housed as described for the lifespan experiment. Mated female flies were kept on the experimental food types for 7 days before being frozen in liquid nitrogen. 6 replicas of 5 flies per condition were used for all metabolic measurements.

Triacylglyceride measurement. Flies per condition were homogenised in 0.05% Tween 20 (Sigma-Aldrich, Dorset, UK) according to Gronke et al., 2003 [55]. TAG content was quantified using the Triglyceride Infinity Reagent (Thermo Fisher Scientific, Surrey, UK).

Glycogen measurement. Flies were homogenised in 200µl saturated Na_2SO_4 solution and centrifuged for 1 min. 80µl of each sample was transferred to new Eppendorf tubes and 800µl chloroform:methanol (1:1) solution was added. Samples were centrifuged for 5 minutes and the supernatant was removed. The remaining pellet, containing precipitated glycogen, was resuspended in 1ml anthrone solution (anthrone in 50 ml 70% H_2SO_4) and incubated at 90°C for 20 minutes. 200µl of each sample was dispensed into the wells of a flat-bottomed 96-well plate, and the absorbance in each well was measured at 620nm and compared against a set of glycogen standards ranging from 0-2µg/µl (protocol adapted from Van Handel, 1965 [56]).

Trehalose measurement. Trehalose levels were measured using the Glucose Infinity Reagent (Thermo Fisher Scientific, Surrey, UK), as described in Broughton et al., 2005 [24].

ACKNOWLEDGEMENTS

We thank Helena Cochemé, Nazif Alic and Jorge Iván Castillo-Quan for advice, and we are grateful to members of the Partridge and Gems laboratories for insightful discussions. We also thank Cathy Slack and Linda Partridge for providing the total S6K antibody. We acknowledge the following funding: the Royal Society (UF100158), and the Biotechnology and Biological Sciences Research Council, UK (BB/I011544/1) (M.D.W.P.); (BB/D526945/1) (S.E.).

Conflict of interest statement

The authors of this manuscript declare no conflict of interests.

REFERENCES

1. Jiang J, Jaruga E, Repnevskaya M, Jazwinski S. An intervention resembling caloric restriction prolongs life span and retards aging in yeast. The FASEB Journal. 2000;14:2135–2137.

2. Klass M. Aging in the nematode Caenorhabditis elegans: major biological and environmental factors influencing life span. Mechanisms of ageing and development 1977; 6:413–429.

3. McCay C. The effect of retarded growth upon the length of life span and upon the ultimate body size. J Nutr. 1935; 10:63–79.

4. Blackwell BN, Bucci TJ, Hart RW, Turturro A. Longevity, Body Weight, and Neoplasia in Ad Libitum-Fed and Diet-Restricted C57BL6 Mice Fed NIH-31 Open Formula Diet. Toxicologic Pathology. 1995; 23:570–582.

5. Weindruch RH, Kristie JA, Cheney KE, Walford RL. Influence of controlled dietary restriction on immunologic function and aging. Federation Proceedings. 1979; 38:2007–2016.

6. Ingram DK, Weindruch R, Spangler EL, Freeman JR, Walford RL. Dietary restriction benefits learning and motor performance of aged mice. J Gerontol. 1987; 42:78–81.

7. Stewart J, Mitchell J, Kalant N. The effects of life-long food restriction on spatial memory in young and aged Fischer 344 rats measured in the eight-arm radial and the Morris water mazes. Neurobiology of aging. 1989; 10:669–675.

8. Steinkraus K, Smith ED, Davis C, Carr D, Pendergrass WR, Sutphin GL, Kennedy BK, Kaeberlein M. Dietary restriction suppresses proteotoxicity and enhances longevity by an hsf-1-dependent mechanism in Caenorhabditis elegans. Aging Cell. 2008; 7:394–404.

9. Colman RJ, Anderson RM, Johnson SC, Kastman EK, Kosmatka KJ, Beasley TM, Allison DB, Cruzen C, Simmons HA, Kemnitz JW, Weindruch R. Caloric restriction delays disease onset and mortality in rhesus monkeys. Science. 2009; 325:201–204.

10. Martin DE, Hall MN. The expanding TOR signaling network. Current Opinion in Cell Biology. 2005; 17:158–166.

11. Kaeberlein M, Powers RW, Steffen KK, Westman EA, Hu D, Dang N, Kerr EO, Kirkland KT, Fields S, Kennedy BK. Regulation of yeast replicative life span by TOR and Sch9 in response to nutrients. Science. 2005; 310:1193–1196.

12. Vellai T, Takacs-Vellai K, Zhang Y, Kovacs AL, Orosz L, Müller F. Genetics: influence of TOR kinase on lifespan in C. elegans. Nature. 2003; 426:620.

13. Kapahi P, Zid BM, Harper T, Koslover D, Sapin V, Benzer S. Regulation of Lifespan in Drosophila by Modulation of Genes in the TOR Signaling Pathway. Curr Biol. 2004; 14:885–890.

14. Harrison DE, Strong R, Sharp ZD, Nelson JF, Astle CM, Flurkey K, Nadon NL, Wilkinson JE, Frenkel K, Carter CS, Pahor M, Javors MA, Fernandez E et al. Rapamycin fed late in life extends lifespan in genetically heterogeneous mice. Nature. 2010; 460:392–395.

15. Khapre RV, Kondratova AA, Patel S, Dubrovsky Y, Wrobel M, Antoch MP, Kondratov RV. BMAL1-dependent regulation of the mTOR signaling pathway delays aging. Aging. 2014; 6:48–57.

16. Johnson SC, Yanos ME, Kayser E-B, Quintana A, Sangesland M, Castanza A, Uhde L, Hui J, Wall VZ, Gagnidze A, Oh K, Wasko BM, Ramos FJ et al. mTOR inhibition alleviates mitochondrial disease in a mouse model of Leigh syndrome. Science. 2013; 342:1524–1524.

17. Ye L, Widlund AL, Sims CA, Lamming DW, Guan Y, Davis JG, Sabatini DM, Harrison DE, Vang O, Baur JA. Rapamycin doses sufficient to extend lifespan do not compromise muscle mitochondrial content or endurance. Aging. 2013; 5:539–550.

18. Komarova E, Antoch M, Novototskaya L, Chernova O, Paszkiewicz G, Leontieva O, Blagosklonny MV, Gudkov A. Rapamycin extends lifespan and delays tumorigenesis in heterozygous p53+/- mice. Aging. 2014; 4:709–714.

19. Popovich I, Anisimov V, Zabezhinski M, Semenchenko A, Tyndyk M, Yurova M, Blagosklonny MV. Lifespan extension and cancer prevention in HER-2/neu transgenic mice treated with low intermittent doses of rapamycin. Cancer Biology & Therapy. 2014; 15:586–592.

20. Fontana L, Partridge L, Longo VD. Extending healthy life span--from yeast to humans. Science. 2010; 328:321–326.

21. Min K-J, Yamamoto R, Buch S, Pankratz M, Tatar M. Drosophila lifespan control by dietary restriction independent of insulin-like signaling. Aging Cell. 2008; 7:199–206.

22. Grandison RC, Piper MDW, Partridge L. Amino-acid imbalance explains extension of lifespan by dietary restriction in Drosophila. Nature. 2009; 462:1061–1064.

23. Grönke S, Clarke D-F, Broughton S, Andrews TD, Partridge L. Molecular evolution and functional characterization of Drosophila insulin-like peptides. PLoS Genetics. 2010; 6:e1000857.

24. Broughton SJ, Piper MDW, Ikeya T, Bass TM, Jacobson J, Driege Y, Martinez P, Hafen E, Withers DJ, Leevers SJ, Partridge L. Longer lifespan, altered metabolism, and stress resistance in Drosophila from ablation of cells making insulin-like ligands. Proc Natl Acad Sci U S A. 2005; 102:3105–3110.

25. Slack C, Werz C, Wieser D, Alic N, Foley A, Stocker H, Withers DJ, Thornton JM, Hafen E, Partridge L. Regulation of lifespan, metabolism, and stress responses by the Drosophila SH2B protein, Lnk. PLoS Genetics. 2010; 6:e1000881.

26. Chen D, Thomas EL, Kapahi P. HIF-1 modulates dietary restriction-mediated lifespan extension via IRE-1 in Caenorhabditis elegans. PLoS Genetics. 2009; 5:e1000486.

27. Kaeberlein TL, Smith ED, Tsuchiya M, Welton KL, Thomas JH, Fields S, Kennedy BK, Kaeberlein M. Lifespan extension in Caenorhabditis elegans by complete removal of food. Aging Cell. 2006; 5:487–494.

28. Broughton SJ, Slack C, Alic N, Metaxakis A, Bass TM, Driege Y, Partridge L. DILP-producing median neurosecretory cells in the Drosophila brain mediate the response of lifespan to nutrition. Aging Cell. 2010; 9:336–346.

29. Slack C, Giannakou ME, Foley A, Goss M, Partridge L. dFOXO-independent effects of reduced insulin-like signaling in Drosophila. Aging Cell. 2011; 10:735–748.

30. Blagosklonny MV. Once again on rapamycin-induced insulin resistance and longevity: despite of or owing to. Aging. 2012; 4:350–358.

31. McElwee JJ, Schuster E, Blanc E, Thomas JH, Gems D. Shared transcriptional signature in Caenorhabditis elegans Dauer larvae and long-lived daf-2 mutants implicates detoxification system in longevity assurance. The Journal of Biological Chemistry. 2004; 279:44533–44543.

32. McElwee JJ, Schuster E, Blanc E, Piper MDW, Thomas JH, Patel DS, Selman C, Withers DJ, Thornton JM, Partridge L, Gems D. Evolutionary conservation of regulated longevity assurance mechanisms. Genome Biology. 2007; 8:R132.

33. Gems D, Doonan R. Antioxidant defense and aging in C. elegans. Cell Cycle. 2009; 8:1–7.

34. Doonan R, McElwee JJ, Matthijssens F, Walker GA, Houthoofd K, Back P, Matscheski A, Vanfleteren JR, Gems D. Against the oxidative damage theory of aging: superoxide dismutases protect against oxidative stress but have little or no effect on life span in Caenorhabditis elegans. Genes & Development. 2008; 22:3236–3241.

35. Blagosklonny MV. Ageing ROS or TOR. Cell Cycle. 2008; 7:3344–3354.

36. Blagosklonny MV. Cell senescence: hypertrophic arrest beyond the restriction point. Journal of Cellular Physiology. 2006; 209:592–597.

37. Gems D, de la Guardia Y. Alternative Perspectives on Aging in Caenorhabditis elegans: Reactive Oxygen Species or Hyperfunction? Antioxidants & Redox Signaling. 2013; 19:321–329.

38. Blagosklonny MV. Aging and Immortality: Quasi-programmed senescence and its pharmacologic inhibition. Cell Cycle. 2006; 5:2087–2102.

39. Skorupa DA, Dervisefendic A, Zwiener J, Pletcher SD. Dietary composition specifies consumption, obesity, and lifespan in Drosophila melanogaster. Aging Cell. 2008; 7:478–490.

40. Chippindale AK, Leroi M, Kim SB, Rose MR. Phenotypic plasticity and selection in Drosophila life-history evolution . I . Nutrition and the cost of reproduction. J Evol Biol. 1993; 6:171–193.

41. Bradley TJ, Simmons FH. An analysis of resource allocation in response to dietary yeast in Drosophila melanogaster. Journal of Insect Physiology. 1997; 43:779–788.

42. Liao C-Y, Rikke BA, Johnson TE, Gelfond JAL, Diaz V, Nelson JF. Fat maintenance is a predictor of the murine lifespan response to dietary restriction. Aging Cell. 2011; 10:629–639.

43. Harrison DE, Archer JR, Astle CM. Effects of food restriction on aging: separation of food intake and adiposity. Proc Natl Acad Sci U S A. 1984; 81:1835–1838.

44. Miller RA, Buehner G, Chang Y, Harper JM, Sigler R, Smith-Wheelock M. Methionine-deficient diet extends mouse lifespan, slows immune and lens aging, alters glucose, T4, IGF-I and insulin levels, and increases hepatocyte MIF levels and stress resistance. Aging Cell. 2005; 4:119–125.

45. Katewa SD, Demontis F, Kolipinski M, Hubbard A, Gill MS, Perrimon N, Melov S, Kapahi P. Intramyocellular Fatty-Acid Metabolism Plays a Critical Role in Mediating Responses to Dietary Restriction in Drosophila melanogaster. Cell Metabolism. 2012; 16:97–103.

46. Böhni R, Riesgo-Escovar J, Oldham S, Brogiolo W, Stocker H, Andruss BF, Beckingham K, Hafen E. Autonomous control of cell and organ size by CHICO, a Drosophila homolog of vertebrate IRS1-4. Cell. 1999; 97:865–875.

47. Zhang H, Stallock JP, Ng JC, Reinhard C, Neufeld TP. Regulation of cellular growth by the Drosophila target of rapamycin dTOR. Genes & Development. 2000; 14:2712–2724.

48. Bjedov I, Toivonen JM, Kerr F, Slack C, Jacobson J, Foley A, Partridge L. Mechanisms of life span extension by rapamycin in the fruit fly Drosophila melanogaster. Cell Metabolism. 2010; 11:35–46.

49. Teleman AA, Chen Y, Cohen SM. 4E-BP functions as a metabolic brake used under stress conditions but not during normal growth. Genes & Development. 2005; 19:1844–1848.

50. Grönke S, Mildner A, Fellert S, Tennagels N, Petry S, Müller G, Jäckle H, Kühnlein RP. Brummer lipase is an evolutionary conserved fat storage regulator in Drosophila. Cell Metabolism. 2005; 1:323–330.

51. Bass TM, Grandison RC, Wong R, Martinez P, Partridge L, Piper MDW. Optimization of dietary restriction protocols in Drosophila. J Gerontol A Biol Sci Med Sci. 2007; 62:1071–1081.

52. Sgrò CM, Partridge L. Laboratory adaptation of life history in Drosophila. The American Naturalist. 2001; 158:657–658.

53. Priest N, Mackowiak B, Promislow D. The role of parental age effects on the evolution of aging. Evolution. 2002; 56:927–935.

54. Stewart MJ, Berry CO, Zilberman F, Thomas G, Kozma SC. The Drosophila p70s6k homolog exhibits conserved regulatory elements and rapamycin sensitivity. Proc Natl Acad Sci U S A. 1996; 93:10791–10796.

55. Grönke S, Beller M, Fellert S, Ramakrishnan H, Jäckle H, Kühnlein RP. Control of fat storage by a Drosophila PAT domain protein. Current Biology. 2003; 13:603–606.

56. Van Handel E. Microseparation of Glycogen, Sugars, and Lipids. Analytical Biochemistry. 1965; 11:266–271.

Research Paper

Multiple dietary supplements do not affect metabolic and cardiovascular health

Andreea Soare[1,2*], Edward P. Weiss[1,3*], John O. Holloszy[1], and Luigi Fontana[1,4,5]

[1] Division of Geriatrics and Nutritional Sciences, Department of Medicine, Washington University School of Medicine, St. Louis, MO 63130, USA
[2] Department of Endocrinology and Diabetes, University Campus Bio-Medico, Rome, Italy
[3] Department of Nutrition and Dietetics, St. Louis University, St. Louis, MO 63130, USA
[4] Department of Medicine, Salerno University School of Medicine, Salerno, Italy
[5] CEINGE Biotecnologie Avanzate, Napoli, Italy
* These authors contributed equally to this research

Key words: supplements, endothelial function, arterial stiffness, inflammation, oxidative stress
Received: 8/12/13; Accepted: 8/31/13; Published: 9/4/13 **doi:** 10.18632/aging.100597
Correspondence to: Luigi Fontana, MD/PhD; **E-mail:** fontana@dom.wustl.edu

Abstract: Dietary supplements are widely used for health purposes. However, little is known about the metabolic and cardiovascular effects of combinations of popular over-the-counter supplements, each of which has been shown to have anti-oxidant, anti-inflammatory and pro-longevity properties in cell culture or animal studies. This study was a 6-month randomized, single-blind controlled trial, in which 56 non-obese (BMI 21.0-29.9 kg/m^2) men and women, aged 38 to 55 yr, were assigned to a dietary supplement (SUP) group or control (CON) group, with a 6-month follow-up. The SUP group took 10 dietary supplements each day (100 mg of resveratrol, a complex of 800 mg each of green, black, and white tea extract, 250 mg of pomegranate extract, 650 mg of quercetin, 500 mg of acetyl-l-carnitine, 600 mg of lipoic acid, 900 mg of curcumin, 1 g of sesamin, 1.7 g of cinnamon bark extract, and 1.0 g fish oil). Both the SUP and CON groups took a daily multivitamin/mineral supplement. The main outcome measures were arterial stiffness, endothelial function, biomarkers of inflammation and oxidative stress, and cardiometabolic risk factors. Twenty-four weeks of daily supplementation with 10 dietary supplements did not affect arterial stiffness or endothelial function in nonobese individuals. These compounds also did not alter body fat measured by DEXA, blood pressure, plasma lipids, glucose, insulin, IGF-1, and markers of inflammation and oxidative stress. In summary, supplementation with a combination of popular dietary supplements has no cardiovascular or metabolic effects in non-obese relatively healthy individuals.

INTRODUCTION

Non-vitamin, non-mineral dietary supplements are widely used for health purposes and sometimes as a substitute to a healthy diet or conventional medical treatments. Nearly 1 in 7 adults takes supplements regularly, and approximately 40% have taken one or more dietary supplements during their life [1]. However, despite the widespread and growing use of these over-the-counter products, insight into the potential beneficial or harmful biological effects of these compounds in humans is frequently lacking.

Some individuals, especially heavy supplement users, typically consume combinations of dietary supplements because they believe that multiple compounds can act through complimentary, additive or synergistic mechanisms to convey a greater biologic effect than can be achieved by any individual supplement [2]. The present study was a randomized clinical trial to evaluate the effectiveness of supplementation with a combination of some of the most self-prescribed dietary supplements (i.e. resveratrol, curcumin, green/black/white tea extract, quercetin, acetyl-l-carnitine, lipoic acid, pomegranate, cinnamon bark, sesamin, and fish oil), in

lean and overweight middle-aged men and women eating a Western diet. It has been reported that these compounds exert powerful protective effects against inflammation, oxidative stress/free radical damage, insulin resistance, and protein glycation in cell culture and laboratory animal studies [3-24]. We evaluated the combined effects of these supplements on arterial stiffness, endothelial function, markers of inflammation, oxidative stress, glucose and lipid metabolism, and blood pressure.

RESULTS

Study Participants

Screening, enrollment, and follow-up information is presented in Fig. 1. The study participants were generally healthy, as reflected by the following: BMI, 25.0±2.3 kg/m^2; total cholesterol, 187±32 mg/dL; triglycerides, 79±53 mg/dL; fasting glucose, 82±9 mg/dL; and systolic and diastolic blood pressures of 109±12 and 68±8 mmHg, respectively. The proportions of men and women did not differ between groups (p=0.65). The average age of participants was slightly lower in the SUP group (means±SD: 44±6 vs. 47±5 yr, p=0.05). BMI did not differ (p=0.65) between the SUP (25.2±2.0 kg/m^2) and control (24.9±2.5 kg/m^2) groups. Based on monthly pill compliance queries, 96% of the participants in the SUP group took all of the prescribed doses of the supplements. All participants in both groups complied with the vitamin/mineral supplementation regimen.

There were no differences between groups in PWV, AI, blood pressure, and endothelium-dependent and endothelium-independent brachial artery vasodilation (Table 1). No changes in body weight or % total body fat occurred in either study group (Table 2). Plasma lipid concentrations and indices of glucoregulation did not change in either group (Table 2). No differences between groups were observed for markers of inflammation, oxidative stress and glycation, and blood counts (Table 2). Serum insulin and IGF-1 concentrations did not change in either group (Table 2). Since completing the randomized trial, all but one of the participants in the SUP group continued for another 6 months on the supplementation regimen. Even with this longer, 12 month period of supplementation, no changes in any outcome were observed (data not shown).

No serious adverse events occurred. Serum markers of liver and kidney function were unaffected by supplementation. Other adverse events were limited to mild gastrointestinal discomfort associated with taking the large number of oral supplements in 19% of the participants.

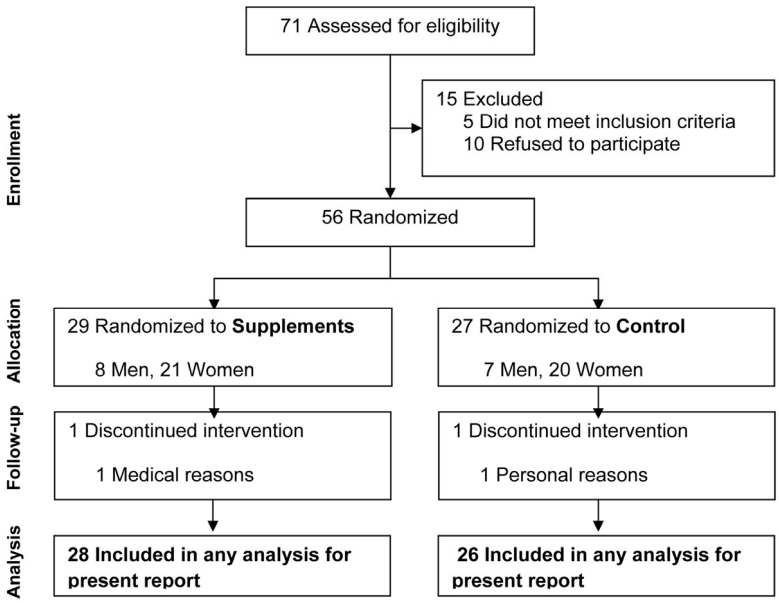

Figure 1. Consort diagram reflecting flow of study participants through the study.

Table 1. Effect of 6 months of nutritional supplements or control on indices of arterial stiffness, vasomotor function, and blood pressure.

	Supplements(n=28)	Control (n=26)	Adjusted Difference Between Groups	Between Group *P* value
Pulse wave velocity, m/s				
Baseline	5.4 ± 0.3	5.2 ± 0.2		
6 months	4.8 ± 0.3	5.3 ± 0.2		
Change	-0.5 ± 0.4	0.1 ± 0.3	-0.3 ± 0.4	0.36
Augmentation index, %				
Baseline	11.7 ± 2.6	12.3 ± 2.8		
6 months	12.5 ± 2.8	13.0 ± 2.3		
Change	0.8 ± 1.1	0.7 ± 1.1	0.4 ± 1.5	0.77
Flow-mediated dilation, %				
Baseline	5.0 ± 0.5	4.1 ± 0.4		
6 months	4.5 ± 0.4	4.4 ± 0.3		
Change	-0.5 ± 0.5	0.3 ± 0.3	-0.3 ± 0.5	0.54
GTN-mediated dilation, %				
Baseline	16.1 ± 1.3	14.6 ± 1.2		
6 months	14.2 ± 1.6	13.3 ± 0.9		
Change	-1.9 ± 1.1	-1.3 ± 1.4	-0.2 ± 1.7	0.93
Systolic BP, mmHg				
Baseline	108 ± 2	109 ± 2		
6 months	108 ± 2	107 ± 3		
Change	0 ± 1	-2 ± 1	1 ± 2	0.48
Diastolic BP, mmHg				
Baseline	69 ± 1	66 ± 2		
6 months	69 ± 1	64 ± 2		
Change	0 ± 1	-2 ± 1*	2 ± 1	0.08

Values are arithmetic means ± SE except for mean differences between groups, which have been adjusted for baseline values. Between-group P values reflect the between-group comparison change-scores from ANCOVAs that included baseline values as the covariate. *Significant ($p \leq 0.05$) within-group change. GTN, nitroglycerine; BP, blood pressure. Several subjects in the supplement group (n=15) and control group (n=14) did not undergo testing for GTN-mediated dilation because systolic blood pressure was below 100 mmHg, which is a contraindication to GTN administration.

DISCUSSION

Our findings indicate that daily use of multiple dietary supplements has no effect on arterial stiffness (i.e. pulse wave velocity and augmentation index), endothelial function (i.e. brachial artery flow-dependent vasodilatation) or blood pressure in nonobese men and women. Furthermore, supplementation with these compounds did not affect key metabolic variables implicated in the biology of aging, and in the pathogenesis of cardiovascular disease, including plasma markers of inflammation, oxidative stress and glycation, plasma lipids, growth factors, or body composition.

Reports from studies conducted mainly on cells in culture or in experimental animals suggest that these compounds promote metabolic health and may have anti-aging effects [4-24]. In particular, resveratrol, quercetin, curcumin, acetyl-L-carnitine, lipoic acid, fish oil, sesamin, pomegranate, cinnamon bark, and green tea extracts have all been reported to have powerful anti-oxidant and/or anti-inflammatory properties [4-24].

Table 2. Risk factors for cardiovascular disease and diabetes, and circulating markers of oxidative stress, chronic inflammation, in response to 6 months of nutritional supplementation or control.

	Supplements (n=28)	Control (n=26)	Adjusted Difference Between Groups	Between Group *P* value
Body Mass and Composition				
Body mass, kg				
Baseline	73.8 ± 2.3	72.8 ± 1.8		
6 months	74.2 ± 2.5	73.1 ± 1.7		
Change	0.3 ± 0.4	0.2 ± 0.4	0.1 ± 0.6	0.91
Body fat, %				
Baseline	30.1 ± 1.1	30.2 ± 1.7		
6 months	29.9 ± 1.0	30.3 ± 1.8		
Change	-0.2 ± 0.3	0.2 ± 0.3	-0.2 ± 0.4	0.70
Lipids				
Triglycerides, mg/dL				
Baseline	79 ± 12	78 ± 8		
6 months	75 ± 6	87 ± 8		
Change	-4 ± 11	8 ± 4	-12 ± 8	0.16
Total cholesterol, mg/dL				
Baseline	186 ± 6	189 ± 6		
6 months	186 ± 6	192 ± 5		
Change	-1 ± 4	4 ± 4	-5 ± 5	0.32
LDL-cholesterol, mg/dL				
Baseline	110 ± 6	114 ± 6		
6 months	111 ± 5	115 ± 5		
Change	1 ± 3	1 ± 4	-1 ± 5	0.80
HDL-cholesterol, mg/dL				
Baseline	61 ± 3	61 ± 3		
6 months	59 ± 3	60 ± 3		
Change	-2 ± 2	-1 ± 2	-1 ± 2	0.59
Glucoregulatory Function				
Fasting glucose, mg/dL				
Baseline	80 ± 2	84 ± 2		
6 months	83 ± 2	85 ± 2		
Change	3 ± 2	1 ± 2	-1 ± 2	0.70
Fasting insulin, μU/mL				
Baseline	3.3 ± 0.3	2.8 ± 0.3		
6 months	3.6 ± 0.4	2.9 ± 0.3		
Change	0.3 ± 0.3	0.1 ± 0.2	0.3 ± 0.4	0.41
HOMA-IR				
Baseline	0.64 ± 0.06	0.60 ± 0.06		
6 months	0.74 ± 0.09	0.63 ± 0.06		
Change	0.10 ± 0.06	0.03 ± 0.04	0.08 ± 0.08	0.32

Table 2. (continued). Risk factors for cardiovascular disease and diabetes, and circulating markers of oxidative stress, chronic inflammation, in response to 6 months of nutritional supplementation or control.

	Supplements (n=28)	Control (n=26)	Adjusted Difference Between Groups	Between Group *P* value
Inflammatory Cytokines and Oxidative Stress Markers				
CRP, mg/L				
Baseline	1.69 ± 0.48	1.21 ± 0.52		
6 months	1.51 ± 0.20	1.44 ± 0.56		
Change	-0.17 ± 0.49	0.23 ± 0.10*	-0.20 ± 0.43	0.46
TNFα, pg/mL				
Baseline	1.92 ± 0.09	2.10 ± 0.18		
6 months	1.94 ± 0.09	2.13 ± 0.19		
Change	0.02 ± 0.05	0.03 ± 0.14	-0.05 ± 0.14	0.70
IL-6, pg/mL				
Baseline	1.26 ± 0.26	1.39 ± 0.31		
6 months	1.35 ± 0.23	1.68 ± 0.32		
Change	0.08 ± 0.08	0.29 ± 0.20	-0.22 ± 0.20	0.27
Protein carbonyl, nmol/mg				
Baseline				
6 months	0.83 ± 0.03	0.79 ± 0.03		
Change	0.76 ± 0.03	0.82 ± 0.03		
	-0.07 ± 0.04	0.03 ± 0.03	-0.06 ± 0.04	0.14
AGEs, ng/mL				
Baseline	307 ± 14	272 ± 13		
6 months	287 ± 12	270 ± 12		
Change	-20 ± 13	-2 ± 12	1 ± 14	0.96
White Cell Counts and Growth Factors				
WBC, k/cumm				
Baseline	5.1 ± 0.2	4.8 ± 0.2		
6 months	5.0 ± 0.2	5.1 ± 0.3		
Change	-0.1 ± 0.2	0.3 ± 0.2	-0.3 ± 0.3	0.20
Lymphocytes, k/cumm				
Baseline	1.50 ± 0.05	1.42 ± 0.09		
6 months	1.42 ± 0.06	1.44 ± 0.10		
Change	-0.08 ± 0.04*	0.02 ± 0.05	-0.10 ± 0.06	0.11
IGF-1, ng/mL				
Baseline	145 ± 6	148 ± 7		
6 months	151 ± 7	144 ± 6		
Change	6 ± 5	-4 ± 4	9 ± 6	0.15

Values are arithmetic means ± SE except for mean differences between groups which have been adjusted for baseline values. Between-group P values reflect the between-group comparison change-scores from ANCOVAs that included baseline values as the covariate. *Significant ($p \leq 0.05$) within-group change. Triglyceride data were also adjusted for a significant effect of age on the baseline to follow up changes. Within-group P values are from paired t-tests. LDL, low density lipoprotein; HDL, high density lipoprotein; HOMA-IR, homeostasis model assessment of insulin resistance; CRP, C-reactive protein, TNFα, tumor necrosis factor α; IL-6, interleukin-6; AGEs, advanced glycation end products; WBC, white blood cells; IGF-1, insulin-like growth factor-1. To convert units to SI units, multiply the conventional units by the following conversion factors: triglycerides x 0.0113 = mmol/L; total, LDL-, and HDL-cholesterol x 0.0259 = mmol/L; glucose x 0.0555 = mmol/L; insulin x 6.945 = pmol/L.

However, in our study we did not see any reduction in markers of inflammation or oxidative stress. Oxidative stress and inflammation are major players in the pathogenesis of arterial aging and endothelial dysfunction, which is a precursor of atherosclerosis [25-29]. Nevertheless, pulse wave velocity, augmentation index and endothelium-dependent vasorelaxation did not improve in the supplement group. Furthermore, supplementation with these compounds did not alter other well-accepted cardiometabolic risk factors, including blood pressure, insulin resistance, and serum cholesterol, triglyceride and advanced glycation end-products concentrations. Endothelial function can be improved with just a single infusion of the anti-oxidant, vitamin C [30]. Because all the supplements that we used have been reported to have powerful anti-inflammatory and anti-oxidant effects, it is interesting that no biological change in endothelial function was observed. In contrast, it has been shown that 6-mo or 1-yr supplementation with DHEA-s results in significant improvements of glucose tolerance, arterial stiffness and inflammation [31].

One possible explanation for the lack of beneficial metabolic effects of these over-the counter dietary supplements could be the low phytochemical bioavailability or inadequate supplement potency of the phytochemicals contained in some of these compounds which are available without prescription [32]. Nonetheless, the fact remains that millions of individuals in USA and Europe are consuming these supplements, sometimes instead of a healthy diet and conventional medical treatment, which might contain hazard trace amounts of pesticides and heavy metals, including lead, arsenic, mercury, and cadmium [1,33]. A placebo was not provided to control group participants in the present study, which might be viewed as a limitation. However, while a "placebo effect" might have been an explanation for significant changes in the supplement group, we did not observe changes. Therefore, in this context, the lack of a placebo is not a limitation. Moreover, although the sample size was relatively small, there was no suggestion of clinically significant differences from the between-group estimates, despite multiple comparisons. Finally, it is conceivable that some supplements might have had beneficial effects that where counteracted by negative effects of others. However, this seems unlikely and people rarely take isolated supplements, and many of these compounds are contained in foods and beverages that are consumed regularly by millions of people. Moreover, heavy supplement users believe that these compounds work better in combination, because as with food and beverages, they provide a mix of phyto-chemicals that interact and potentiate their effect (e.g. resveratrol in wine, cathechins in green and black tea, pomegranate in fruits, curcumin in spices, etc.).

Findings from the present study suggest that a combination of several popular nutritional supplements, which are commonly taken with the intention of promoting healthy longevity and preventing chronic disease, have no effects on arterial stiffness, endothelial function, inflammation, oxidative stress, and other chronic disease risk factors in non-obese men and women. Additional randomized controlled studies are still needed to assess the potential benefits of these and other dietary supplements in obese metabolically abnormal individuals.

METHODS

Participants. Non-obese (BMI 21.0-29.9 kg/m^2) men and women, aged 38-65y were recruited from the Saint Louis area. Participants were free of chronic disease based on a medical history, physical examination, blood and urine chemistries, and electrocardiogram. Exclusion criteria included chronic use of medications or dietary supplements, tobacco use, alcohol abuse, and habitual vigorous exercise. Participants consented to participate in the study, which was approved by the Washington University Institutional Review Board.

Study design. The study was a 6-month single-blind controlled trial in which participants were randomized (1:1 ratio with stratification for sex) to a nutritional supplement (SUP) group or control (CON) group. At the end of the RCT, the participants who had been randomized to SUP continued taking the supplements for another 6-mo, while those who had been in the CON group crossed over to the supplementation regimen for 6-mo. Technicians who performed outcomes assessments were blinded to study group assignments. Participants fasted overnight (12-hr) and refrained from exercise for 24-hr before testing. For follow-up tests, participants in the SUP group were instructed to take their nutritional supplements upon waking in the morning prior to testing. The primary outcome, carotid-femoral pulse wave velocity (PWV), was measured by using Doppler flow measures. Another index of arterial stiffness, carotid artery augmentation index (AI) was measured using applanation tonometry. Endothelium-dependent and endothelium-independent brachial artery vasodilation were evaluated by using ultrasound imaging to measure flow-mediated dilation and glyceryl trinitrate- (GTN)-mediated dilation, respectively.

Intervention. Participants in the SUP group took the following dietary supplements: resveratrol (100 mg/day), quercetin (650 mg/day), acetyl-l-carnitine HCL (500/mg/day), alpha-lipoic acid (600 mg/day),

curcumin complex (900 mg/day; standardized to 95% total curcuminoids, plus piperine 5 mg), pomegranate extract (250 mg/day; standardized to 70% ellagic acid), fish oil (1 g/day, containing 300 mg of eicosapentaenoic acid and 200 mg docosahexaenoic acid), cinnamon bark (1.7 g/day), green/white/black tea complex (800 mg/day each of green, black, and white tea extract) and sesamin (1 g/day; standardized to 500 mg sesamin lignans). Sesamin was formulated by Scivation, Inc. (Burlington, NC, USA) and all others by Swanson Health Products (Fargo, ND, USA). Both groups received a daily multivitamin/mineral supplement (Daily Multi-Vitamin & Mineral, Swanson, Fargo, ND, USA) and were advised to maintain their usual diet and physical activity. Participants met with a member of the research team each month to receive supplements and to answer questions about compliance with the supplementation regimen, changes in diet, physical activity, medical conditions, and medication use, and adverse events.

Body weight and composition. Weight and height were measured with a calibrated balance beam scale and wall-mounted stadiometer, respectively, with the participant wearing only a hospital gown and underwear. BMI was calculated (kg/m^2). Body composition was evaluated using dual energy X-ray absorptiometry (Delphi W, software version 11.2, Hologic Corp., Waltham, MA). Bilateral brachial artery blood pressure was measured with a calibrated monitor (Dinamap 1846 SX, Critkon, Inc, Tampa, FL) according to JNC 7 guidelines.

Circulating biomarkers of disease risk and aging. Blood samples were collected from a forearm vein into separate tubes containing sodium heparin, EDTA, and no additives. Plasma and serum were isolated by centrifugation (3500 g, 15 min, 4º C) and stored at -80º C for later batch analyses. Samples were analyzed for plasma concentrations of glucose (glucose oxidase method, 2300 Stat Plus, YSI Inc., Yellow Springs, OH) and insulin (chemiluminescence assay, Immulite 1000, Siemens USA, Malvern, PA). The homeostasis model assessment of insulin resistance (HOMA-IR) was calculated from fasting glucose and insulin. ELISA assay kits were used to measure serum concentrations of inflammatory cytokines (tumor necrosis factor α (TNFα), interleukin-6 (IL-6), C-reactive protein (CRP), Quantikine, R&D Systems, Minneapolis, MN), oxidative stress markers (protein carbonyls (Cell Biolabs, San Diego, CA) and advanced glycation end-product (AGE) N-1-carboxymethyl lysine (MBL International, Woburn, MA)), and insulin-like growth factor-1 (IGF-1, Diagnostic Systems Laboratories, Webster, TX). Plasma lipids and blood counts were measured by a CLIA-certified clinical laboratory at the medical center.

Indices of arterial stiffness. Carotid artery augmentation index (AI) was measured by using applanation tonometry according to published guidelines [34]. Twenty digital pulse waves were recorded with a tonometer (Millar Instruments, Inc., Model #TCB-500, Houston, TX) and analyzed with Windaq software (version 2.31, DATAQ Instruments, Inc., Akron, OH). The the maximum and minimum voltage on each wave form was identified and used to calculate pulse pressure (PP). The second derivative of the pulse wave was generated and used to identify the "shoulder" on the upstroke of the raw wave form. Augmentation pressure (AP) was calculated as the difference between the peak voltage and the voltage at the shoulder. Augmentation index was calculated as $AI = 100 \times AP/PP$ for each of the 20 waveforms; the resulting values were averaged. Because AI is dependent on heart rate, AI values were adjusted to a standardized heart rate of 75 beats/min based on the inverse relationship of 4.8 AI units per 10 beats/min HR [35]. The technician visually inspected all waveforms to ensure that the landmarks had been properly identified and to omit waveforms that were of suboptimal quality due to artifacts or irregular heartbeats. When analyses were questionable (e.g. large variation in AI values among waveforms), the waveforms were re-analyzed by another technician. If discrepancies between the analyses occurred, the technicians reviewed the analyses together and if the differences could not be remediated, the data were excluded.

Pulse wave velocity (PWV) was determined according to standard procedures1 by using transcutaneous Doppler flow measurements (Model 806-CB, Parks Medical Electronics, Inc., Aloha, OR) at the right common carotid artery and the right femoral artery. Twenty Doppler wave forms were simultaneously recorded (Windaq software, version 2.31, DATAQ Instruments, Inc., Akron, OH) at the two sites. Pulse transit time was determined as the difference in pulse arrival times (based on the "foot" of the pulse wave, as determined from the second derivative of the pulse wave) for the carotid and femoral sites. Pulse transit distances between the aorta and the carotid site and the aorta and the femoral site were measured over the skin using the second intercostal space as a landmark for the aorta, with the difference between these distances being considered the pulse propagation distance [36]. PWV was calculated for each of the 20 pulses as the quotient of the propagation distance (in meters) and transit time (in seconds) and the 20 values were averaged. Quality

control procedures were identical to those described above for the AI method.

Vascular function. Brachial artery flow mediated dilation (FMD) was used to measure endothelium-dependent vasodilation and glyceryl trinitrate- (GTN)-mediated dilation was used to measure endothelium-independent vasodilation. The participant's right arm was immobilized with the shoulder abducted at 70-90º and elbow fully extended. Ultrasound images were acquired using an ultrasound system (Agilent SONOS 5500, Andover, Massachusetts) equipped with an 11-3L linear array transducer. The probe was secured using a stereotactic clamp (Noga Engineering, Ltd.) to maintain constant positioning over the artery throughout the procedure. Ultrasound images were fed to a computer for real time quantification of arterial diastolic diameter (30 ± 2 measures/sec) using Vascular Imaging Analysis software (VIA, version 9.60) [37]. Baseline diameter was recorded for 2 minutes before a pneumatic cuff (Hokanson E20 Rapid Cuff Inflator and AG101 Cuff Inflator Air Source, PMS Instruments, Ltd., Maidenhead, UK) was inflated to 200 mmHg on the right forearm to occlude blood flow. After 5 minutes of occlusion, the pressure in the cuff was rapidly released and arterial diameter was recorded continuously for 5 minutes. FMD was calculated as the percent increase in diameter from baseline to peak diameter, where baseline diameter was the average diastolic diameter over the 2-minute baseline and peak diameter was recorded as the 10-second average of the highest diastolic diameter after cuff deflation. After the FMD assessment, and after the diameter of the artery returned to baseline, a second 2-minute baseline data collection was performed, followed by administration of 0.4 mg sublingual GTN spray. Brachial artery diameter was evaluated again 5 minutes after GTN administration. GTN-mediated dilation was calculated as the percentage increase in arterial diameter from baseline to 5 minutes after GTN administration.

Statistical power and analyses. Sample size estimates were calculated for PWV, as a measure of arterial stiffness and for interleukin-6 (IL-6) and C-reactive protein (CRP) as inflammatory markers. Calculations were based on data collected in our laboratory during previous studies. These studies included a randomized controlled trial on the effects of 50 mg/d oral DHEA supplementation on markers of aging in older adults [31] and cross-sectional [38] and longitudinal studies [39] on the effects of calorie restriction on markers of aging in middle-aged adults. For all sample size calculations, the alpha error rate was set at 0.05, tests were designated as two-tailed, desired power was set to 0.80, and the ratio of participants to be randomized to the intervention and no-treatment control groups was 1:1. Results indicate that 21 subjects per group would be sufficient for detecting a 3.1 m/sec improvement in pulse wave velocity, 27 subjects per groups would be sufficient for detecting a 0.86 ng/mL reduction in IL-6, and 12 subjects per groups would be sufficient for detecting a 1.60 mg/L reduction in CRP. Therefore, our proposed sample size of 56 participants (28 per group) was sufficient to detect biologically relevant changes in arterial stiffness and inflammation.

Power analyses were performed for PWV, IL-6, and CRP to determine sample size. Respective results indicated that sample sizes of 21, 27, and 12 subjects per group would be adequate for detecting significant effects. Therefore, 28 subjects per group was chosen.
Baseline characteristics were compared with independent t-tests and chi-square tests. Outcomes were analyzed with analysis of covariance, in which baseline values were included as a covariate. Paired t-tests were used for within-group paired comparisons. Significance was accepted at $p \leq 0.05$ and tests were two-tailed. Analyses were conducted with SAS for Windows XP Pro (version 9.3, SAS Institute, Cary, NC).

ACKNOWLEDGEMENTS

Drs. Soare, Weiss, and Fontana had full access to all of the data in the study and take responsibility for the integrity of the data and the accuracy of the data analysis.

Conflicts of Interest Statement

The authors declare no conflicts of interest.

REFERENCES

1. Blendon RJ, Benson JM, Botta MD, Weldon KJ. Users' views of dietary supplements. JAMA Intern Med 2013;173:74-6.
2. Denham BE. Dietary supplements--regulatory issues and implications for public health. JAMA 2011; 306:428-9.
3. Almeida IM, Barreira JC, Oliveira MB, Ferreira IC. Dietary antioxidant supplements: benefits of their combined use. Food Chem Toxicol 2011; 49:3232-7.
4. Baur JA, Sinclair DA. Therapeutic potential of resveratrol: the in vivo evidence. Nature reviews. Drug discovery. 2006; 5:493-506.
5. Das S, Das DK. Anti-inflammatory responses of resveratrol. Inflammation & allergy drug targets. 2007;6:168-173.
6. Chan MM. Inhibition of tumor necrosis factor by curcumin, a phytochemical. Biochem. Pharmacol. 1995; 49:1551-1556.
7. Ruby AJ, Kuttan G, Babu KD, Rajasekharan KN, Kuttan R. Anti-tumour and antioxidant activity of natural curcuminoids. Cancer Lett. 1995; 94:79-83.
8. Balentine D, Paetau-Robinson I. Tea as a source of dietary antioxidants with a potential role in prevention of chronic

diseases. In: Mazza G, BD O, eds. Herbs, Botanicals & Teas. Lancaster: Technomic Publishing Co., Inc.; 2000:265-287.

9. Aneja R, Odoms K, Denenberg AG, Wong HR. Theaflavin, a black tea extract, is a novel anti-inflammatory compound. Crit. Care Med. 2004; 32:2097-2103.

10. Bors W, Heller W, Michel C, Saran M. Flavonoids as antioxidants: determination of radical-scavenging efficiencies. Methods Enzymol. 1990; 186:343-355.

11. García-Mediavilla V, Crespo I, Collado PS, Esteller A, Sánchez-Campos S, Tuñón MJ, González-Gallego J. The anti-inflammatory flavones quercetin and kaempferol cause inhibition of inducible nitric oxide synthase, cyclooxygenase-2 and reactive C-protein, and down-regulation of the nuclear factor kappaB pathway in Chang Liver cells. Eur. J. Pharmacol. 2007; 557:221-229.

12. Mackraj I, Govender T, Ramesar S. The antihypertensive effects of quercetin in a salt-sensitive model of hypertension. J. Cardiovasc. Pharmacol. 2008; 51:239-245.

13. Rivera L, Moron R, Sanchez M, Zarzuelo A, Galisteo M. Quercetin ameliorates metabolic syndrome and improves the inflammatory status in obese Zucker rats. Obesity. 2008; 16:2081-2087.

14. Hagen TM, Liu J, Lykkesfeldt J, Wehr CM, Ingersoll RT, Vinarsky V, Bartholomew JC, Ames BN. Feeding acetyl-L-carnitine and lipoic acid to old rats significantly improves metabolic function while decreasing oxidative stress. Proc. Natl. Acad. Sci. U. S. A. 2002; 99:1870-1875.

15. Aviram M, Dornfeld L, Rosenblat M, Volkova N, Kaplan M, Coleman R, Hayek T, Presser D, Fuhrman B. Pomegranate juice consumption reduces oxidative stress, atherogenic modifications to LDL, and platelet aggregation: studies in humans and in atherosclerotic apolipoprotein E-deficient mice. Am. J. Clin. Nutr. 2000; 71:1062-1076.

16. Aviram M, Dornfeld L. Pomegranate juice consumption inhibits serum angiotensin converting enzyme activity and reduces systolic blood pressure. Atherosclerosis. 2001; 158:195-198.

17. Lin CC, Wu SJ, Chang CH, Ng LT. Antioxidant activity of Cinnamomum cassia. Phytother. Res. 2003; 17:726-730.

18. Reddy AM, Seo JH, Ryu SY, Kim YS, Min KR. Cinnamaldehyde and 2 methoxycinnamaldehyde as NF-kappaB inhibitors from Cinnamomum cassia. Planta Med. 2004; 70:823-827.

19. Qin B, Nagasaki M, Ren M, Bajotto G, Oshida Y, Sato Y. Cinnamon extract (traditional herb) potentiates in vivo insulin-regulated glucose utilization via enhancing insulin signaling in rats. Diabetes Res. Clin. Pract. 2003; 62:139-148.

20. Qin B, Nagasaki M, Ren M, Bajotto G, Oshida Y, Sato Y. Cinnamon extract prevents the insulin resistance induced by a high-fructose diet. Horm. Metab. Res. 2004; 36:119-125.

21. Ashakumary L, Rouyer I, Takahashi Y, Ide T, Fukuda N, Aoyama T, Hashimoto T, Mizugaki M, Sugano M. Sesamin, a sesame lignan, is a potent inducer of hepatic fatty acid oxidation in the rat. Metabolism. 1999; 48:1303-1313.

22. Arachchige PG, Takahashi Y, Ide T. Dietary sesamin and docosahexaenoic and eicosapentaenoic acids synergistically increase the gene expression of enzymes involved in hepatic peroxisomal fatty acid oxidation in rats. Metabolism. 2006; 55:381-390.

23. Hirose N, Inoue T, Nishihara K, Sugano M, Akimoto K, Shimizu S and Yamada H. Inhibition of cholesterol absorption and synthesis in rats by sesamin. J. Lipid Res. 1991; 32:629-638.

24. Calder PC. Polyunsaturated fatty acids, inflammation, and immunity. Lipids. 2001; 36:1007-1024.

25. Noma K, Goto C, Nishioka K, Jitsuiki D, Umemura T, Ueda K, Kimura M, Nakagawa K, Oshima T, Chayama K, Yoshizumi M, Liao JK, Higashi Y. Roles of rho-associated kinase and oxidative stress in the pathogenesis of aortic stiffness. J Am Coll Cardiol. 2007; 49:698-705.

26. Abramson JL, Weintraub WS and Vaccarino V. Association between pulse pressure and C-reactive protein among apparently healthy US adults. Hypertension 2002; 39: 197-202.

27. Mattace-Raso FUS, van der Cammen TJM, van der Meer IM, Schalekamp MADH, Asmar R, Hofman A and Witteman JCM. C-reactive protein and arterial stiffness in older adults: The Rotterdam Study. Atherosclerosis 2004; 176:111-116.

28. Davignon J, Ganz P. Role of endothelial dysfunction in atherosclerosis. Circulation 2004; 109:III27-32.

29. Hürlimann D, Forster A, Noll G, Enseleit F, Chenevard R, Distler O, Béchir M, Spieker LE, Neidhart M, Michel BA, Gay RE, Lüscher TF, Gay S, Ruschitzka F. Anti-tumor necrosis factor-alpha treatment improves endothelial function in patients with rheumatoid arthritis. Circulation 2002; 106:2184-7.

30. Eskurza I, Monahan KD, Robinson JA, Seals DR. Effect of acute and chronic ascorbic acid on flow-mediated dilatation with sedentary and physically active human ageing. J Physiol 2004; 556:315-24.

31. Weiss EP, Villareal DT, Ehsani AA, Fontana L, Holloszy JO. Dehydroepiandrosterone replacement therapy in older adults improves indices of arterial stiffness. Aging Cell 2012; 11: 876-84.

32. Williamson G, Manach C. Bioavailability and bioefficacy of polyphenols in humans. II. Review of 93 intervention studies. Am J Clin Nutr 2005; 81:243-55.

33. Office UGA. Herbal dietary supplements: examples of deceptive or questionable marketing practices and potentially dangerous advice. Publication No GAO-10-662T. http://www.gao.gov/new.items/d10662t.pdf (12 August 2013)

34. Laurent S, Cockcroft J, Van Bortel L, Boutouyrie P, Giannattasio C, Hayoz D, Pannier B, Vlachopoulos C, Wilkinson I, Struijker-Boudier H; European Network for Non-invasive Investigation of Large Arteries. Expert consensus document on arterial stiffness: methodological issues and clinical application. Eur Heart J 2006; 27:2588-2605.

35. Wilkinson IB, Mohammad NH, Tyrrell S, Hall IR, Webb DJ, Paul VE, Levy T, Cockcroft JR. Heart rate dependency of pulse pressure amplification and arterial stiffness. Am J Hypertens 2002; 15:24-30.

36. Karamanoglu M. Errors in estimating propagation distance in pulse wave velocity. Hypertension 2003; 41:e8.

37. Sidhu JS, Newey VR, Nassiri DK, Kaski JC. A rapid and reproducible on line automated technique to determine endothelial function. Heart 2002; 88:289-92.

38. Fontana L, Meyer TE, Klein S, Holloszy JO. Long-term calorie restriction is highly effective in reducing the risk for atherosclerosis in humans. Proc Natl Acad Sci USA 2004; 101:6659-63.

39. Fontana L, Villareal DT, Weiss EP, Racette SB, Steger-May K, Klein S, Holloszy JO; Washington University School of Medicine CALERIE Group.Calorie restriction or exercise: effects on coronary heart disease risk factors. A randomized, controlled trial. Am J Physiol Endocrinol Metab 2007; 293:197-202.

Editorial

Using PDE inhibitors to harness the benefits of calorie restriction: lessons from resveratrol

Jay H. Chung

doi: 10.18632/aging.100442

Resveratrol is a polyphenolic compound produced in some plants in response to stress, such as injury or infection [1] and is present most notably in red wine. A number of seemingly unrelated health benefits have been attributed to resveratrol, including protection against type 2 diabetes, cancer, heart disease, inflammation and neurodegenerative diseases. However, what these diseases have in common is their association with aging. Therefore, when resveratrol was reported to be a Sirt1 activating compound (STAC) [2], it captured the imagination of the field of aging.

The controversy regarding the mechanism of action for resveratrol arose when a series of papers demonstrated that it activated Sirt1 only if the substrate is attached to a fluorophore or a bulky amino acid [3-7]. However, resveratrol activated Sirt1 in vivo. One potential explanation is that the peptide modifications somehow mimicked the structure of the substrate in vivo. Another potential explanation is that resveratrol indirectly activates Sirt1 by targeting another protein. It has been known for some time that resveratrol indirectly activates AMP-activated protein kinase (AMPK) [8], a well-known regulator of energy metabolism that is also activated by calorie restriction (CR) [9,10]. We and others showed that resveratrol-mediated activation of AMPK increases NAD^+, the cofactor for Sirt1, as well as Sirt1 activity [11,12]. Consistent with the central role of AMPK in resveratrol action, the metabolic effects of resveratrol disappeared in AMPK knock-out mice [12]. These findings, in conjunction with the observation that resveratrol-mediated activation of AMPK does not require Sirt1 [12], indicated that AMPK is upstream of Sirt1 and that the direct target of resveratrol is upstream of AMPK.

One of the proposed mechanisms by which resveratrol activates AMPK is inhibition of ATP production. However, except at high concentrations of resveratrol (>100 μM), ATP levels do not decrease in the time frame of AMPK activation [13,14], suggesting another mechanism of action. In response to conditions that decrease serum glucose such as CR, glucagon and catecholamines are released. These hormones stimulate adenylate cyclases (AC), resulting in increased cAMP production. To explain the CR-mimetic effects of resveratrol, we measured cAMP levels in resveratrol-treated myotubes and discovered that resveratrol, at low micromolar concentrations (<10 μM), increased cAMP levels [15]. After ruling out the possibility that resveratrol activates AC, we discovered that resveratrol increased cAMP levels by competitively inhibiting a number of cAMP phosphodiesterases (PDEs), which degrade cAMP. We tested PDEs 1-5 and found that resveratrol inhibits PDEs 1, 3 and 4. cAMP, in turn, activates AMPK by increasing the activities of the AMPK kinases CamKKβ and, in some conditions LKB1, via cAMP effector proteins Epac1 (cAMP guanine-nucleotide exchange factor) or PKA, respectively. In addition, PKA-mediated phosphory-lation of S434 has been shown to activate Sirt1 [16]. Thus, increasing cAMP levels can activate Sirt1 by a number of pathways.

Since there are 11 PDE family members, each with different properties and tissue expression patterns, it would be impossible to mimic all of resveratrol effects with just one PDE inhibitor. However, PDE4 is the predominant PDE activity in skeletal muscle, the tissue where the metabolic effects of resveratrol are best elucidated. We found that the PDE4 inhibitor rolipram was sufficient to activate AMPK and Sirt1 in myotubes and to reproduce, at least qualitatively, the metabolic effects of resveratrol in skeletal muscle, as well as to improve glucose tolerance in obese mice [15]. It is unlikely that inhibition of PDE4 alone or of cAMP PDEs together explains all of the effects seen with resveratrol. The target(s) of resveratrol will most likely depend on the tissue, the effects of interest and the organism being studied.

One area where we lack understanding is the intracellular concentration of resveratrol. The serum level of unmodified resveratrol is low (submicromolar to low micromolar) because most resveratrol in serum is present in the conjugated form (e.g. glucuronide). However, tissues such as skeletal muscle have glucuronidases, which can potentially removed the conjugate and increase the intracellular levels of unmodified resveratrol far above those in the serum.

The mechanism by which novel chemical entity (NCE) STACs activate Sirt1 in vivo is also under question

because like resveratrol, they do not activate Sirt1 against native substrates in vitro, suggesting that they may activate Sirt1 indirectly in vivo [5,7]. Interestingly, analyses of off-target activities of NCE STACs SRT1720, 2183 and 1460 showed that they are stronger PDE inhibitors than resveratrol [7], raising the possibility that they too may be activating Sirt1 in vivo by inhibiting PDEs, at least in part.

In addition to resveratrol, other natural compounds that have been identified as STACs such as butein, fisetin and quercetin have also been identified to be PDE inhibitors [2,17]. This raises the question as to why so many compounds that are identified as STACs using the flurophore-tagged substrate turn out to be PDE inhibitors. We can only speculate at this point, but one possibility is that by coincidence, the structure of the Sirt1 STAC-binding pocket has some similarity to the PDE catalytic pocket.

Whether resveratrol can activate Sirt1 directly in addition to activating it indirectly (via PDE inhibition) remains to be seen. Even if resveratrol can activate Sirt1 directly in vivo, it is not clear how much this effect will add to the well-known anti-inflammatory and anti-diabetic effects produced by PDE4 inhibitors alone (e.g. the FDA-approved PDE4 inhibitor roflumilast) [18]. This question may take a while to answer.

In conclusion, the discovery of the resveratrol-PDE link suggests that PDE4 inhibitors, possibly in combination with other PDE inhibitors, may be useful for mimicking CR and for treating aging-related diseases.

ACKNOWLEDGEMENTS

This work was funded by the intramural program at the National Heart Lung and Blood Institute of the National Institutes of Health.

Jay H. Chung, MD/PhD
Laboratory of Obesity and Aging Research, Genetics and Developmental Biology Center, National Heart Lung and Blood Institute, National Institutes of Health, Bethesda, MD 20892
Email: chungj@nhlbi.nih.gov

Received: 3/3/12; Published: 3/4/12

REFERENCES

1. Signorelli P and Ghidoni R. The Journal of nutritional biochemistry. 2005;16:449-466.
2. Howitz KT, Bitterman KJ, Cohen HY. et. al. Nature. 2003; 425:191-196.
3. Beher D, Wu J, Cumine S. et. al. Chem Biol Drug Des. 2009; 74:619-624.
4. Borra MT, Smith BC, and Denu J M. J Biol Chem. 2005; 280:17187-17195.
5. Dai H, Kustigian L, Carney D. et. al. J Biol Chem. 2010; 285:32695-32703.
6. Kaeberlein M, McDonagh T, Heltweg B. et. al. J Biol Chem. 2005; 280:17038-17045.
7. Pacholec, M., Bleasdale, J. E., Chrunyk, B. et. al. J Biol Chem. 2010; 285:8340-8351.
8. Hardie DG and Carling D. Eur J Biochem. 1997; 246:259-273.
9. Edwards AG, Donato AJ, Lesniewski LA. et. al. Mech Ageing Dev. 2010; 131:739-742.
10. Palacios OM, Carmona JJ, Michan S. et. al. Aging. 2009; 1: 771-783.
11. Canto C, Jiang LQ, Deshmukh AS. et. al. Cell Metab. 2010; 11:213-219.
12. Um JH, Park SJ, Kang H. et. al. Diabetes. 2010;59:554-563.
13. Suchankova G, Nelson LE, Gerhart-Hines Z. et. al. Biochem Biophys Res Commun. 2009; 378:836-841.
14. Dasgupta B and Milbrandt J. Proc Natl Acad Sci U S A. 2007; 104: 7217-7222.
15. Park SJ, Ahmad, F, Philp A. et. al. Cell. 2012; 148:421-433.
16. Gerhart-Hines Z, Dominy E, Jr, Blattler SM. et. al. Mol Cell. 2011; 44:851-863.
17. Kuppusamy UR and Das NP. Biochem Pharmacol. 1992; 44:1307-1315.
18. Field SK. Clin Med Insights Circ Respir Pulm Med. 2011; 5:57-70.

Research Paper

Long-term calorie restriction, but not endurance exercise, lowers core body temperature in humans

Andreea Soare[1,2], Roberto Cangemi[1,3], Daniela Omodei[1,4], John O. Holloszy[1], and Luigi Fontana[1,5]

[1] Division of Geriatrics and Nutritional Sciences and Center for Human Nutrition, Washington University School of Medicine, St. Louis, Missouri, USA
[2] Department of Endocrinology and Diabetes, University Campus Bio-Medico, Rome, Italy
[3] Department of Experimental Medicine, University of Rome "La Sapienza," Italy
[4] CEINGE Biotecnologie Avanzate, Napoli, Italy
[5] Division of Nutrition and Aging, Istituto Superiore di Sanità, Rome, Italy

Key words: Calorie Restriction, endurance exercise, core body temperature, metabolism, thyroid hormone
Received: 3/21/11; Accepted: 3/26/11; Published: 3/27/11 **doi:** 10.18632/aging.100280
Corresponding author: Luigi Fontana, MD/PhD; **E-mail:** lfontana@dom.wustl.edu

Abstract: Reduction of body temperature has been proposed to contribute to the increased lifespan in calorie restricted animals and mice overexpressing the uncoupling protein-2 in hypocretin neurons. However, nothing is known regarding the long-term effects of calorie restriction (CR) with adequate nutrition on body temperature in humans. In this study, 24-hour core body temperature was measured every minute by using ingested telemetric capsules in 24 men and women (mean age 53.7±9.4 yrs) consuming a CR diet for an average of 6 years, 24 age- and sex-matched sedentary (WD) and 24 body fat-matched exercise-trained (EX) volunteers, who were eating Western diets. The CR and EX groups were significantly leaner than the WD group. Energy intake was lower in the CR group (1769±348 kcal/d) than in the WD (2302±668 kcal/d) and EX (2798±760 kcal/d) groups (P<0.0001). Mean 24-hour, day-time and night-time core body temperatures were all significantly lower in the CR group than in the WD and EX groups (P≤0.01). Long-term CR with adequate nutrition in lean and weight-stable healthy humans is associated with a sustained reduction in core body temperature, similar to that found in CR rodents and monkeys. This adaptation is likely due to CR itself, rather than to leanness, and may be involved in slowing the rate of aging.

INTRODUCTION

Calorie restriction (CR) without malnutrition increases lifespan and healthspan in rodents and non-human primates [1, 2]. Several studies have documented a lowering of core body temperature by CR in mice, rats and rhesus monkeys [3-6]. Interestingly, ad-libitum-fed transgenic mice overexpressing the uncoupling protein 2 in hypocretin neurons (Hcrt-UCP2) also have a lower core body temperature, and a 16% greater life expectancy than wild type animals, independently of caloric intake [7]. In the Baltimore Longitudinal Study of Aging (BLSA) men with a core body temperature below the median lived significantly l onger than men with body temperature above the median in the absence of CR [8].

In mammals body temperature is tightly regulated by hypothalamic neurons. The neurons located in the preoptic area integrate central and peripheral (e.g. environmental and metabolic) signals, and by modulating the autonomic and hormonal control of heat production and heat loss, maintain core body temperature nearly constant at different ambient temperatures [9]. It is well know that nutrition is a major regulator of energy production and body temperature [10]. To maintain body temperature higher than the ambient temperature, mammals utilize a

substantial amount of energy. Reducing core body temperature when food availability is scarce is an effective strategy to save energy. The metabolic and molecular adaptations that mediate a reduction in core body temperature may contribute to the anti-aging effects of CR.

No information on the effects of long-term CR without malnutrition on 24-h core body temperature in humans has been published. The purpose of the present study was to measure the core body temperature in healthy, weight-stable members of the Calorie Restriction Society, who have been consuming CR diets, containing adequate protein and micronutrients, for years. Mean 24-hour, day-time and night-time core body temperatures of the CR group were compared with values obtained in two comparison groups: 1) age- and sex-matched sedentary subjects consuming a Western diet (WD), and 2) age-, sex-, and body fat-matched endurance runners consuming a WD.

RESULTS

Body composition. Mean BMI values were different between the three groups (Table 1). Total body fat were similar in the CR and EX groups, and lower than in the WD group (Table 1).

Nutrient intake. The CR subjects consumed a variety of foods which supplied more than 100% of the Recommended Daily Intake (RDI) for all the essential nutrients. Foods with a high nutrient-to-energy ratio such as vegetables, fruits, nuts, dairy products, egg whites, wheat and soy proteins, and lean meat were consumed, whereas processed foods, rich in refined carbohydrates, free sugars and partially hydrogenated oils, were avoided. Energy intake was lower in the CR group (1769±348 kcal/d) than in either the EX group (2798±760 kcal/d) or WD group (2302±668 kcal/d) (P≤0.0001). Energy intake in the CR group was ~23% and ~37% below that of the WD and EX groups,

Table 1. Characteristics of the study subjects

	CR group (n=24)	EX group (n=24)	WD group (n=24)	P value
Age (yrs)	53.7±9.4	52.7±10	53.7±10.2	ns
Sex (M/F)	20/4	20/4	20/4	
Height (m)	1.74±0.1	1.75±0.1	1.79±0.1	ns
Weight (Kg)	58.2±5.9[1,2]	68.4±9.6[1]	78.7±15.5	0.0001
BMI (kg/m^2)	19.3±1.3[1,2]	22.2±2.1[1]	24.4±2.8	0.0001
Lean mass (kg)	47.9±6.7[3]	54.5±8.9	56.5±12.9	0.010
Total body fat (%)	13.0±5.3[1]	15.2±5.1[1]	21.8±6.8	0.0001
Body surface area (m^2)	1.70±0.11[1,4]	1.83±0.16[3]	1.97±0.25	0.0001

Values are means ± SD

[1,3] Significantly different from Western diet group: [1]P≤0.006; [3]P≤0.03

[2,4] Significantly different from the EX group: [2]P≤0.006; [4]P≤0.05

respectively. The percentage of total energy intake derived from protein, carbohydrate, fat and alcohol was 21%, 50%, 29% and 0.1%, respectively in the CR group, ~17%, 49%, 32% and 2% in the EX group, and ~16%, 46%, 34% and 4% in the WD group.

Core body temperature. Mean 24-h, day-time and night-time core body temperature were significantly lower in the CR group than in the EX or WD groups (Table 2). Mean 24-h core body temperature correlated linearly with % body fat (r = 0.298; p=0.01) (Figure 1), but not with age (r = 0.011; p=0.929), body weight (r = 0.066; p=0.581), lean body mass (r = 0.026; p=0.834), or body surface area (r = 0.004; p=0.976). The correlation between 24-h core body temperature and % body fat became stronger (r = 0.539; p=0.0001) when the EX participants were excluded from the analysis. In contrast, there was no correlation between 24-h core body temperature and % body fat when the CR individuals were excluded from the analysis (r = 0.056; p=0.706).

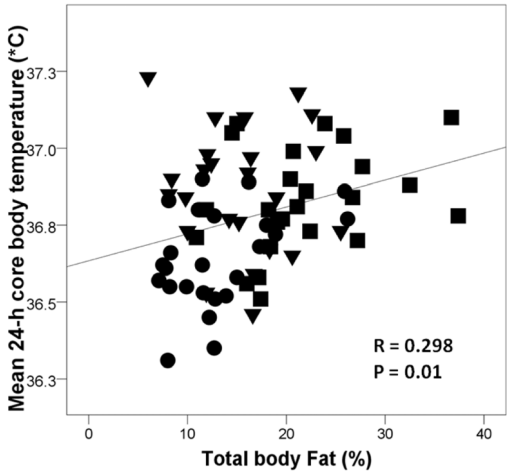

Figure 1. Relationship between mean 24-h core body temperature and % body fat measured by DEXA in the CR group (●), endurance runners (▼), and sedentary Western diet group (■). Pearson correlation was used to assess associations between continuous variables.

Table 2. Core body temperature

	CR group (n=24)	EX group (n=24)	WD group (n=24)	P value
Mean 24-h temperature	36.64±0.16[1,2]	36.86±0.20	36.83±0.17	0.0001
Day-time temperature (8 am to 10.30 pm)	36.78±0.23[3,4]	36.97±0.22	36.95±0.26	0.01
Night-time temperature (2 to 5 am)	36.35±0.17[1,4]	36.54±0.29	36.56±0.20	0.004

Values are means ± SD
[1,3] Significantly different from Western diet group: [1]P≤0.006; [3]P<0.05
[2,4] Significantly different from the EX group: [2]P≤0.0001; [4]P<0.02

DISCUSSION

In this study, mean 24-hour, day-time and night-time core body temperature were all significantly lower in the CR group than in the WD and EX groups. This reduction in 24-h core body temperature is consistent with findings in CR rodents and monkeys studies [3-6], and may contribute at least in part to the anti-aging effects of CR.

Although we found a significant correlation between % body fat and 24 h body temperature, it seems likely that the reduction in core body temperature induced by CR is largely related to CR itself, rather than changes in body composition. Mean 24-hours, day-time and night-time core body temperature were ~0.2 °C lower in the CR than in the EX group, even though percent body fat was similarly low in these groups. However, energy intake was ~37% lower in the CR than in the EX groups. It has been hypothesized that the CR-mediated reduction in body temperature relates to the induction of an energy conservation mechanism during CR [11]. In humans, monkeys and rodents long-term CR (but not endurance exercise) reduces the circulating levels of triiodothyronine [12-15] which controls energy homeostasis, body temperature, and cell respiration [16, 17]. The decrease in T3 could play a role in mediating the decrease in body temperature, and the reductions in T3 and temperature could influence the rate of aging by reducing metabolic rate and oxidative stress.

It is interesting in this context that body temperature is also reduced in the long-lived dwarf and growth hormone receptor KO mice [18, 19]. As in CR rodents, circulating levels of IGF-1, insulin and thyroid hormones are reduced in the dwarf and growth hormone receptor KO mice [20]. In contrast, in humans practicing long-term CR do not have lower circulating IGF-1 levels [21], suggesting that a down-regulation of the IGF-1 pathway is not involved in mediating the reduction in body temperature. The importance of a reduction of body temperature in modulating longevity has been also supported by the data obtained from the Hcrt-UCP2 mice and the Baltimore Longitudinal Study of Aging (BLSA). Overexpression of the uncoupling protein 2 in hypocretin neurons causes an elevation of hypothalamic temperature that leads to a 0.3-0.5°C reduction in core body temperature, and a significant increase in longevity, independently of caloric intake [7]. In the Baltimore Longitudinal Study of Aging (BLSA), men with core body temperatures below the median lived significantly longer than men with body temperatures above the median in the absence of CR [8].

Data from weight loss studies have shown that short-term (6 mos) CR significantly decreases core body temperature in overweight subjects that are actively losing weight [22]. However, in overweight men and women who had achieved a "stable" lower body weight using a low-calorie liquid diet, there was no change in core body temperature [22]. Consistently, no difference in core body temperature between weight-stable obese and normal-weight subjects has been detected, suggesting that in steady-state obese subjects maintain their core body temperature normal probably by increasing heat dissipation from peripheral regions [23, 24]. In contrast, in our study we have found that long-term CR, but not endurance exercise, chronically reduces core body temperature in weight-stable lean individuals. One possible explanation for the reduced 24-h core body temperature in the CR practitioners may be a protective physiological adaptation to save energy. This hypothesis is supported by the finding that the reduced core body temperature in the CR group is associated with lower circulating levels triiodothyronine, insulin, leptin and total testosterone, which are key nutrient-sensing metabolic/anabolic hormones [12, 25, 26]. The combination of decreased core body temperature and lower circulating levels of serum triiodothyronine, leptin, and anabolic hormones (i.e. testosterone, insulin) is a clear indication that these individuals are in a state of "sensing" severe energy restriction.

In conclusion, the results of this study provide evidence that long-term CR, with adequate intake micronutrients, in healthy, weight-stable individuals is associated with a reduction of mean 24-hour, day-time and night-time core body temperature, similar to that found in calorie-restricted rodents and monkeys.

METHODS

Study participants. Three groups (24 participants/group) were studied. One group (CR group) had been consuming a CR diet with adequate nutrients for a 6±3 years (range 3-15 yrs) and were members of the Calorie Restriction Society, who we asked to come to St. Louis to participate in this study. The CR Society members practice severe CR, because they believe that CR will markedly increase their disease-free longevity. Most of them live in North America, although there are also some CR Society members in England, Scandinavia and Japan. The second group (EX group), were endurance runners who had been running an average of 46 miles/wk (range 22-89 miles/wk) for 20±10 yrs (range 7-34 yrs), and were recruited from the St.Louis area. The EX group was matched on age, sex, and percent

body fat with the CR group. The third group (WD group) were healthy sedentary (regular exercise <1h/week) normal weight individuals, recruited from the St.Louis area, who were eating a WD. The WD group was matched on age and sex with the CR and EX groups. The characteristics of the study participants are shown in Table 1. None of the participants had evidence of chronic disease, smoked cigarettes, or were taking medications that could affect the outcome variables. All participants reported weight stability, defined as less than a 2-kg change in body weight in the preceding 6-mos. This study was approved by the Human Studies Committee of Washington University School of Medicine, and all participants gave informed consent before their participation.

Body composition. Total body fat mass and fat free mass were determined by dual-energy X-ray absorptiometry (DXA) (QDR 1000/w, Hologic, Waltham, MA).

Dietary assessment. Participants recorded all food and beverage intakes for 7 consecutive days. Food records were analysed by using the NDS-R program (version 4.03_31).

Core body temperature measurement. Twenty-four hour core body temperature was measured every minute using radiofrequency telemetered thermometers (CorTemp, HQ Inc, Palmetto, FL). Each thermometer pill contains a crystal quartz oscillator which transmits core temperature readings within ± 0.1 °C through a low frequency radio wave to an external receiver/data logger [27]. All the subjects tested were on a stable diet, at a stable weight, and without acute illness or recent hospitalization. The participants were instructed to refrain from exercise for at least 48 hours prior to CorTemp pill ingestion. Mean 24-hour, daytime (8 AM-10:30 PM), and nighttime (2 AM-5 AM) temperatures were computed.

Statistical analysis. One-way analysis of variance (ANOVA) was used to compare group variables, followed by Tukey post-hoc testing when indicated. One-way ANOVA with Games-Howell was performed for distributions where equal variances could not be assumed. Statistical significance was set at $P < 0.05$ for all tests. All data were analyzed by using SPSS software, version 13.0 (SPSS Inc, Chicago). All values are expressed as means±SD.

ACKNOWLEDGEMENTS

Funding/Support: Supported by NIH General Clinical Research Center Grant RR00036, P30DK056341 from the National Institute of Diabetes And Digestive And Kidney Diseases, Istituto Superiore di Sanità/National Institutes of Health Collaboration Program Grant, a grant from the Longer Life Foundation (an RGA/Washington University Partnership) and a donation from the Scott and Annie Appleby Charitable Trust.

Role of the Sponsor: The funding agency had no role in the analysis or interpretation of the data or in the decision to submit the report for publication.

CONFLICT OF INTERESTS STATEMENT

The authors of this manuscript have no conflict of interests to declare.

REFERENCES

1. Anderson RM, Shanmuganayagam D, Weindruch R. Caloric restriction and aging: studies in mice and monkeys. Toxicol Pathol. 2009; 37:47-51.

2. Fontana L, Coleman RJ, Holloszy J, Weindruch R. Calorie restriction in non-human and human primates. In HANDBOOK OF THE BIOLOGY OF AGING, SEVENTH EDITION (Elsevier Inc., London, UK), 2011; 447-461.

3. Duffy PH, Feuers RJ, Leakey JA, Nakamura K, Turturro A, Hart RW. Effect of chronic caloric restriction on physiological variables related to energy metabolism in the male Fischer 344 rat. Mech Ageing Dev. 1989; 48:117-133.

4. Duffy PH, Feuers RJ, Hart RW. Effect of chronic caloric restriction on the circadian regulation of physiological and behavioral variables in old male B6C3F1 mice. Chronobiol Int. 1990; 7:291-303.

5. Rikke BA, Yerg III JA, Battaglia ME, Nagy TR, Allison DB, Johnson TE. Strain variation in the response of body temperature to dietary restriction. Mechanisms of Ageing and Development 2003; 124:663-678.

6. Lane MA, Baer DJ, Rumpler WV, Weindruch R, Ingram DK, Tilmont EM, Cutler RG, Roth GS. Calorie restriction lowers body temperature in rhesus monkeys, consistent with postulated antiaging mechanisms in rodents. Proc. Natl. Acad. Sci U.S.A. 1996; 93:4159–4164.

7. Conti B, Sanchez-Alavez M, Winsky-Sommerer R, Morale MC, Lucero J, Brownell S, Fabre V, Huitron-Resendiz S, Henriksen S, Zorrilla EP, de Lecea L, Bartfai T. Transgenic mice with a reduced core body temperature have an increased life span. Science 2006; 314:825-828.

8. Roth GS, Lane MA, Ingram DK, Mattison JA, Elahi D, Tobin JD, Muller D, Metter EJ. Biomarkers of caloric restriction may predict longevity in humans. Science. 2002; 297:811.

9. Boulant JA. Role of the preoptic-anterior hypothalamus in thermoregulation and fever. Clin Infect Dis. 2000; 31 Suppl 5:S157-161.

10. Lowell BB, Spiegelman BM. Towards a molecular understanding of adaptive thermogenesis. Nature. 2000; 404:652-660.

11. Sacher, G. A. (1977) in Handbook of the Biology of Aging, eds. Finch, C. E. & Hayflick, L. (Van Nostrand Reinhold, New York), 1977; 582-638.

12. Fontana L, Klein S, Holloszy J.O, Premachandra B.N. Effect of Long-term Calorie Restriction with Adequate Protein and Micronutrients on Thyroid Hormones. Journal of Clinical Endocrinology & Metabolism 2006;91:3232-3235.

13. Roth GS, Handy AM, Mattison JA, Tilmont EM, Ingram DK, Lane MA. Effects of dietary caloric restriction and aging on thyroid hormones of rhesus monkeys. Horm Metab Res 2002; 34:378-382.

14. Herlihy JT, Stacy C, Bertrand HA. Long-term food restriction depresses serum thyroid hormone concentrations in the rat. Mech Ageing Dev 1990; 53:9-16.

15. Maglich JM, Watson J, McMillen PJ, Goodwin B, Willson TM, Moore JT. The nuclear receptor CAR is a regulator of thyroid hormone metabolism during caloric restriction. J Biol Chem 2004;279:19832-19838.

16. Braverman LE, Utiger RD. Werner & Ingbar's The Thyroid. A fundamental and clinical text, 9th edn. Lippincott, New York. 2004

17. Tapia G, Fernandez V, Varela P, Cornejo P, Guerrero J, Videla LA**.** Thyroid hormone-induced oxidative stress triggers nuclear factor-kappaB activation and cytokine gene expression in rat liver. Free Radic Biol Med 2003; 35:257-265.

18. Schonholz DH, Osborn CM. Temperature studies in dwarf mice. Anat Rec. 1949; 105:605.

19. Hauck SJ, Hunter WS, Danilovich N, Kopchick JJ, Bartke A. Reduced Levels of Thyroid Hormones, Insulin, and Glucose, and Lower Body Core Temperature in the Growth Hormone Receptor/Binding Protein Knockout Mouse. Exp Biol Med Vol. 2001; 226:552–558.

20. Bartke A. Growth hormone and aging: a challenging controversy. Clin Interv Aging. 2008; 3:659-665.

21. Fontana L, Weiss EP, Villareal DT, Klein S, Holloszy JO. Long-term effects of calorie or protein restriction on serum IGF-1 and IGFBP-3 concentration in humans. Aging Cell. 2008; 7:681-687.

22. Heilbronn, L. K., de Jonge, L., Frisard, M. I., DeLany, J. P., Larson-Meyer, D. E., Rood, J., Nguyen, T., Martin, C. K., Volaufova, J., Most, M. M., Greenway, F. L., Smith, S. R., Deutsch, W. A., Williamson, D. A. et al. Effect of 6-month calorie restriction on biomarkers of longevity, metabolic adaptation, and oxidative stress in overweight individuals: a randomized controlled trial. Journal of the American Medical Association 2006; 295:1539-1548.

23. Savastano DM, Gorbach AM, Eden HS, Brady SM, Reynolds JC, Yanovski JA. Adiposity and human regional body temperature. Am J Clin Nutr 2009; 90:1124–1131.

24. Jequier E, Gygax PH, Pittet P, Vannotti A. Increased thermal body insulation: relationship to the development of obesity. J Appl Physiol 1974; 36:674–678.

25. Fontana L, Klein S, Holloszy JO. Effects of long-term calorie restriction and endurance exercise on glucose tolerance, insulin action and adipokine production. Age 2010; 32:97-108.

26. Cangemi R, Friedmann AJ, Holloszy JO, Fontana L. Effects of long-term calorie restriction on serum sex hormones concentration in men. Aging Cell 2010; 9:236-242.

27. Byrne C, Lim CL. The ingestible telemetric body core temperature sensor: a review of validity and exercise applications. Br J Sports Med. 2007; 41:126-133.

Research Paper

Adult-onset, short-term dietary restriction reduces cell senescence in mice

Chunfang Wang[1], Mandy Maddick[1], Satomi Miwa[1], Diana Jurk[1], Rafal Czapiewski[2], Gabriele Saretzki[2], Sabine A.S. Langie[3], Roger W.L. Godschalk[4], Kerry Cameron[1], Thomas von Zglinicki[1]

[1] Centre for Integrated Systems Biology of Ageing and Nutrition, Institute for Ageing and Health, Newcastle University, Newcastle Upon Tyne, UK
[2] Crucible Laboratory, Institute for Ageing and Health, Newcastle University, Newcastle Upon Tyne, UK
[3] Human Nutrition Research Centre and Centre for Brain Ageing and Vitality, Institute for Ageing and Health, Newcastle University, Newcastle Upon Tyne, UK
[4] Nutrition and Toxicology Research Institute Maastricht (NUTRIM), Department of Health Risk Analysis and Toxicology, Maastricht University, Netherlands

Key words: Dietary restriction, caloric restriction, mice, senescence, telomeres, ageing
Received: 08/18/10; accepted: 09/09/10; published on line: 09/11/10 **doi:** 10.18632/aging.100196
Corresponding author: Thomas von Zglinicki, PhD; **E-mail:** t.vonzglinicki@ncl.ac.uk

Abstract: Dietary restriction (DR) extends the lifespan of a wide variety of species and reduces the incidence of major age-related diseases. Cell senescence has been proposed as one causal mechanism for tissue and organism ageing. We show for the first time that adult-onset, short-term DR reduced frequencies of senescent cells in the small intestinal epithelium and liver of mice, which are tissues known to accumulate increased numbers of senescent cells with advancing age. This reduction was associated with improved telomere maintenance without increased telomerase activity. We also found a decrease in cumulative oxidative stress markers in the same compartments despite absence of significant changes in steady-state oxidative stress markers at the whole tissue level. The data suggest the possibility that reduction of cell senescence may be a primary consequence of DR which in turn may explain known effects of DR such as improved mitochondrial function and reduced production of reactive oxygen species.

INTRODUCTION

Dietary restriction (DR), whereby total caloric intake is reduced but adequate nutrition is maintained, results in an extension of lifespan. Additionally, DR has been shown to delay the onset and severity of cancer and other diseases associated with ageing [1]. The DR response has been remarkably robust in a wide range of animal species, although both evolutionary models and genetic experiments question its universality in different inbred strains of mice and, importantly, in humans [2,3]. The molecular and cellular mechanisms underlying the response to DR have been intensely examined. It has been proposed that DR prolonged lifespan for example by attenuating oxidative damage, reducing production of reactive oxygen species (ROS), increasing DNA repair capacity, altering the growth hormone/IGF-1 axis, decreasing signaling through the mTOR substrate S6K1 or improving hormesis [4-8]. However, we are still far from a mechanistic and integrative understanding of the DR response [1,9].

This is even more true for the response to adult-onset, short-term DR. While the effect on lifespan becomes less robust if DR is implemented in older animals [10,11], there are still strong beneficial effects on cancer incidence [11-15], immune response [14,16] and cognitive function [17]. Preliminary data from non-human primates [18] and clinical trials [19] have suggested that late onset DR could have at least some beneficial effects in humans.

Recently, evidence is mounting that cellular senescence, which was originally described as the permanent loss of replicative capacity in human fibroblasts *in vitro* [20], is a complex phenotype, possibly causally contributing to aging *in vivo* [21-23]. Senescent cells are found with increasing frequency in many tissues of aging rodents, primates and humans [24-28]. High frequencies of senescent cells have been associated with age-related diseases like osteoarthritis and atherosclerosis [29,30] and were also found in mouse models of accelerated aging [31-34]. Senescent cells are not simply incompetent of proliferating; they display major alterations to their gene expression profiles [35] and secrete bioactive molecules including matrix-degrading enzymes [36], inflammatory cytokines [21,22,37] and ROS [23]. Thus, cell senescence may well be an important driver for the aging process *in vivo* [38,39].

If this concept were correct, one would hypothesize that a reduction of cell senescence might be part, and potentially a causal part, of the beneficial action of DR. This would be interesting because less senescent cells could explain the anti-inflammatory and anti-oxidative action of DR. However, there are few data to support such a hypothesis. There is good evidence that both life-long and adult-onset DR limit T cell senescence in mice and primates [14,40-42], at least partially by maintaining sensitivity to stress-induced apoptosis [43]. However, T cell senescence might be very different from senescence of cells in solid tissues. For instance, while a DNA damage response is the major driver for growth arrest [44] and phenotypic changes [23] in fibroblast senescence, its role in T cell senescence is less well established. Moreover, sensitivity to apoptotic stimuli is generally high in senescent T cells, but decreases during senescence in fibroblasts and other solid tissue cells.

There is very little data available on the impact of DR on cell senescence in solid mammalian tissues. Early data [45,46] showed reduced proliferative activity in various tissues of young mice under DR but improved maintenance of replicative activity and capacity in old mice under life-long DR, which might be due to a decreased accumulation of senescent cells. Krishnamurthy et al. [26] showed that DR reduced staining for senescence-associated β-Galactosidase (sen-β-Gal) and the expression of $p16^{INK4a}$ and $p19^{Arf}$ in the kidney. However, the specificity and sensitivity of sen-β-Gal as a marker for senescent cells *in vivo* has been repeatedly questioned [47,48]. Moreover, $p16^{INK4a}$ and $p19^{Arf}$ expression was similarly changed in postmitotic tissues like brain cortex and heart, suggesting that expression from the INK4A locus might be a better indicator for aging than for cell senescence. Further indirect evidence for decreased cell senescence under DR came from a study showing reduced levels of IGFBP3, a major secretion product of senescent epithelial and mesenchymal cells, following long-term DR [49]. However, while frequencies of senescent cells increased during aging in skin of rhesus monkeys [50] and baboons [25], no decrease of sen-β-Gal-positive epithelial cells and no increase in proliferation-competent skin fibroblasts was found after 9-12 years of DR in rhesus monkeys [50]. To our knowledge, there is no data reporting an effect of shorter term DR on cell senescence in solid tissues.

We tested the impact of short-term (3 months), adult-onset DR on cellular senescence in mice. We concentrated on the small intestine, a highly proliferative organ, and on liver with a slow cell turnover under non-pathological conditions. We had shown before that senescent cell frequencies in these organs increase significantly during normal aging in mice [28]. Using sensitive and specific markers for senescent cells [51,52], we found that short-term, adult-onset DR significantly reduced the frequencies of senescent liver hepatocytes, especially in the centrilobular area, and of senescent intestinal enterocytes in the transient amplifying zone. DR also improved telomere maintenance in liver and intestine and reduced cumulative oxidative stress markers in the same tissue compartments. We propose that reduction of cell senescence might be a primary effect of DR which may explain improved mitochondrial function and reduced ROS production.

RESULTS

Adult-onset, short-term DR reduced the frequencies of senescent cells in small intestine and liver

Male C57/BL mice were subjected to three months of DR by average 26% of food restriction starting at 14 months of age. The study cohort is characterized in supplementary Table S1. We focused on intestinal crypt enterocytes and liver hepatocytes because frequencies of senescent cells in these tissue compartments increased with age or as result of telomere dysfunction in Terc-/- mice [23,28].

We first measured the frequency of intestinal enterocytes showing an active DNA damage response as characterized by nuclear positivity for the DNA damage marker, γ-H2A.X. As we have shown before, there were few γ-H2A.X-positive enterocytes within villi, instead, positive cells centered around the transient amplifying zone in crypts [28]. DR significantly reduced the frequencies of γ-H2A.X-positive intestinal crypt enterocytes (Figure 1A). We compared frequencies of γ-H2A.X-positive and sen-β-Gal-positive

crypt enterocytes, measured on adjacent frozen sections from five AL and five DR mice (Figure 1B). The significant reduction of positive cells by DR was confirmed for both markers, and they were significantly correlated (r^2=0.7080). γ-H2A.X staining on its own may overestimate frequencies of senescent cells, especially in tissue compartments with high proliferative activity such as gut because an active DNA damage response can also be initiated by replication stress in dividing cells. Accordingly, we showed recently that a combination of strong positivity for γ-H2A.X with absence of a proliferation marker results in quantitatively correct estimates of senescent cell frequencies *in vitro* and *in vivo* [52]. Double staining for γ-H2A.X and PCNA in the small intestine (Figure 1C) showed that DR reduced also the frequencies of PCNA positive crypt enterocytes as reported previously [45]. Frequencies of γ-H2A.X positive/PCNA negative intestinal crypt enterocytes in 17 month old mice were 20.0±0.9% under AL conditions and 14.0±1.9% after 3 months DR (Figure 1C). This difference was significant (p=0.02).

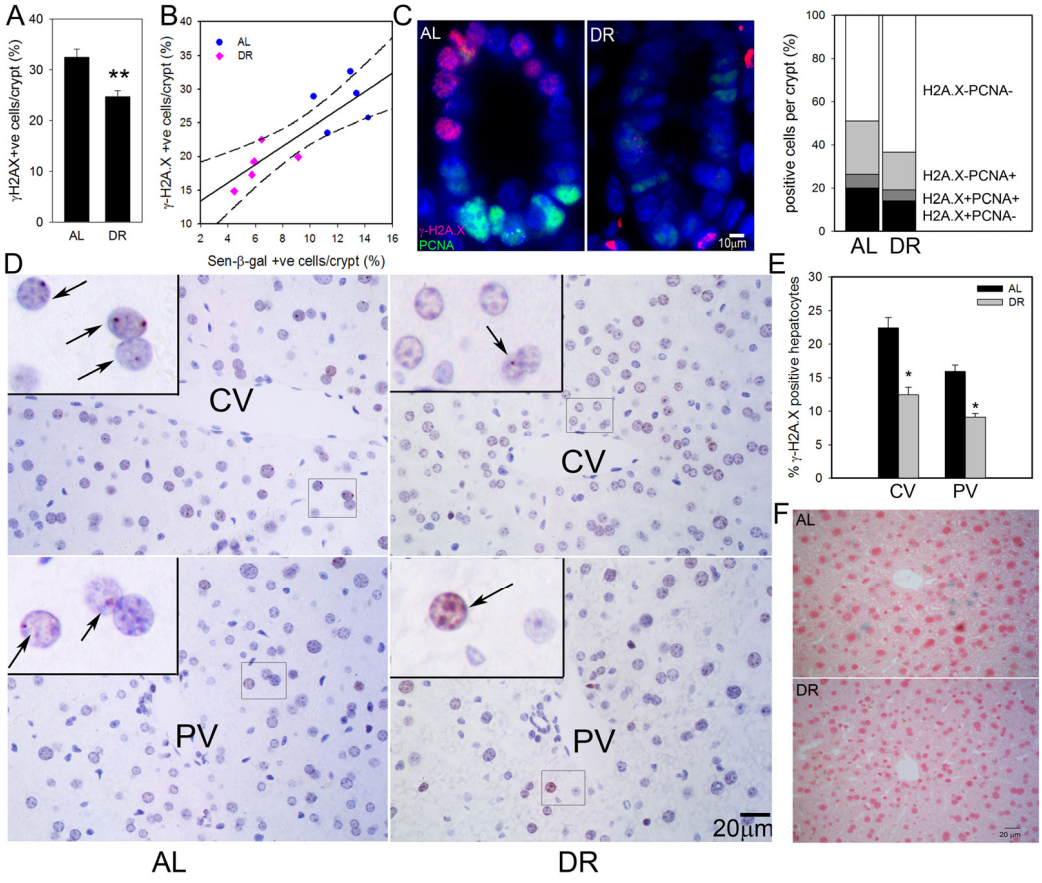

Figure 1. DR reduced frequencies of senescent hepatocytes and intestinal crypt enterocytes. (**A**) Frequencies of γ-H2A.X positive enterocytes per crypt, immunohistochemistry on paraffin sections. ** p<0.005. (**B**) Correlation between sen-β-Gal and γ-H2A.X positive enterocytes (p=0.002). Data points are means per animal (DR: pink; Al: blue). Linear regression (solid line) and 95% confidence intervals (dashed lines) are given. (**C**) Representative images (left) and quantitative evaluation (right) of PCNA and γ-H2A.X double immunofluorescence of intestinal crypts from AL and DR mice. Blue: DAPI; red: γ-H2A.X; green: PCNA. (**D**) Representative images of γ-H2A.X immunohistochemistry in livers from AL (left) and DR (right) mice. Examples of centrilobular (top) and periportal (bottom) areas are shown. CV: central vein; PV: portal vein. Boxed areas are shown at higher magnification. Arrows indicate nuclei containing γ-H2A.X foci (red). (**E**) Quantification of γ-H2A.X positive hepatocytes. * p<0.05. (F) Representative images for sen-β-Gal activity. Pink: nuclei; blue: cytoplasmic sen-β-Gal staining. All data are from 5 animals/group, mean±S.E.M.

In liver, frequencies of γ-H2A.X positive hepatocytes were higher in centrilobular than periportal areas (Figure1D) as shown previously [28]. Importantly, the frequencies of γ-H2A.X positive hepatocytes were significantly reduced following 3 months DR by 6.5 ± 1.8% in the centrilobular area and by 3.3 ± 1.2% in the periportal area (Figure 1E). Results were qualitatively confirmed by sen-β-Gal staining on cryosections (Figure 1F). The frequency of PCNA- or Ki67-positive cells in hepatocytes was less than 1% (data not shown). Therefore, γ-H2A.X positivity on its own is regarded as a good estimate of senescent hepatocytes in liver.

Adult-onset, short-term DR improved telomere maintenance in small intestine and liver

Despite the presence of active telomerase, telomeres shorten with age in various tissues of laboratory mice [28,53]. However, even in very old mice, telomeres are much longer than in humans and aging in mice did not measurably increase the degree of co-localisation of DNA damage foci with telomeres [28]. This suggests that telomere shortening may only be a minor contributor to cell senescence in aging wild-type mice. Here, we measured telomere length by quantitative FISH (Q-FISH) in intestinal enterocytes and liver hepatocytes (Figure 2A, B). Following 3 months of DR, the average telomere length per crypt enterocyte nucleus was significantly higher than in AL fed mice (Figure 2A). The effect of DR on hepatocyte telomere length was smaller than in the intestine (Figure 2B), possibly because of the lower rate of proliferation. However, the difference between DR and AL was still significant in the centrilobular areas. Telomerase activity as measured by TRAP in whole liver and intestinal mucosa homogenates was not significantly changed by DR (Figure 2C). If anything, it tended to decrease under DR, possibly due to the anti-proliferative effect of DR, suggesting that other factors than telomerase must be responsible for the improved telomere maintenance under DR. The most probable of these is reduction of oxidative damage to telomeres [54].

Adult-onset, short-term DR reduced some oxidative damage markers in small intestine and liver

Senescent cells are a major source of ROS because mitochondrial dysfunction and, possibly, other ROS-producing mechanisms are part of the senescent phenotype [23,55-57]. Long-term DR is well known to reduce oxidative stress and mitochondrial ROS production [8,58]. We measured several markers of oxidative damage in small intestine and liver to test whether adult-onset, short-term DR impacts on oxidative stress in the same tissues as it reduced cell senescence.

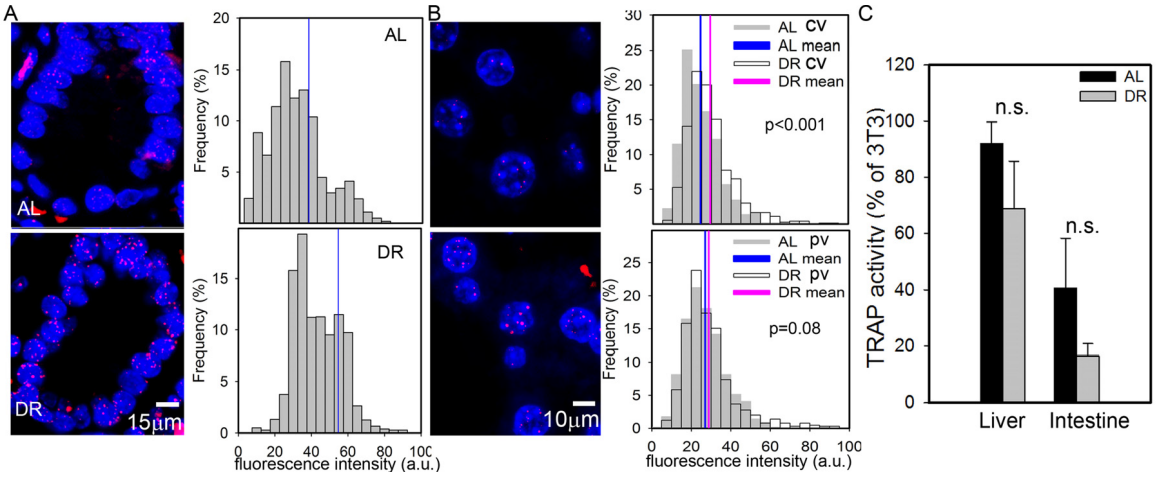

Figure 2. DR improves telomere maintenance. (**A**) Representative Q-FISH images (left panels, red: telomeres, blue: nuclei) and distribution of enterocyte telomere fluorescence intensity per nucleus (right panels, n≥2230 nuclei, 5 animals) in intestinal crypts. Mean nuclear telomere fluorescence intensity is indicated by blue vertical lines. p<0.001, Mann-Whitney rank sum test. (**B**) Representative Q-FISH images (left panels, red: telomeres, blue: nuclei) and distribution of hepatocyte telomere fluorescence intensity in centrilobular (CV, top, n≥560 nuclei) and periportal (PV, bottom, n≥650 nuclei) in liver areas. Mean fluorescence intensities are indicated for AL (blue) and DR (pink). P-values for AL vs DR were calculated by Mann-Whitney rank sum test. (**C**) Telomerase catalytic activity (% of TRAP activity in 3T3 cells) in whole liver (left, n=4) and intestinal mucosa (right, n=5) homogenates. Data are mean±S.E.M. n.s.: not significant (T-test).

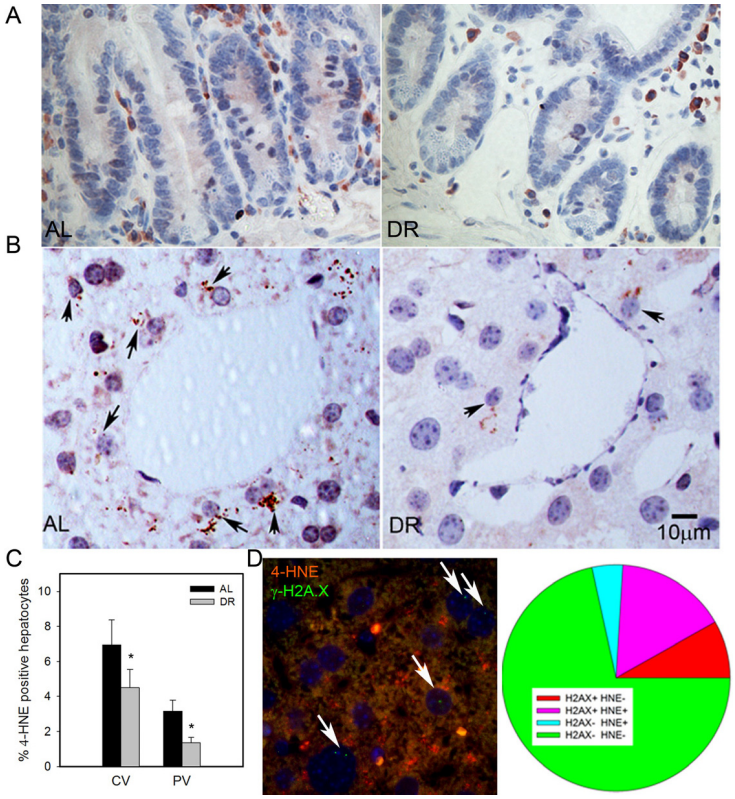

Figure 3. DR decreased lipid peroxidation in liver. (**A**) Representative 4-HNE immunohistochemistry in small intestine from AL (left) and DR(right) mice. Brown: 4-HNE staining; blue: nuclei. (**B**) Representative 4-HNE images from centrilobular areas in liver. Brown: 4-HNE, Blue: nuclei. Arrows indicate examples of positive cells. (**C**) Frequencies of 4-HNE-positive hepatocytes in periportal and centrilobular areas of liver. Data are mean±S.E.M. * $p<0.05$, n=5 animals/group. (**D**) Co-localisation of γ-H2A.X (green) and 4-HNE (red) in AL liver. Representative image, double immunofluorescence, cryosection. Cells with nuclei (DAPI, blue) positive for γ-H2A.X are marked by arrows. Cells were scored as either single positive (H2AX+ HNE – or H2A.X- HNE +), double positive (H2A.X+ HNE+) or double negative (H2A.X- HNE -). Data are from four animals from the AL group.

4-HNE is a major end product of lipid peroxidation and has been shown to accumulate in tissues with age [59]. We found few 4-HNE positive cells in intestinal crypts, and almost all were located in the lamina propria (Figure 3A). Confirming earlier results [28], HNE-positive hepatocytes were more frequent in centrilobular than in periportal areas. Importantly, frequencies of HNE-positive hepatocytes decreased under DR in both areas (Figure 3B, C $p<0.05$). To directly see whether there was an association between cell senescence and oxidative stress in liver hepatocytes, we performed a double staining for γ-H2A.X and 4-HNE (Figure 3D). Quantitative evaluation showed that the majority of senescent hepatocytes (as measured by γ-H2A.X) were also positive for 4-HNE and, vice versa, about three quarters of 4-HNE-positive hepatocytes were probably senescent (Figure 3D), thus confirming a cell-specific association between senescence and a marker of oxidative damage.

Broad-band autofluorescence originates mainly from oxidised and cross-linked cell components, like advanced glycation end products (AGEs) and lipofuscin and is thus regarded as a good cumulative marker for oxidative damage [23,60-62]. Short-term DR significantly reduced the intensity of broad-band autofluorescence from intestinal crypt enterocytes (Figure 4A) and in centrilobular areas of the liver (Figure 4B). The reduction of autofluorescence in the periportal areas of the liver by DR was not significant (Figure 4B), in accordance with this compartment showing the least reduction of senescent cells.

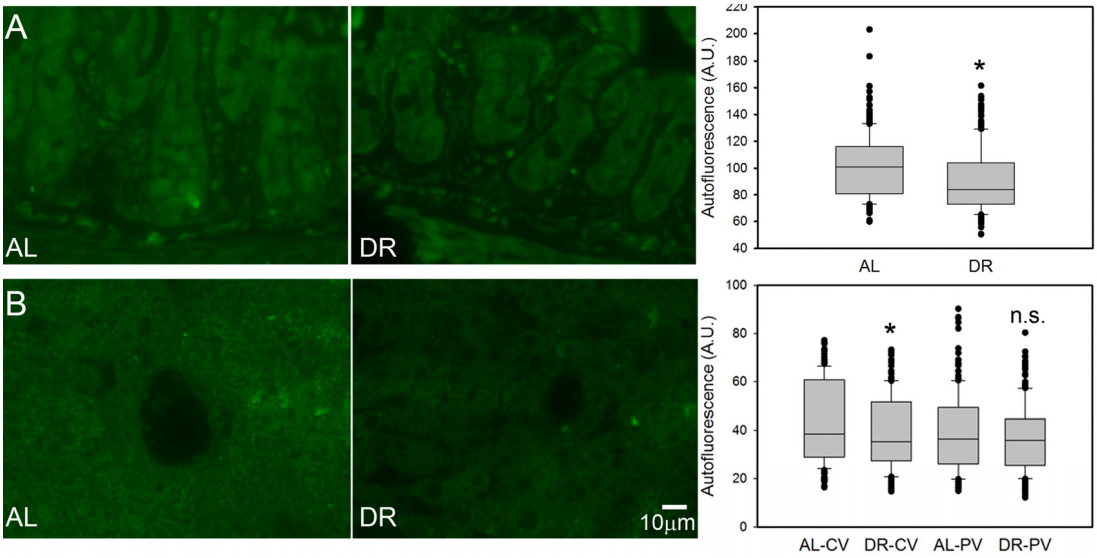

Figure 4. DR decreased the intensity of broad-band autofluorescence. (**A**) Representative autofluorescence images (left) and quantitative data (right) in small intestinal crypts under AL (left) and DR (right). (**B**) Representative autofluorescence images from centrilobular areas in liver (AL left, DR right) and quantitative data in periportal and centrilobular areas. All data are mean±S.E.M from 5 animals/group. *p<0.05; n.s. not significant (T-test).

8-oxodG (a marker for oxidative DNA damage), nitrotyrosine content (a marker for oxidative protein damage) and H_2O_2 release rate from tissue homogenate are indicative of steady-state levels of oxidative stress/ oxidative damage. These markers were measured in whole liver homogenates. None of them were significantly different between AL and DR mice (Figure 5). Similarly, DR did not change 8-oxodG levels in homogenates of the intestinal mucosa (data not shown).

DISCUSSION

This is the first study to show that short-term DR reduced frequencies of senescent cells in solid tissues. It is important to note that the magnitude of the reductions, amounting to between 3.3 and 6.5% depending on the tissue compartment, is very substantial given the short duration of the treatment. Frequencies of senescent cells increase with age in intestinal crypts and liver at rates below 0.5% per month [28], indicating that 3 months DR probably reduced levels of senescent cells beyond that at the start of the treatment. Available data indicate that senescent hepatocytes are turned over slowly in liver [63,64]. Turnover rates of senescent enterocytes in intestinal crypts are unknown. DR could block the induction of senescent cells, increase the rate of their turnover, or both.

Cell senescence *in vitro* is associated with a 3- to 5-fold increase in cellular ROS levels [23,55-57]. Various signaling pathways and feedback loops connect DNA damage response and checkpoint proteins that are activated early and permanently in senescence, notably p21, p16 and Rb, with ROS generation via mitochondrial dysfunction and, potentially, NADPHoxidase activation [23,56,65]. As senescent cells were less in DR, we therefore expected to see lower levels of oxidative stress markers under DR especially in those tissue compartments which showed large reductions of senescent cells. This was indeed the case: autofluorescence was significantly reduced in the intestinal crypts and the centrilobular areas of the liver, but not around the portal vein. While 4-HNE could not be measured in enterocytes, it was more strongly reduced around the central vein than in the periportal areas of the liver. Without increases in telomerase activity, telomere length was better maintained under DR in the crypt enterocytes and in the centrilobular, but not periportal, areas of the liver. Autofluorescence, 4-HNE and telomere maintenance in the absence of changes in telomerase activity are all regarded as cumulative markers of oxidative damage [54,59,62]. In contrast, we did not find any significant effect of DR on the markers of oxidative damage measured in whole tissue homogenates. This was not surprising because 8-oxodG and H_2O_2 release as acute parameters are less sensitive

than the cumulative markers mentioned above. Moreover, an average decrease in the number of senescent cells by about 5% in liver would result in less than 10% decrease in total ROS, which is within the experimental error for these measurements. As there are very few senescent cells in villi, the expected impact of the observed decreases in senescent cell frequencies in the crypts on ROS in the whole intestinal mucosa would be even lower.

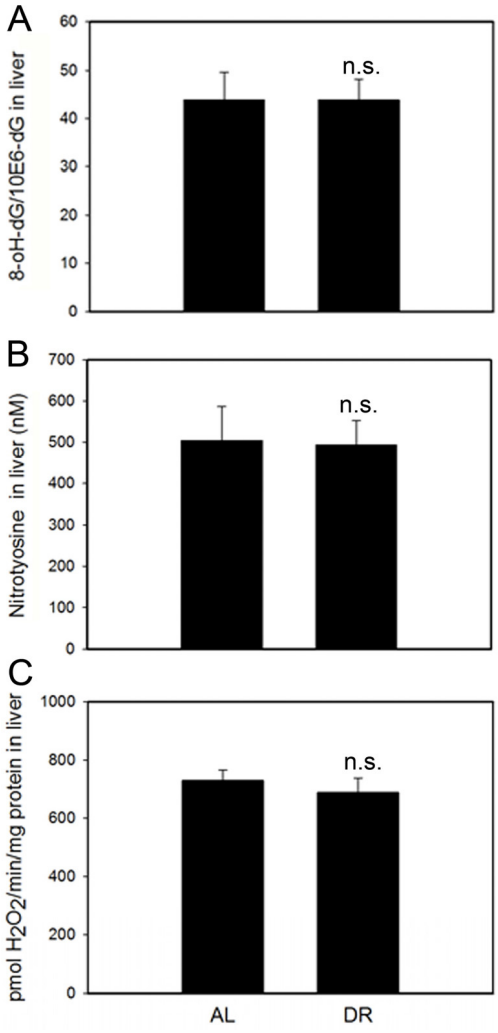

Figure 5. DR does not change oxidative damage markers measured in whole liver homogenates. (**A**) 8-oxodG levels in liver homogenates from AL and DR mice measured by HPLC with electrochemical detection. n=9 animals/group. (**B**) Nitrotyrosine levels in liver homogenates from AL and DR mice measured by ELISA; n=6 animals/ group. (C) Steady state hydrogen peroxide release from liver homogenates from AL and DR mice measured by Amplex Red fluorimetry; n=12 animals/ group. All data are mean ±S.E.M.; n.s.: not significant (T-test).

Taken together, our data suggest that at least some of the beneficial effects of DR that have been repeatedly described in the literature, such as improved mitochondrial coupling and reduced ROS release [8,58], could be quantitatively explained as an indirect effect, mediated via reduction of senescent cells. Mitochondria are dysfunctional (i.e. produce more superoxide despite lower membrane potential and induce a retrograde response) not only in senescent human fibroblasts *in vitro* [57]. The same changes were triggered by telomere dysfunction in mouse cells and tissues including the intestinal crypt epithelium. In this system, as in human fibroblasts, mitochondrial dysfunction was dependent on signaling through p21, the central mediator of cell senescence [23,32].

Our results lead to the question of how DR could impact directly on cell senescence. One interesting candidate may be signaling through the mTOR-S6K1 pathway. DR reduced phosphorylation and activity of Akt1, mTOR and its downstream targets S6K1 and 4E-BP1 [66]. Knockout of S6K1 mimics the effects of DR [67]. Importantly, S6K1 is intimately involved in the regulation of cell senescence. S6K1 phosphorylation and activity is altered in replicative senescence [68]. mTOR activation induced senescence in human fibroblasts [69] and the activation state of the mTOR pathway has been shown to be relevant for the decision between reversible arrest and cell senescence in models of DNA damage-independent senescence [70]. Wnt1-driven activation of the mTOR pathway caused epithelial stem cell senescence and loss after a short hyperproliferative period [71]. A mechanistic clue comes from a recent paper showing that activated S6K1 binds more tightly to Mdm2, inhibiting Mdm2-mediated p53 ubiquitination and thus stabilizing p53-dependent DNA damage signaling [72]. Accordingly, suppression of mTOR-S6K1 signaling as occurring under DR would lead to Mdm2 nuclear transduction, activate p53 degradation and reduce thus signaling towards apoptosis and/or senescence.

In conclusion, the data are compatible with the idea that reduction of cellular senescence is a primary effect of DR, possibly mediated via suppression of signaling through mTOR-S6K1, and that this reduction in turn might be sufficient to account for the improvement of mitochondrial function and reduction of ROS production that are known to occur under DR.

METHODS

Animals. From a group of 90 male C57/BL mice aged 14.2 ± 1.2 months, 45 animals were subjected to DR, while the other 45 animals, matched for body mass, food intake and age, served as ad libitum-fed (AL)

controls. The experiment lasted for 3 months with an average food restriction of 26%. All mice were sacrificed at the end of the experiment. Five mice per group were perfused by whole animal fixation with 4% paraformaldeyde followed by dissection. Tissues were paraffin-embedded and 5μm sections were prepared from small intestine and liver. Tissues from five additional mice per group were frozen in OTC for cryosectioning. Tissues from further animals were frozen in liquid N_2. The intestinal mucosa was stripped from the muscle layer before freezing. Further details of the experimental protocol can be found as supplementary material, Tab. S1. The project was approved by the Faculty of Medical Sciences Ethical Review Committee, Newcastle University.

Histochemistry, immunofluorescence, telomere Q-FISH and telomerase activity. Sen-β-Gal histochemistry, immunohistochemistry and telomere Q-FISH were performed as described [28]. The antibodies used and the dilution factors were: anti-γ-H2A.X (#9718, Cell Signalling, Herts, UK, 1:250), anti-PCNA (#ab27Abcam, Cambridge, UK, 1:1,000) and anti-4-HNE (#MHH-030n, Japan Institute for the Control of Aging, Japan, 1:500). Incubation with all primary antibodies was overnight at 4°C.

For double immunofluorescence, blocked sections were incubated with anti-PCNA and anti- γ-H2A.X antibodies together in PBS at 4°C overnight and incubated with Alexa-555-conjugated goat anti-rabbit antibody and biotinylated anti-mouse antibody for 45 min in PBS. Subsequently, tissue sections were washed 3 times and incubated with 0.2% Fluorescein Avidin-DCS in PBS for 30min. Images were taken in a Leica DM5500B microscope with 40x objective. 30-40 crypts were scored for each animal.

Telomerase activity was measured using the TeloTAGGG Telomerase PCR ELISA kit (Roche) according to the manufacturer's recommendations.

Autofluorescence. Autofluorescence was measured on unstained, non-deparaffinized tissue sections using a Leica DM5500B microscope. The sample was excited at 458nm and fluorescence emission captured above 475nm.

8-oxodG. The base oxidation product 8-oxo-7,8-dihydro-2'-deoxyguanosine (8-oxodG) was detected by HPLC with electrochemical detection (ECD). Ground frozen tissues (30-100 mg, n=4-9 per group) were thawed and genomic DNA was obtained using standard phenol extraction [73]. The DNA extraction procedure was optimized to minimize artificial induction of 8-oxodG, by using radical-free phenol, minimizing exposure to oxygen and by addition of 1 mM deferoxamine mesylate and 20 mM TEMPO (2,2,6,6-tetramethylpiperidine-N-oxyl), according to the European Standards Committee on Oxidative DNA Damage [74]. HPLC-ECD was based on a method described earlier [75]. Briefly, 30 μg DNA was digested to deoxyribonucleosides by treatment with nuclease P1 [0.02 U/μl] for 90min at 37 °C and subsequently with alkaline phosphatase [0.014 U/μl]. for 45min at 37 °C. The digest was then injected into a Gynkotek 480 isocratic pump (Gynkotek, Bremen, Germany) coupled with a Midas injector (Spark Holland, Hendrik Ido Ambacht, the Netherlands) and connected to an Supelcosil™ LC-18S column (250 X 4.6 mm) (Supelco Park, Bellefonte, PA) and an electrochemical detector (Antec, Leiden, the Netherlands). The mobile phase consisted of 10% aqueous methanol containing 94 mM KH_2PO_4, 13 mM K_2HPO_4, 26 mM NaCl and 0.5 mM EDTA. Elution was performed at a flow rate of 1.0 ml/min with a lower absolute detection limit of 40 fmol for 8-oxo-dG, or 1.5 residues/10^6 2'-deoxyguanosine (dG). dG was simultaneously monitored at 260 nm.

Nitrotyrosine measurement. Ground frozen tissues (8-32mg, n=5 per group) were thawed and total protein was extracted using Microplate BCA™ protein assay kit (Thermo Scientific, UK). Nitrotyrosine was detected by oxiSelect™ Nitrotyrosine ELISA kit (Cell Biolabs, INC, UK) according to the protocol provided by the manufacturer.

H_2O_2 release. Ground frozen tissue was homogenized in PBS and used immediately for the assay. The rate of hydrogen peroxide release was monitored fluorometrically as resorufin formation due to oxidation of Amplex Red (10-acetyl-3,7-dihydroxyphenoxazine, purchased from Invitrogen, 50μM) in the presence of horseradish peroxidase (2U/ml), at an excitation 544 nm and an emission 590 nm using a FLUOstar Omega (BMG Labtech). Superoxide dismutase (75U/ml) was included in the assay buffer. The slope was converted into the rate of hydrogen peroxide release with a standard curve. Protein concentration was measured using Bio-Rad DC protein assay kit.

ACKNOWLEDGMENTS

We thank Adele Kitching and Julie Wallace for technical support with the mice; Dr Glyn Nelson for his technical support in the nitrotyrosine measurement and Lou M. Maas for his technical support in the 8-oxodG analysis. This work was funded by BBSRC and EPSRC (CISBAN). Part of the work was subsidized by the Centre for Brain Ageing and Vitality, which is funded

through the Lifelong Health and Wellbeing cross council initiative by the MRC, BBSRC, EPSRC and ESRC.

CONFLICT OF INTERESTS STATEMENT

The authors of this manuscript have no conflict of interests to declare.

REFERENCE

1. Masoro EJ. Dietary restriction: current status. Aging (Milano) 2001; 13: 261-262

2. Liao CY, Rikke BA, Johnson TE, Diaz V, Nelson JF. Genetic variation in the murine lifespan response to dietary restriction: from life extension to life shortening. Aging Cell 2010; 9:92-95

3. Shanley DP, Kirkwood TB. Caloric restriction does not enhance longevity in all species and is unlikely to do so in humans. Biogerontology 2006; 7: 165-168

4. Yu BP. Aging and oxidative stress: modulation by dietary restriction. Free Radic Biol Med 1996; 21: 651-668

5. Sohal RS, Weindruch R. Oxidative stress, caloric restriction, and aging. Science 1996; 273: 59-63

6. Zainal TA, Oberley TD, Allison DB, Szweda LI, Weindruch R. Caloric restriction of rhesus monkeys lowers oxidative damage in skeletal muscle. FASEB J 2000; 14: 1825-1836

7. Guo ZM, Yang H, Hamilton ML, Van Remmen H, Richardson A. Effects of age and food restriction on oxidative DNA damage and antioxidant enzyme activities in the mouse aorta. Mech Ageing Dev 2001; 122: 1771-1786

8. Gredilla R, Barja G. Minireview: the role of oxidative stress in relation to caloric restriction and longevity. Endocrinology 2005; 146: 3713-3717

9. Anderson RM, Weindruch R. Metabolic reprogramming in dietary restriction. Interdiscip Top Gerontol 2007; 35: 18-38

10. Lipman RD, Smith DE, Bronson RT, Blumberg J. Is late-life caloric restriction beneficial? Aging (Milano) 1995; 7: 136-139

11. Spindler SR. Rapid and reversible induction of the longevity, anticancer and genomic effects of caloric restriction. Mech Ageing Dev 2005; 126: 960-966

12. Pugh TD, Oberley TD, Weindruch R. Dietary intervention at middle age: caloric restriction but not dehydroepiandrosterone sulfate increases lifespan and lifetime cancer incidence in mice. Cancer Res 1999; 59: 1642-1648

13. Volk MJ, Pugh TD, Kim M, Frith CH, Daynes RA, Ershler WB, Weindruch R. Dietary restriction from middle age attenuates age-associated lymphoma development and interleukin 6 dysregulation in C57BL/6 mice. Cancer Res 1994; 54: 3054-3061

14. Weindruch R, Walford RL. Dietary restriction in mice beginning at 1 year of age: effect on life-span and spontaneous cancer incidence. Science 1982; 215: 1415-1418

15. Dhahbi JM, Kim HJ, Mote PL, Beaver RJ, Spindler SR. Temporal linkage between the phenotypic and genomic responses to caloric restriction. Proc Natl Acad Sci U S A 2004; 101: 5524-5529

16. Kubo C, Johnson BC, Day NK, Good RA. Calorie source, calorie restriction, immunity and aging of (NZB/NZW)F1 mice. J Nutr 1984; 114: 1884-1899

17. Means LW, Higgins JL, Fernandez TJ. Mid-life onset of dietary restriction extends life and prolongs cognitive functioning. Physiol Behav 1993; 54: 503-508

18. Anderson RM, Shanmuganayagam D, Weindruch R. Caloric restriction and aging: studies in mice and monkeys. Toxicol Pathol 2009; 37: 47-51

19. Racette SB, Weiss EP, Villareal DT, Arif H, Steger-May K, Schechtman KB, Fontana L, Klein S, Holloszy JO. One year of caloric restriction in humans: feasibility and effects on body composition and abdominal adipose tissue. J Gerontol A Biol Sci Med Sci 2006; 61: 943-950

20. Hayflick L, Moorhead PS. The serial cultivation of human diploid cell strains. Exp Cell Res 1961; 25: 585-621

21. Rodier F, Coppe JP, Patil CK, Hoeijmakers WA, Munoz DP, Raza SR, Freund A, Campeau E, Davalos AR, Campisi J. Persistent DNA damage signalling triggers senescence-associated inflammatory cytokine secretion. Nat Cell Biol 2009; 11: 973-979

22. Kuilman T, Peeper DS. Senescence-messaging secretome: SMS-ing cellular stress. Nat Rev Cancer 2009; 9:81-94

23. Passos JF, Nelson G, Wang C, Richter T, Simillion C, Proctor CJ, Miwa S, Olijslagers S, Hallinan J, Wipat A, Saretzki G, Rudolph KL, Kirkwood TB, et al. Feedback between p21 and reactive oxygen production is necessary for cell senescence. Mol Syst Biol 2010; 6: 347

24. Dimri GP, Lee X, Basile G, Acosta M, Scott G, Roskelley C, Medrano EE, Linskens M, Rubelj I, Pereira-Smith O, et al. A biomarker that identifies senescent human cells in culture and in aging skin in vivo. Proc Natl Acad Sci U S A 1995; 92: 9363-9367

25. Herbig U, Ferreira M, Condel L, Carey D, Sedivy JM. Cellular senescence in aging primates. Science 2006; 311: 1257

26. Krishnamurthy J, Torrice C, Ramsey MR, Kovalev GI, Al-Regaiey K, Su L, Sharpless NE. Ink4a/Arf expression is a biomarker of aging. J Clin Invest 2004; 114: 1299-1307

27. Jeyapalan JC, Ferreira M, Sedivy JM, Herbig U. Accumulation of senescent cells in mitotic tissue of aging primates. Mech Ageing Dev 2007; 128: 36-44

28. Wang C, Jurk D, Maddick M, Nelson G, Martin-Ruiz C, von Zglinicki T. DNA damage response and cellular senescence in tissues of aging mice. Aging Cell 2009; 8:311-323

29. Chang E, Harley CB. Telomere length and replicative aging in human vascular tissues. Proc Natl Acad Sci U S A 1995; 92: 11190-11194

30. Price JS, Waters JG, Darrah C, Pennington C, Edwards DR, Donell ST, Clark IM. The role of chondrocyte senescence in osteoarthritis. Aging Cell 2002; 1:57-65

31. Baker DJ, Perez-Terzic C, Jin F, Pitel K, Niederlander NJ, Jeganathan K, Yamada S, Reyes S, Rowe L, Hiddinga HJ, Eberhardt NL, Terzic A, van Deursen JM. Opposing roles for p16Ink4a and p19Arf in senescence and ageing caused by BubR1 insufficiency. Nat Cell Biol 2008; 10:825-836

32. Choudhury AR, Ju Z, Djojosubroto MW, Schienke A, Lechel A, Schaetzlein S, Jiang H, Stepczynska A, Wang C, Buer J, Lee HW, von Zglinicki T, Ganser A, et al. Cdkn1a deletion improves stem cell function and lifespan of mice with dysfunctional telomeres without accelerating cancer formation. Nat Genet 2007; 39: 99-105

33. Rudolph KL, Chang S, Lee HW, Blasco M, Gottlieb GJ, Greider C, DePinho RA. Longevity, stress response, and cancer in aging telomerase-deficient mice. Cell 1999; 96:701-712

34. Tyner SD, Venkatachalam S, Choi J, Jones S, Ghebranious N, Igelmann H, Lu X, Soron G, Cooper B, Brayton C, Hee Park S, Thompson T, Karsenty G, et al. p53 mutant mice that display early ageing-associated phenotypes. Nature 2002; 415:45-53

35. Shelton DN, Chang E, Whittier PS, Choi D, Funk WD. Microarray analysis of replicative senescence. Curr Biol 1999; 9: 939-945

36. Krtolica A, Parrinello S, Lockett S, Desprez PY, Campisi J. Senescent fibroblasts promote epithelial cell growth and tumorigenesis: a link between cancer and aging. Proc Natl Acad Sci U S A 2001; 98:12072-12077

37. Coppe JP, Patil CK, Rodier F, Sun Y, Munoz DP, Goldstein J, Nelson PS, Desprez PY, Campisi J. Senescence-associated secretory phenotypes reveal cell-nonautonomous functions of oncogenic RAS and the p53 tumor suppressor. PLoS Biol 2008; 6: 2853-2868

38. Campisi J, Sedivy J. How does proliferative homeostasis change with age? What causes it and how does it contribute to aging? J Gerontol A Biol Sci Med Sci 2009; 64:164-166

39. Tchkonia T, Morbeck D, von Zglinicki T, van Deursen J, Lustgarten J, Scrable H, Koshla S, Jensen MD, Kirkland JL. Fat tissue, aging and cellular senescence. Aging Cell 2010: epub ahead of print.

40. Miller RA. Age-related changes in T cell surface markers: a longitudinal analysis in genetically heterogeneous mice. Mech Ageing Dev 1997; 96: 181-196

41. Messaoudi I, Warner J, Fischer M, Park B, Hill B, Mattison J, Lane MA, Roth GS, Ingram DK, Picker LJ, Douek DC, Mori M, Nikolich-Zugich J. Delay of T cell senescence by caloric restriction in aged long-lived nonhuman primates. Proc Natl Acad Sci U S A 2006; 103: 19448-19453

42. Messaoudi I, Fischer M, Warner J, Park B, Mattison J, Ingram DK, Totonchy T, Mori M, Nikolich-Zugich J. Optimal window of caloric restriction onset limits its beneficial impact on T-cell senescence in primates. Aging Cell 2008; 7: 908-919

43. Spaulding CC, Walford RL, Effros RB. The accumulation of non-replicative, non-functional, senescent T cells with age is avoided in calorically restricted mice by an enhancement of T cell apoptosis. Mech Ageing Dev 1997; 93: 25-33

44. d'Adda di Fagagna F, Reaper PM, Clay-Farrace L, Fiegler H, Carr P, Von Zglinicki T, Saretzki G, Carter NP, Jackson SP. A DNA damage checkpoint response in telomere-initiated senescence. Nature 2003; 426: 194-198

45. Wolf NS, Penn PE, Jiang D, Fei RG, Pendergrass WR. Caloric restriction: conservation of in vivo cellular replicative capacity accompanies life-span extension in mice. Exp Cell Res 1995; 217: 317-323

46. Pendergrass WR, Li Y, Jiang D, Fei RG, Wolf NS. Caloric restriction: conservation of cellular replicative capacity in vitro accompanies life-span extension in mice. Exp Cell Res 1995; 217: 309-316

47. Severino J, Allen RG, Balin S, Balin A, Cristofalo VJ. Is beta-galactosidase staining a marker of senescence in vitro and in vivo? Exp Cell Res 2000; 257: 162-171

48. Kurz DJ, Decary S, Hong Y, Erusalimsky JD. Senescence-associated (beta)-galactosidase reflects an increase in lysosomal mass during replicative ageing of human endothelial cells. J Cell Sci 2000; 113: 3613-3622

49. Kim KS, Kim MS, Seu YB, Chung HY, Kim JH, Kim JR. Regulation of replicative senescence by insulin-like growth factor-binding protein 3 in human umbilical vein endothelial cells. Aging Cell 2007; 6: 535-545

50. Pendergrass WR, Lane MA, Bodkin NL, Hansen BC, Ingram DK, Roth GS, Yi L, Bin H, Wolf NS. Cellular proliferation potential during aging and caloric restriction in rhesus monkeys (Macaca mulatta). J Cell Physiol 1999; 180:123-130

51. von Zglinicki T, Saretzki G, Ladhoff J, d'Adda di Fagagna F, Jackson SP. Human cell senescence as a DNA damage response. Mech Ageing Dev 2005; 126: 111-117

52. Lawless C, Wang C, Jurk D, Merz A, Zglinicki TV, Passos JF. Quantitative assessment of markers for cell senescence. Exp Gerontol 2010: epub ahead of print

53. Flores I, Canela A, Vera E, Tejera A, Cotsarelis G, Blasco MA. The longest telomeres: a general signature of adult stem cell compartments. Genes Dev 2008; 22: 654-667

54. von Zglinicki T. Oxidative stress shortens telomeres. Trends Biochem Sci 2002; 27: 339-344

55. Macip S, Igarashi M, Fang L, Chen A, Pan ZQ, Lee SW, Aaronson SA. Inhibition of p21-mediated ROS accumulation can rescue p21-induced senescence. EMBO J 2002; 21: 2180-2188

56. Takahashi A, Ohtani N, Yamakoshi K, Iida S, Tahara H, Nakayama K, Nakayama KI, Ide T, Saya H, Hara E. Mitogenic signalling and the p16INK4a-Rb pathway cooperate to enforce irreversible cellular senescence. Nat Cell Biol 2006; 8: 1291-1297

57. Passos JF, Saretzki G, Ahmed S, Nelson G, Richter T, Peters H, Wappler I, Birket MJ, Harold G, Schaeuble K, Birch-Machin MA, Kirkwood TB, von Zglinicki T. Mitochondrial dysfunction accounts for the stochastic heterogeneity in telomere-dependent senescence. PLoS Biol 2007; 5: e110

58. Merry BJ. Oxidative stress and mitochondrial function with aging--the effects of calorie restriction. Aging Cell 2004; 3: 7-12

59. Chen JJ, Yu BP. Alterations in mitochondrial membrane fluidity by lipid peroxidation products. Free Radic Biol Med 1994; 17: 411-418

60. Sitte N, Merker K, Grune T, von Zglinicki T. Lipofuscin accumulation in proliferating fibroblasts in vitro: an indicator of oxidative stress. Exp Gerontol 2001; 36:475-486

61. Gerstbrein B, Stamatas G, Kollias N, Driscoll M. In vivo spectrofluorimetry reveals endogenous biomarkers that report healthspan and dietary restriction in Caenorhabditis elegans. Aging Cell 2005; 4: 127-137

62. Sohal RS, Marzabadi MR, Galaris D, Brunk UT. Effect of ambient oxygen concentration on lipofuscin accumulation in cultured rat heart myocytes--a novel in vitro model of lipofuscinogenesis. Free Radic Biol Med 1989; 6: 23-30

63. Panda S, Isbatan A, Adami GR. Modification of the ATM/ATR directed DNA damage response state with aging and long after hepatocyte senescence induction in vivo. Mech Ageing Dev 2008; 129: 332-340

64. Krizhanovsky V, Yon M, Dickins RA, Hearn S, Simon J, Miething C, Yee H, Zender L, Lowe SW. Senescence of activated stellate cells limits liver fibrosis. Cell 2008; 134: 657-667

65. Schilder YD, Heiss EH, Schachner D, Ziegler J, Reznicek G, Sorescu D, Dirsch VM. NADPH oxidases 1 and 4 mediate cellular senescence induced by resveratrol in human endothelial cells. Free Radic Biol Med 2009; 46: 1598-1606

66. Jiang W, Zhu Z, Thompson HJ. Dietary energy restriction modulates the activity of AMP-activated protein kinase, Akt, and mammalian target of rapamycin in mammary carcinomas, mammary gland, and liver. Cancer Res 2008; 68: 5492-5499

67. Selman C, Tullet JM, Wieser D, Irvine E, Lingard SJ, Choudhury AI, Claret M, Al-Qassab H, Carmignac D, Ramadani F, Woods A, Robinson IC, Schuster E, et al. Ribosomal protein S6 kinase 1 signaling regulates mammalian life span. Science 2009; 326: 140-144

68. Zhang H, Hoff H, Marinucci T, Cristofalo VJ, Sell C. Mitogen-independent phosphorylation of S6K1 and decreased ribosomal S6 phosphorylation in senescent human fibroblasts. Exp Cell Res 2000; 259: 284-292

69. Zhuo L, Cai G, Liu F, Fu B, Liu W, Hong Q, Ma Q, Peng Y, Wang J, Chen X. Expression and mechanism of mammalian target of rapamycin in age-related renal cell senescence and organ aging. Mech Ageing Dev 2009; 130: 700-708

70. Korotchkina LG, Leontieva OV, Bukreeva EI, Demidenko ZN, Gudkov AV, Blagosklonny MV. The choice between p53-induced senescence and quiescence is determined in part by the mTOR pathway. Aging (Albany NY) 2010; 2: 344-352

71. Castilho RM, Squarize CH, Chodosh LA, Williams BO, Gutkind JS. mTOR mediates Wnt-induced epidermal stem cell exhaustion and aging. Cell Stem Cell 2009; 5: 279-289

72. Lai KP, Leong WF, Chau JF, Jia D, Zeng L, Liu H, He L, Hao A, Zhang H, Meek D, Velagapudi C, Habib SL, Li B. S6K1 is a multifaceted regulator of Mdm2 that connects nutrient status and DNA damage response. EMBO J 2010; 29: 2994-3006

73. Godschalk RW, Maas LM, Van Zandwijk N, van 't Veer LJ, Breedijk A, Borm PJ, Verhaert J, Kleinjans JC, van Schooten FJ. Differences in aromatic-DNA adduct levels between alveolar macrophages and subpopulations of white blood cells from smokers. Carcinogenesis 1998; 19: 819-825

74. ESCODD. Comparison of different methods of measuring 8-oxoguanine as a marker of oxidative DNA damage. Free Radic Res 2000; 32: 333-341

75. de Kok TM, ten Vaarwerk F, Zwingman I, van Maanen JM, Kleinjans JC. Peroxidation of linoleic, arachidonic and oleic acid in relation to the induction of oxidative DNA damage and cytogenetic effects. Carcinogenesis 1994; 15: 1399-1404

SUPPLEMENTAL MATERIAL

Table S1. Characterisation of the experimental cohort.

Parameter	Ad libitum (AL)	Dietary restriction (DR)	*P* - value
Mean age at death (months)	17.24±1.20	17.33±1.19	0.822
Animal deaths during experiment other than tumours	3	2	0.738
Macroscopic tumour incidence	6	2	0.150
Mean body mass (g)	39.38±0.37	34.26±2.24	<0.001
Mean food intake (g)	3.59±0.41	2.67±0.00	<0.001
Mean daily body temperature (^{o}C)	35.98±0.11	35.72±0.09	0.002
Mean daily physical activity (arbitrary units)	13.64±2.33	19.63±13.44	0.252

Ninety male mice were taken from a long-established colony of the C57/BL (ICRFa) strain which had been selected for use in studies of intrinsic ageing because it is free from specific age-associated pathologies and thus provides a good general model of ageing (Rowlatt et al 1976).

Mice were housed in cages of groups of 4-6 which did not change from weaning. Mice were provided with sawdust and paper bedding and had *ad libitum* access to water. Mice were divided into 2 groups (N=45/group), matched for age, body mass and food intake. There were eight cages in each group. One group was dedicated to ad libitum (AL) feeding and the other group to dietary restriction (DR). The experiment lasted 3 months.

AL fed mice had access to standard rodent pelleted chow in a hopper at all times (CRM(P), Special Diets Services, Witham, UK). The body mass of each mouse was measured twice a week (±0.01g; Sartorius top-pan balance, Epsom, UK). Body mass of the DR group was always recorded before food was given.
DR mice were offered an average of 26% food restriction relative to the AL group. Mean body mass and food intake were calculated across the whole experiment.

7 mice were culled or found dead in the cage during the experiment (4 AL and 3 DR). AL animals that were culled during the experiment for reasons other than tumors were due to paralysis and bladder stones and one was found dead in the cage with the cause unknown. DR animals were culled due to peritonitis in both cases. One AL mouse was culled due to a tail tumor and 1 DR mouse was culled due to a kidney tumor during the experiment. The other macroscopic tumors were noted when dissecting. Tumors in AL mice were found in the liver, kidney, pancreas, small intestine and colon. One tumor was located in the pancreas of DR mouse when dissecting.

Prior to the experiment, one mouse in each cage (N=8AL and N=8DR) was implanted intraperitoneally with a wireless E-mitter (Model PDT-4000 E-Mitter, Mini-Mitter, OR, USA) to monitor body temperature and activity continuously *in vivo*. Mean values were calculated over the whole duration of the experiment.

At the end of the experiment all mice were dissected. Tissues from five mice per group were frozen for cryosectioning (mean age of AL: 17.80±1.10mo and DR: 17.60±1.34mo, $P = 0.803$) and five mice per group were fixed in 4% paraformaldeyde by whole animal perfusion followed by dissection (all aged exactly 17 mo).

REFERENCE

Rowlatt C, Chesterman FC, Sheriff U. Lifespan, age changes and tumour incidence in an ageing C57BL mouse colony. Laboratory Animals. 1976; 10: 419-442.

Research paper

Diet and exercise signals regulate SIRT3 and activate AMPK and PGC-1α in skeletal muscle

Orsolya M. Palacios[1,7], Juan J. Carmona[2,3,4,7], Shaday Michan[5], Ke Yun Chen[1], Yasuko Manabe[6], Jack Lee Ward III[1], Laurie J. Goodyear[6], and Qiang Tong[1]

[1] USDA/ARS Children's Nutrition Research Center, Department of Pediatrics, Baylor College of Medicine, Houston, TX 77030, USA

[2] Howard Hughes Medical Institute & Paul F. Glenn Laboratories for the Biological Mechanisms of Aging, Department of Pathology, Harvard Medical School, Boston, MA 02115, USA

[3] Massachusetts General Hospital Cancer Center, Charlestown, MA 02129, USA

[4] Department of Society, Human Development, and Health, Harvard School of Public Health, Boston, MA 02115, USA

[5] Paul F. Glenn Laboratories for the Biological Mechanisms of Aging, Department of Pathology, Harvard Medical School, Boston, MA 02115, USA

[6] Joslin Diabetes Center & Brigham and Women's Hospital, Harvard Medical School, Boston, MA 02115, USA

[7] These authors contributed equally to this work

Running title: Diet and exercise regulate SIRT3 in skeletal muscle

Key words: SIRT3, AMPK, PGC-1α, caloric restriction, skeletal muscle, exercise, high-fat diet

Correspondence: Qiang Tong, PhD, Children's Nutrition Research Center, Baylor College of Medicine, 1100 Bates Street, Houston, TX 77030, USA

Received: 06/04/09; accepted: 08/13/09; published on line: 08/15/09 **doi:** 10.18632/aging.100075

E-mail: qtong@bcm.edu

Abstract: SIRT3 is a member of the sirtuin family of NAD^+-dependent deacetylases, which is localized to the mitochondria and is enriched in kidney, brown adipose tissue, heart, and other metabolically active tissues. We report here that SIRT3 responds dynamically to both exercise and nutritional signals in skeletal muscle to coordinate downstream molecular responses. We show that exercise training increases SIRT3 expression as well as associated CREB phosphorylation and PGC-1α up-regulation. Furthermore, we show that SIRT3 is more highly expressed in slow oxidative type I soleus muscle compared to fast type II extensor digitorum longus or gastrocnemius muscles. Additionally, we find that SIRT3 protein levels in skeletal muscle are sensitive to diet, for SIRT3 expression increases by fasting and caloric restriction, yet it is decreased by high-fat diet. Interestingly, the caloric restriction regimen also leads to phospho-activation of AMPK in muscle. Conversely in SIRT3 knockout mice, we find that the phosphorylation of both AMPK and CREB and the expression of PGC-1α are down regulated, suggesting that these key cellular factors may be important components of SIRT3-mediated biological signals *in vivo*.

INTRODUCTION

The sirtuin family of proteins possesses NAD^+-dependent deacetylase activity and/or ADP ribosyltransferase activity. The seven mammalian sirtuins (SIRT1-7) sirtuins (SIRT1-7) are localized differentially within the cell and have a variety of functions [1, 2]. SIRT1 is the most extensively studied member of the family and regulates diverse biological processes ranging from DNA repair and genome stability to glucose and lipid

homeostasis [3, 4]. Although three specific sirtuins, SIRT3-5, are found in the mitochondria [5, 6], not much is known about their function *in vivo* [7]. SIRT4 has been shown to regulate amino acid-stimulated insulin secretion by targeting glutamate dehydrogenase [8], and it was recently demonstrated that SIRT5 participates in the urea cycle [9]. Among the mitochondrial sirtuins, SIRT3 possesses the most robust deacetylase activity [10-12]. Indeed, significantly higher levels of mitochondrial protein acetylation were detected in the livers of SIRT3-null mice, compared to those of SIRT4 or SIRT5 knockout animals [13]. However, little is known about the physiological role of SIRT3 despite the fact that a number of SIRT3 substrates and co-precipitating proteins have been identified: acetyl-CoA synthetase 2 [14], Ku70 [15], FOXO3a [16], subunit 9 of mitochondrial Complex I (NDUFA9) [17], glutamate dehydrogenase [13, 18] and isocitrate dehydrogenase 2 [18].

SIRT3 has been linked to longevity in men [19, 20] and aberrant expression of this sirtuin correlates with node-positive breast cancer in clinical biopsies from women [21]—suggesting that SIRT3 serves as an important diagnostic and therapeutic target in human health/aging and disease, affecting men and women in unique ways. In human cells, we have shown that SIRT3, along with SIRT4, is required for Nampt-mediated cell survival after genotoxic stress, wherein maintenance of mitochondrial NAD^+ levels inhibits apoptosis [22]. Previously we also reported in murine brown adipose tissue that the RNA level of SIRT3 increases by cold exposure and caloric restriction (CR) and that constitutive expression of SIRT3, in brown pre-adipocytes, stimulates downstream CREB-mediated expression of PGC-1α and other mitochondrial-related genes [10]. In this study, we investigated the physiological conditions that regulate SIRT3 in skeletal muscle, a metabolically active organ vital for insulin-mediated glucose disposal and lipid catabolism. Notably, skeletal muscle strongly influences whole-body lipid metabolism, as lipid catabolism provides up to 70% of the energy usage for resting muscle [23]. In this tissue, the balance between fatty acid availability and fatty acid oxidation rates plays an important role in regulating insulin responses, and intramuscular fatty acid metabolites like diacylglycerol may cause insulin resistance [24]. Therefore, studying the role of molecular factors and pathways acting in muscle under various dietary and environmental conditions will be critical for better understanding metabolism, health, and disease.

In skeletal muscle, the peroxisome proliferator-activated receptor gamma coactivator-1α (PGC-1α), a nuclear receptor co-activator, plays multiple roles in metabolic regulation [25, 26]. It stimulates mitochondrial biogenesis [27], induces muscle fiber-type switch, and increases oxidative capacity in skeletal muscle cells [28]. In addition to transcriptional activation by CREB [29], it has been shown that AMP-activated protein kinase (AMPK) also increases PGC-1α expression [30, 31] and activates it by direct phosphorylation [32]. AMPK is also a key molecular sensor and regulator of muscle metabolism.

AMPK is a ubiquitous heterotrimeric serine/threonine protein kinase, which functions as a fuel sensor in many tissues, including skeletal muscle [33]. AMPK is allosterically activated by AMP and by phosphorylation at Thr172 in the catalytic α-subunit, mainly by an upstream AMPK kinase, LKB1 [34, 35]. Importantly, AMPK is stimulated by cellular stresses that deplete ATP and elevate AMP, such as diet restriction/hypo-glycemia [36], exercise [37], and muscular contraction [38]. Activated AMPK stimulates ATP-generating catabolic pathways, such as cellular glucose uptake and fatty acid α-oxidation. AMPK activation also represses ATP-consuming processes, such as lipogenesis, to restore intracellular energy balance [33, 39].

Our work seeks to further elucidate the role of sirtuins within health and disease, with particular focus on muscle tissue in this study. We report here that expression of SIRT3 in skeletal muscle is sensitive to various signals from both diet and exercise, leading to downstream activation of AMPK and up-regulation of PGC-1α. SIRT3 is therefore a potential key regulator of skeletal muscle biology, responding to important environmental cues and activating cellular factors *in vivo*.

RESULTS

SIRT3 is regulated in skeletal muscle by exercise training

We first assayed the SIRT3 expression profile *in vivo* to compare the whole-body distribution of SIRT3, specifically across muscles to tissues like adipose and kidney, where SIRT3 has been previously described. As predicted, the SIRT3 tissue distribution pattern mirrors that of SIRT3 mRNA [11]. Indeed, SIRT3 exhibits high expression in important metabolically active tissues like kidney, brown fat, liver, and brain (Figure 1). When comparing expression across muscle samples, we noticed that SIRT3 protein levels were higher in the slow-twitch soleus muscle compared to the fast-twitch muscles like extensor digitorum longus and gastro-cnemius, in agreement with higher mitochondrial content and the oxidative feature of the soleus muscle.

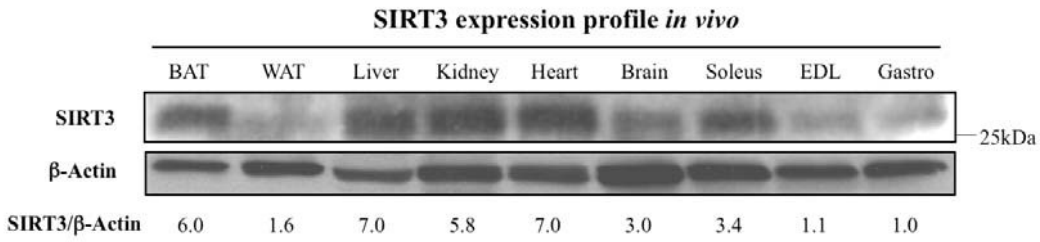

Figure 1. Tissue distribution of SIRT3 protein. The SIRT3 protein is abundantly expressed in the brown adipose tissue (BAT), liver, kidney, heart, brain, and soleus muscle, but very low in white adipose tissue (WAT), the extensor digitorum longus muscle (EDL), or the gastrocnemius muscle (Gastro). For each sample, 50 μg of protein was loaded into a 10% acrylamide gel, electrophoresed, and transferred to a nitrocellulose membrane. The membrane was probed using an anti-SIRT3 serum or an anti-β-actin antibody. Blots were quantified with ImageQuant and SIRT3/actin ratios are provided; since gastrocnemius (Gastro) has the lowest SIRT3 expression *in vivo*, normalization (l.0) was set with respect to this tissue.

To study the role of SIRT3 in muscle within the context of exercise biology, we next tested if SIRT3 protein levels were sensitive to an established voluntary exercise protocol [40]. Using a specific anti-mouse SIRT3 polyclonal antibody, we found that SIRT3 protein increased selectively in triceps, the muscle that undergoes training in the wheel-caged system, but not in cardiac muscle samples from those same animals (Figure 2A). In contrast to SIRT3, exercise training failed to alter SIRT1 protein levels in triceps (data not shown). The specificity of our antibody for detecting the endogenous ~28kDa SIRT3 protein was confirmed by using SIRT3 knockout tissue lysates (Supplemental Figure 1). Notably, induction of SIRT3 in skeletal muscle was higher in female mice when compared to that of male littermates (Figure 2B). In agreement with this up-regulation, we also observed increased SIRT3 levels in the gastrocnemius muscle of rats exercised on a treadmill-based exercise paradigm [41] (Supplemental Figure 2). Even one week of treadmill training was sufficient to increase SIRT3 protein amount (Supplemental Figure 2B). The up-regulation of SIRT3 (Figure 2B) correlated with enhanced downstream phosphorylation of CREB at Ser133 (Figure 2C) and PGC-1α induction (Figure 2D). Lastly, citrate synthase activity, a mitochondrial marker for exercise training, was significantly higher in trained muscles than in the respective sedentary control group (Figure 2E). Collectively, these data suggest that the up-regulation of SIRT3 by exercise is an important and conserved molecular consequence of training.

SIRT3 expression in skeletal muscle is sensitive to dietary intake

Previously we had demonstrated how CR stimulates the *in vivo* expression of SIRT3 in brown fat [10]. Thus we hypothesized that perhaps SIRT3 expression in muscles is also sensitive to nutritional signals, especially given how different muscles contain various levels of SIRT3 (Figure 1) and vary inherently with respect to energetic/metabolic potential. To test this hypothesis, we measured the SIRT3 levels in leg muscles of mice in either CR or *ad libitum* (AL) cohorts after twelve months. CR is an effective environmental method known to extend lifespan in a number of model organisms, from yeast and nematodes to rodents, yet the underlying molecular mechanisms by which this pathway acts *in vivo* remain largely unknown [42].

Here we found that the CR diet significantly increased levels of SIRT3 protein in skeletal muscle, compared to the AL control diet (Figure 3A). In addition, twenty-four hours of fasting was sufficient to induce the muscle expression of SIRT3 (Figure 3B). Conversely, SIRT3 protein level was significantly decreased following three months of energy-dense, high-fat feeding (Figure 3C), indicating that the SIRT3 expression in muscle fluctuates in response to dietary nutrient uptake. We next measured the effect of CR on AMPK—an enzyme whose activity is dependent on changes in metabolic/energetic potential [30, 31].

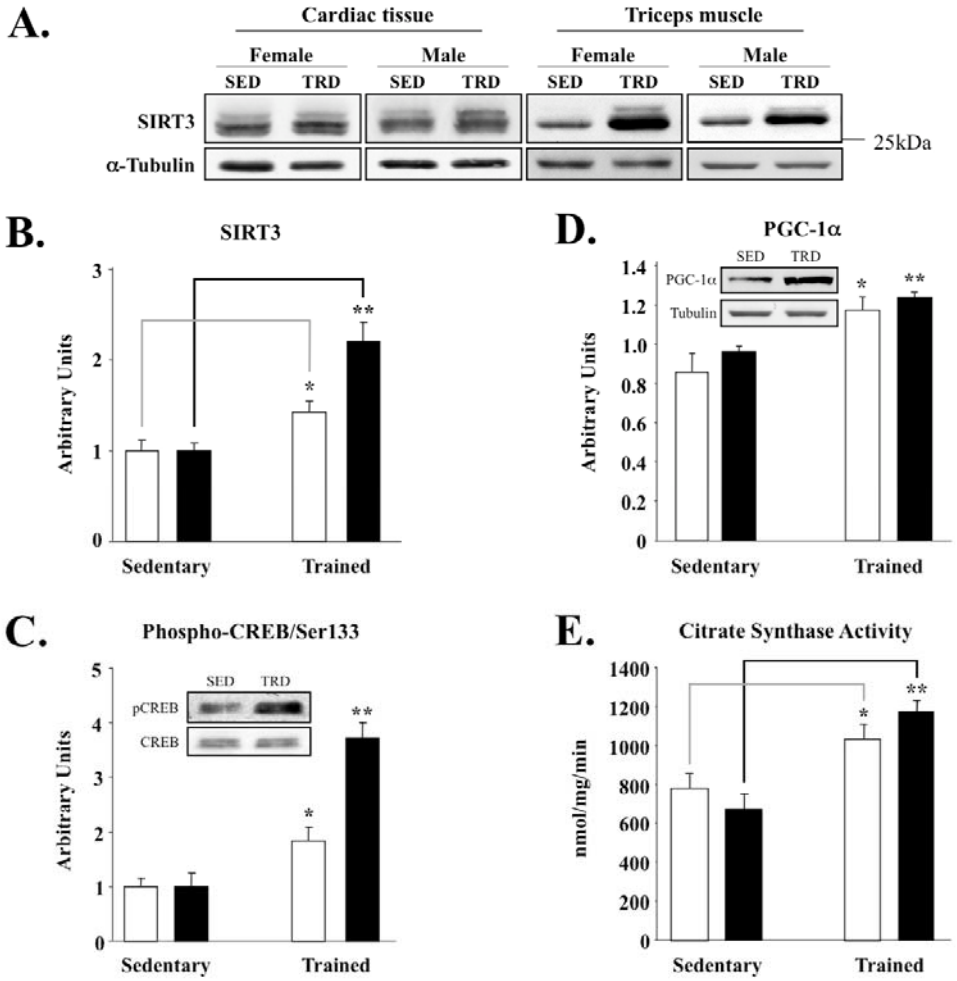

Figure 2. Skeletal muscle-specific induction of SIRT3 and associated factors in exercise-trained mice. (**A**) Triceps or cardiac muscle tissue was homogenized and 50 μg of protein was analyzed by Western blot, using anti-SIRT3 serum (Covance) and α-tubulin control; representative blots are shown here and throughout. SED = sedentary and TRD = trained. (**B**) Quantification of SIRT3 band intensities using ImageQuant from blots with animals grouped by sex. Males are plotted as clear bars and females as shaded bars. Total number of animals used per cohort and graphed are as follows: sedentary males, N = 7; sedentary females, N = 5; exercised males, N = 8; exercised females, N = 6. (**C**) Phospho-CREB/Ser133 and total CREB protein. Band intensities of phospho-CREB and CREB were quantified and phospho-CREB content was normalized relative to total CREB content; inset provides sample blots of male triceps tissue. (**D**) Induction of PGC-1α correlates with enhanced SIRT3 expression in triceps; samples processed and analyzed, as above. Inset blots are of male triceps tissue. (**E**) Citrate synthase activity was measured as a mitochondrial marker from the same triceps samples, as described previously [40]. N = 2, *P < 0.05, **P < 0.01.

Since AMPK is activated during decreased energy levels, we hypothesized that AMPK may be activated under CR. In nematodes, for example, it has recently been shown that AMPK is critical for mediating key downstream biological effects that enable lifespan extension by caloric/dietary restriction [43]. Our data here show that AMPK is hyper-phospho-activated at Thr172 of its catalytic α-subunit, which was quantified and determined to be three to four times higher than the AL control diet (Figure 3D). Together these data provided novel connections between caloric intake, SIRT3 and AMPK that merit more analysis.

Loss of SIRT3 significantly impacts activation of AMPK, CREB and PGC-1α expression

We next tested if the lack of SIRT3 would impact AMPK and other related factors like CREB and/or

PGC-1α in skeletal muscle. Consistent with our previous data, we found that SIRT3-null animals had 50% lower levels of AMPK phosphorylation compared to the wild-type littermate control group (Figure 4A). In our exercise model (Figure 2A-D), SIRT3 up-regulation enhanced downstream activation of CREB and PGC-1α. Accordingly, in the SIRT3-null mice, activating phosphorylation of CREB at Ser122 was also reduced (Figure 4B), which correlated with lowered transcriptional activation of *pgc-1α* (Figure 4C). This result is consistent with previously published data, which show that both AMPK and CREB activate *pgc-1α* expression *in vivo* [29].

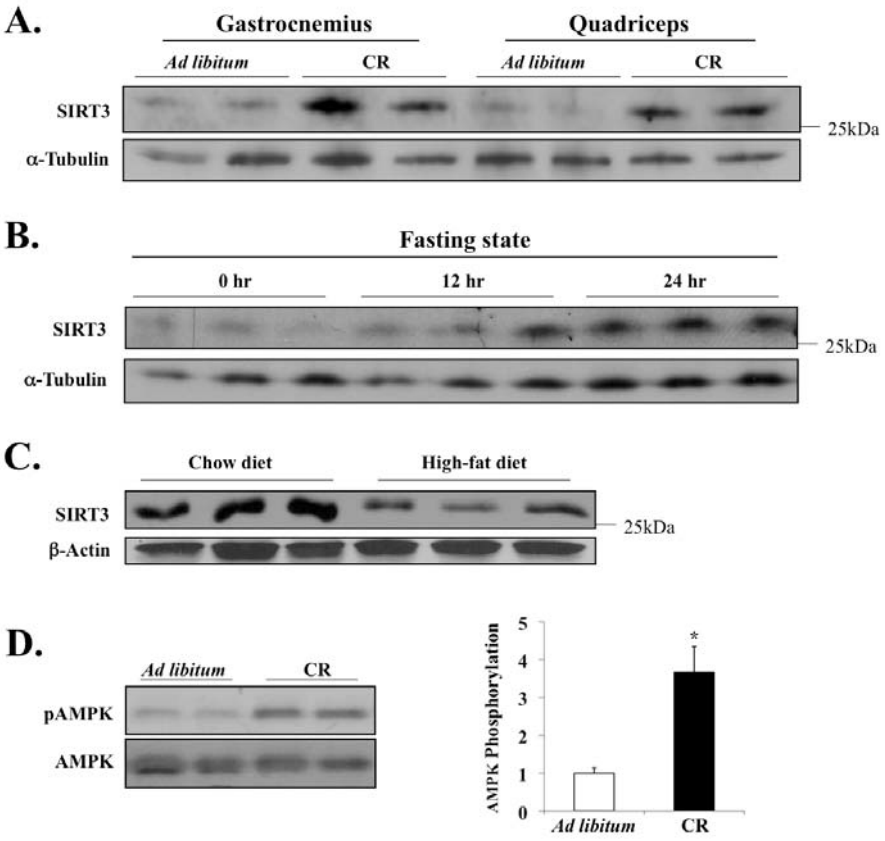

Figure 3. Diet-sensitive expression of SIRT3 and AMPK in muscle tissue. (**A**) Mice were fed NIH-31 standard feed *ad libitum* or NIH-31/NIA-fortified diet (Harlan Teklad) with a daily food allotment of 60% of the control mice to establish caloric restriction (CR); twelve months after the onset of CR, tissues were harvested to examine SIRT3 expression. (**B**) Mice were deprived of food for 24 hours, and SIRT3 level in EDL muscle was determined by Western blot analysis. (**C**) SIRT3 protein expression is decreased in murine hind-leg muscle after 3 months of high-fat diet feeding; total hind-leg tissue protein was isolated and analyzed. (**D**) AMPK T-172 phosphorylation and AMPK total protein in the quadriceps of the caloric restricted mice were assayed; AMPK phosphorylation was determined as phospho-AMPK normalized by total AMPK. N=3, *P < 0.05.

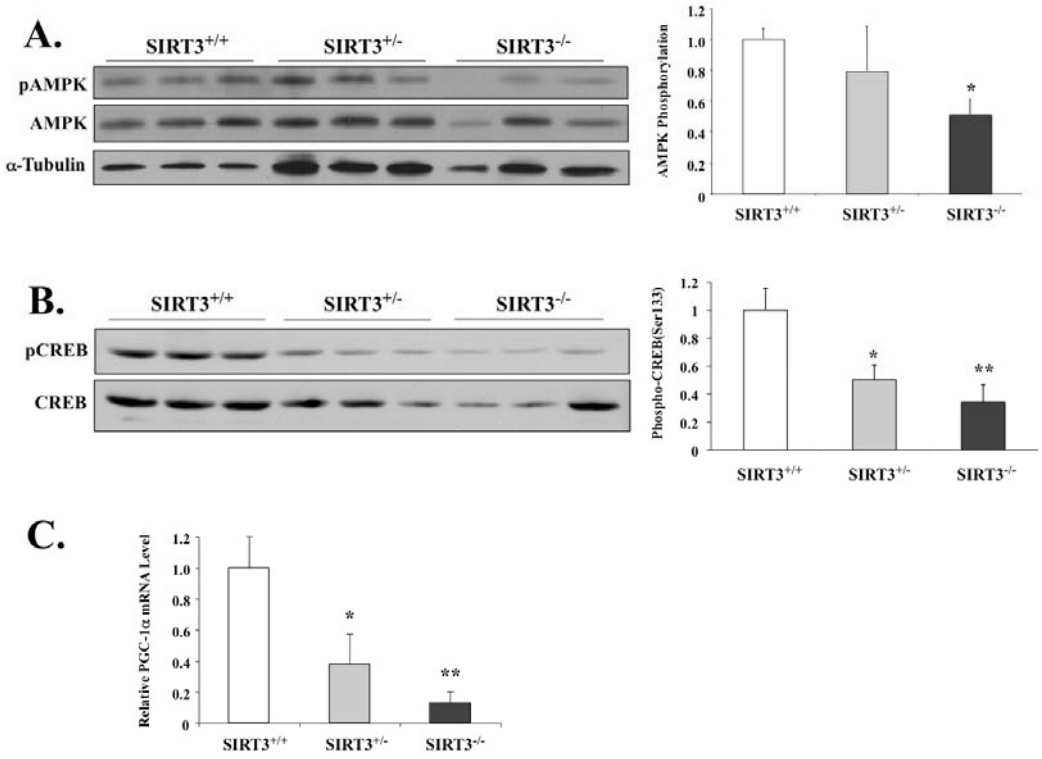

Figure 4. SIRT3-deficient mice have lower phosphorylation levels of AMPK and CREB, as well as decreased PGC-1α mRNA. (**A**) AMPK T-172 phosphorylation and AMPK total protein in the EDL muscles of the male wild-type mice or mice with heterozygous or homozygous SIRT3 gene deficiency were determined by Western blot analysis. AMPK phosphorylation was determined as phospho-AMPK normalized by total AMPK. N=3, *P < 0.05. (**B**) CREB phosphorylation and CREB total protein in the EDL muscles of the wild-type mice or mice with heterozygous or homozygous SIRT3 gene deficiency were determined by Western blotting analysis. CREB phosphorylation was determined as phospho-CREB normalized by total CREB. N=3, *P < 0.05, **P<0.01. (**C**) Quatitative RT-PCR shows *pgc-1*α mRNA level reduced in the gastrocnemius of SIRT3 knockout mice. *P < 0.05, **P<0.01.

DISCUSSION

Here we have found that SIRT3 is differentially expressed *in vivo*, with the greatest expression observed in metabolically active tissues like skeletal muscle, where SIRT3 undergoes dynamic regulation by different environmental regimens. SIRT3 protein level is decreased by high-fat feeding, while it is increased by short-term fasting (24-hour) or long-term nutrient deprivation (12-month CR) and exercise training. In this study we also show that loss of SIRT3 significantly inhibits AMPK and CREB phosphorylation, which decreases PGC-1α transcriptional expression in muscle. Consequently, we propose a new model in which SIRT3 leads to potential downstream changes in response to important environmental signals (Figure 5). This model suggests that SIRT3 levels may respond to various nutritional/energetic and physiological challenges by regulating muscle energy homeostasis *via* factors like AMPK and PGC-1α.

Given our study, it will be interesting to test whether SIRT3-null animals show any defects under certain environmental challenges. Despite the hyper-acetylation of mitochondrial proteins in SIRT3 knockout mice, the significance of these biochemical changes is unclear. A recent study of SIRT3-deficient mice by another group did not find defects in basal metabolism nor adaptive thermogenesis, while the mice were housed in standard dietary/sedentary conditions [13]. Similarly, we found normal treadmill performance in SIRT3 knockout mice while under standard housing (unpublished observations). Upon challenge with various environmental

signals, however, these animals may respond differently. Accordingly, we are actively testing how challenges by CR/fasting/high-fat diet and exercise may affect the SIRT3-null mice and alter key downstream cellular factors in muscle cells.

The mechanism(s) by which different environmental variables modulate SIRT3 and activate AMPK in muscle (and other tissues that highly express SIRT3) remains to be fully elucidated. For example, activation of acetyl-CoA synthetase 2 (AceCS2) by SIRT3 [44, 45] may elevate the AMP/ATP ratio and consequently activate AMPK. Alternatively, a recent proteomics-based approach has identified many novel SIRT3-interacting partners in human cells, including the ATP synthase (mitochondrial F1 complex) alpha/beta subunits and the ubiquinol-cytochrome c reductase hinge protein, UQCRH [46]. Since these proteins (together with NDUFA9 [17]) serve as critical components of the ATP-generating machinery in cells, SIRT3 may also potentially modulate the AMP/ATP ratio *via* these factors to activate AMPK. Moreover, we too have purified additional putative SIRT3-binding proteins from HeLa cells (using a related cross-linking/immunoaffinity purification method [47]), which include mitochondrial acetoacetyl CoA thiolase (also referred to as α-ketothiolase), malate dehydrogenase, thioredoxin 2 (Trx-2), Hsp60, and lactate dehydrogenase (unpublished data). Since some of these enzymes are important regulators of muscle energy homeostasis, our data further substantiate that SIRT3 may modulate ATP/energy levels *via* key targets to activate AMPK. It is intriguing to note that a study of an independent line of SIRT3-knockout mice indicated that the ATP level is significantly reduced in several tissues [17], although the effect of SIRT3 deficiency on muscle ATP level has not been reported.

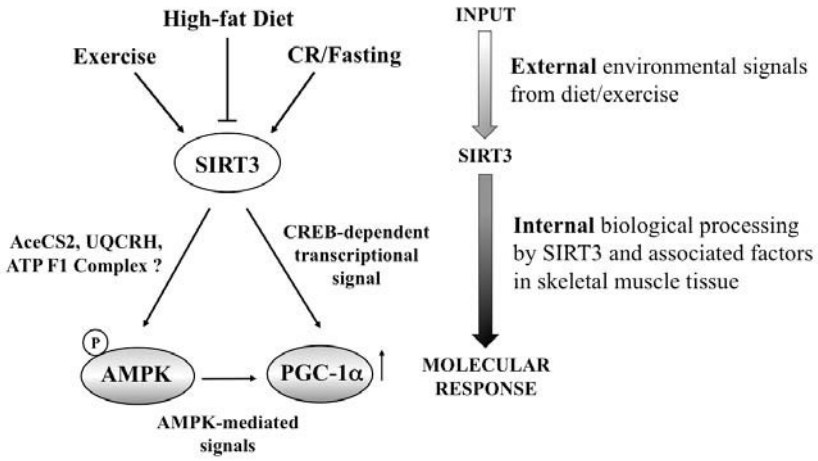

Figure 5. Schematic diagram of potential SIRT3 action in the skeletal myocyte. Collectively, our data support a working model in which SIRT3 responds dynamically to various nutritional and physiological signals to potentially impact muscle energy homeostasis *via* AMPK and PGC-1α. Since AMPK can also phosphorylate and activate CREB [52], SIRT3 may activate CREB directly or through AMPK. Given its dynamic role, SIRT3 action within the skeletal muscle cells may serve as an important diagnostic and therapeutic target for impacting human health and disease.

Interestingly, it has also been shown that activation of AMPK, upon glucose nutrient restriction of muscle stem cells, causes an increase in the cellular NAD^+/NADH ratio, consistent with a positive feedback loop needed for prolonged SIRT1 activation [48], as may occur in our SIRT3 model and merits testing. Indeed a second *in vitro* study independently validates a similar NAD^+/NADH model *via* AMPK [49]. Strikingly, AMPK activation (as occurs with CR) may also result in lifespan extension [50-52], and future study will reveal if SIRT3 is involved in this process. It is known that activated AMPK directly phosphorylates PGC-1α [32] and CREB [53]—and that both AMPK and CREB are involved in the transactivation of PGC-1α [54, 55]. Lastly, both SIRT3 and SIRT1 promote mitochondrial biogenesis and fatty acid oxidation *via* PGC-1α but in different ways. SIRT3 promotes PGC-1α expression while SIRT1 activates PGC-1α by direct deacetylation [56]. However, we have found that exercise training regulates SIRT3 but not SIRT1 expression in muscle. At present, it remains to be considered how these two key sirtuin enzymes may work cooperatively within certain tissues in response to environmental signals.

Furthermore, it is important to consider that a phenotype may be tissue-specific, especially if SIRT3 has different biological roles in the body. For example, in the rennin-angiotensin system, which plays a key role in the pathophysiology of cardiac and renal disease in humans, targeted disruption of the angiotensin receptor (*Agtr1a* gene in mice) yields animals with less cardiac and vascular injury, prolonged lifespan, increased number of mitochondria, and dramatic up-regulation of SIRT3 in kidney tissue—a possible site of SIRT3 action that may contribute, at least in part, to the phenotype that is observed [57]. Another interesting place of molecular action is in brown adipose tissue (BAT), in which SIRT3 has been previously shown to respond dynamically to CR and regulate fat cell physiology *via* PGC-1α [10]. With the recent discovery of BAT in humans (reviewed in [58]), there are now new opportunities to explore the role of SIRT3 in diabetes and obesity research [59]. Moreover, after intense swimming, it has been reported that the expression of SIRT3 and PGC-1α increases in white blood cells to activate the antioxidant response [60]. Lastly, in human skeletal muscle, it has been reported that SIRT3 and PGC-1α expression decline with age and correlate with a sedentary proteomic profile found in people with decreased metabolic output [61]. With exercise, however, these authors observed that the effect is reversed. Collectively, these data suggest that SIRT3 function is perhaps varied throughout the body and specialized to meet the unique metabolic/energetic capacities found within various tissues, particularly in response to environmental cues.

Thus it will be interesting to test whether inducible tissue-specific SIRT3-null mice show global metabolic defects from exercise and/or diet regimens in various parts of the body, especially with aging. This inducible genetic approach will also allow us to bypass potential compensatory effects resulting from the lack of SIRT3 during development. Additionally, a mouse model with increased SIRT3 over-expression in muscle (and/or other specific tissues) will also be a valuable tool for further elucidating the biological role(s) of this sirtuin *in vivo*. All of this work will be important as we fight against aging and associated disorders ranging from type 2 diabetes (and other metabolic diseases) to breast cancer, in which expression of SIRT3 is aberrant. Therefore, small-molecule activators of SIRT3, currently in development and testing [62], may provide novel and key therapeutic routes for the treatment of a variety of common diseases, perhaps by mimicking the beneficial molecular effects of exercise and/or caloric restriction *in vivo*.

EXPERIMENTAL PROCEDURES

Animals, diet and exercise. Ethics statement: Protocols for animal use were in accordance with the guidelines of the Institutional Animal Care and Use Committees of Baylor College of Medicine and the Joslin Diabetes Center and the National Institutes of Health. For the caloric restriction experiment, C57BL/6 male mice were singly caged. At 8 weeks of age, control mice were fed *ad libitum* with NIH-31 standard diet (Harlan Teklad), while food consumption was measured daily. Caloric restricted mice were fed with NIH-31/NIA-fortified diet (Harlan Teklad) with a daily food allotment of 90%, 70% and then 60% of the amount consumed by the control mice—at the first, second, and third week, respectively. From then on, daily food allotment stabilized at 60% of *ad libitum* food intake for the caloric restricted mice. 12 months later, mice were dissected to collect tissues for analysis. For the fasting experiment, food was removed from 3 months old C57BL/6 male mice at 6pm for 24 hours. For the high-fat diet feeding experiment, 8-week-old male mice were fed a control diet or a 35% fat-enriched chow (Bio-Serv) for three months. Various tissues were also harvested from mice fed the control diet to examine SIRT3 gene expression by Western blot analysis at the termination of the study. For the exercise study [40], 7-week-old male and female FVB/NJ mice were wheel-cage trained for 6 weeks and fed PicoLab Mouse Diet 20 (LabDiet/Purina). In brief, mice were housed in individual cages with or without rodent running wheels

(Nalgene, Rochester, NY) and the animals could exercise voluntarily during a 6-week training period. At the end of the 6 weeks, mice were euthanized, triceps muscles were removed and subsequently analyzed for SIRT3, CREB, phospho-CREB/Ser122, and PGC-1α protein expression [10]. Citrate synthase activity was measured as a mitochondrial marker post-exercise training from triceps samples, as described previously [40].

Sirt3-knockout mice. Mice in which the *Sirt3* gene (Accession: NM_022433) was targeted by gene trapping were obtained from the Texas Institute for Genomic Medicine (Houston, TX, USA). Briefly, these mice were created by generating embryonic stem (ES) cells (Omnibank No. OST341297) with a retroviral promoter trap that functionally inactivates one allele of the *Sirt3* gene, as described previously [63]. Sequence analysis indicated that retroviral insertion occurred in the intron preceding coding exon 2 (Supplemental Figure 1). Targeted 129/SvEvBrd embryonic stem cells were injected into C57BL/6 albino blastocysts. The chimeras (129/SvEvBrd) were then crossed with C57BL/6 albinos to produce the heterozygotes. Heterozygotes were then mated and the offspring were genotyped using PCR, containing two primers flanking the trapping cassette insertion site TG0003-5' (ATCTCGCAGATAGGCTATCAGC) and TG0003-3' (AACCACGTAACCTTACCCAAGG), as well as a third primer LTR rev, a reverse primer located at the 5' end of the trapping cassette (ATAAACCCTCTTGCAG TTGCATC). Primer pair TG0003-5' and TG0003-3' amplify a 336bp fragment from the wild-type allele, while primer pair TG0003-5' and LTR rev amplify a 160bp fragment from the knockout allele.

Antibodies and Western blots. The antibodies used for Western blot analysis included: anti-mouse SIRT3 serum raised against the C-terminus (DLMQRERGKLD GQDR, Genemed Synthesis, Inc.) and used for the tissue distribution and high-fat diet analyses; anti-mouse and anti-rat SIRT3 serum was also developed against the C-terminal regions of each respective protein (Covance), and the anti-mouse serum was validated for specificity using brown fat, cardiac tissue, and soleus muscle from SIRT3 knockout mice (Supplemental Fig. 1), then used for analyzing the exercise samples. Other antibodies used included the following: anti-phospho-CREB/Ser133 (Cell Signaling); anti-CREB (Cell Signaling); anti-phospho-AMPK (Cell Signaling); AMPK (Cell Signaling); anti-PGC-1α (Calbiochem); β-actin antibody (Santa Cruz); and α-tubulin (Abcam).

ACKNOWLEDGEMENTS

We thank Dr. E. O'Brian Smith for assistance with statistical analysis, Dr. Martin Young for valuable discussions/suggestions, and Margaret Nguyen for technical assistance. O.M.P. was supported by a National Institutes of Health (NIH) training grant (T32 HD007445) and J.J.C. by a Howard Hughes Medical Institute Predoctoral Fellowship. L.J.G. received support from a NIH grant (RO1DK068626). This work was also supported by grants to Q. T. from the U.S. Department of Agriculture (CRIS 6250-51000-049) and the NIH (RO1DK075978).

CONFLICT OF INTERESTS STATEMENT

The authors of this article report no conflict of interest(s).

REFERENCES

1. Michishita E, Park J Y, Burneskis J M, Barrett J C, Horikawa I. Evolutionarily conserved and nonconserved cellular localizations and functions of human SIRT proteins. Mol Biol Cell. 2005; 16: 4623-4635.

2. North B J, Verdin E. Sirtuins: Sir2-related NAD-dependent protein deacetylases. Genome Biol. 2004; 5: 224.

3. Haigis M C, Guarente L P. Mammalian sirtuins--emerging roles in physiology, aging, and calorie restriction. Genes Dev. 2006; 20: 2913-2921.

4. Michan S, Sinclair D. Sirtuins in mammals: insights into their biological function. Biochem J. 2007; 404: 1-13.

5. Hallows W C, Albaugh B N, Denu J M. Where in the cell is SIRT3?--functional localization of an NAD+-dependent protein deacetylase. Biochem J. 2008; 411: e11-3.

6. Cooper H M, Spelbrink J N. The human SIRT3 protein deacetylase is exclusively mitochondrial. Biochem J. 2008; 411: 279-285.

7. Guarente L. Mitochondria--a nexus for aging, calorie restriction, and sirtuins? Cell. 2008; 132: 171-176.

8. Haigis M C, Mostoslavsky R, Haigis K M, Fahie K, Christodoulou D C, Murphy A J, Valenzuela D M, Yancopoulos G D, Karow M, Blander G, Valenzuela D M, Yancopoulos G D, Karow M, Blander G, Wolberger C, Prolla T A, Weindruch R, Alt F W, Guarente L. SIRT4 inhibits glutamate dehydrogenase and opposes the effects of calorie restriction in pancreatic beta cells. Cell. 2006; 126: 941-954.

9. Nakagawa T, Lomb D J, Haigis M C, Guarente L. SIRT5 Deacetylates carbamoyl phosphate synthetase 1 and regulates the urea cycle. Cell. 2009; 137: 560-570.

10. Shi T, Wang F, Stieren E, Tong Q. SIRT3, a mitochondrial sirtuin deacetylase, regulates mitochondrial function and thermogenesis in brown adipocytes. J Biol Chem. 2005; 280: 13560-13567.

11. Onyango P, Celic I, McCaffery J M, Boeke J D, Feinberg A P. SIRT3, a human SIR2 homologue, is an NAD-dependent deacetylase localized to mitochondria. Proc Natl Acad Sci U S A. 2002; 99: 13653-13658.

12. Schwer B, North B J, Frye R A, Ott M, Verdin E. The human silent information regulator (Sir)2 homologue hSIRT3 is a mitochondrial nicotinamide adenine dinucleotide-dependent deacetylase. J Cell Biol. 2002; 158: 647-657.

13. Lombard D B, Alt F W, Cheng H L, Bunkenborg J, Streeper R S, Mostoslavsky R, Kim J, Yancopoulos G, Valenzuela D, Murphy A, Yang Y, Chen Y, Hirschey M D, Bronson R T, Haigis M, Guarente L P, Farese R V, Jr, Weissman S, Verdin E, Schwer B. Mammalian Mammalian Sir2 homolog SIRT3 regulates global mitochondrial lysine acetylation. Mol Cell Biol. 2007; 27:8807-8814.

14. Schwer B, Bunkenborg J, Verdin R O, Andersen J S, Verdin E. Reversible lysine acetylation controls the activity of the mitochondrial enzyme acetyl-CoA synthetase 2. Proc Natl Acad Sci U S A. 2006; 103:10224-10229.

15. Sundaresan N R, Samant S A, Pillai V B, Rajamohan S B, Gupta M P. SIRT3 is a stress responsive deacetylase in cardiomyocytes that protects cells from stress-mediated cell death by deacetylation of Ku-70. Mol Cell Biol. 2008; 6384-6401.

16. Jacobs K M, Pennington J D, Bisht K S, Aykin-Burns N, Kim H S, Mishra M, Sun L, Nguyen P, Ahn B H, Leclerc J, Deng C X, Spitz D R, Gius D. SIRT3 interacts with the daf-16 homolog FOXO3a in the mitochondria, as well as increases FOXO3a dependent gene expression. Int J Biol Sci. 2008; 4: 291-299.

17. Ahn B H, Kim H S, Song S, Lee I H, Liu J, Vassilopoulos A, Deng C X, Finkel T. A role for the mitochondrial deacetylase Sirt3 in regulating energy homeostasis. Proc Natl Acad Sci U S A. 2008; 105: 14447-144452.

18. Schlicker C, Gertz M, Papatheodorou P, Kachholz B, Becker C F, Steegborn C. Substrates and Regulation Mechanisms for the Human Mitochondrial Sirtuins Sirt3 and Sirt5. J Mol Biol. 2008; 790-801.

19. Bellizzi D, Dato S, Cavalcante P, Covello G, Di Cianni F, Passarino G, Rose G, De Benedictis G. Characterization of a bidirectional promoter shared between two human genes related to aging: SIRT3 and PSMD13. Genomics. 2007; 89: 143-150.

20. Bellizzi D, Rose G, Cavalcante P, Covello G, Dato S, De Rango F, Greco V, Maggiolini M, Feraco E, Mari V, Franceschi C, Passarino G, De Benedictis G. A novel VNTR enhancer within the SIRT3 gene, a human homologue of SIR2, is associated with survival at oldest ages. Genomics. 2005; 85:258-263.

21. Ashraf N, Zino S, Macintyre A, Kingsmore D, Payne A P, George W D, Shiels P G. Altered sirtuin expression is associated with node-positive breast cancer. Br J Cancer. 2006; 95: 1056-1061.

22. Yang H, Yang T, Baur J A, Perez E, Matsui T, Carmona J J, Lamming D W, Souza-Pinto N C, Bohr V A, Rosenzweig A, de Cabo R, Sauve A A, Sinclair D A. Nutrient-sensitive mitochondrial NAD+ levels dictate cell survival. Cell. 2007; 130: 1095-1107.

23. Smith A G, Muscat G E. Skeletal muscle and nuclear hormone receptors: implications for cardiovascular and metabolic disease. Int J Biochem Cell Biol. 2005; 37:2047-2063.

24. Yu C, Chen Y, Cline G W, Zhang D, Zong H, Wang Y, Bergeron R, Kim J K, Cushman S W, Cooney G J, Atcheson B, White M F, Kraegen E W, Shulman G I. Mechanism by Which Fatty Acids Inhibit Insulin Activation of Insulin Receptor Substrate-1 (IRS-1)-associated Phosphatidylinositol 3-Kinase Activity in Muscle. J Biol Chem. 2002; 277:50230-50236.

25. Finck B N, Kelly, D P. PGC-1 coactivators: inducible regulators of energy metabolism in health and disease. J Clin Invest. 2006; 116: 615-622.

26. Handschin, C. and B.M. Spiegelman, Peroxisome Proliferator-Activated Receptor {gamma} Coactivator 1 Coactivators, Energy Homeostasis, and Metabolism. Endocr Rev. 2006; 728-735.

27. Wu Z, Puigserver P, Andersson U, Zhang C, Adelmant G, Mootha V, Troy A, Cinti S, Lowell B, Scarpulla R C, Spiegelman B M. Mechanisms controlling mitochondrial biogenesis and respiration through the thermogenic coactivator PGC-1. Cell. 1999; 98: 115-124.

28. Lin J, Wu H, Tarr P T, Zhang C Y, Wu Z, Boss O, Michael L F, Puigserver P, Isotani E, Olson E N, Lowell B B, Bassel-Duby R, Spiegelman B M. Transcriptional co-activator PGC-1 alpha drives the formation of slow-twitch muscle fibres. Nature. 2002; 418: 797-801.

29. Lopez-Lluch G, Irusta P M, Navas P, de Cabo R. Mitochondrial biogenesis and healthy aging. Exp Gerontol. 2008; 43:813-819.

30. Bergeron R, Ren J M, Cadman K S, Moore I K, Perret P, Pypaert M, Young L H, Semenkovich C F, Shulman G I. Chronic activation of AMP kinase results in NRF-1 activation and mitochondrial biogenesis. Am J Physiol Endocrinol Metab. 2001; 281: 1340-1346.

31. Zong H, Ren J M, Young L H, Pypaert M, Mu J, Birnbaum M J, Shulman G I. AMP kinase is required for mitochondrial biogenesis in skeletal muscle in response to chronic energy deprivation. Proc Natl Acad Sci U S A. 2002; 99: 15983-15987.

32. Jager S, Handschin C, St-Pierre J, Spiegelman B M. AMP-activated protein kinase (AMPK) action in skeletal muscle via direct phosphorylation of PGC-1{alpha}. Proc Natl Acad Sci U S A. 2007; 104: 12017-12022.

33. Kahn B B, Alquier T, Carling D, Hardie D G. AMP-activated protein kinase: ancient energy gauge provides clues to modern understanding of metabolism. Cell Metab. 2005; 1: 15-25.

34. Hawley S A, Boudeau J, Reid J L, Mustard K J, Udd L, Makela T P, Alessi D R, Hardie D G. Complexes between the LKB1 tumor suppressor, STRADalpha/beta and MO25alpha/beta are upstream kinases in the AMP-activated protein kinase cascade. J Biol. 2003; 2: 28.1-28.16

35. Woods A, Johnstone S R, Dickerson K, Leiper F C, Fryer L G, Neumann D, Schlattner U, Wallimann T, Carlson M, Carling D. LKB1 is the upstream kinase in the AMP-activated protein kinase cascade. Curr Biol. 2003; 13: 2004-2008.

36. Itani S I, Saha A K, Kurowski T G, Coffin H R, Tornheim K, Ruderman N B. Glucose Autoregulates Its Uptake in Skeletal Muscle: Involvement of AMP-Activated Protein Kinase. Diabetes. 2003; 52: 1635-1640.

37. Fujii N, Hayashi T, Hirshman M F, Smith J T, Habinowski S A, Kaijser L, Mu J, Ljungqvist O, Birnbaum M J, Witters L A, Thorell A, Goodyear L J. Exercise induces isoform-specific increase in 5'AMP-activated protein kinase activity in human skeletal muscle. Biochem Biophys Res Commun. 2000; 273:1150-1155.

38. Hutber C A, Hardie D G, Winder W W. Electrical stimulation inactivates muscle acetyl-CoA carboxylase and increases AMP-activated protein kinase. Am J Physiol. 1997; 272: 262-266.

39. Kemp B E, Stapleton D, Campbell D J, Chen Z P, Murthy S, Walter M, Gupta A, Adams J J, Katsis F, van Denderen B, Jennings I G, Iseli T, Michell B J, Witters L A. AMP-activated protein kinase, super metabolic regulator. Biochem Soc Trans. 2003; 31: 162-168.

40. Rockl K S, Hirshman M F, Brandauer J, Fujii N, Witters L A, Goodyear L J. Skeletal muscle adaptation to exercise training: AMP-activated protein kinase mediates muscle fiber type shift. Diabetes. 2007; 56(8): 2062-2069.

41. Koh H J, Hirshman M F, He H, Li Y, Manabe Y, Balschi J A, Goodyear L J. Adrenaline is a critical mediator of acute exercise-

induced AMP-activated protein kinase activation in adipocytes. Biochem J. 2007; 403: 473-481.
42. Guarente L, Picard F. Calorie restriction--the SIR2 connection. Cell. 2005; 120: 473-482.
43. Greer E L, Dowlatshahi D, Banko M R, Villen J, Hoang K, Blanchard D, Gygi S P, Brunet A. An AMPK-FOXO pathway mediates longevity induced by a novel method of dietary restriction in C. elegans. Curr Biol. 2007; 17: 1646-1656.
44. North B J, Sinclair D A. Sirtuins: a conserved key unlocking AceCS activity. Trends Biochem Sci. 2007; 32: 1-4.
45. Hallows W C, Lee S, Denu J M. Sirtuins deacetylate and activate mammalian acetyl-CoA synthetases. Proc Natl Acad Sci U S A. 2006; 103: 10230-10235.
46. Law I K, Liu L, Xu A, Lam K S, Vanhoutte P M, Che C M, Leung P T, Wang Y. Identification and characterization of proteins interacting with SIRT1 and SIRT3: implications in the anti-aging and metabolic effects of sirtuins. Proteomics. 2009; 9: 2444-2456.
47. Nakatani Y, Ogryzko V. Immunoaffinity purification of mammalian protein complexes. Methods Enzymol. 2003; 370: 430-444.
48. Fulco M, Cen Y, Zhao P, Hoffman E P, McBurney M W, Sauve A A, Sartorelli V. Glucose restriction inhibits skeletal myoblast differentiation by activating SIRT1 through AMPK-mediated regulation of Nampt. Dev Cell. 2008; 14: 661-673.
49. Canto C, Gerhart-Hines Z, Feige J N, Lagouge M, Noriega L, Milne J C, Elliott P J, Puigserver P, Auwerx J. AMPK regulates energy expenditure by modulating NAD+ metabolism and SIRT1 activity. Nature. 2009; 458: 1056-1060.
50. McCarty, M.F., Chronic activation of AMP-activated kinase as a strategy for slowing aging. Med Hypotheses. 2004; 63: 334-339.
51. Apfeld J, O'Connor G, McDonagh T, DiStefano P S, Curtis R. The AMP-activated protein kinase AAK-2 links energy levels and insulin-like signals to lifespan in C. elegans. Genes Dev. 2004; 18: 3004-3009.
52. Dagon Y, Avraham Y, Magen I, Gertler A, Ben-Hur T, Berry E M. Nutritional status, cognition, and survival: a new role for leptin and AMP kinase. J Biol Chem. 2005; 280: 42142-42148.
53. Thomson D M, Herway S T, Fillmore N, Kim H, Brown J D, Barrow J R, Winder W W. AMP-activated protein kinase phosphorylates transcription factors of the CREB family. J Appl Physiol. 2008; 104: 429-438.
54. Handschin C, Rhee J, Lin J, Tarr P T, Spiegelman B M. An autoregulatory loop controls peroxisome proliferator-activated receptor gamma coactivator 1alpha expression in muscle. Proc Natl Acad Sci U S A. 2003; 100: 7111-7116.
55. Herzig S, Long F, Jhala U S, Hedrick S, Quinn R, Bauer A, Rudolph D, Schutz G, Yoon C, Puigserver P, Spiegelman B, Montminy M. CREB regulates hepatic gluconeogenesis through the coactivator PGC-1. Nature. 2001; 413: 179-183.
56. Gerhart-Hines Z, Rodgers J T, Bare O, Lerin C, Kim S H, Mostoslavsky R, Alt F W, Wu Z, Puigserver P. Metabolic control of muscle mitochondrial function and fatty acid oxidation through SIRT1/PGC-1alpha. Embo J. 2007; 26: 1913-1923.
57. Benigni A, Corna D, Zoja C, Sonzogni A, Latini R, Salio M, Conti S, Rottoli D, Longaretti L, Cassis P, Morigi M, Coffman T M, Remuzzi G. Disruption of the Ang II type 1 receptor promotes longevity in mice. J Clin Invest. 2009; 119: 524-530.
58. Farmer S R. Obesity: Be cool, lose weight. Nature. 2009; 458: 839-840.
59. Capel F, Viguerie N, Vega N, Dejean S, Arner P, Klimcakova E, Martinez J A, Saris W H, Holst C, Taylor M, Oppert J M, Sorensen T I, Clement K, Vidal H, Langin D. Contribution of energy restriction and macronutrient composition to changes in adipose tissue gene expression during dietary weight-loss programs in obese women. J Clin Endocrinol Metab. 2008; 93: 4315-4322.
60. Ferrer M D, Tauler P, Sureda A, Tur J A, Pons A. Antioxidant regulatory mechanisms in neutrophils and lymphocytes after intense exercise. J Sports Sci. 2009; 27: 49-58.
61. Lanza I R, Short D K, Short K R, Raghavakaimal S, Basu R, Joyner M J, McConnell J P, Nair K S. Endurance exercise as a countermeasure for aging. Diabetes. 2008; 57: 2933-2942.
62. Jin L, Galonek H, Israelian K, Choy W, Morrison M, Xia Y, Wang X, Xu Y, Yang Y, Smith J J, Hoffmann E, Carney D P, Perni R B, Jirousek M R, Bemis J E, Milne J C, Sinclair D A, Westphal C H. Biochemical characterization, localization, and tissue distribution of the longer form of mouse SIRT3. Protein Sci. 2009; 18(3): 514-525.
63. Zambrowicz B P, Friedrich G A, Buxton E C, Lilleberg S L, Person C, Sands A T. Disruption and sequence identification of 2,000 genes in mouse embryonic stem cells. Nature. 1998; 392: 608-611.
64. Cooper H M, Huang J Y, Verdin E, Spelbrink J N. A new splice variant of the mouse SIRT3 gene encodes the mitochondrial precursor protein. PLoS ONE. 2009; 4: e4986.

SUPPLEMENTARY FIGURES

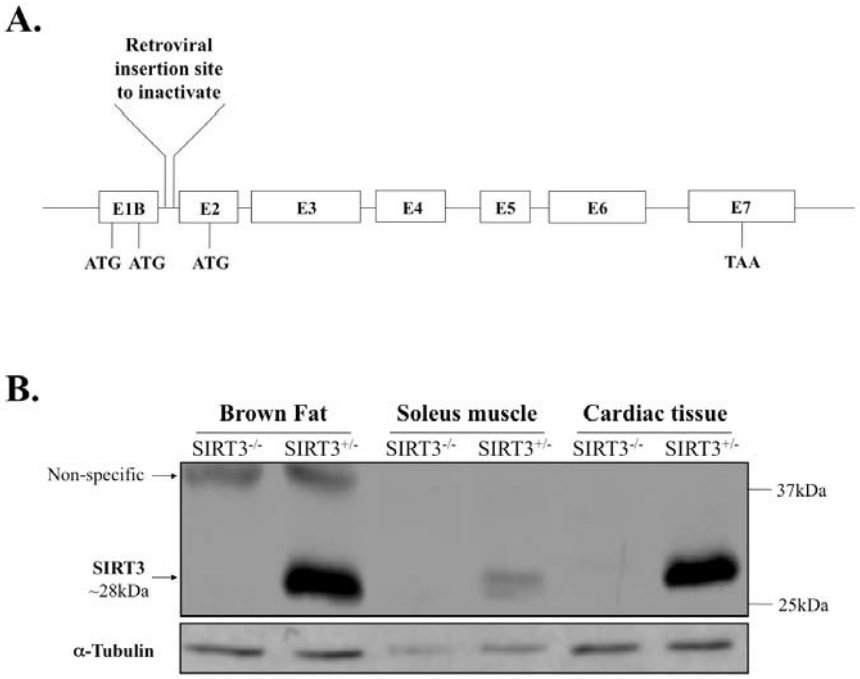

Supplemental Figure 1. Murine *Sirt3* gene structure and inactivation. (**A**) Annotated *Sirt3* gene structure [62, 64], showing retroviral insertion site for inactivation of SIRT3 in the null mice. Lines indicate relative position of known ATG start codons; the stop codon, TAA, is indicated in exon 7 (E7). Nomenclature for the exon designations shown here is taken from Cooper et al. [62]. (**B**) SIRT3 protein levels were assayed from mice tissues with either homozygous or heterozygous *Sirt3* gene deficiency, using standard Western blot analysis (as before).

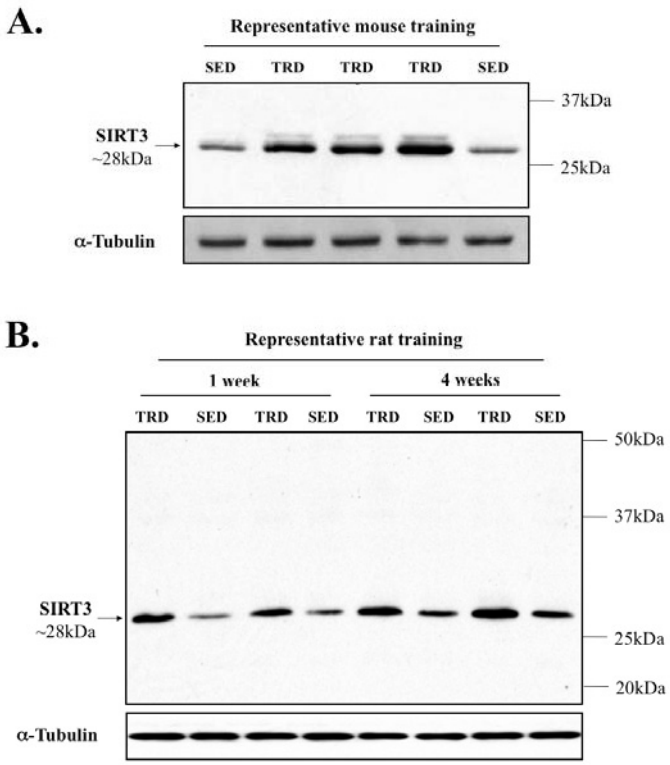

Supplemental Figure 2. SIRT3 up-regulation by exercise is conserved in rodents. (**A**) Representative Western blot panels of mice muscle samples used for quantification in Figure 2, and **(B**) rat muscle showing that SIRT3 up-regulation occurs as early as 1-week on a previously established treadmill-based exercise paradigm [41]. Remarkably, the molecular size of the mouse and rat SIRT3 proteins is conserved.